frontiers | Research Topics

Recent advances in synthesizing and utilizing nitrogen-containing heterocycles

Edited by
Hyun-Joon Ha, Hsyueh-Liang Wu and Takashi Ohshima

Published in
Frontiers in Chemistry

ISSN 1664-8714
ISBN 978-2-8325-4918-6
DOI 10.3389/978-2-8325-4918-6

About Frontiers

Frontiers is more than just an open access publisher of scholarly articles: it is a pioneering approach to the world of academia, radically improving the way scholarly research is managed. The grand vision of Frontiers is a world where all people have an equal opportunity to seek, share and generate knowledge. Frontiers provides immediate and permanent online open access to all its publications, but this alone is not enough to realize our grand goals.

Frontiers journal series

The Frontiers journal series is a multi-tier and interdisciplinary set of open-access, online journals, promising a paradigm shift from the current review, selection and dissemination processes in academic publishing. All Frontiers journals are driven by researchers for researchers; therefore, they constitute a service to the scholarly community. At the same time, the *Frontiers journal series* operates on a revolutionary invention, the tiered publishing system, initially addressing specific communities of scholars, and gradually climbing up to broader public understanding, thus serving the interests of the lay society, too.

Dedication to quality

Each Frontiers article is a landmark of the highest quality, thanks to genuinely collaborative interactions between authors and review editors, who include some of the world's best academicians. Research must be certified by peers before entering a stream of knowledge that may eventually reach the public - and shape society; therefore, Frontiers only applies the most rigorous and unbiased reviews. Frontiers revolutionizes research publishing by freely delivering the most outstanding research, evaluated with no bias from both the academic and social point of view. By applying the most advanced information technologies, Frontiers is catapulting scholarly publishing into a new generation.

What are Frontiers Research Topics?

Frontiers Research Topics are very popular trademarks of the *Frontiers journals series*: they are collections of at least ten articles, all centered on a particular subject. With their unique mix of varied contributions from Original Research to Review Articles, Frontiers Research Topics unify the most influential researchers, the latest key findings and historical advances in a hot research area.

Find out more on how to host your own Frontiers Research Topic or contribute to one as an author by contacting the Frontiers editorial office: frontiersin.org/about/contact

Recent advances in synthesizing and utilizing nitrogen-containing heterocycles

Topic editors

Hyun-Joon Ha — Hankuk University of Foreign Studies, Republic of Korea
Hsyueh-Liang Wu — National Taiwan Normal University, Taiwan
Takashi Ohshima — Kyushu University, Japan

Citation

Ha, H.-J., Wu, H.-L., Ohshima, T., eds. (2024). *Recent advances in synthesizing and utilizing nitrogen-containing heterocycles*. Lausanne: Frontiers Media SA. doi: 10.3389/978-2-8325-4918-6

Table of contents

frontiers | Frontiers in Chemistry

TYPE Editorial
PUBLISHED 10 May 2024
DOI 10.3389/fchem.2024.1421449

OPEN ACCESS

EDITED AND REVIEWED BY
Iwao Ojima,
Stony Brook University, United States

*CORRESPONDENCE
Takashi Ohshima,
ohshima@phar.kyushu-u.ac.jp
Hsyueh-Liang Wu,
hlw@ntnu.edu.tw
Hyun-Joon Ha,
hjha@hufs.ac.kr

RECEIVED 22 April 2024
ACCEPTED 26 April 2024
PUBLISHED 10 May 2024

CITATION
Ohshima T, Wu H-L and Ha H-J (2024), Editorial: Recent advances in synthesizing and utilizing nitrogen-containing heterocycles. *Front. Chem.* 12:1421449. doi: 10.3389/fchem.2024.1421449

Editorial: Recent advances in synthesizing and utilizing nitrogen-containing heterocycles

Takashi Ohshima[1]*, Hsyueh-Liang Wu[2]* and Hyun-Joon Ha[3]*

[1]Graduate School of Pharmaceutical Sciences, Kyushu University, Fukuoka, Japan, [2]Department of Chemistry, National Taiwan Normal University, Taipei, Taiwan, [3]Department of Chemistry, Hankuk University of Foreign Studies, Yongin, Republic of Korea

KEYWORDS

aziridine, azetidine, pyrrolidine, imidazolidine, pyrazole, triazoles, piperidine, pyridine

Editorial on the Research Topic
Recent advances in synthesizing and utilizing nitrogen-containing heterocycles

Exploring the vast landscape of nitrogen-containing heterocycles, commonly known as aza-heterocycles, reveals their ubiquitous presence in natural products, pharmaceuticals, agrochemicals, and functional materials. Consequently, synthesizing these compounds has garnered significant attention, driven by the need to develop more efficient methods for their preparation and utilization as versatile building blocks. The importance of nitrogen-containing heterocycles has increased due to their expanding role as ligands in transition-metal catalysis and organocatalysis. Despite extensive studies into their synthesis and applications, ongoing demand remains for more efficient and general preparation methods to diversify the structural backbones and improve their biological activities. Moreover, their usage as ligands and catalysts is continuously being investigated in various chemical reactions.

This Research Topic, "Recent Advances in Synthesizing and Utilizing Nitrogen-Containing Heterocycles," curated by Professors Ohshima, Wu, and Ha, features a Research Topic of groundbreaking research, illuminating innovative synthetic methods, strategies for selectivity and reactivity modulation, and diverse applications in functional molecule design. This editorial presents ten original research articles and one perspective piece, highlighting essential findings and their broader implications in the field of heterocyclic chemistry, offering promising insights into the future of this vibrant scientific area.

The Innovative Synthetic Methods section showcases pioneering strategies for constructing nitrogen-containing heterocycles. Murakami et al. present a copper-catalyzed method for synthesizing imidazolidine and imidazolidinone by reacting aziridines with imines and isocyanates, respectively. This approach involves transforming 3-membered heterocyclic rings into 5-membered ones, yielding a diverse array of 2-substituted imidazolidines and substituted imidazolidinones with high functional group compatibility. Lee et al. introduce a novel method for constructing functionalized dihydropyridinone rings via the annulation of an amide tethered with an alkyne moiety at the α-carbon. This process includes the formation of O-silyl N,O-ketene acetal and silver-mediated addition, proving a new route for the total synthesis of phenanthroindolizidine and phenanthroquinolizidine alkaloids.

Kim et al. descrive a new single-atom deletion strategy for the late-stage conversion of alkaloids, employing oxidative ring contraction followed by chemoselective reduction to convert the 6-membered piperidine moiety of (allo)securinine into a 5-membered pyrrolidine, facilitating access to (allo) norsecurinine.

In the Selectivity and Reactivity Control domain, it is demonstrated that modifications to the catalyst, reaction conditions, or substrate structure can significantly enhance selectivity and reactivity, suggesting a new control strategy in heterocyclic synthesis. Kuriyama et al., focusing on La(OTf)3-catalyzed reactions, illuminate the efficiency and versatility of modern synthetic strategies. Their method utilizing La(OTf)3-catalyzed intramolecular regioselective aminolysis method to convert cis-3,4-epoxy amines into highly strained 4-membered ring azetidines over 5-membered ring pyrrolidines. This approach achieves high yields even with acid-sensitive and Lewis basic functional groups, marking a significant advancement in synthetic organic chemistry. Srivastava and Ha develop an innovative approach for constructing nitrogen-containing heterocycles via aziridine ring-opening reactions. In this reaction, the regioselectivity depends on the functional groups of the alkyl substituents. Employing aziridine rings substituted with ketone or silylated hydroxy group as substrates has proven to efficiently facilitate ring-opening and subsequent cyclizations, converting 3-membered heterocyclic rings into 5- or 6-membered ones. Noda et al. investigate the reactivity of rhodium alkyl nitrenes derived from substituted hydroxylamine precursors for synthesizing 5-membered pyrrolidines, focusing on modulating the regioselectivity between benzylic and tertiary C–H bonds by adding of Brønsted acids or by modifying oxygen substituents. Their findings deepen the understanding of metallonitrene structures and provide valuable insights for the selective synthesis of N-heterocycles. This study underscores the profound impact of precursor structures and additives on nitrene reactivity, paving the way for substrate-controlled synthesis, which is crucial for medicinal chemistry and drug development. Kim et al. develop a novel and highly efficient strategy for the C4-selective (hetero)arylation of pyridines using N-aminopyridinium salts. This method overcomes the poor site-selectivity often encountered in conventional methods by using N-aminopyridinium salts instead of pyridine as substrates. This metal-free method proceeds at room temperature with a base, eliminating the need for catalysts or oxidants. It allows the incorporation of various electron-rich (hetero)aryl groups onto pyridines, facilitating the synthesis of valuable C4-(hetero)aryl pyridine derivatives, crucial in agrochemicals, pharmaceuticals, and functional materials. In a complementary contribution, Choi et al. explore the compatibility of various functional groups in the hydrazinolysis of amides with ammonium salts. The resulting acyl hydrazide can be readily converted into the corresponding ester through acylpyrazole. Utilizing a Functional Group Evaluation (FGE) kit comprising 26 additives, including nitrogen-containing heterocycles like imidazole and indole, this study rapidly assesses the compatibility of functional groups crucial for drug discovery research. Furthermore, this innovative research unveils the positive effects of carboxylic acid additives, suggesting the utility of this evaluation kit in developing new reaction systems.

The Applications for Functional Molecules segment transcends the boundaries of traditional synthesis by exploring the applications of nitrogen-containing heterocycles across various scientific fields.

Further expanding the synthetic repertoire, Namioka et al. present an efficient method for preparing organomagnesium intermediates with protected azido groups, utilizing Amphos for azide protection. This technique facilitates the synthesis of diverse functionalized azides and their subsequent conversion into a wide array of 1,2,3-triazoles through click reactions. This advancement contributes significantly to synthetic organic chemistry, pharmaceutical sciences, and materials chemistry by providing a versatile approach to synthesize azides and triazoles, pivotal as synthetic intermediates and bioactive compounds. Mohamadpour et al. introduce a groundbreaking, green photosynthesis method for synthesizing 3,4-dihydropyrimidin-2-(1H)-one/thione derivatives which exhibit widespread biological applications such as antihypertensive, antiviral, antitumor, antibacterial, α-1a-antagonism, antioxidant, and anti-inflammatory actions, from aryl aldehydes, β-ketoesters, and urea/thiourea. This method employs a novel halogenated dicyanobenzene-based photosensitizer, 3DPAFIPN, as a donor-acceptor photocatalyst triggered by visible light. Utilizing blue LED technology enables a sustainable, energy-efficient reaction process in an ethanol medium at room temperature. The perspective offered by Ha brings to light the practicality and environmental benefits of using proline-derived organocatalysis and pot-economical synthesis. The synthesis of (−)-quinine serves as a prime example of overcoming synthetic challenges through organocatalysis, showcasing the method's potential in streamlining the environmentally benign production of complex organic compounds. The discussion includes various organocatalysis techniques and their success in enhancing reaction conditions, emphasizing the significance of organocatalysts in modern synthetic organic chemistry.

This Research Topic showcases the dynamic and ever-evolving landscape of research on nitrogen-containing heterocycles and lays the groundwork for future investigations. It is a testament to the collaborative spirit of the scientific community, driven by a shared commitment to unravel the complexities of chemistry for the advancement of knowledge and society.

We extend our deepest appreciation to all the contributors, whose dedication and groundbreaking work enrich our collective understanding and pave the way for future innovations. Their diverse insights and findings reflect the multifaceted nature of chemistry's quest to harness the potential of nitrogen-containing heterocycles, promising new avenues for discovery and application.

Author contributions

TO: Writing–original draft, Writing–review and editing. H-LW: Writing–original draft, Writing–review and editing. H-JH: Writing–original draft, Writing–review and editing.

Funding

The author(s) declare that financial support was received for the research, authorship, and/or publication of this article. MEXT KAKENHI (Grant JP21A204, JP21H05207, and JP21H05208) 2024 HUFS grant.

Acknowledgments

TO acknowledges financial support from MEXT KAKENHI (Grant JP21A204, JP21H05207, and JP21H05208). H-JH acknowledges financial support from the 2024 HUFS grant.

Conflict of interest

The authors declare that the research was conducted in the absence of any commercial or financial relationships that could be construed as a potential conflict of interest.

Publisher's note

frontiers | Frontiers in Chemistry

TYPE Original Research
PUBLISHED 31 July 2023
DOI 10.3389/fchem.2023.1237878

OPEN ACCESS

EDITED BY
Takashi Ohshima,
Kyushu University, Japan

REVIEWED BY
Yoshitaka Hamashima,
University of Shizuoka, Japan
Rajendra Rohokale,
University of Florida, United States

*CORRESPONDENCE
Suguru Yoshida,
s-yoshida@rs.tus.ac.jp

RECEIVED 10 June 2023
ACCEPTED 17 July 2023
PUBLISHED 31 July 2023

CITATION
Namioka R, Suzuki M and Yoshida S (2023), Synthesis of 1,2,3-triazoles using Grignard reactions through the protection of azides.
Front. Chem. 11:1237878.
doi: 10.3389/fchem.2023.1237878

Synthesis of 1,2,3-triazoles using Grignard reactions through the protection of azides

Rina Namioka[1], Minori Suzuki[1,2] and Suguru Yoshida[1]*

[1]Department of Biological Science and Technology, Faculty of Advanced Engineering, Tokyo University of Science, Tokyo, Japan, [2]Laboratory of Chemical Bioscience, Institute of Biomaterials and Bioengineering, Tokyo Medical and Dental University (TMDU), Tokyo, Japan

An efficient method to prepare organomagnesium intermediates having a protected azido group is reported. Protection of azido groups with di-(*tert*-butyl)(4-(dimethylamino)phenylphosphine (amphos) and following iodine–magnesium exchange realized the preparation of organomagnesium intermediates, which served in the synthesis of diverse azides by transformation with various electrophiles followed by deprotection with elemental sulfur. Furthermore, click reactions of azides with alkynes enabled synthesizing a wide variety of 1,2,3-triazoles.

KEYWORDS

azides, triazoles, protection, click chemistry, iodine–magnesium exchange, turbo Grignard reagent, phosphazide, phosphines

1 Introduction

Azides are a significant class of compounds in a broad range of research fields, including synthetic organic chemistry, pharmaceutical sciences, and materials chemistry (Figure 1A) (Bräse and Banert, 2010; Banert, 2016; Yoshida, 2020). Triazole formations by copper-catalyzed azide–alkyne cycloaddition (CuAAC) (Rostovtsev et al., 2002; Tornøe et al., 2002; Meldal and Tornøe, 2008) or strain-promoted azide–alkyne cycloaddition (SPAAC) (Agard et al., 2004; Ning et al., 2008; Dommerholt et al., 2010) have served as click reactions. Azides are also frequently used in organonitrogen syntheses through the Staudinger reduction which takes place smoothly by the treatment of phosphines at ambient temperature (Staudinger and Meyer, 1919; Saxon and Bertozzi, 2000). Despite the importance of azides in synthetic organic chemistry, it is not always easy to synthesize azides owing to the electrophilic nature of azido groups which are susceptible to various nucleophiles, such as carbanions (Tanimoto and Kakiuchi, 2013). In particular, the preparation of carbanions having azido groups is, thus, a challenging issue (Figure 1B). For example, Nagaki and coworkers reported that treatment of 4-bromophenyl azide with *n*-butyllithium at −78°C under microflow conditions followed by protonation afforded phenyl azides in low yield (Figure 1C–1) (Ichinari et al., 2020), notably showing that the preparation of 4-azidophenyllithium is a challenging transformation, even under microflow conditions. An alternative preparation method for the 4-azidophenyllithium equivalent was successfully developed from 1,4-dibromobenzene (**3**) under microflow conditions through triazene formation with sulfonyl azide **4** and the subsequent bromine–lithium exchange, leading to aryllithium **5**, as a carbanion, having a masked azide moiety (Figure 1C–2) (Ichinari et al., 2020). Although this elegant method allowed us to synthesize a limited variety of 4-substituted phenyl azides, a new approach to prepare carbanions bearing masked azide moieties leading to a wide array of azides is sought after.

10.3389/fchem.2023.1237878

In this study, we conceived an idea of preparing carbanions having "protected" azido groups through the treatment of azides with di(tert-butyl)(4-(dimethylamino)phenylphosphine (amphos) (Figure 1D). Previously, we found that amphos smoothly reacts with azides to furnish phosphazides without denitrogenation, and phosphazides can be transformed into azides through deprotection with elemental sulfur (Meguro et al., 2018). Azide protection realized various transformations, such as selective click reactions of diazides and Grignard reactions using carbonyl compounds having azide moieties due to the good stability of phosphazides as protected azides (Aimi et al., 2021). Herein, we describe an efficient method to prepare organomagnesium intermediates by

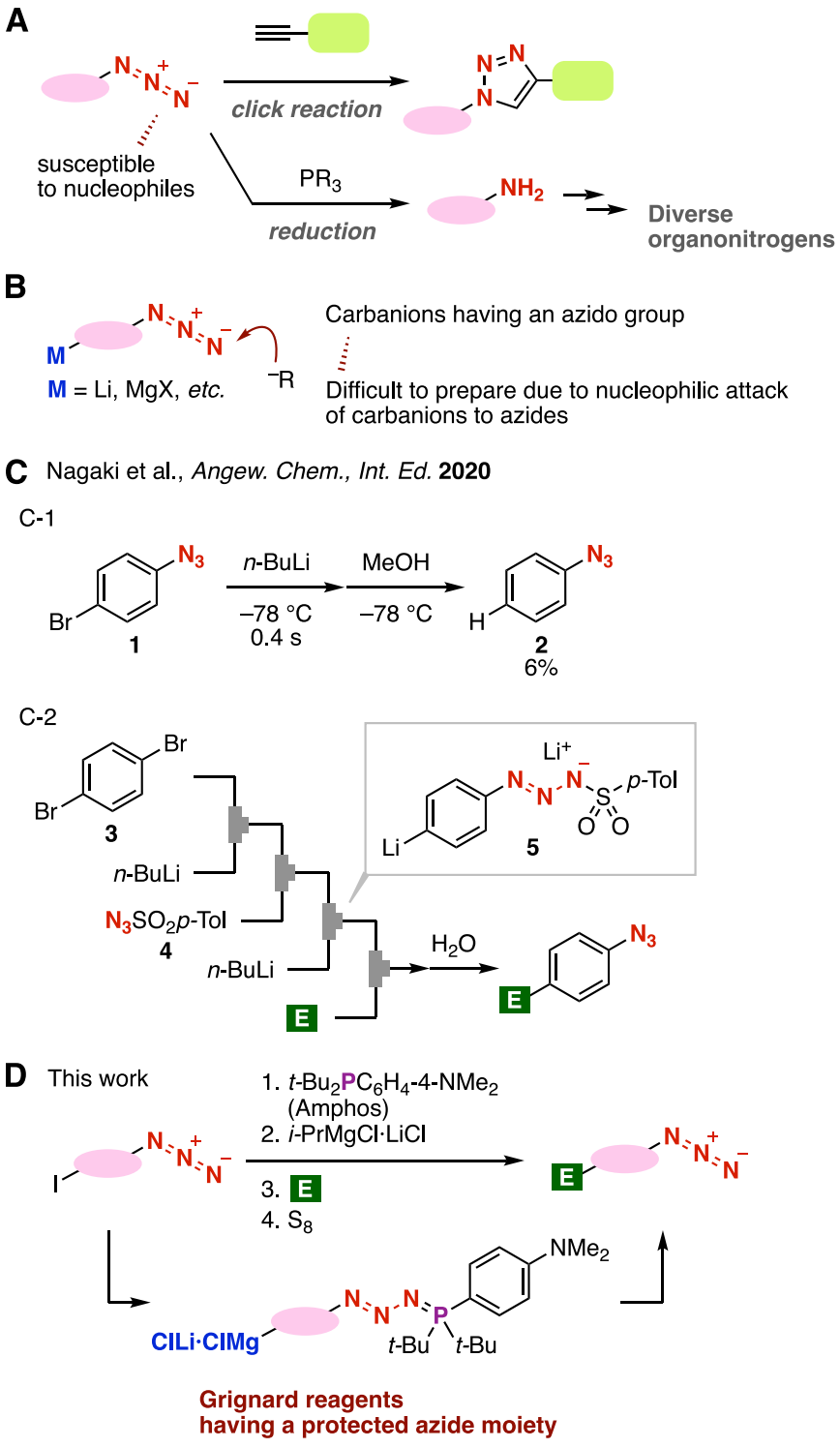

FIGURE 1
(A) Transformations of azides. **(B)** Carbanions having an azido group. **(C)** Nagaki's work. **(D)** Overview of this work.

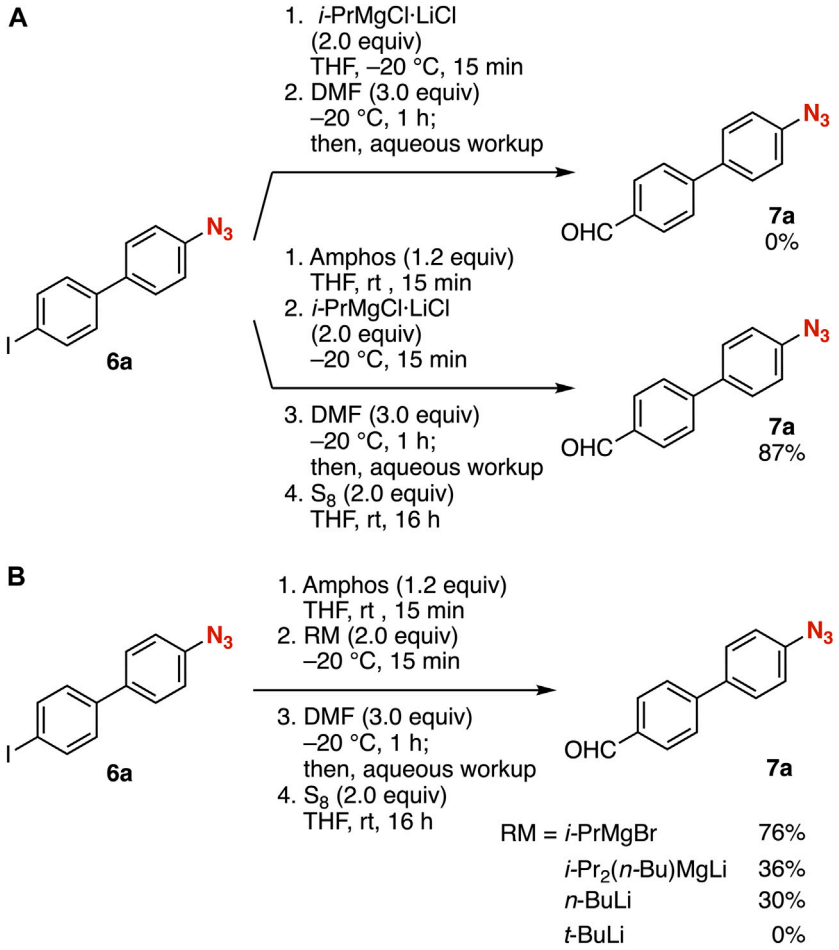

FIGURE 2
(A) Synthesis of **7a** from **6a** with or without the protection of the azido group. **(B)** Screening reagents for the iodine–metal exchange.

iodine–magnesium exchange with a turbo Grignard reagent after the phosphazide formation of iodine-substituted azides, enabling facile synthesis of diverse 1,2,3-triazoles by Grignard reactions and following CuAAC reactions.

2 Results and discussion

First, we attempted the iodine–magnesium exchange of 4-(4-iodophenyl)phenyl azide (**6a**) with an isopropylmagnesium chloride lithium chloride complex (Krasovskiy and Knochel, 2004; Bao et al., 2015) in THF at −20°C followed by the addition of *N*,*N*-dimethylformamide (DMF) (Figure 2A, route 1). As a result, the desired aldehyde **7a** was not obtained due to the decomposition of the azido group. In contrast, we succeeded in the synthesis of aldehyde **7a** from iodide **6a** in high yield via phosphazide formation (Figure 2A, route 2). Treatment of azide **6a** with amphos at room temperature followed by iodine–magnesium exchange with the isopropylmagnesium chloride lithium complex in THF at −20°C and subsequent addition of DMF resulted in efficient formylation. Following deprotection of the phosphazide moiety with elemental sulfur provided azide **7a** in good yield without damaging the azido group. The iodine–magnesium exchange with isopropylmagnesium bromide instead of the turbo Grignard reagent also proceeded efficiently (Figure 2B). Aldehyde **7a** was prepared in moderate yield when using *i*-Pr_2(*n*-Bu)MgLi (Inoue et al., 2001) or *n*-butyllithium for the iodine–metal exchange. Metalation using *tert*-butyllithium resulted in a complex mixture of products.

A wide range of azides **8** were successfully synthesized by the addition of electrophiles to the organomagnesium intermediate prepared *in situ* from azide **6a** (Figure 3). Various aldehydes **9** efficiently reacted with the organomagnesium intermediate, enabling us to synthesize the corresponding alcohols **8a**–**8e** in good yields, leaving azide, benzyl alcohol, chloro, methoxy, and thienyl moieties intact. Tertiary alcohol **8f** or **8g** was prepared from azide **6a** using acetone (**10a**) or α,α,α-trifluoroacetophenone (**10b**), respectively, as an electrophile. Allylation of the Grignard reagent prepared from **6a** took place to afford the azide **8h** after deprotection with elemental sulfur. Bromide **8i** was synthesized by bromination of the carbanion with *N*-bromosuccinimide (NBS), followed by treatment with S_8.

We succeeded in the synthesis of aldehydes **7b**–**7f** from a range of azides **6** through phosphazide formation, iodine–magnesium exchange, formylation with DMF, and deprotection with S_8 (Figure 4). For example, 4-formyl- or 3-formylphenyl azide **7b** or

10.3389/fchem.2023.1237878

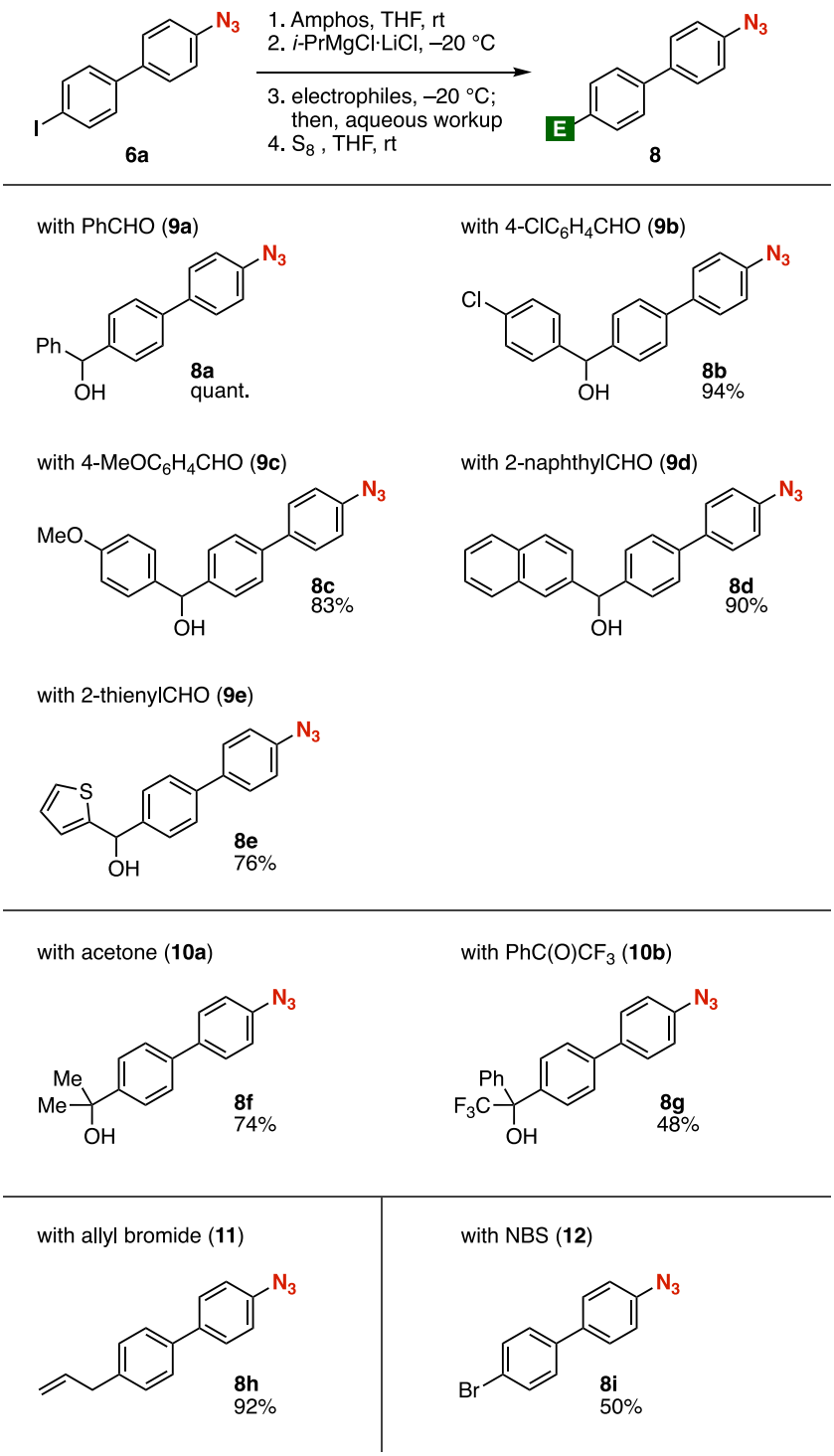

FIGURE 3
Synthesis of azides **8** from azide **6a** and various electrophiles. NBS, *N*-bromosuccinimide.

7c were prepared from 4-iodo- or 3-iodophenyl azide (**6b** or **6c**), respectively. We accomplished the synthesis of trisubstituted benzene **7d** from 4-azido-3-methylphenyl iodide (**6d**) through the phosphazide formation of the *ortho* methyl-substituted phenyl azide moiety. When using 4-azido-2-chlorophenyl iodide (**6e**), protection of the azido group, iodine–magnesium exchange, formylation, and deprotection proceeded smoothly for furnishing aldehyde **7e** without damaging aldehyde, azide, and chloro moieties. Moreover, we achieved the preparation of the carbanion intermediate having an alkyl azide moiety from azide **6f** through phosphazide formation and subsequent iodine–magnesium exchange, which successfully served in formylation with DMF.

10.3389/fchem.2023.1237878

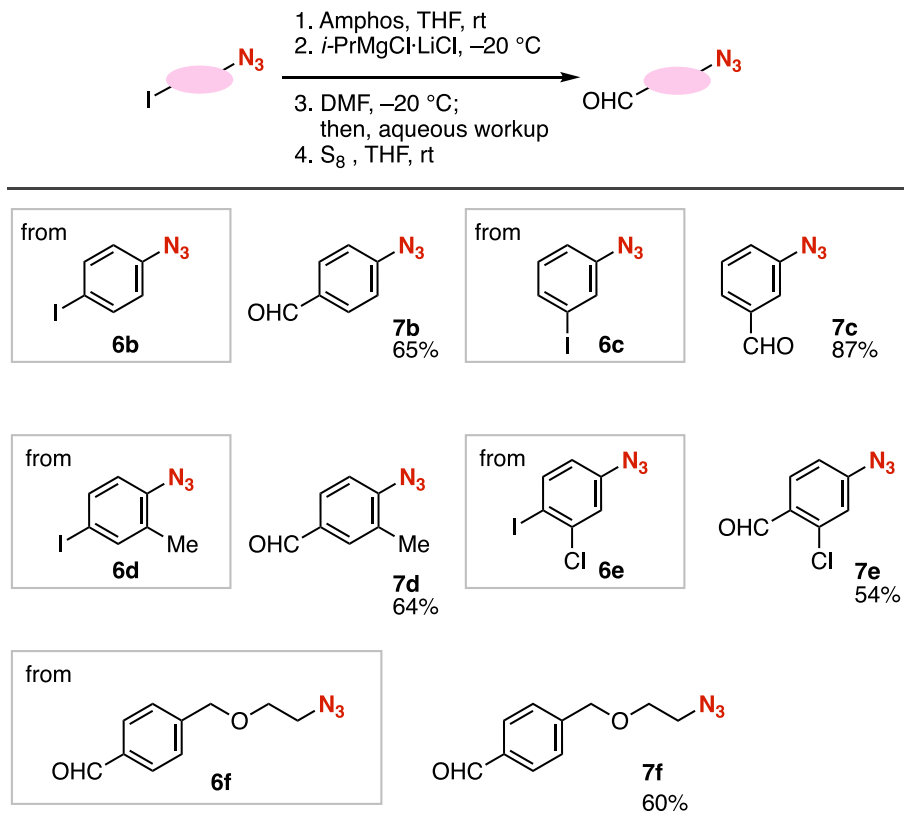

FIGURE 4
Synthesis of azides **7** from various azides **6**.

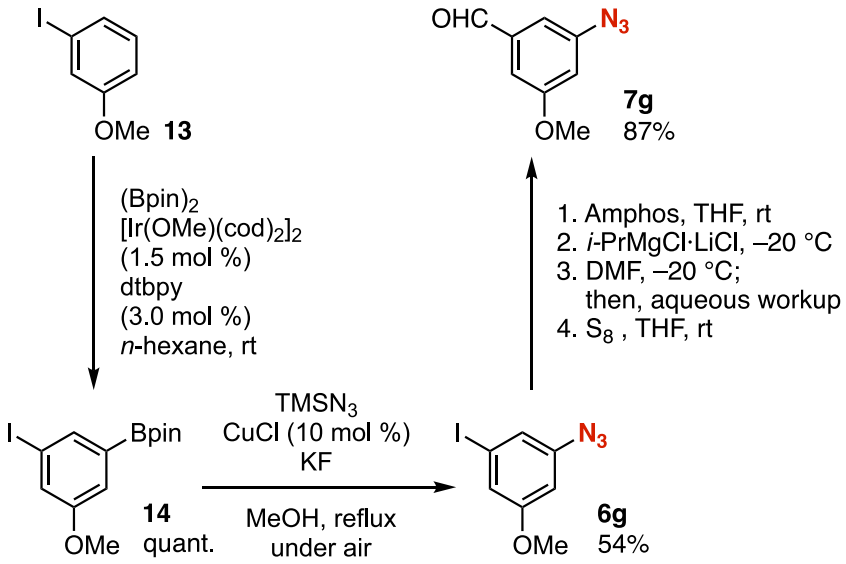

FIGURE 5
Synthesis of azide **7g**.

Azides bearing the iodo group can be synthesized by formal C–H azidation (Yoshida et al., 2014; Nishiyama et al., 2019) through Ir-catalyzed C–H borylation (Cho et al., 2002; Ishiyama et al., 2002; Mkhalid et al., 2010) and subsequent Cu-catalyzed azidation (Li et al., 2010). Thus, transformations of aryl iodides via the protection of the azido group allowed us to prepare a wide range of highly

10.3389/fchem.2023.1237878

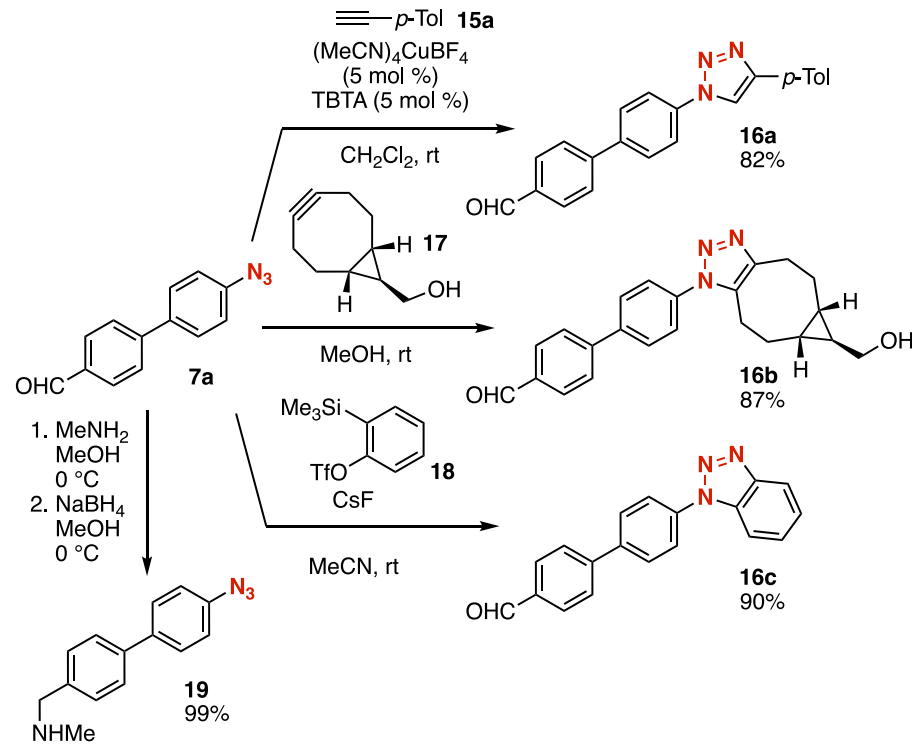

FIGURE 6
Transformations of azide **7a**.

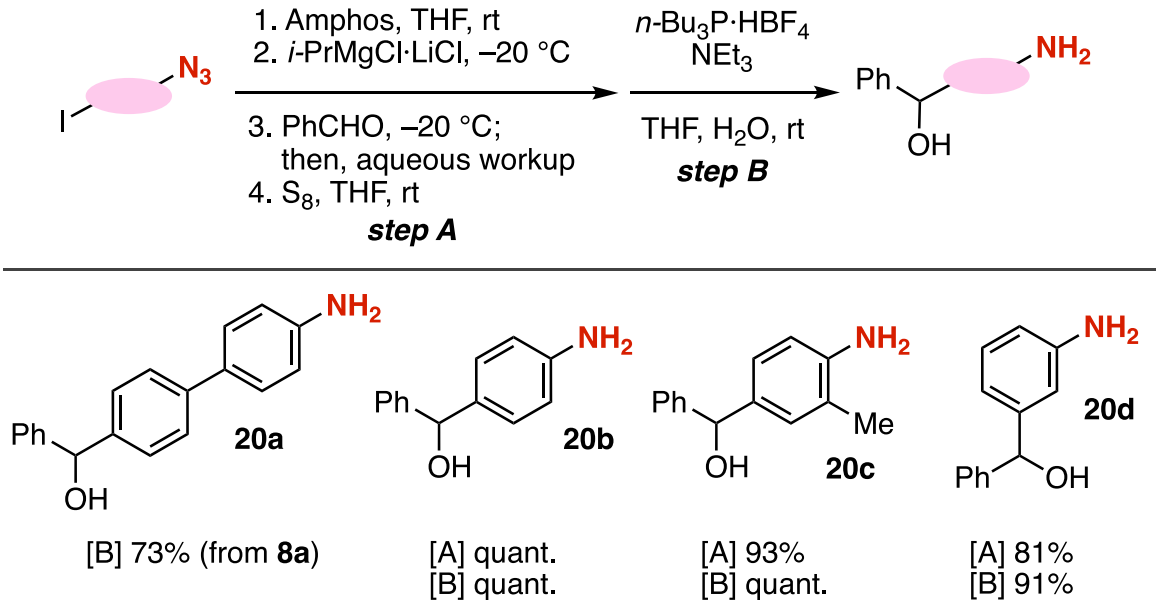

FIGURE 7
Transformations to anilines **20**.

functionalized aryl azides from simple aryl iodides. For example, C–H borylation of *m*-iodoanisole catalyzed by iridium proceeded smoothly without damaging the iodo group (Figure 5). Subsequent azidation of the resulting arylboron **14**, catalyzed by copper, took place efficiently. Then, we succeeded in the transformation of aryl iodide **6g** via phosphazide formation and the iodine–magnesium exchange to provide benzaldehyde **7g,** leaving the methoxy, formyl, and azido groups untouched.

10.3389/fchem.2023.1237878

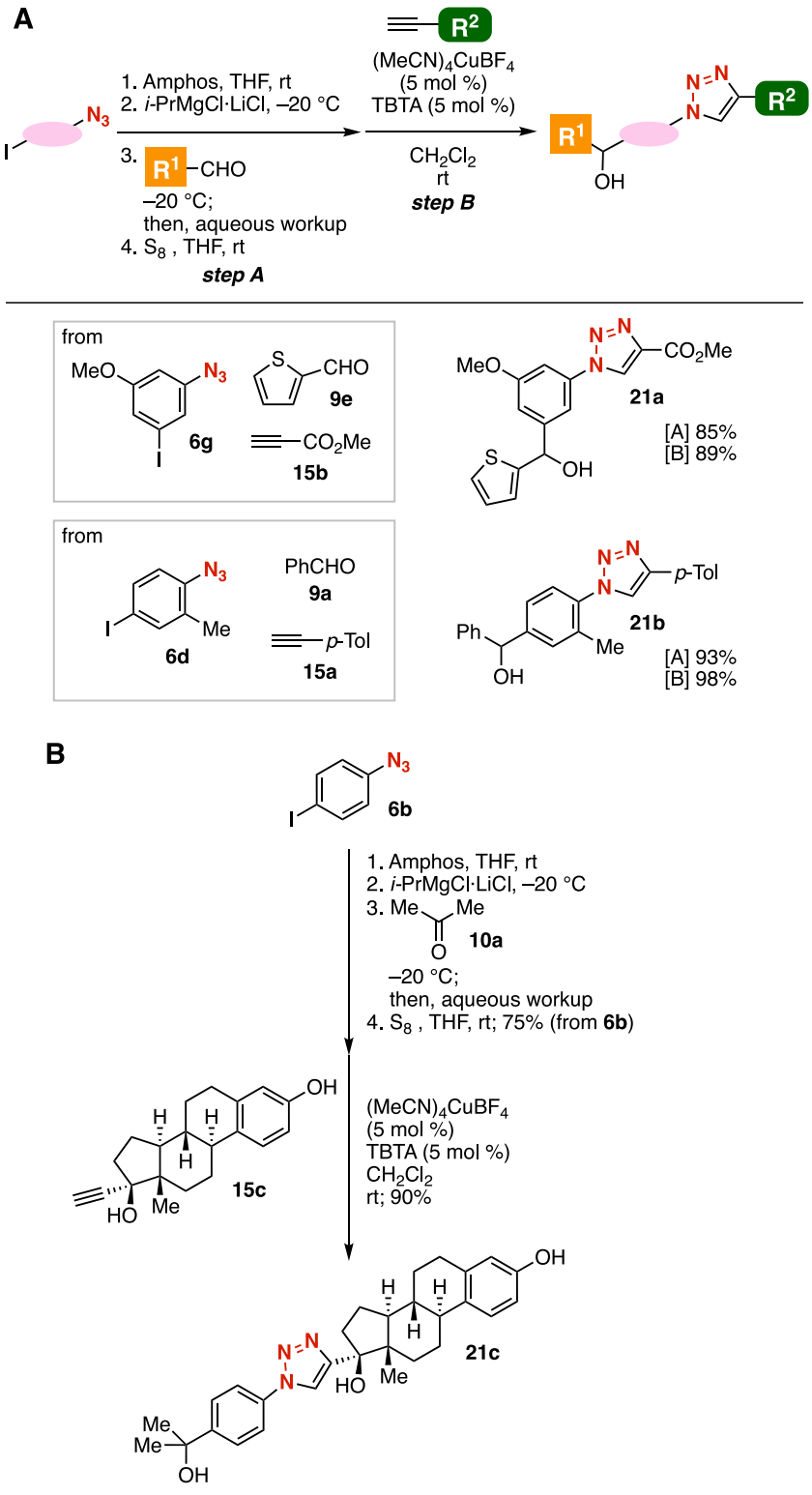

FIGURE 8
(A) Synthesis of triazoles **21a** and **21b**. **(B)** Synthesis of triazole **21c**.

A wide variety of 1,2,3-triazoles were easily synthesized from azide **7a** without damaging the formyl group (Figure 6). Indeed, we accomplished the synthesis of triazole **16a** in high yield by the CuAAC reaction of azide **7a** with terminal alkyne **15a** in the presence of a catalytic amount of $(MeCN)_4CuBF_4$ and tris[(1-benzyl-1*H*-1,2,3-triazol-4-yl)methyl]amine (TBTA) (Chan et al., 2004). Triazole

formation of azide **7a** with cycloalkyne **17** proceeded smoothly to afford triazole **16b** in good yield without copper catalysis (Dommerholt et al., 2010). We succeeded in the cycloaddition of azide **7a** with benzyne generated from *o*-silylaryl triflate **18** to provide benzotriazole **16c** having an aldehyde moiety (Shi et al., 2008). Reductive amination of aldehyde **7a** also took place avoiding the reduction of the azido group. Thus, further transformations enabled us to diversify azides after reactions of azide-substituted carbanion equivalents.

Amino alcohols **20a**–**20d** were efficiently synthesized from azides by transformations of carbanions through the protection of azido groups followed by the Staudinger reduction (Figure 7). We achieved the synthesis of amino alcohol **20a** from azide **8a** with tri-(*n*-butyl)phosphonium tetrafluoroborate in the presence of triethylamine (Meguro et al., 2017). The Grignard reaction of azide-substituted carbanion equivalents with aldehyde **9a** and the following Staudinger reduction realized the preparation of a number of amino alcohols **20b**–**20d** in good yields. Considering the pivotal role of amines and alcohols in the preparation of azaheterocycles, the synthesis of amino alcohols from iodine-substituted azides is poised to make significant contributions to the field of synthetic organic chemistry.

Grignard reactions of azide-substituted carbanion equivalents and the subsequent CuAAC reaction enabled us to synthesize a broad variety of 1,2,3-triazoles from diverse azides, aldehydes, and terminal alkynes (Figure 8). After treatment of 3-iodo-5-methoxyphenyl azide (**6g**) with amphos followed by the iodine–magnesium exchange, the Grignard reaction with 2-thienyl aldehyde (**9e**) and deprotection with elemental sulfur resulted in the efficient synthesis of the corresponding alcohol in good yield (Figure 8A). Then, we succeeded in the preparation of triazole **21a** by the CuAAC reaction with alkyne **15b** bearing an ester moiety. This approach is clearly advantageous over a synthetic route without azide protection, as esters can readily react with carbanions like Grignard reagents. Consequently, the synthesis of triazole **21a** from azide **6g**, aldehyde **9e**, and alkyne **15b** was achieved in short steps. Furthermore, triazole **21b** was efficiently prepared from azide **6d**, aldehyde **9a**, and alkyne **15a**. We achieved the synthesis of triazole **21c** bearing an estradiol scaffold from 4-iodophenyl azide (**6b**), acetone (**10a**), and ethinyl estradiol (**15c**) by a simple protocol through phosphazide formation.

3 Materials and method

For general experimental and instrumental methods, synthetic procedures, and full compound characterization, see the Supplementary Materials.

3.1 Synthesis of aldehyde **7a** from aryl iodide **6a**

To a solution of 4-azido-4'-iodo-1,1'-biphenyl (**6a**) (96.8 mg, 0.301 mmol) dissolved in THF (4.0 mL) was added di(*tert*-butyl)(4-(dimethylamino)phenyl)phosphine (amphos) (95.9 mg, 0.361 mmol, and 1.2 equiv) at room temperature. After stirring for 15 min at the same temperature, we slowly added *i*PrMgCl·LiCl (1.3 M, THF solution, 0.50 mL, 0.650 mmol, and 2.2 equiv) to it at −20°C. After stirring for 30 min at the same temperature, we also slowly added *N*,*N*-dimethylformamide (70.0 μL, 0.904 mmol, and 3.0 equiv) to the solution. After stirring for 1 h at −20°C, we slowly added water (5 mL) to it. The mixture was extracted with EtOAc (10 mL × 3). The combined organic extract was washed with brine (10 mL) and dried with Na_2SO_4. After filtration, the filtrate was concentrated under reduced pressure. We added S_8 (19.7 mg, 0.614 mmol, and 2.0 equiv) to the residue dissolved in THF (4.0 mL) at room temperature. After stirring for 16 h at the same temperature, the mixture was concentrated under reduced pressure. The residue was purified by preparative TLC (*n*-hexane/EtOAc = 1/1) to give 4-(4-azidophenyl)benzaldehyde (**7a**) (55.6 mg, 0.249 mmol, and 83%) as a pale yellow solid.

3.2 4-Azido-4′-iodo-1,1′-biphenyl (**6a**)

Pale yellow solid; Mp 122–124°C; TLC R_f 0.65 (*n*-hexane/EtOAc = 10/1); ^{1}H NMR ($CDCl_3$, 400 MHz): δ 7.07–7.13 (AA'BB', 2H), 7.25–7.33 (AA'BB', 2H), 7.51–7.57 (AA'BB', 2H), and 7.74–7.79 (AA'BB', 2H); ^{13}C{^{1}H} NMR ($CDCl_3$, 101 MHz): δ 93.1, 119.5, 128.2, 128.6 (two signals overlapped), 136.7, 137.9, and 139.6; IR (Nujol, cm^{-1}): 810, 1,296, 1,306, 1,377, 1,388, 1,463, 1,478, 2,106, 2,139, 2,855, 2,924, and 2,953; and HRMS (FAB) *m/z*: $[M]^{+}$ calcd for $C_{12}H_8IN_3^{+}$ 320.9763; found 320.9779.

4 Conclusion

In conclusion, we succeeded in the preparation of organomagnesium intermediates having protected azido groups. Various azides were successfully synthesized by the Grignard reaction of carbanions having phosphazide moieties with various electrophiles followed by deprotection with elemental sulfur. Since a broad range of organonitrogens, such as amines and triazoles, are easily prepared from azides, reactions involving carbanion equivalents with azide moieties, followed by subsequent transformations, are poised to significantly contribute to organonitrogen synthesis. Our laboratory is currently engaged in further studies, including the preparation and transformations of carbanions with phosphazide moieties.

Data availability statement

The original contributions presented in the study are included in the article/Supplementary Materials; further inquiries can be directed to the corresponding author.

Author contributions

SY directed the study, conceived the experiments, and wrote the paper. RN and MS planned and performed the experiments and wrote the paper. All authors contributed to the article and approved the submitted version.

Funding

This work was supported by JSPS KAKENHI, grant number JP22H02086 (SY), and the Asahi Glass Foundation (SY).

Conflict of interest

The authors declare that the research was conducted in the absence of any commercial or financial relationships that could be construed as a potential conflict of interest.

Publisher's note

All claims expressed in this article are solely those of the authors and do not necessarily represent those of their affiliated organizations, or those of the publisher, the editors, and the reviewers. Any product that may be evaluated in this article, or claim that may be made by its manufacturer, is not guaranteed or endorsed by the publisher.

Supplementary material

The Supplementary Material for this article can be found online at: https://www.frontiersin.org/articles/10.3389/fchem.2023.1237878/full#supplementary-material

References

Agard, N. J., Prescher, J. A., and Bertozzi, C. R. (2004). A strain-promoted [3 + 2] Azide–Alkyne cycloaddition for covalent modification of biomolecules in living systems. *J. Am. Chem. Soc.* 126, 15046–15047. doi:10.1021/ja044996f

Aimi, T., Meguro, T., Kobayashi, A., Hosoya, T., and Yoshida, S. (2021). Nucleophilic transformations of azido-containing carbonyl compounds *via* protection of the azido group. *Chem. Commun.* 57, 6062–6065. doi:10.1039/d1cc01143j

Banert, K. (2016). The chemistry of unusually functionalized azides. *Synthesis* 48, 2361–2375. doi:10.1055/s-0035-1561454

Bao, R. L.-Y., Zhao, R., and Shi, L. (2015). Progress and developments in the turbo grignard reagent *i*-PrMgCl·LiCl: A ten-year journey. *Chem. Commun.* 51, 6884–6900. doi:10.1039/c4cc10194d

Bräse, S., and Banert, K. (2010). *Organic azides: Syntheses and applications*. Chichester: John Wiley and Sons, Ltd.

Chan, T. R., Hilgraf, R., Sharpless, K. B., and Fokin, V. V. (2004). Polytriazoles as copper(I)-Stabilizing ligands in catalysis. *Org. Lett.* 6, 2853–2855. doi:10.1021/ol0493094

Cho, J.-Y., Tse, M. K., Holmes, D., Maleczka, R. E., Jr, and Smith, M. R., III (2002). Remarkably selective iridium catalysts for the elaboration of aromatic C-H bonds. *Science* 295, 305–308. doi:10.1126/science.1067074

Dommerholt, J., Schmidt, S., Temming, R., Hendriks, L. J. A., Rutjes, F. P. J. T., van Hest, J. C. M., et al. (2010). Readily accessible bicyclononynes for bioorthogonal labeling and three-D imensional imaging of living cells. *Angew. Chem. Int. Ed.* 49, 9612–9615. doi:10.1002/ange.201003761

Ichinari, D., Ashikari, Y., Mandai, K., Aizawa, Y., Yoshida, J.-i., and Nagaki, A. (2020). A novel approach to functionalization of aryl azides through the generation and reaction of organolithium species bearing masked azides in flow microreactors. *Angew. Chem. Int. Ed.* 59, 1583–1587. doi:10.1002/ange.201912419

Inoue, A., Kitagawa, K., Shinokubo, H., and Oshima, K. (2001). Selective Halogen–Magnesium exchange reaction via organomagnesium ate complex. *J. Org. Chem.* 66, 4333–4339. doi:10.1021/jo015597v

Ishiyama, T., Takagi, J., Hartwig, J. F., and Miyaura, N. (2002). A stoichiometric aromatic C–H borylation catalyzed by iridium(I)/2,2'-Bipyridine complexes at room temperature. *Angew. Chem. Int. Ed.* 41, 3056–3058. doi:10.1002/1521-3773(20020816)41:16<3056::aid-anie3056>3.0.co;2-#

Krasovskiy, A., and Knochel, P. (2004). A LiCl-mediated Br/Mg exchange reaction for the preparation of functionalized aryl- and heteroarylmagnesium compounds from organic bromides. *Angew. Chem. Int. Ed.* 43, 3333–3336. doi:10.1002/anie.200454084

Li, Y., Gao, L.-X., and Han, F.-S. (2010). Reliable and diverse synthesis of aryl azides through copper-catalyzed coupling of boronic acids or esters with $TMSN_3$. *Chem. Eur. J.* 16, 7969–7972. doi:10.1002/chem.201000971

Meguro, T., Yoshida, S., and Hosoya, T. (2017). Aromatic azido-selective reduction via the staudinger reaction using tri-*n*-butylphosphonium tetrafluoroborate with triethylamine. *Chem. Lett.* 46, 473–476. doi:10.1246/cl.161159

Meguro, T., Yoshida, S., Igawa, K., Tomooka, K., and Hosoya, T. (2018). Transient protection of organic azides from click reactions with alkynes by phosphazide formation. *Org. Lett.* 20, 4126–4130. doi:10.1021/acs.orglett.8b01692

Meldal, M., and Tornøe, C. W. (2008). Cu-catalyzed Azide–Alkyne cycloaddition. *Chem. Rev.* 108, 2952–3015. doi:10.1021/cr0783479

Mkhalid, I. A. I., Barnard, J. H., Marder, T. B., Murphy, J. M., and Hartwig, J. F. (2010). C–H activation for the construction of C–B bonds. *Chem. Rev.* 110, 890–931. doi:10.1021/cr900206p

Ning, X., Guo, J., Wolfert, M. A., and Boons, G.-J. (2008). Visualizing metabolically labeled glycoconjugates of living cells by copper-free and fast huisgen cycloadditions. *Angew. Chem. Int. Ed.* 47, 2253–2255. doi:10.1002/anie.200705456

Nishiyama, Y., Misawa, Y., Hazama, Y., Oya, K., Yoshida, S., and Hosoya, T. (2019). Synthesis of diverse 3-Azido-5-(azidomethyl)benzene Derivatives via formal C–H azidation and functional group-selective transformations. *Heterocycles* 99, 1053–1072. doi:10.3987/com-18-s(f)72

Rostovtsev, V. V., Green, L. G., Fokin, V. V., and Sharpless, K. B. (2002). A stepwise huisgen cycloaddition process: Copper(I)-Catalyzed regioselective "ligation" of azides and terminal alkynes. *Angew. Chem. Int. Ed.* 41, 2596–2599. doi:10.1002/1521-3773(20020715)41:14<2596::aid-anie2596>3.0.co;2-4

Saxon, E., and Bertozzi, C. R. (2000). Cell surface engineering by a modified staudinger reaction. *Science* 287, 2007–2010. doi:10.1126/science.287.5460.2007

Shi, F., Waldo, J. P., Chen, Y., and Larock, R. C. (2008). Benzyne click chemistry: Synthesis of benzotriazoles from benzynes and azides. *Org. Lett.* 10, 2409–2412. doi:10.1021/ol800675u

Staudinger, H., and Meyer, J. (1919). Über neue organische Phosphorverbindungen III. Phosphinmethylenderivate und Phosphinimine. *Helv. Chim. Acta* 2, 635–646. doi:10.1002/hlca.19190020164

Tanimoto, H., and Kakiuchi, K. (2013). Recent applications and developments of organic azides in total synthesis of natural products. *Nat. Prod. Commun.* 8, 1021–1034. doi:10.1177/1934578x1300800730

Tornøe, C. W., Christensen, C., and Meldal, M. (2002). Peptidotriazoles on solid phase: [1,2,3]-Triazoles by regiospecific copper(I)-Catalyzed 1,3-Dipolar cycloadditions of terminal alkynes to azides. *J. Org. Chem.* 67, 3057–3064. doi:10.1021/jo011148j

Yoshida, S., Misawa, Y., and Hosoya, T. (2014). Formal C–H-Azidation-Based shortcut to Diazido building blocks for the versatile preparation of photoaffinity labeling probes. *Eur. J. Org. Chem.* 2014, 3991–3995. doi:10.1002/ejoc.201402516

Yoshida, S. (2020). Sequential conjugation methods based on triazole formation and related reactions using azides. *Org. Biomol. Chem.* 18, 1550–1562. doi:10.1039/c9ob02698c

frontiers | Frontiers in Chemistry

TYPE Original Research
PUBLISHED 01 September 2023
DOI 10.3389/fchem.2023.1254632

OPEN ACCESS

EDITED BY
Takashi Ohshima,
Kyushu University, Japan

REVIEWED BY
Tao Shi,
The Scripps Research Institute, United States
Matsubara Ryosuke,
Kobe University, Japan
Jin Kyoon Park,
Pusan National University, Republic of Korea

*CORRESPONDENCE
Sungwoo Hong,
hongorg@kaist.ac.kr

RECEIVED 07 July 2023
ACCEPTED 17 August 2023
PUBLISHED 01 September 2023

CITATION
Kim K, You E and Hong S (2023), Nucleophilic C4-selective (hetero) arylation of pyridines for facile synthesis of heterobiaryls.
Front. Chem. 11:1254632.
doi: 10.3389/fchem.2023.1254632

Nucleophilic C4-selective (hetero) arylation of pyridines for facile synthesis of heterobiaryls

Kewon Kim[1,2], Euna You[1,2] and Sungwoo Hong[1,2]*

[1]Department of Chemistry, Korea Advanced Institute of Science and Technology (KAIST), Daejeon, Republic of Korea, [2]Center for Catalytic Hydrocarbon Functionalizations, Institute for Basic Science (IBS), Daejeon, Republic of Korea

The synthesis of heterobiaryl compounds holds significant value in organic chemistry due to their extensive range of applications. Herein, we report a highly efficient strategy for conducting C4-selective (hetero) arylation of pyridines using *N*-aminopyridinium salts. The reaction proceeds readily at room temperature in the presence of a base, thus eliminating the requirement for catalysts or oxidants. This method allows for the installation of various electron-rich (hetero) aryl groups on pyridines, resulting in the streamlined synthesis of highly valuable C4-(hetero) aryl pyridine derivatives, which are otherwise challenging to acquire via conventional methods. This simple and straightforward method will facilitate access to a range of heterobiaryl compounds thereby promoting their application in various scientific disciplines.

KEYWORDS

C-H (hetero) arylation, pyridinium salt, C4-selectivity, heterobiaryl, metal-free

Introduction

Pyridine, a prominent component in the realms of agrochemicals, pharmaceuticals, and functional materials (Vitaku et al., 2014; Zhong, et al., 2014), is often a key constituent of *N*-heterobiaryl scaffolds due to their rigid and adaptable three-dimensional structures (Wu and Chan, 2006; Ghoteimi et al., 2023; Yang et al., 2016; Lee, H. et al., 2019; Jo, W. et al., 2020; Li, H. et al., 2021; Shao et al., 2021; Nguyen, N. H. et al., 2022; Takahashi, F., and Yorimitsu, H., 2023). These structures are frequently used in the fabrication of therapeutic agents or as ligands for metal catalyst complexes. For instance, LJH685, a selective RSK inhibitor, has been designed to treat triple-negative breast cancer (TNBC) (Cui et al., 2022), and Etoricoxib (Chauret et al., 2001), a selective cyclooxygenase-2 inhibitor, has been developed for its anti-inflammatory effects. As a result, the synthesis of arylated pyridine scaffolds has become a hot topic, with a majority of strategies employing transition metal catalysts (Li et al., 2014; Lee, D. et al., 2015; Zuo et al., 2015; Jiao et al., 2016; Lutz et al., 2016; Jia et al., 2018; Gu, X. et al., 2022). The Baran group, for example, introduced a Minisci-type Ag-catalyzed arylation of pyridine and other heteroarenes (Seiph et al., 2010) (Scheme 1A). In addition, modified versions of the Suzuki-Miyaura reaction using heteroaryl halides and Pd catalysts have been reported (Ichikawa et al., 2017) (Scheme 1B). However, despite their synthetic versatility, these methods demand high temperatures and exhibit limited functional group tolerance. The advent of photocatalyzed reactions utilizing diazonium salts (Bartolomeu et al., 2019) and diaryliodonium salts (Tobisu et al., 2013) as aryl radical precursors marked a significant advance (Scheme 1C). Although these reactions are achievable at room temperature, the poor site selectivity of pyridine continues to pose a challenge.

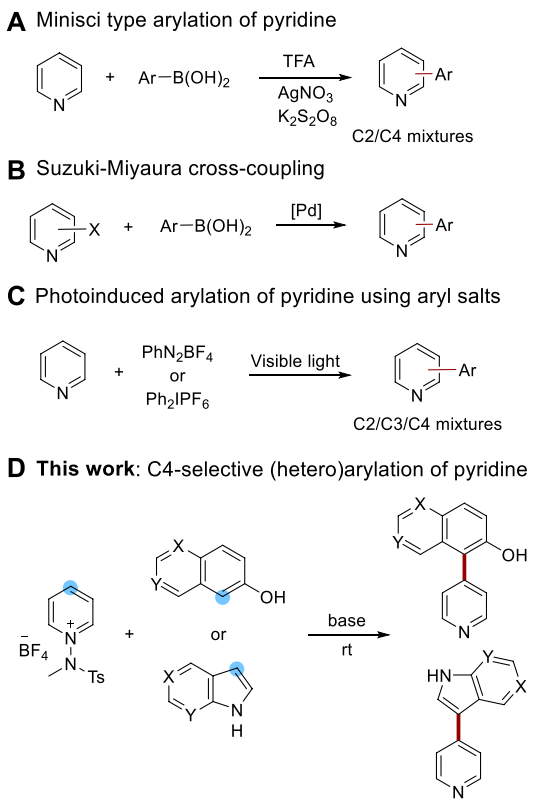

SCHEME 1
Synthetic approaches to (hetero) arylation of pyridine cores.

Recently, pyridinium salts have emerged as versatile synthetic tools for pyridine functionalization, delivering mild conditions and superior site selectivity (Kim et al., 2021; Shin et al., 2021; Choi et al., 2022; Kim et al., 2022a; Kim et al., 2022b; Kim et al., 2022c). As pyridine surrogates, *N*-substituted pyridinium salts have bolstered the development of numerous visible-light induced reactions where radicals are produced via photocatalysts or electron donor-acceptor (EDA) complex formations. These radicals initiate a hydrogen atom transfer (HAT) or react with unsaturated carbon species, giving rise to complex radical species that can be sequestered in the pyridinium salts (Kim et al., 2019; Lee et al., 2020; Mathi et al., 2020). Of particular interest is the site-selective functionalization controlled by the *N*-substituents attached to the pyridinium salts (Jung et al., 2019). Beyond radical pathways, two-electron pathways have also been investigated, with pyridine or other heteroarene salts acting as electrophiles, demonstrating impressive reactivity and site selectivity (Okamoto et al., 1963; Okamoto et al., 1966; Lemire et al., 2004; Donohoe et al., 2009; Chupakhin et al., 2017). While one reference exists on pyridine C4 selective arylation using Grignard reagents, there are inherent compatibility challenges with various functional groups during the arylation process. As a result, the substrate scope is constrained, with only a single example reported (Katritzky and Beltrami, 1979). Despite these advances, the direct cross-coupling of pyridinium salts with other (hetero) arenes under mild conditions is still an underexplored field. Motivated by the versatile reactivity and excellent selectivity of *N*-substituted pyridinium salts, we aimed to design a method for C4-selective (hetero) arylation of pyridine under mild reaction conditions. We hypothesized that electron-rich (hetero) arenes, such as indoles and naphthol, would undergo nucleophilic addition to electrophilic pyridinium salts, leading to the formation of *N*-(hetero) biaryl compounds incorporating pyridine. This new approach enables the synthesis of a variety of *N*-(hetero) biaryl building blocks, known to be invaluable scaffolds in the sphere of medicinal chemistry (Marchais-Oberwinkler et al., 2008; Guo et al., 2011; Tsuji, T. et al., 2020; Yuan et al., 2020; Chaudhary, 2021).

Result and discussion

First, we conducted a comprehensive screening of reaction conditions to facilitate the incorporation of an indole moiety onto pyridine, employing pyridinium salt **1a** and 5-methoxyindole **2a**. We assessed the efficiency of various organic and inorganic bases (Table 1, entries 1–5). Cs_2CO_3 failed to show any significant conversion, while DBU and NaO*t*Bu generated moderate yields. Notably, alongside the desired product **3b**, we also detected minor side product **N1**, which exhibited a bond formation between the nitrogen of the indole and the C4 position of the pyridine. Specifically, side product **3b′** resulted from an additional nucleophilic addition of the free N–H from the desired product, **3b**, to another pyridinium salt. When a stronger base, NaH, was used, the yield of the desired product **3b** was slightly improved. Prior research has suggested that the choice of base cation can affect the reactivity and selectivity (Kobayashi et al., 2015; Chen and Wu, 2017). To investigate the potential influence of base cations on our reaction, we further scrutinized various *tert*-butoxide species with differing cations, due to the similar conversion but milder basicity of NaO*t*Bu in comparison with NaH (entries 5 and 6). Remarkably, LiO*t*Bu yielded a result similar to NaO*t*Bu but demonstrated significantly superior selectivity for the indole C3 position. Subsequently, we explored the effects of ratio of **2a** and LiO*t*Bu (entries 7–13). A lower base quantity resulted in a decreased yield, and it was concluded that an optimal condition involved the use of 2.0 equiv of base (entry 10). When 2.0 equiv of **2a** was used, the yield significantly improved (entry 13). This enhancement can be attributed to the unfavorable formation of **3b′** in the presence of excess **2a**. Additionally, we evaluated other solvents with varying polarities, but DMSO proved to be superior (entries 14 and 15). Without the base, the reaction did not proceed (entry 16). Considering these optimization results, we selected entry 13 as the optimal condition for the introduction of the indole group at the pyridine C4 position.

Utilizing the optimized conditions for heteroarylations, we explored the scope of the reaction by including various functional groups on indoles (Table 2). The reactions showed consistent performance across a variety of indoles, from simple indoles to those substituted with electron-donating groups, such as methoxy, and methyl groups (**3a**–**3e**). Various halogen groups, spanning from iodo to fluoro, resulted in satisfactory conversions in the reaction (**3f**–**3i**). Electron-withdrawing groups, including nitro (**3j**), cyano (**3k**), amide (**3l**), and aldehyde (**3m**) groups, were successfully accommodated under the reaction conditions, leading to good conversions. Remarkably, even in the presence of a strong base, the hydroxyl group (**3n**) yielded a significant output. We also tested azaindole (**3o**) and pyrrolopyrimidine (**3p**), both of which are common derivatives of indoles found in medicinal chemistry.

10.3389/fchem.2023.1254632

TABLE 1 Optimization of reaction conditions.[a]

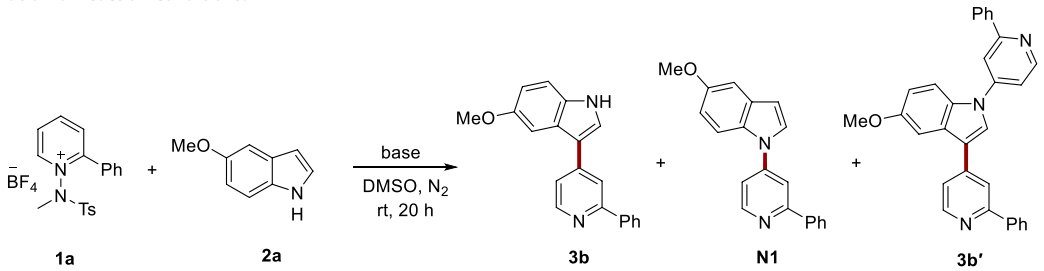

1a **2a** **3b** **N1** **3b′**

Entry	**1a** (equiv)	**2a** (equiv)	Base (equiv)	Yield[b] (**3b/N1/3b′**) (%)
1	1.5	1.0	Cs_2CO_3 (2.0)	trace/trace/trace
2	1.5	1.0	NaO*t*Bu (2.0)	48/17/9
3	1.5	1.0	DBU (2.0)	38/trace/trace
4	1.5	1.0	NaH (2.0)	51/13/12
5	1.5	1.0	KO*t*Bu (2.0)	26/9/5
6	1.5	1.0	LiO*t*Bu (2.0)	48/3/7
7	1.0	1.0	LiO*t*Bu (1.2)	46/6/4
8	1.0	1.0	LiO*t*Bu (1.5)	49/5/4
9	1.0	1.0	LiO*t*Bu (1.8)	55/5/5
10	1.0	1.0	LiO*t*Bu (2.0)	57/5/4
11	1.0	1.0	LiO*t*Bu (2.5)	55/4/4
12	1.0	1.5	LiO*t*Bu (2.0)	73/8/trace
13	**1.0**	**2.0**	**LiO*t*Bu (2.0)**	**82/8/trace**
14[c]	1.0	2.0	LiO*t*Bu (2.0)	18/2/trace
15[d]	1.0	2.0	LiO*t*Bu (2.0)	trace/trace/trace
16	1.0	2.0	no base	trace/trace/trace

Entry 13 was selected as an optimal condition.

[a]Reaction conditions: **1a** or **2a** was used as a limiting reagent (0.1 mmol for 1.0 equiv) in DMSO (1.0 mL) under N_2 atmosphere at rt for 20 h.

[b]NMR, yields were measured with the caffeine as an internal standard.

[c]DMF, was used instead of DMSO.

[d]THF, was used instead of DMSO.

Pleasingly, the reactions proceeded well, highlighting the applicability of this method for the synthesis of these vital indole derivatives.

Subsequently, we systematically evaluated a series of pyridinium salts with diverse substituents to examine their reactivity and suitability with the established reaction conditions. The utilization of unsubstituted pyridinium salts resulted in comparatively lower yields (**3q**) than when 2-substituted pyridinium salts were used. When pyridinium salts carried an aryl substituent, the reaction progressed efficiently, suggesting that the aryl group present on the pyridinium salts enhances the reaction (**3r**–**3t**). The incorporation of other aryl groups, such as thiophene (**3u**) and pyridine (**3v**), into the pyridinium salt successfully yielded the corresponding products. We found that the reaction proceeded successfully when using C2-ester pyridinium salt **3w**. Additionally, we expanded the applicability of our method by facilitating reactions with quinolinium salt (**3x**). When we used a pyridinium salt derived from a pharmaceutical compound, vismodegib, the reaction produced the desired product **3y** in 40% yield.

We discovered that 2-naphthol could be effectively installed at the C4 position of pyridine in the presence of a base. Following the screening of reaction conditions using pyridinium salt **1a** and 2-naphthol **4a** as model substrates, we identified an optimized reaction condition that led to high conversion yields towards compound **5a** (see Supplementary Table S1 for details). In the naphthol scope (Table 3), we noted a promising tolerance towards a variety of functional groups. The reaction progressed smoothly for substrates containing electron-donating groups such as methyl and methoxy groups (**5a**–**5e**). Halogen groups, including bromo (**5f**), chloro (**5g**), and fluoro (**5h**), were also compatible with the reaction conditions. Furthermore, electron-withdrawing groups, like cyano, amide, ester, ketone, and aldehyde groups, resulted in excellent conversion (**5i**–**5m**). The nucleophilic alcohol group also showed favorable conversion (**5n**). Motivated by this broad functional group tolerance, we extended our investigation to other heteroarenes as naphthol derivatives (**5o**–**5r**). Pleasingly,

10.3389/fchem.2023.1254632

TABLE 2 Nucleophilic heteroarylation of pyridine with indoles.[a]

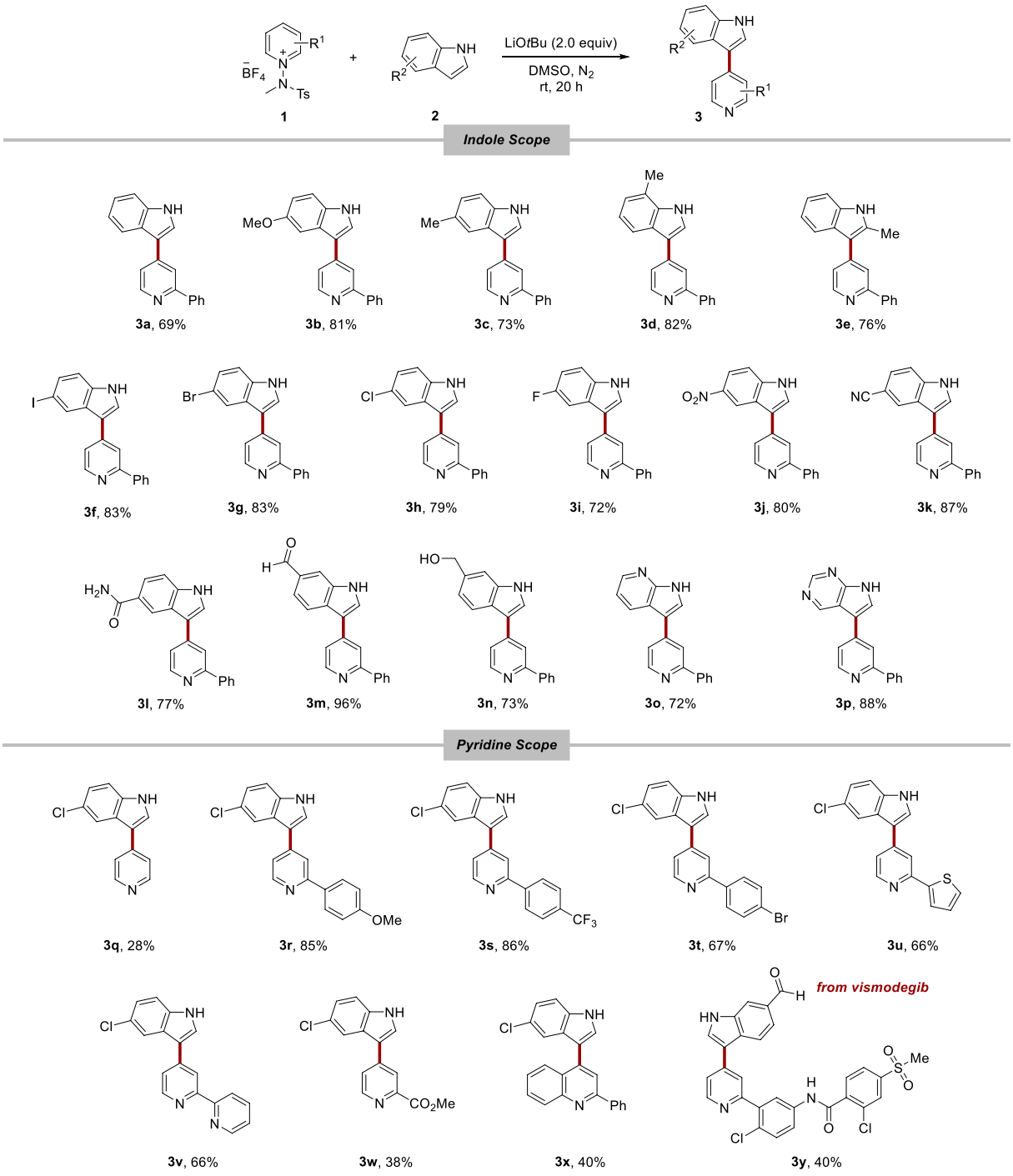

[a]Reaction conditions: **1** (0.1 mmol), **2** (2.0 equiv) and LiO*t*Bu (2.0 equiv) in DMSO (1.0 mL) under N_2 atmosphere at rt for 20 h. Isolated yields.

the reactions involving quinoline (**5o**), isoquinoline (**5p**), and benzothiophene (**5r**) proceeded well. However, benzofuran (**5q**) exhibited lower compatibility with the reaction conditions. Within the pyridine scope, improved conversion was observed with pyridine salts bearing a phenyl group compared to simple pyridine salts (**5s**–**5v**). Pyridinium salts substituted with thiophene (**5w**) and pyridine (**5x**) resulted in high conversions. Pleasingly, excellent yields were observed with the pyridinium salt carrying an ester group (**5y**) and the quinolinium salt (**5z**). Furthermore, a promising conversion was demonstrated when using the pyridinium salt derived from vismodegib (**5aa**), indicating the efficiency of this method in introducing a naphthol moiety even in the late stage of complex, pyridine-containing molecules.

10.3389/fchem.2023.1254632

TABLE 3 Nucleophilic arylation of pyridine with 2-naphthols.[a]

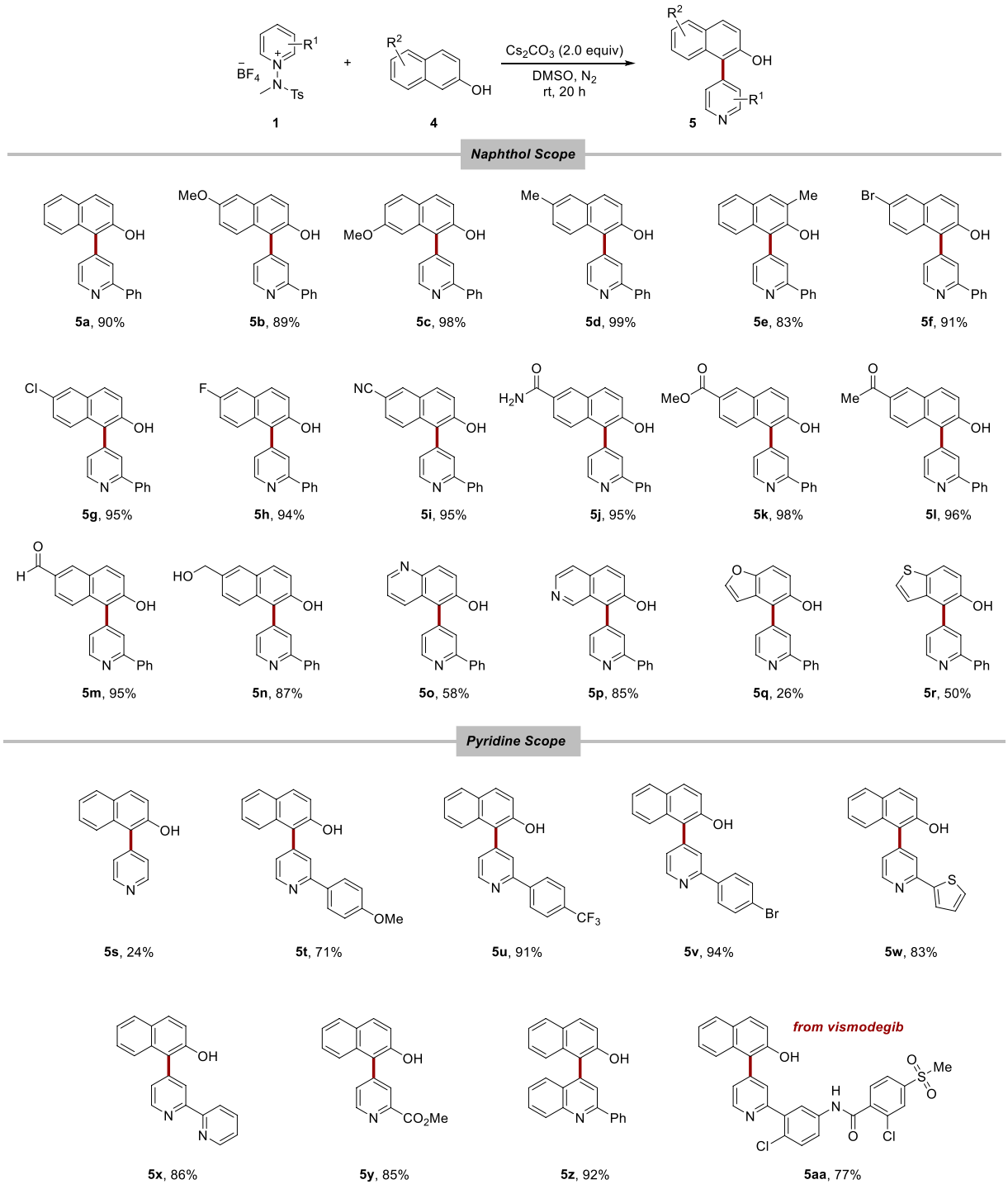

[a]Reaction conditions: **1** (1.5 equiv), **4** (0.1 mmol), and Cs_2CO_3 (2.0 equiv) in DMSO (1.0 mL) under N_2 atmosphere at rt for 20 h. Isolated yields.

To further elucidate the reaction mechanism, we conducted several control experiments. When the hydroxyl group of 2-naphthol was protected with an acyl group, the desired product was not observed, implying that the deprotonation of the hydroxyl group is a critical step (Scheme 2A). Blocking the C1 position of 2-naphthol with a methyl group halted the reaction. This evidence, together with the synthesis of **5e**, distinctly indicates that under the optimal reaction conditions, the most reactive site of 2-naphthol towards the pyridinium salt is the C1 position (Scheme 2B). In the context of indoles, when *N*-methylated indole was used as a

10.3389/fchem.2023.1254632

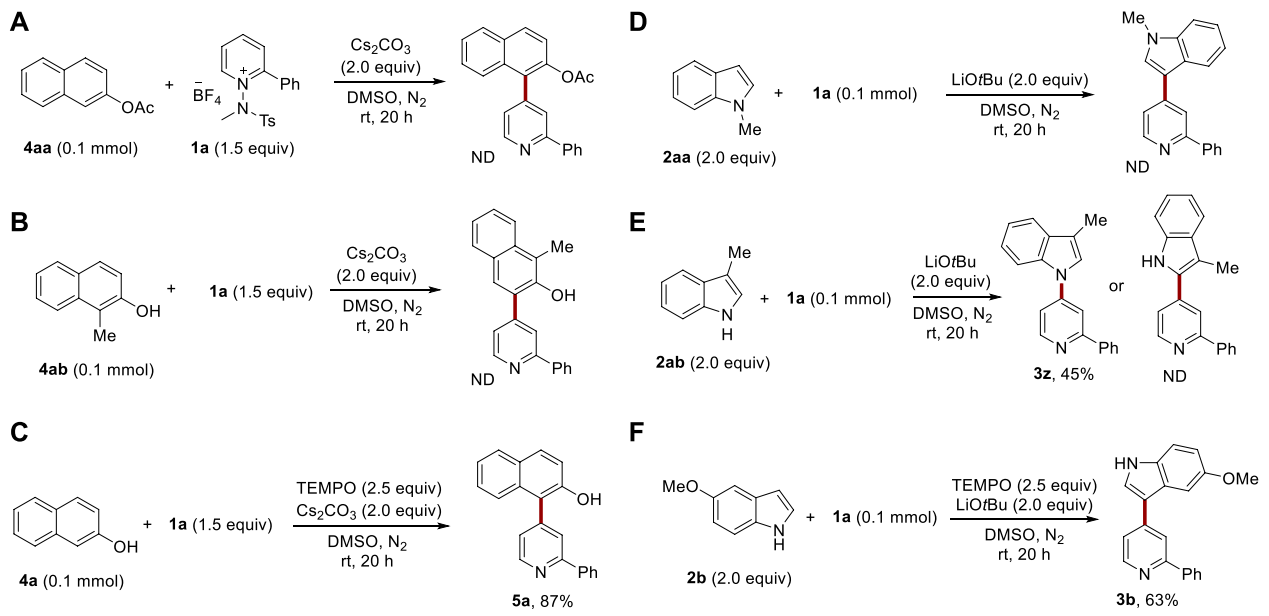

SCHEME 2
Mechanistic studies.

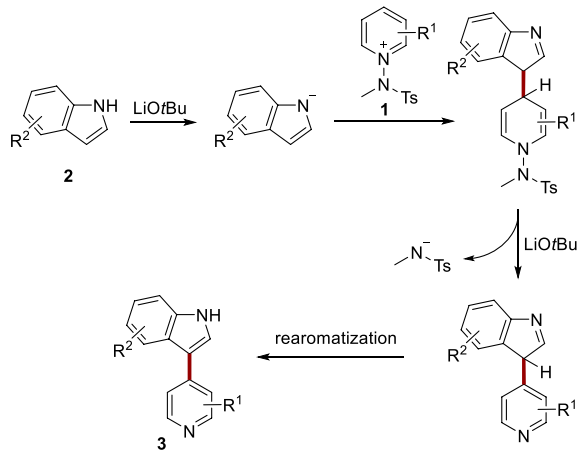

SCHEME 3
Proposed reaction mechanisms.

substrate, no reaction was observed, highlighting that a free N–H is vital for the reaction to proceed (Scheme 2D). When the C3 position of indole was blocked, the only significant product observed was **3z**, which resulted from the nucleophilic attack of nitrogen from **2ab** on the pyridinium salt (Scheme 2E). The addition of a radical scavenger, (2,2,6,6-tetramethylpiperidine-1-oxyl) (TEMPO) did not inhibit reactivity, suggesting that the reaction proceeded via an ionic pathway (Schemes 2C, F).

Given the experimental evidence, a plausible reaction mechanism for the arylation of pyridine with indole is depicted in Scheme 3. The reaction commences with the base-induced deprotonation of indole, followed by nucleophilic addition to the pyridinium salt **1**. This addition is succeeded by the base-assisted aromatization of the pyridine moiety, leading to the release of a tosyl amine anion. Intriguingly, this anionic tosyl amine could potentially function as a base for the rearomatization of indole. Upon completion of the reaction, the reaction mixture is subjected to mild acidic workup, leading to the formation of the desired product **3**. A similar pathway is expected for naphthol and is outlined in Supplementary Scheme S1.

Conclusion

In summary, we have developed a mild and selective nucleophilic (hetero) arylation of pyridine with exclusive C4 selectivity at the pyridine ring. This method employs *N*-aminopyridinium salts as electrophiles, enabling the facile and efficient synthesis of (hetero) arylated pyridine derivatives incorporating a wide range of aromatic functionalities. With the assistance of a base, indoles, naphthols, and their respective heteroarene derivatives can undergo nucleophilic addition onto the pyridine, eliminating the need for additional protection or deprotection steps. Interestingly, these nucleophilic (hetero) arenes exhibit unique and selective reactivity when engaging with the pyridinium salt. This selective behavior allows for meticulous control over the regiochemistry of the arylation reaction, facilitating the introduction of (hetero) aryl groups at the C4 position of pyridine. Given the observed extensive functional group tolerance, the developed protocols have the potential to yield a vast array of heterobiaryl scaffolds, which are indispensable building blocks in medicinal chemistry. These insights will contribute to the ongoing evolution of synthetic methods, simultaneously unlocking new possibilities for the discovery and development of innovative pharmaceutical compounds.

Data availability statement

The original contributions presented in the study are included in the article/Supplementary Material, further inquiries can be directed to the corresponding author.

Author contributions

KK: Investigation, Methodology, Writing–original draft, Writing–review and editing. EY: Investigation, Methodology, Writing–review and editing. SH: Conceptualization, Funding acquisition, Project administration, Resources, Supervision, Visualization, Writing–original draft, Writing–review and editing.

Funding

This research was supported financially by Institute for Basic Science (IBS-R010-A2).

Conflict of interest

The authors declare that the research was conducted in the absence of any commercial or financial relationships that could be construed as a potential conflict of interest.

Publisher's note

All claims expressed in this article are solely those of the authors and do not necessarily represent those of their affiliated organizations, or those of the publisher, the editors and the reviewers. Any product that may be evaluated in this article, or claim that may be made by its manufacturer, is not guaranteed or endorsed by the publisher.

Supplementary material

The Supplementary Material for this article can be found online at: https://www.frontiersin.org/articles/10.3389/fchem.2023.1254632/full#supplementary-material

References

Bartolomeu, A. A., Silva, R. C., Brocksom, T. J., Noel, T., and de Oliveira, K. T. (2019). Photoarylation of pyridines using aryldiazonium salts and visible light: An EDA approach. *J. Org. Chem.* 84, 10459–10471. doi:10.1021/acs.joc.9b01879

Chaudhary, A. (2021). Recent development in the synthesis of heterocycles by 2-naphthol-based multicomponent reactions. *Mol. Divers.* 25, 1211–1245. doi:10.1007/s11030-020-10076-4

Chauret, N., Yergey, J. A., Brideau, C., Friesen, R. W., Mancini, J., Riendeau, D., et al. (2001). *In vitro* metabolism considerations, including activity testing of metabolites, in the discovery and selection of the COX-2 inhibitor Etoricoxib (MK-0663). *Bioorg. Med. Chem. Lett.* 11, 1059–1062. doi:10.1016/s0960-894x(01)00135-4

Chen, J., and Wu, J. (2017). Transition-metal-free C3 arylation of indoles with aryl halides. *Angew. Chem. Int. Ed.* 56, 3951–3955. doi:10.1002/anie.201612311

Choi, W., Kim, M., Lee, K., Park, S., and Hong, S. (2022). C4-Selective C–H borylation of pyridinium derivatives driven by electron donor-acceptor complexes. *Org. Lett.* 24, 9452–9457. doi:10.1021/acs.orglett.2c03882

Chupakhin, O. N., Shchepochkin, A. V., and Charushin, V. N. (2017). Atom- and step-economical nucleophilic arylation of azaaromatics via electrochemical oxidative cross C–C coupling reactions. *Green Chem.* 19, 2931–2935. doi:10.1039/c7gc00789b

Cui, Y. M., Li, W., Shen, T. Z., Tao, Y. X., Liu, B. Q., Li, X. L., et al. (2022). Design, synthesis and anti-breast cancer evaluation of biaryl pyridine analogues as potent RSK inhibitors. *Bioorg. Med. Chem. Lett.* 59, 128565. doi:10.1016/j.bmcl.2022.128565

Donohoe, T. J., Connolly, M. J., and Walton, L. (2009). Regioselective nucleophilic addition to pyridinium salts: A new route to substituted dihydropyridones. *Org. Lett.* 11, 5562–5565. doi:10.1021/ol902402v

Ghoteimi, R., Braka, A., Rodriguez, C., Cros-Perrial, E., Duvauchelle, V., Uttaro, J. P., et al. (2023). Second-generation CD73 inhibitors based on a 4,6-Biaryl-2-thiopyridine scaffold. *ChemMedChem* 18, e202200594. doi:10.1002/cmdc.202200594

Gu, X., Liu, K., Yang, L., Xie, C., Li, M., and Wang, J. J. (2022). Nickel-catalyzed enantioselective alpha-heteroarylation of ketones via C–F bond activation to construct all-carbon quaternary stereocenters. *Chem. Sci.* 13, 12498–12502. doi:10.1039/d2sc03409c

Guo, P., Joo, J. M., Rakshit, S., and Sames, D. (2011). C–H arylation of pyridines: High regioselectivity as a consequence of the electronic character of C–H bonds and heteroarene ring. *J. Am. Chem. Soc.* 133, 16338–16341. doi:10.1021/ja206022p

Ichikawa, T., Netsu, M., Mizuno, M., Mizusaki, T., Takagi, Y., Sawama, Y., et al. (2017). Development of a unique heterogeneous palladium catalyst for the suzuki-miyaura reaction using (Hetero)aryl chlorides and chemoselective hydrogenation. *Adv. Synth. Catal.* 359, 2269–2279. doi:10.1002/adsc.201700156

Jia, F., Yin, C., Zeng, Y., Sun, R., Ge, Y. C., Xu, D., et al. (2018). Mechanism of direct C–H arylation of pyridine via a transient activator strategy: A combined computational and experimental study. *J. Org. Chem.* 83, 10389–10397. doi:10.1021/acs.joc.8b01480

Jiao, J., Murakami, K., and Itami, K. (2016). Palladium-catalyzed C–H arylation of pyridines with aryl triflates. *Chem. Lett.* 45, 529–531. doi:10.1246/cl.160133

Jo, W., Baek, S. Y., Hwang, C., Heo, J., Baik, M. H., and Cho, S. H. (2020). ZnMe2-Mediated, direct alkylation of electron-deficient N-heteroarenes with 1,1-diborylalkanes: Scope and mechanism. *J. Am. Chem. Soc.* 142, 13235–13245. doi:10.1021/jacs.0c06827

Jung, S., Lee, H., Moon, Y., Jung, H.-Y., and Hong, S. (2019). Site-selective C–H acylation of pyridinium derivatives by photoredox catalysis. *ACS Catal.* 9, 9891–9896. doi:10.1021/acscatal.9b03367

Katritzky, A. R., Beltrami, H., and Sammers, M. P. (1979). Preparation of 4-aryl-ad 4-Heteroaryl-pyridines: Regiospecific nucleophilic attack γ to a quaternaryl nitrogen atom. *J. Chem. Soc. Chem. Commun.* 137. doi:10.1039/C39790000137

Kim, C., Jeong, J., Vellakkaran, M., and Hong, S. (2022a). Photocatalytic decarboxylative pyridylation of carboxylic acids using in situ-generated amidyl radicals as oxidants. *ACS Catal.* 12, 13225–13233. doi:10.1021/acscatal.2c04417

Kim, M., Koo, Y., and Hong, S. (2022b). N-functionalized pyridinium salts: A new chapter for site-selective pyridine C–H functionalization via radical-based processes under visible light irradiation. *Acc. Chem. Res.* 55, 3043–3056. doi:10.1021/acs.accounts.2c00530

Kim, M., Shin, S., Koo, Y., Jung, S., and Hong, S. (2022c). Regiodivergent conversion of alkenes to branched or linear alkylpyridines. *Org. Lett.* 24, 708–713. doi:10.1021/acs.orglett.1c04156

Kim, M., You, E., Park, S., and Hong, S. (2021). Divergent reactivity of sulfinates with pyridinium salts based on one-versus two-electron pathways. *Chem. Sci.* 12, 6629–6637. doi:10.1039/d1sc00776a

Kim, N., Lee, C., Kim, T., and Hong, S. (2019). Visible-light-induced remote C(sp3)–H pyridylation of sulfonamides and carboxamides. *Org. Lett.* 21, 9719–9723. doi:10.1021/acs.orglett.9b03879

Kobayashi, S., Yoo, W.-J., Nguyen, V. Q., and Guiteras Capdevila, M. (2015). Lithium tert-butoxide-mediated carboxylation reactions of unprotected indoles and pyrroles with carbon dioxide. *Heterocycles* 90, 1196–1204. doi:10.3987/com-14-s(k)94

Lee, D. J., Ko, D., and Yoo, E. J. (2015). Rhodium(II)-Catalyzed cycloaddition reactions of non-classical 1,5-dipoles for the formation of eight-membered heterocycles. *Angew. Chem. Int. Ed.* 54, 13715–13718. doi:10.1002/anie.201506764

Lee, H. E., Lee, M. J., and Park, J. K. (2019). Rapid base- and metal-free oxidative C-H cyclization for the synthesis of benzo[4,5]imidazo[1,2-a]pyridine derivatives. *Asian J. Org. Chem.* 8, 1659–1663. doi:10.1002/ajoc.201900347

Lee, K., Lee, S., Kim, N., Kim, S., and Hong, S. (2020). Visible-light-enabled trifluoromethylative pyridylation of alkenes from pyridines and triflic anhydride. *Angew. Chem. Int. Ed.* 59, 13379–13384. doi:10.1002/anie.202004439

Lemire, A., Grenon, M., Pourashraf, M., and Charette, A. B. (2004). Nucleophilic addition to 3-substituted pyridinium salts: Expedient syntheses of (-)-L-733,061 and (-)-CP-99,994. *Org. Lett.* 6, 3517–3520. doi:10.1021/ol048624n

Li, H., Tang, X., Pang, J. H., Wu, X., Yeow, E. K. L., Wu, J., et al. (2021). Polysulfide anions as visible light photoredox catalysts for aryl cross-couplings. *J. Am. Chem. Soc.* 143, 481–487. doi:10.1021/jacs.0c11968

Li, Y., Liu, W., and Kuang, C. (2014). Direct arylation of pyridines without the use of a transition metal catalyst. *Chem. Commun.* 50, 7124–7127. doi:10.1039/c4cc02546f

Lutz, J. P., Chau, S. T., and Doyle, A. G. (2016). Nickel-catalyzed enantioselective arylation of pyridine. *Chem. Sci.* 7, 4105–4109. doi:10.1039/c6sc00702c

Marchais-Oberwinkler, S., Kruchten, P., Frotscher, M., Ziegler, E., Neugebauer, A., Bhoga, U., et al. (2008). Substituted 6-Phenyl-2-naphthols. Potent and selective nonsteroidal inhibitors of 17β-hydroxysteroid dehydrogenase type 1 (17β-HSD1): Design, synthesis, biological evaluation, and pharmacokinetics. *J. Med. Chem.* 51, 4685–4698. doi:10.1021/jm800367k

Mathi, G. R., Jeong, Y., Moon, Y., and Hong, S. (2020). Photochemical carbopyridylation of alkenes using N-alkenoxypyridinium salts as bifunctional reagents. *Angew. Chem. Int. Ed.* 59, 2049–2054. doi:10.1002/anie.201913320

Nguyen, N. H., Oh, S. M., Park, C. M., and Shin, S. (2022). Ortho-selective C–H arylation of phenols with N-carboxyindoles under brønsted acid- or Cu(I)-Catalysis. *Chem. Sci.* 13, 1169–1176. doi:10.1039/d1sc06157g

Okamoto, T., Hirobe, M., Mizushima, C., and Ohsawa, A. (1963). Reaction of N-aminopyridinium derivatives. II. The reactions of 1-(N-acylalkylamino) pyridinium salt derivatives with cyanide ion, A new synthesis of primary amines. *Chem. Pharm. Bull.* 11, 780–785. doi:10.1248/cpb.11.780

Okamoto, T., Hirobe, M., and Ohsawa, A. (1966). Reaction of N-aminopyridinium derivatives. V. Syntheses of 1-(N-methylacetamido) alkylpyridinium salts and their reaction with cyanide ion. *Chem. Pharm. Bull.* 14, 518–523. doi:10.1248/cpb.14.518

Seiph, I. B., Su, S., Rodriguez, R. A., Fujiwara, Y., Sobel, A. L., Baran, P. S., et al. (2010). Direct C–H arylation of electron-deficient heterocycles with arylboronic acids. *J. Am. Chem. Soc.* 132, 13194–13196. doi:10.1021/ja1066459

Shao, Y.-D., Han, D.-D., Dong, M.-M., Yang, X.-R., and Cheng, D.-J. (2021). A one-pot stepwise approach to axially chiral quinoline-3-carbaldehydes enabled by iminium–allenamine cascade catalysis. *Org. Chem. Front.* 8, 605–612. doi:10.1039/d0qo01339k

Shin, S., Lee, S., Choi, W., Kim, N., and Hong, S. (2021). Visible-light-induced 1,3-aminopyridylation of [1.1.1]Propellane with N-aminopyridinium salts. *Angew. Chem. Int. Ed.* 60, 7873–7879. doi:10.1002/anie.202016156

Takahashi, F., and Yorimitsu, H. (2023). Stereoselective synthesis of tetraarylethylenes enabled by reductive anti-1,2-dimetallation of alkynes. *Chem. Eur. J.* 29, e202203988. doi:10.1002/chem.202203988

Tobisu, M., Furukawa, T., and Chatani, N. (2013). Visible light-mediated direct arylation of arenes and heteroarenes using diaryliodonium salts in the presence and absence of a photocatalyst. *Chem. Lett.* 42, 1203–1205. doi:10.1246/cl.130547

Tsuji, T., Tanaka, T., Tanaka, T., Yazaki, R., and Ohshima, T. (2020). Catalytic Aerobic Cross-Dehydrogenative Coupling of Azlactones en Route to α,α-Disubstituted α-Amino Acids. *Org. Lett.* 22, 4164–4170. doi:10.1021/acs.orglett.0c01248

Vitaku, E., Smith, D. T., and Njardarson, J. T. (2014). Analysis of the structural diversity, substitution patterns, and frequency of nitrogen heterocycles among U.S. FDA approved pharmaceuticals. *J. Med. Chem.* 57, 10257–10274. doi:10.1021/jm501100b

Wu, J., and Chan, A. S. C. (2006). P-phos: A family of versatile and effective atropisomeric dipyridylphosphine ligands in asymmetric catalysis. *Acc. Chem. Res.* 39, 711–720. doi:10.1021/ar0680015

Yang, C., Mehmood, F., Lam, T. L., Chan, S. L., Wu, Y., Yeung, C. S., et al. (2016). Stable luminescent iridium(III) complexes with bis(N-heterocyclic carbene) ligands: Photo-stability, excited state properties, visible-light-driven radical cyclization and CO2 reduction, and cellular imaging. *Chem. Sci.* 7, 3123–3136. doi:10.1039/c5sc04458h

Yuan, S., Chang, J., and Yu, B. (2020). Construction of biologically important biaryl scaffolds through direct C–H bond activation: Advances and prospects. *Top. Curr. Chem.* 378, 23. doi:10.1007/s41061-020-0285-9

Zhong, M., Peng, E., Huang, N., Huang, Q., Huq, A., Lau, M., et al. (2014). Discovery of functionalized bisimidazoles bearing cyclic aliphatic-phenyl motifs as HCV NS5A inhibitors. *Bioorg. Med. Chem. Lett.* 24, 5731–5737. doi:10.1016/j.bmcl.2014.10.057

Zuo, X., Wu, W., and Su, W. (2015). Visible-light photoredox catalysis:direct arylation of elec-tron-deficient heterocycles and arenes with aryl diazonium salts. *Acta Chim. Sin.* 73, 1298–1301. doi:10.6023/A15040284

frontiers | Frontiers in Chemistry

TYPE Original Research
PUBLISHED 19 September 2023
DOI 10.3389/fchem.2023.1251299

OPEN ACCESS

EDITED BY
Takashi Ohshima,
Kyushu University, Japan

REVIEWED BY
Rajendra Rohokale,
University of Florida, United States
Tao Shi,
The Scripps Research Institute, United States
Hiroyuki Morimoto,
Kyushu Institute of Technology, Japan

*CORRESPONDENCE
Yoshiharu Iwabuchi,
y-iwabuchi@tohoku.ac.jp

RECEIVED 01 July 2023
ACCEPTED 22 August 2023
PUBLISHED 19 September 2023

CITATION
Kuriyama Y, Sasano Y and Iwabuchi Y (2023), Azetidine synthesis by La(OTf)$_3$-catalyzed intramolecular regioselective aminolysis of *cis*-3,4-epoxy amines. *Front. Chem.* 11:1251299. doi: 10.3389/fchem.2023.1251299

Azetidine synthesis by La(OTf)$_3$-catalyzed intramolecular regioselective aminolysis of *cis*-3,4-epoxy amines

Yuse Kuriyama, Yusuke Sasano and Yoshiharu Iwabuchi*

Department of Organic Chemistry, Graduate School of Pharmaceutical Sciences, Tohoku University, Sendai, Japan

Azetidine is a prevalent structural motif found in various biologically active compounds. In this research paper, we report La(OTf)$_3$-catalyzed intramolecular regioselective aminolysis of *cis*-3,4-epoxy amines to afford azetidines. This reaction proceeded in high yields even in the presence of acid-sensitive and Lewis basic functional groups.

KEYWORDS

azetidine, epoxide, catalytic reaction, regioselectivity, cyclization, Lewis acid, synthetic methods

1 Introduction

Arranging specific polar functional groups in three-dimensional space is a basic strategy for imparting a specific bioactive function to organic molecules and is universally found in nature and used in medicinal chemistry. The regioselective nucleophilic ring opening of epoxides is an efficient strategy for constructing contiguous chiral centers, and many methods have been developed to achieve this reaction (Caron and Sharpless, 1985; Faiz and Zahoor, 2016; Wang, 2017; Rodríguez-Berríos et al., 2023). Aminolysis of epoxides is a useful reaction for the synthesis of sterically complex nitrogen-containing compounds such as alkaloids. However, the regioselective aminolysis of epoxides poses a significant challenge, especially when Lewis and Brønsted acid promoters are used as catalysts. This is because the acid added to activate the epoxide is usually quenched by the high basicity of amine nucleophiles.

In the course of our study on the total synthesis of biologically active natural products (Uesugi et al., 2015), our research group discovered that lanthanoid (III) trifluoromethanesulfonate (Ln(OTf)$_3$) functions as an excellent catalyst for the regioselective nucleophilic ring opening of epoxides, which led us to exploit the synthetic use of Ln(OTf)$_3$ as a catalyst for epoxide ring-opening reactions. Thus, we have demonstrated that a catalytic amount of europium (III) trifluoromethanesulfonate (Eu(OTf)$_3$) enables the introduction of alcohols and thiols, as well as aryl and aliphatic amines, onto the C3 position of 2,3-epoxy alcohols with high regioselectivity (Scheme 1A) (Uesugi et al., 2014). Eu(OTf)$_3$ also efficiently catalyzed the C4-selective aminolysis of a 3,4-epoxy alcohol, the synthetic use of which was demonstrated by the efficient synthesis of the antipsychotic agent (+)-nemonapride (Uesugi et al., 2017). Furthermore, the lanthanum (III) trifluoromethanesulfonate (La(OTf)$_3$) catalyst induced anti-Baldwin 5-*endo*-*tet* cyclization of *trans*-3,4-epoxy amines via C4-selective intramolecular epoxide aminolysis to give 3-hydroxypyrrolidines in high yields (Scheme 1B) (Kuriyama et al., 2021). Interestingly, the La(OTf)$_3$ catalyst was found to promote the C3-selective intramolecular aminolysis of a *cis*-

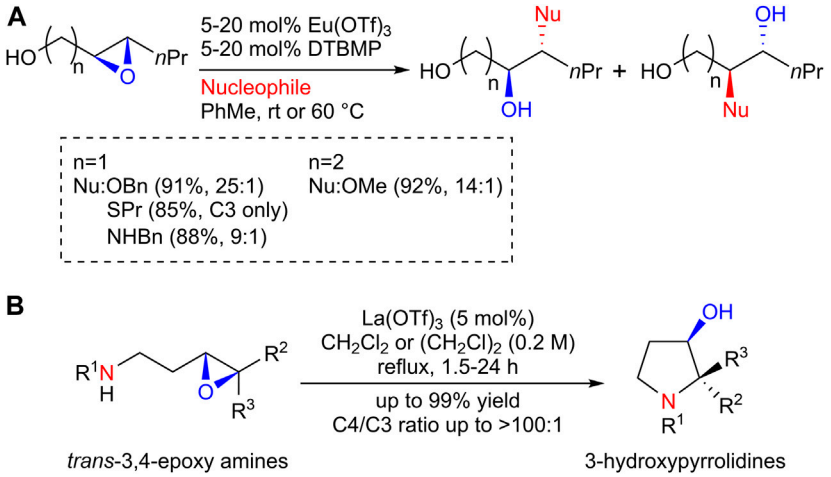

SCHEME 1
(A) Eu(OTf)$_3$-catalyzed regioselective ring-opening reaction of epoxy alcohols; **(B)** La(OTf)$_3$-catalyzed regioselective ring-opening reaction of *trans*-3,4-epoxy amines.

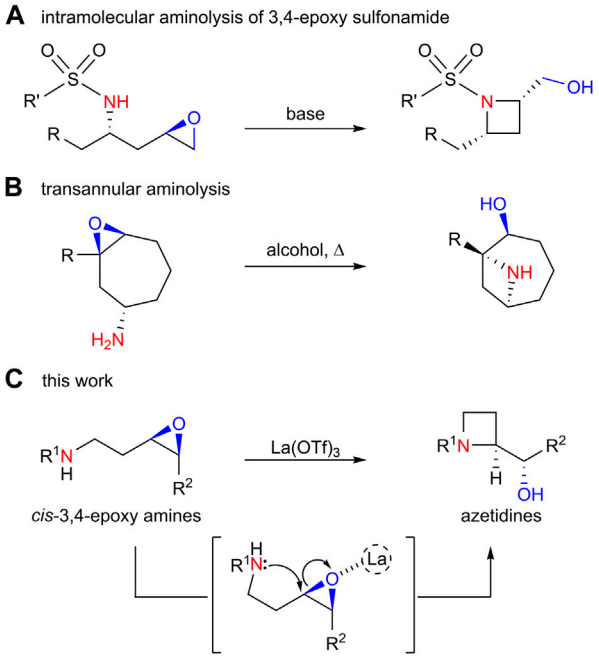

SCHEME 2
Azetidine syntheses by aminolysis reaction of epoxides; **(A)** intramolecular aminolysis of 3,4-epoxy sulfonamide; **(B)** transannular aminolysis; **(C)** this work.

3,4-epoxy amine to give an azetidine in high yield, which led to the development of a novel synthetic route for azetidines, as reported herein.

Azetidine is a structural motif found in various natural products and pharmaceuticals. This strained structure has encouraged synthetic chemists to develop strategies for the synthesis of azetidines (Hameed et al., 2017; Parmar et al., 2021; Yoda et al., 2011). Intramolecular S_N2 reactions are often used to form azetidine rings in which a nitrogen atom attacks a carbon atom connected to a leaving group [halogen (Betz et al., 2019; Rowe et al., 2019; Dherange et al., 2022), mesylate (Bose et al., 1994), *etc.*]. The intramolecular aminolysis of 3,4-epoxy amines could be an alternative method for constructing an azetidine ring with a carbonyl group adjacent to the azetidine ring, which could be a useful scaffold for further functionalization. However, such reactions have rarely been reported, except the intramolecular aminolysis of 3,4-epoxy sulfonamide (Scheme 2A) (Moulines et al., 1993; Breternitz and Schaumann, 1999; Medjahdi et al., 2009; Faigl et al., 2012) and transannular aminolysis of 3,4-epoxy amine (Scheme 2B) (Shimokawa et al., 2011; Shing and So, 2011; Wang et al., 2018; Hocine et al., 2023). To the best of our knowledge, the intramolecular aminolysis of an unprotected linear 3,4-epoxy amine (rather than amide) has not been reported before. Herein, we describe further investigations to clarify the optimum conditions and substrate scope for the La(OTf)$_3$-catalyzed highly regioselective 4-*exo*-*tet* cyclization of linear 3,4-epoxy amines to afford azetidines (Scheme 2C).

2 Materials and methods

2.1 General information

All reactions were carried out in an argon atmosphere with dehydrated solvents under anhydrous conditions unless otherwise noted. Dehydrated THF and CH_2Cl_2 were purchased from Kanto Chemical Co., Inc., and the other solvents were dehydrated and distilled according to standard protocols. Reagents were obtained from commercial suppliers and used without further purification unless otherwise noted.

Reactions were monitored by thin-layer chromatography (TLC) on 0.25 mm Merck silica gel plates (60F-254). Column chromatography was performed using Silica Gel 60N (Kanto Chemical Co., Inc., spherical, neutral, particle size 63–210 mm)

and NH-DM1020 (Fuji Silysia Chemical Ltd., spherical, particle size 100 μm); flash column chromatography was performed using Silica Gel 60N (Kanto Chemical Co., Inc., spherical, neutral, particle size 40–50 mm), unless otherwise noted.

Melting points were measured using a Yazawa BY-2 and Buchi M-565 and were uncorrected. Infrared (IR) spectra were obtained using a JASCO FT-IR-4600 instrument and are reported as wavenumbers. Proton nuclear magnetic resonance (^{1}H-NMR) spectra were recorded using a JEOL JMN-AL400 (400 MHz) and a JEOL ECA-600 (600 MHz) spectrometer. Chemical shift (δ) is reported in parts per million (ppm) downfield relative to tetramethyl silane (TMS; 0.0 ppm) in $CDCl_3$ and benzene (7.16 ppm) in C_6D_6. The coupling constants (J) are reported in Hz. Carbon-13 nuclear magnetic resonance (^{13}C-NMR) spectra were recorded on a JEOL JMN-AL400 (100 MHz) spectrometer. Chemical shifts are reported in ppm relative to the centerline of the triplet of $^{13}CDCl_3$ (77.0 ppm) and $^{13}C_6D_6$ (128.0 ppm). Low-resolution mass spectra (MS) were recorded on JEOL JMS-DX303, JMS-T100GC, and JEOL JMS-700 instruments. High-resolution mass spectra (HRMS) were recorded on JEOL JMS-T100GC and JEOL JMS-700 mass spectrometers using electron impact (EI) and on a Thermo Scientific Exactive Mass Spectrometer using electrospray ionization (ESI).

2.2 General procedure

2.2.1 Synthesis of *cis*-3,4-epoxy amines (1aa–1ka, 1ab and 1ac)

Et_3N (2.5 eq) and MsCl (1.5 eq) were added to a solution of epoxy alcohol (1 eq) in CH_2Cl_2 (0.5 M) at 0°C, and the mixture was stirred for 10 min at room temperature. Then, saturated aqueous $NaHCO_3$ was added to the mixture at 0°C, and the mixture was extracted thrice with CH_2Cl_2. The combined organic layers were dried over anhydrous $MgSO_4$, filtered, and concentrated under reduced pressure. The resulting crude product was used immediately in the subsequent reaction without further purification.

Alkyl amine (3.0 eq) and NaI (10 mol%) were added to a solution of the crude product in DMSO (0.5 M) at room temperature (ca. 25°C), and the mixture was stirred for 2 days at ambient temperature. The mixture was diluted with H_2O and extracted with Et_2O. The combined organic layers were washed thrice with brine, dried over anhydrous Na_2SO_4, filtered, and concentrated under reduced pressure. The resulting residue was purified using column chromatography to yield the corresponding epoxy amines.

2.2.2 Synthesis of *cis*-3,4-epoxy anilines (1la–1na)

A pre-mixed solution of $NaOCl{\cdot}5H_2O$ (1.5 eq) in saturated aqueous NaHCO was added dropwise to a cooled and well-stirred mixture of epoxy alcohol (1.0 eq) and TEMPO (1 mol%) in CH_2Cl_2 (0.2 M) and saturated aqueous $NaHCO_3$ containing KBr (10 mol%), and the resulting mixture was stirred for 10 min at 0°C. Then, saturated aqueous $Na_2S_2O_3$ was added at 0°C, and the mixture was extracted with CH_2Cl_2. The combined organic layers were washed with brine, dried over $MgSO_4$, filtered, and concentrated under reduced pressure. The resulting crude product was used immediately in the subsequent reaction without purification (Lucio Anelli et al., 1987).

$ArNH_2$ (1.0 eq) was added to a solution of the abovementioned crude product in CH_2Cl_2. After the mixture was stirred for 10 min at 0°C, $NaBH(OAc)_3$ (1.2 eq) was added at 0°C and stirred at room temperature. Then saturated aqueous $NaHCO_3$ was added, and the resulting mixture was extracted thrice with CH_2Cl_2. The combined organic layers were dried over anhydrous Na_2SO_4, filtered, and concentrated under reduced pressure. The resulting residue was purified using column chromatography to yield the corresponding epoxy anilines.

2.2.3 Optimized conditions of intramolecular aminolysis of *cis*-3,4-epoxy amines

$La(OTf)_3$ (5 mol%) was added to a solution of *cis*-3,4-epoxy amine (1 eq) in $(CH_2Cl)_2$ (0.2 M) at room temperature, and the mixture was stirred under reflux. Upon completion of the reaction, the mixture was cooled to 0°C, and saturated aqueous $NaHCO_3$ was added. The mixture was extracted thrice with CH_2Cl_2. The combined organic layers were dried over Na_2SO_4, filtered, and then concentrated under reduced pressure. The resulting residue was purified using column chromatography to yield the corresponding azetidine.

3 Results

The feasibility of azetidine synthesis via $Ln(OTf)_3$-catalyzed intramolecular aminolysis of *cis*-3,4-epoxy amines was investigated using *cis*-3,4-epoxy amine **1aa**, prepared from *cis*-3-hexen-1-ol in three steps, as a model substrate (Table 1). Preliminary experiments revealed the optimum conditions for the intramolecular aminolysis of *trans*-3,4-epoxy amines to yield pyrrolidine; catalytic $La(OTf)_3$ in refluxing CH_2Cl_2 did not complete the reaction (Kuriyama et al., 2021). Therefore, 1,2-dichloroethane (DCE) was used for refluxing instead of CH_2Cl_2 for 2.5 h to afford azetidine **2aa** in 81% yield, along with a trace amount of pyrrolidine **3aa** (**2aa**/**3aa** = >20:1) (Table 1, entry 1). Solvents with almost the same boiling points similar to that of DCE were screened. The selectivity for benzene (PhH) was lower than that for DCE (Table 1, entry 2). Coordinative solvents such as MeCN and THF exhibited good selectivity, but some of the substrate **1aa** remained (Table 1, entries 3 and 4). Subsequently, the acids were screened using DCE as the solvent. Using $Sc(OTf)_3$ instead of $La(OTf)_3$ required a longer reaction time and afforded **2aa** in moderate yield (Table 1, entry 5). LiOTf afforded a complex mixture of products. $Ni(ClO_4)_2{\cdot}6H_2O$, the catalyst reported by Yamamoto for the intermolecular aminolysis of 3,4-epoxy alcohols (Wang and Yamamoto, 2015), and TfOH, a Brønsted acid, gave low yields of **2aa** because some substrate **1aa** remained; the reaction gave a complex mixture (Table 1, entries 7 and 8). In the absence of acids in refluxing DCE, no reaction occurred after 2.5 h (Table 1, entry 9). In contrast, although **1aa** was completely consumed after 24 h, **2aa** was not detected, and a complex mixture was obtained (Table 1, entry 10). Based on the aforementioned examination, the optimum conditions were identified as 5 mol% $La(OTf)_3$ in refluxing DCE.

With the optimum conditions established, the effects of the substituents on the amino groups were evaluated (Figure 1). Azetidine formation proceeded smoothly in the presence of

TABLE 1 Optimization of reaction conditions.

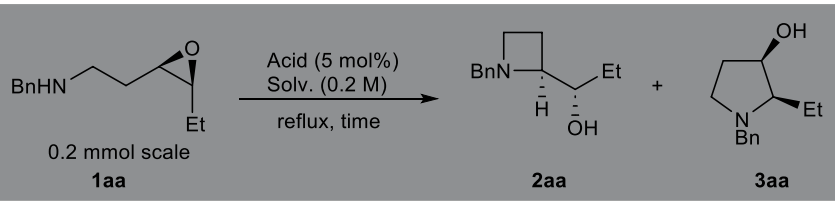

Entry	Acid	Solv	NMR Yield of **2aa**[a)]	**2aa/3aa**
1	$La(OTf)_3$	$(CH_2Cl)_2$	81% (2.5 h)	>20:1
2	$La(OTf)_3$	PhH	81% (2.5 h)	16:1
3	$La(OTf)_3$	EtOAc	77% (12 h)	>20:1
4	$La(OTf)_3$	MeCN	58% (12 h)	>20:1
5	$Sc(OTf)_3$	$(CH_2Cl)_2$	62% (4.5 h)	>20:1
6	LiOTf	$(CH_2Cl)_2$	N.D. (6 h)	–
7	$Ni(ClO_4)_2{\cdot}6H_2O$	$(CH_2Cl)_2$	13% (6 h)	–
8	TfOH[b]	$(CH_2Cl)_2$	10% (6 h)	–
9	–	$(CH_2Cl)_2$	N.R. (2.5 h)	–
10	–	$(CH_2Cl)_2$	N.D. (24 h)	–

[a]NMR yield was determined using mesitylene.
[b]15 mol%.

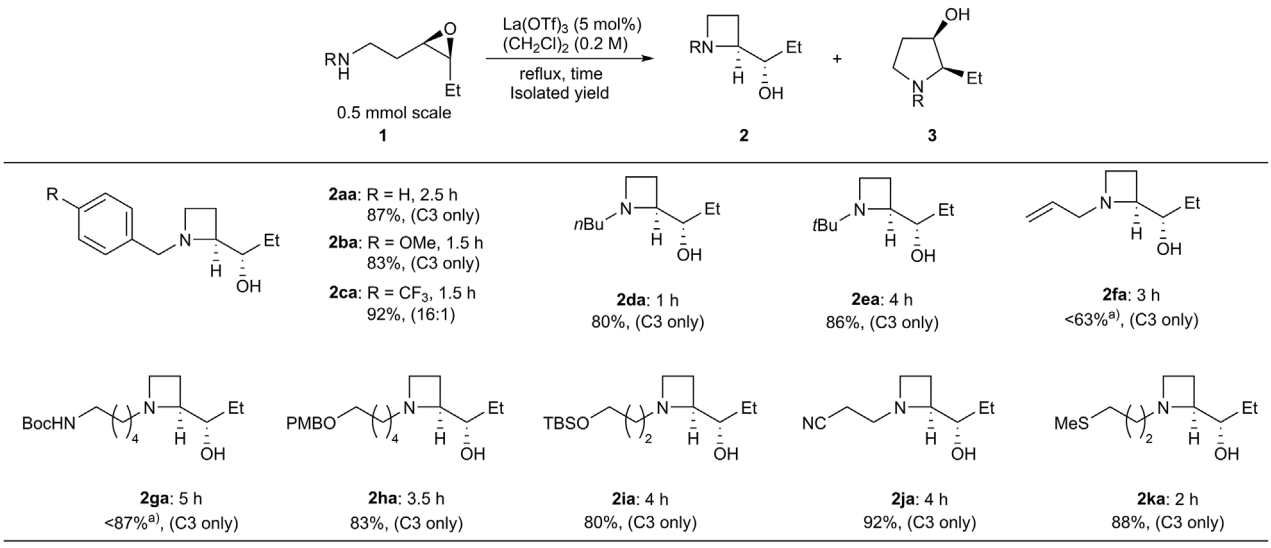

FIGURE 1
Substrate scope of the regioselective aminolysis.

electron-rich and electron-deficient benzyl groups (**2ba**, **2ca**). Substrates with an *n*-butyl amine moiety afforded azetidine **2da** in high yield with high regioselectivity. A substrate with a bulky *tert*-butyl amine afforded azetidine **2ea** in high yield. Substrates with π-basic allyl group also afforded the corresponding azetidine **2fa** in moderate yield. Acid-prone functional groups, such as Boc, PMB, and TBS groups, were tolerated to afford azetidines (**2ga**–**2ia**) in high yields. Nitrile and sulfide functionalities hardly affected the yields of azetidines (**2ja** and **2ka**). Interestingly, epoxy aniline **1la** gave azetidine **2la** in only 39% yield because of the competing formation of tetrahydroquinoline **4** via electrophilic aromatic substitution, whereas the corresponding *trans*-epoxy aniline efficiently underwent C4-selective intramolecular aminolysis to give pyrrolidine in high yield (Table 2) (Barvainiene et al., 2007;

TABLE 2 Substrate scope of epoxy anilines.

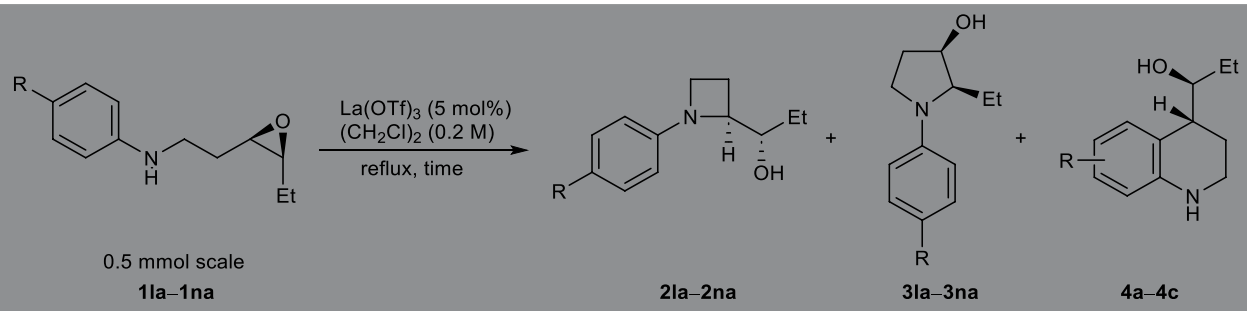

R	Time (h)	Isolated yield		
		2	3	4
H (**1la**)	5	39%	19%	21%
MeO (**1ma**)	5	38%	<12%[a]	<29%[b]
NO_2[c] (**1na**)	7	N.R.		

[a]A negligible amount of undetermined byproduct was contaminated.
[b]Isomers of tetrahydroquinoline were obtained as an inseparable mixture.
[c]0.25 mmol scale.

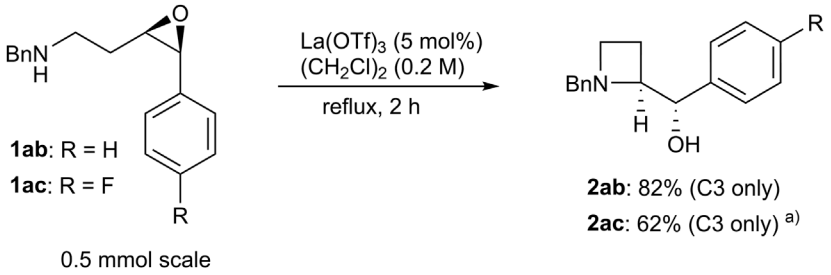

SCHEME 3
Aryl-substituted epoxy amine; a) A tiny amount of pyrrolidine was observed in the crude product (C3/C4 = >20:1).

Wipf and Maciejewski, 2008; Mühlhaus et al., 2019). While epoxy aniline **1ma** bearing an electron-donating methoxy group underwent aminolysis as did **1la**, epoxy aniline **1na** bearing an electron-withdrawing nitro group did not undergo the reaction. The effect of the functional groups adjacent to the epoxide was evaluated. Apart from the cation stabilization at the benzylic position, phenyl-substituted epoxide **1ab** underwent aminolysis at the homobenzylic position, rather than the benzylic position, to afford azetidine **2ab** in high yields (Scheme 3). Azetidine **2ac** was also given in moderate yield from 4-fluorophenyl-substituted epoxide **1ac**.

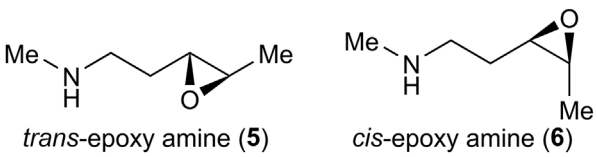

FIGURE 2
Substrates studied computationally.

4 Discussion

Density functional theory (DFT) calculations were performed to gain insight into the opposite regioselectivity between *trans*- and *cis*-epoxy amines. Simplified *trans*- and *cis*-epoxy amines **5** and **6** were used as substrates to reduce computational costs (Figure 2). When naked lanthanum (III) is coordinated to *trans*-epoxy amine **5**, the energy of the transition state that yields azetidine by C3-selective aminolysis is lower than that produced by C4-selective aminolysis, which indicates selectivity opposite to that of the experimental results (see Supplementary Material S1). Dimethylamine-coordinated lanthanum (III) was used as the activator. The calculations showed that the energy of the pyrrolidine transition state was lower than that of the azetidine transition state, which was consistent with the experimental results (Figure 3). Calculations of the transition states of *cis*-epoxy amines

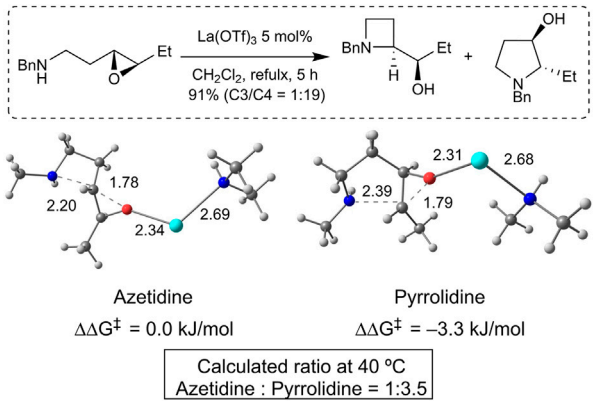

FIGURE 3
DFT studies of the selectivity for *trans*-epoxy amine (PCM (dichloromethane)/ωB97XD/6-311++G**, SDD (La)//PCM (dichloromethane)/ωB97XD/6-31G**, LanL2DZ (La)); lanthanum (light blue), oxygen (red), nitrogen (blue), carbon (gray), and hydrogen (white).

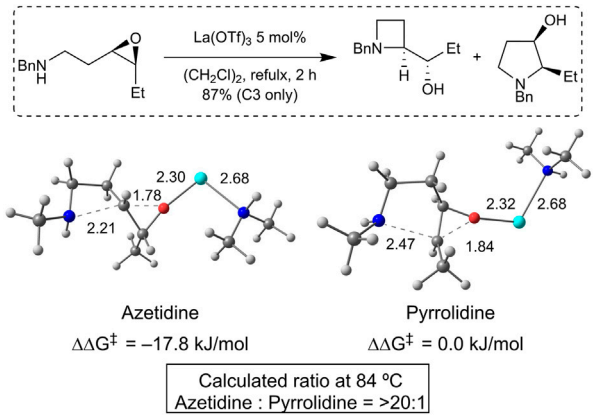

FIGURE 4
DFT studies of the selectivity for *cis*-epoxy amine (PCM (dichloroethane)/ωB97XD/6-311++G**, SDD (La)//PCM (dichloroethane)/ωB97XD/6-31G**, LanL2DZ (La)); lanthanum (light blue), oxygen (red), nitrogen (blue), carbon (gray), and hydrogen (white).

complexed with dimethylamine-coordinated lanthanum (III) showed that the transition state of azetidine was much smaller than that of pyrrolidine, which was consistent with the experimental results (Figure 4). These computational results suggest that lanthanum complexes coordinated by substrates and/or products are likely to contribute to inverse regioselectivity.

5 Conclusion

We have developed the $La(OTf)_3$-catalyzed regioselective intramolecular aminolysis of *cis*-3,4-epoxy amines to afford azetidines. This reaction tolerated various functional groups, including coordinative and acid-prone functional groups. C3-selective aminolysis also proceeded with styrene oxide-type 3,4-epoxy amine, in which the C4 position was the benzylic position. Computational studies suggest that the difference in the regioselectivity of aminolysis between the *cis*- and *trans*-isomers was likely caused by lanthanum (III) coordinated with the substrate and/or product. Further investigations of the Lewis acid-promoted ring-opening reaction of strained heterocycles and its application to successive ring-opening reactions are currently underway. The reactions developed herein are expected to be applied to the synthesis of various highly functionalized bioactive compounds.

Data availability statement

The original contributions presented in the study are included in the article/Supplementary Materials, further inquiries can be directed to the corresponding author.

Author contributions

Investigation: YK, YS, and YI; experiment: YK; writing-original draft preparation: YK and YS; writing-review and editing: YS and YI; funding acquisition: YS and YI. All authors contributed to the article and approved the submitted version.

Funding

This research was partially supported by JSPS KAKENHI Grant Nos. 22H02739 and 21H05210 (Digitalization-driven Transformative Organic Synthesis (Digi-TOS)), and by Research Support Project for Life Science and Drug Discovery (Basis for Supporting Innovative Drug Discovery and Life Science Research (BINDS)) from AMED under Grant Number JP22ama121040.

Conflict of interest

The authors declare that the research was conducted in the absence of any commercial or financial relationships that could be construed as a potential conflict of interest.

Publisher's note

Supplementary material

The Supplementary Material for this article can be found online at: https://www.frontiersin.org/articles/10.3389/fchem.2023.1251299/full#supplementary-material

References

Barvainiene, B., Stanisauskaite, A., and Getautis, V. (2007). Synthesis and thermal reactions of N-(2, 3-epoxypropyl) diphenylamine. *Chem. Heterocycl. Compd.* 43 (6), 718–721. doi:10.1007/s10593-007-0117-7

Betz, K. N., Chiappini, N. D., and Du Bois, J. (2019). Intermolecular sp3-C–H amination for the synthesis of saturated azacycles. *Org. Lett.* 22 (5), 1687–1691. doi:10.1021/acs.orglett.9b04096

Bose, A. K., Mathur, C., Wagle, D. R., Naqvi, R., Manhas, M. S., and Urbanczyk-Lipkowska, Z. (1994). Chiral β-lactams as synthons. Stereospecific synthesis of a 6-epi-lincosamine derivative. *Heterocycles* 2 (39), 491–496.

Breternitz, H.-J., and Schaumann, E. (1999). Ring-opening of N-tosylaziridines by heterosubstituted allyl anions. Application to the synthesis of azetidines and pyrrolidines. *J. Chem. Soc. Perkin Trans.* 1 (14), 1927–1932. doi:10.1039/a902117e

Caron, M., and Sharpless, K. (1985). Titanium isopropoxide-mediated nucleophilic openings of 2, 3-epoxy alcohols. A mild procedure for regioselective ring-opening. *J. Org. Chem.* 50 (9), 1557–1560. doi:10.1021/jo00209a047

Dherange, B. D., Yuan, M., Kelly, C. B., Reiher, C. A., Grosanu, C., Berger, K. J., et al. (2022). Direct deaminative functionalization. *J. Am. Chem. Soc.* 145 (1), 17–24. doi:10.1021/jacs.2c11453

Faigl, F., Kovács, E., Turczel, G., Szöllősy, Á., Mordini, A., Balázs, L., et al. (2012). Novel stereoselective synthesis of 1, 2, 3-trisubstituted azetidines. *Tetrahedron Asymmetry* 23 (22-23), 1607–1614. doi:10.1016/j.tetasy.2012.10.014

Faiz, S., and Zahoor, A. F. (2016). Ring opening of epoxides with C-nucleophiles. *Mol. Divers.* 20, 969–987. doi:10.1007/s11030-016-9686-7

Hameed, A., Javed, S., Noreen, R., Huma, T., Iqbal, S., Umbreen, H., et al. (2017). Facile and green synthesis of saturated cyclic amines. *Molecules* 22 (10), 1691. doi:10.3390/molecules22101691

Hocine, S., Duchamp, E., Mishra, A., Fourquez, J.-M., and Hanessian, S. (2023). Synthesis of aza-bridged perhydroazulene chimeras of tropanes and hederacine a. *J. Org. Chem.* 88 (7), 4675–4686. doi:10.1021/acs.joc.3c00169

Kuriyama, Y., Sasano, Y., Hoshino, Y., Uesugi, S.-i., Yamaichi, A., and Iwabuchi, Y. (2021). Highly regioselective 5-endo-tet cyclization of 3, 4-epoxy amines into 3-hydroxypyrrolidines catalyzed by La (OTf) 3. *Chemistry–A Eur. J.* 27 (6), 1961–1965. doi:10.1002/chem.202004455

Lucio Anelli, P., Biffi, C., Montanari, F., and Quici, S. (1987). Fast and selective oxidation of primary alcohols to aldehydes or to carboxylic acids and of secondary alcohols to ketones mediated by oxoammonium salts under two-phase conditions. *J. Org. Chem.* 52 (12), 2559–2562. doi:10.1021/jo00388a038

Medjahdi, M., Gonzalez-Gomez, J. C., Foubelo, F., and Yus, M. (2009). Stereoselective synthesis of azetidines and pyrrolidines from N-tert-butylsulfonyl (2-aminoalkyl) oxiranes. *J. Org. Chem.* 74 (20), 7859–7865. doi:10.1021/jo9016666

Moulines, J., Bats, J.-P., Hautefaye, P., Nuhrich, A., and Lamidey, A.-M. (1993). Substituent control in the synthesis of azetidines and pyrrolidines by N-tosyl-oxiraneethylamines base-mediated cyclization. *Tetrahedron Lett.* 34 (14), 2315–2318. doi:10.1016/s0040-4039(00)77602-7

Mühlhaus, F., Weißbarth, H., Dahmen, T., Schnakenburg, G., and Gansäuer, A. (2019). Merging regiodivergent catalysis with atom-economical radical arylation. *Angew. Chem.* 131 (40), 14346–14350. doi:10.1002/ange.201908860

Parmar, D. R., Soni, J. Y., Guduru, R., Rayani, R. H., Kusurkar, R. V., and Vala, A. G. (2021). Azetidines of pharmacological interest. *Arch. Pharm.* 354 (11), 2100062. doi:10.1002/ardp.202100062

Rodríguez-Berríos, R. R., Isbel, S. R., and Bugarin, A. (2023). Epoxide-based synthetic approaches toward polypropionates and related bioactive natural products. *Int. J. Mol. Sci.* 24 (7), 6195. doi:10.3390/ijms24076195

Rowe, E. A., Reisman, L., Jefcoat, J. A., and Rupar, P. A. (2019). Comparison of the anionic ring-opening polymerizations of N-(Alkylsulfonyl) azetidines. *Macromolecules* 52 (21), 8032–8039. doi:10.1021/acs.macromol.9b01436

Shimokawa, J., Harada, T., Yokoshima, S., and Fukuyama, T. (2011). Total synthesis of gelsemoxonine. *J. Am. Chem. Soc.* 133 (44), 17634–17637. doi:10.1021/ja208617c

Shing, T. K., and So, K. H. (2011). Facile and enantiospecific syntheses of (6 S, 7 R)-6-Chloro-7-benzyloxy-(7 S)-Halo-and (7 S)-Hydroxy-cocaine and natural (−)-Cocaine from d-(−)-ribose. *Org. Lett.* 13 (11), 2916–2919. doi:10.1021/ol2009686

Uesugi, S.-i., Sasano, Y., Matsui, S., Kanoh, N., and Iwabuchi, Y. (2017). Concise, Protecting-Group-Free Synthesis of (+)-Nemonapride *via* $Eu(OTf)_3$-Catalyzed Aminolysis of 3,4-Epoxy Alcohol. *Chem. Pharm. Bull.* 65 (1), 22–24. doi:10.1248/cpb.c16-00568

Uesugi, S.-i., Watanabe, T., Imaizumi, T., Ota, Y., Yoshida, K., Ebisu, H., et al. (2015). Total synthesis and biological evaluation of irciniastatin a (aka psymberin) and irciniastatin b. *J. Org. Chem.* 80 (24), 12333–12350. doi:10.1021/acs.joc.5b02256

Uesugi, S.-i., Watanabe, T., Imaizumi, T., Shibuya, M., Kanoh, N., and Iwabuchi, Y. (2014). Eu (OTf) 3-catalyzed highly regioselective nucleophilic ring opening of 2, 3-epoxy alcohols: An efficient entry to 3-substituted 1, 2-diol derivatives. *Org. Lett.* 16 (17), 4408–4411. doi:10.1021/ol502264y

Wang, C. (2017). Electrophilic ring opening of small heterocycles. *Synthesis* 49 (24), 5307–5319. doi:10.1055/s-0036-1589102

Wang, C., and Yamamoto, H. (2015). Nickel-catalyzed regio-and enantioselective aminolysis of 3, 4-epoxy alcohols. *J. Am. Chem. Soc.* 137 (13), 4308–4311. doi:10.1021/jacs.5b01005

Wang, P., Gao, Y., and Ma, D. (2018). Divergent entry to gelsedine-type alkaloids: Total syntheses of (−)-gelsedilam,(−)-gelsenicine,(−)-gelsedine, and (−)-gelsemoxonine. *J. Am. Chem. Soc.* 140 (37), 11608–11612. doi:10.1021/jacs.8b08127

Wipf, P., and Maciejewski, J. P. (2008). Titanocene (III)-catalyzed formation of indolines and azaindolines. *Org. Lett.* 10 (19), 4383–4386. doi:10.1021/ol801860s

frontiers | Frontiers in Chemistry

TYPE Original Research
PUBLISHED 21 September 2023
DOI 10.3389/fchem.2023.1267422

OPEN ACCESS

EDITED BY
Hyun-Joon Ha,
Hankuk University of Foreign Studies,
Republic of Korea

REVIEWED BY
Tao Shi,
The Scripps Research Institute,
United States
Rajendra Rohokale,
University of Florida, United States

*CORRESPONDENCE
Sanghee Kim,
pennkim@snu.ac.kr

†These authors have contributed equally to this work

RECEIVED 26 July 2023
ACCEPTED 28 August 2023
PUBLISHED 21 September 2023

CITATION
Lee S, Shin JE, Yoon R, Yoo H and Kim S (2023), Annulation of *O*-silyl *N*,*O*-ketene acetals with alkynes for the synthesis of dihydropyridinones and its application in concise total synthesis of phenanthroindolizidine alkaloids. *Front. Chem.* 11:1267422. doi: 10.3389/fchem.2023.1267422

Annulation of *O*-silyl *N*,*O*-ketene acetals with alkynes for the synthesis of dihydropyridinones and its application in concise total synthesis of phenanthroindolizidine alkaloids

Seokwoo Lee[1,2†], Jae Eui Shin[1†], Ran Yoon[1], Hanbin Yoo[1] and Sanghee Kim[1*]

[1]College of Pharmacy, Seoul National University, Seoul, Republic of Korea, [2]College of Pharmacy, Chungnam National University, Daejeon, Republic of Korea

The formation of *N*-heterocycles with multiple substituents is important in organic synthesis. Herein, we report a novel method for the construction of functionalized dihydropyridinone rings through the annulation of an amide α-carbon with a tethered alkyne moiety. The reaction of the amide with the alkyne was achieved via *O*-silyl *N*,*O*-ketene acetal formation and silver-mediated addition. Furthermore, the developed method was applied for the total synthesis of phenanthroindolizidine and phenanthroquinolizidine alkaloids. By varying the coupling partners, a concise and collective total synthesis of these alkaloids was achieved.

KEYWORDS

***N*-heterocycle, *O*-silyl, *N*,*O*-ketene acetal, dihydropyridinone, total synthesis, phenanthroindolizidine, phenanthroquinolizidine, alkaloid**

1 Introduction

The construction of *N*-heterocycles containing multiple substituents still remains an important synthetic challenge (Vo et al., 2014; Nandakumar et al., 2015; He et al., 2021; Chen et al., 2023). We recently described the Ag(I) and Brønsted acid co-catalyzed cyclization of an enamine with a tethered alkyne moiety as a one-pot method for pyridinium formation (Scheme 1A) (Lee et al., 2023). Our proposed mechanism for the transformation involves the addition of a nucleophilic enamine to a silver(I)-complexed alkyne, followed by protonolysis of the resulting vinyl-silver species and subsequent aromatization. Based on this annulation, we envisioned that the nucleophilic addition of the amide α-carbon onto the appended alkyne would form a dihydropyridinone (Scheme 1B). To the best of our knowledge, the reactions of alkynes with amides have not been well explored, although reactions with various types of carbon nucleophiles, especially stabilized carbon nucleophiles such as malonates, β-ketoesters, and diketones, have been well explored (Dénes et al., 2010; Hack et al., 2015; Lin et al., 2021).

Herein, we report the annulation of an amide α-carbon with a tethered alkyne moiety, which is a new complementary process for the functionalization of dihydropyridinone rings.

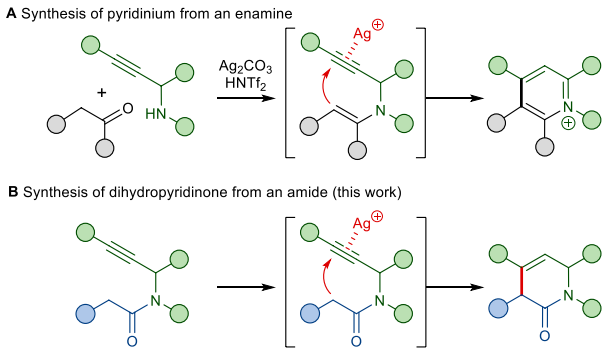

SCHEME 1
Synthesis of *N*-heterocycles via the annulation of an alkyne with a tethered moiety.

In addition, we discuss the application of this C–C bond-forming reaction for the expedient total synthesis of phenanthroindolizidine and phenanthroquinolizidine alkaloids.

2 Results and discussion

We examined the feasibility of the proposed reaction using model substrate **1** (Table 1), which was prepared in two steps from commercially available materials. Based on our previous results on pyridinium formation (Lee et al., 2023), Ag_2CO_3 or $AgNTf_2$ were employed as a catalyst for alkyne activation. Without a base, no conversion of **1** occurred. The addition of a conventional base, such as an alkali metal carbonate or 1,8-diazabicyclo[5.4.0]undec-7-ene (DBU), did not result in product formation (Supplementary Table S1). Despite the reported incompatibility of strong bases and Lewis-acidic metals (Yamamoto, 2000; Yamamoto et al., 2008; Lappert et al., 2009), the strong bases generally used for amide enolate generation, including potassium bis(trimethylsilyl)amide (KHMDS) and LiHMDS, were also examined. However, all of these attempts failed, and most of the starting material decomposed or was recovered (Supplementary Table S1).

We turned our attention to an *O*-silyl *N*,*O*-ketene acetal as a surrogate for the amide enolate. *O*-Silyl *N*,*O*-ketene acetals have been typically used for Mukaiyama-type reactions (Paris et al., 2022) and generated *in situ* by the treatment of an amide with a silylating agent and tertiary amine base (Kobayashi et al., 2011; Downey et al., 2015; Takeda et al., 2017). Previously, Shen and coworkers reported the gold(I)-catalyzed cyclization of alkynes with an *O*-silyl ketene amide or carbamate nucleophiles (Minnihan et al., 2007). However, the reaction of an alkyne with a silyl *N*,*O*-ketene acetal has not been reported.

At the outset of this study, TMSOTf was used as a silylating agent, and various amine bases were screened in the presence of 0.1 equiv of Ag_2CO_3 in dichloroethane (DCE) under reflux conditions. Among the tested amine bases, *N*,*N*-diisopropylethylamine (DIPEA) exhibited the best performance, affording dihydropyridinone **2** in a modest 59% yield along with a mixture of unidentifiable polar side products (Table 1, entry 1). The other sterically hindered base 2,6-lutidine also provided **2**, albeit in a lower yield (46%, entry 2).

After determining the feasibility of the reaction, further screening of the reaction conditions was performed using DIPEA and TMSOTf. Under reflux conditions, the yield of compound **2** was reduced, likely due to the formation of considerable amounts of unidentified side products. A reduction in the reaction temperature led to an increase in the yield of compound **2** (entries 3–5), likely as a result of decreased formation of side products. For example, **2** was

TABLE 1 Conditions for the formation of 2 from 1.[a]

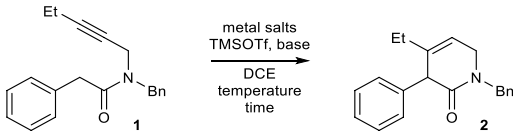

Entry	Metal salts	Base	Temp.	Time (h)	Yield (%)[b]
1	Ag_2CO_3	DIPEA	reflux	1	59 (57)[c]
2	Ag_2CO_3	2,6-lutidine	reflux	1	46
3	Ag_2CO_3	DIPEA	60°C	1	63
4	Ag_2CO_3	DIPEA	40°C	1.5	80
5	Ag_2CO_3	DIPEA	r.t.	6	95 (93)[c]
6	$AgNTf_2$	DIPEA	r.t.	3	96 (93)[c]
7[d]	$AgNTf_2$	DIPEA	r.t.	3	95 (92)[c]
8[e]	$AgNTf_2$	DIPEA	r.t.	3	94 (90)[c]

[a]Reaction conditions: **1** (0.1 mmol), metal salts (0.1 equiv), TMSOTf (4.0 equiv), base (4.0 equiv), DCE (0.05 M).
[b]The chemical yield was estimated via ^{1}H NMR, analysis of the crude reaction mixtures using tetrachloroethane ($C_2H_2Cl_4$) as the internal standard.
[c]Isolation yield.
[d]The reaction was carried out under CH_2Cl_2.
[e]1.0 mmol scale. TMSOTf = Trimethylsilyl trifluoromethanesulfonate, DIPEA = *N*,*N*-Diisopropylethylamine.

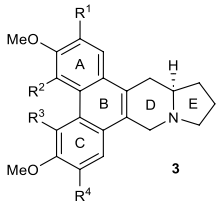

phenanthroindolizidine alkaloids

	R^1	R^2	R^3	R^4
(−)-antofine (**3a**)	OMe	H	H	H
(−)-tylocrebrine (**3b**)	H	H	OMe	H
(−)-isotylocrebrine (**3c**)	H	OMe	OMe	H
(−)-tylophorine (**3d**)	OMe	H	H	OMe

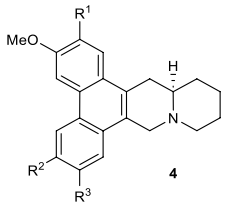

phenanthroquinolizidine alkaloids

	R^1	R^2	R^3
(−)-cryptopleurine (**4a**)	OMe	OMe	H
(−)-boehmeriasin A (**4b**)	H	OMe	OMe
(−)-boehmeriasin B (**4c**)	H	OH	OMe

FIGURE 1
The structures of representative phenanthroindolizidine and phenanthroquinolizidine alkaloids.

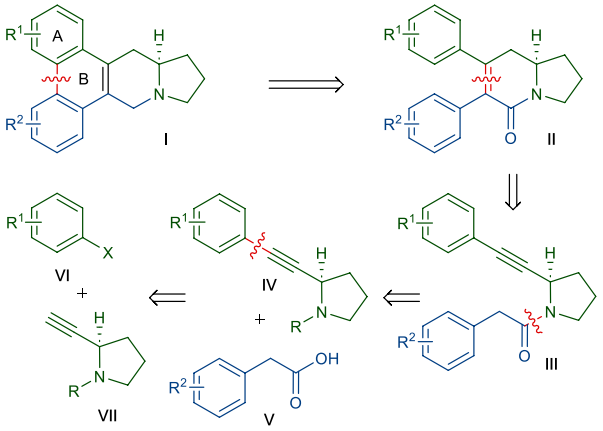

SCHEME 2
Retrosynthetic route for the synthesis of phenanthroindolizidine alkaloids.

formed in an excellent yield of 95% at room temperature, although a longer reaction time was required (entry 5). When Ag_2CO_3 was replaced with $AgNTf_2$, the reaction time was reduced by half (3 h), and the yield was also excellent (96%, entry 6). As in our previous study on the annulation of enamines with alkynes (Lee et al., 2023), the 5-membered heterocycles formed via 5-*exo-dig* cyclization were not observed under the conditions. Other silylating agents did not lead to better yields than TMSOTf (Supplementary Table S2). Several solvents were tested for this transformation. The only other effective solvent was CH_2Cl_2, which furnished **2** with a similar yield (95%, entry 7). Other solvents did not enable the formation of **2** (Supplementary Table S3). Under the optimal conditions, the reaction could be enlarged to a 1.0 mmol scale without a significant decrease in yield (94%, entry 8).

Based on these results, we attempted the total synthesis of phenanthroindolizidine alkaloids (Figure 1). This family of natural products exhibits a wide range of biological effects, including significant anticancer and antiviral activities (De Fatima Pereira et al., 2015; Jia et al., 2021). Therefore, these alkaloids have been the synthetic targets of numerous research groups over the past few decades (Chemler, 2009; Burtoloso et al., 2014).

Our retrosynthetic analysis, based on the above dihydropyridinone synthetic strategy, is depicted in Scheme 2. The B ring of the phenanthroindolizidine skeleton of I could be constructed at the last stage of the synthesis via the biaryl coupling of II. We envisioned that dihydropyridinone ring of II could be formed by the annulation of an amide α-carbon with a tethered alkyne moiety in III, according to the above-mentioned method. An obvious disconnection of the amide bond in III led to the 2-alkyne-pyrrolidine IV and 2-arylacetic acid V. Pyrrolidine derivative IV would be accessed by coupling of an aryl halide VI with the known alkyne VII. According to this retrosynthetic scheme, many members of this phenanthroindolizidine family and analogs could be synthesized by varying the two coupling partners V and VI. Even, this scheme would permit the synthesis of phenanthroquinolizidine alkaloids if 2-alkyne-piperidine was employed instead of VII.

Our synthesis began with the preparation of known alkyne **5** (Scheme 3), which is available in two steps from commercially available *N*-Boc-D-prolinol (Mercado-Marin et al., 2014). The Sonogashira coupling of **5** with 3,4-dimethoxy phenyl iodide afforded **6a** in high yield. Removal of the *N*-Boc group, followed by EDCI-mediated coupling with 2-arylacetic acid **7a**, generated amide **8a** in a good overall yield. Application of the developed reaction conditions to **8a** was successful, resulting in the formation of 3,6-dihydropyridin-2-one **9a** as the major product (90%) after 1 h. Treatment with DBU at 90°C led to the isomerization of **9a** to the thermodynamically more favorable 5,6-dihydropyridinone **10a** (see Supplementary Material). At this stage, we envisaged that **10a** could be obtained directly from the alkyne–amide cyclization. Fortunately, we found modified conditions that allowed the direct formation of **10a** from **8a**. At an elevated temperature of 60°C for 2 h, **10a** was obtained directly from **8a** in a 71% yield.

The oxidative biaryl coupling of **10a** was accomplished with hypervalent iodine reagent phenyliodine(III) bis(trifluoroacetate) (PIFA) to give pentacyclic product **11a** in a 64% yield (Kwon et al., 2015). Finally, the amide group of **11a** was reduced with $LiAlH_4$ to give (−)-antofine (**3a**) in an 85% yield (Iwao et al., 1983). Overall, this asymmetric total synthesis was completed in only 8 steps from *N*-Boc-D-prolinol with a 33% overall yield (5 steps from known **6a** and a 35% overall yield).

With an established route to (−)-antofine, we pursued the total synthesis of (−)-tylocrebrine (**3b**), whose structure differs from that of (−)-antofine (**3a**) due to the presence of a methoxy group at C-5. Unlike the method for B-ring formation in **3a**, radical-mediated oxidative biaryl coupling could not be used for **3b** synthesis because of the regioselectivity problem. Therefore, we planned to employ palladium catalyzed C–H annulation (Ghosh et al., 2022; Thombal et al., 2022).

From intermediate **6a**, (−)-tylocrebrine (**3b**) was readily accessible. First, **6a** was coupled with 2-arylacetic acid **7b** to afford **8b**. The annulation of an amide with a tethered alkyne moiety in **8b** under the abovementioned conditions gave 5,6-dihydropyridinone **10b** directly in a 63% yield. After several

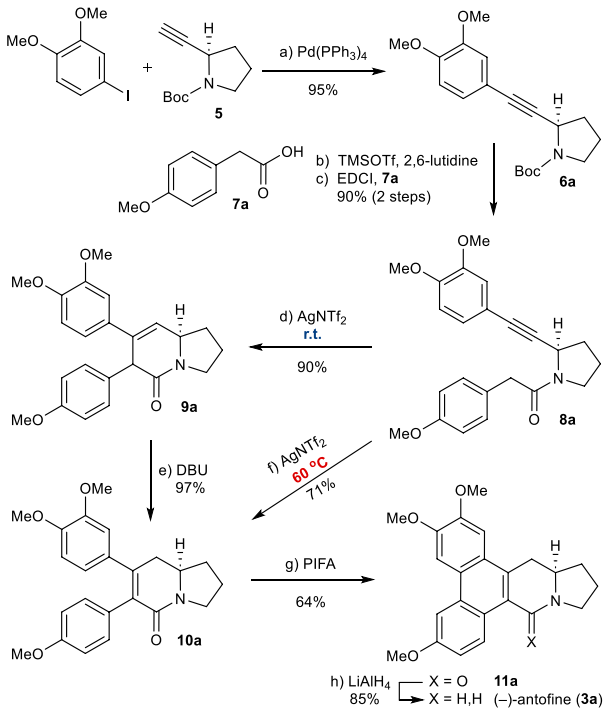

SCHEME 3
Synthesis of (–)-antofine (**3a**). Reagents and conditions: a) $Pd(PPh_3)_4$ (0.05 equiv), piperidine/MeCN (1:1), reflux, 3 h, 95%; b) TMSOTf (2.0 equiv), 2,6-lutidine (3.0 equiv), CH_2Cl_2, 0°C, 10 min; c) **7a** (1.2 equiv), EDCI (1.1 equiv), DMAP (1.1 equiv), CH_2Cl_2, r.t., 12 h, 90% for 2 steps; d) $AgNTf_2$ (0.1 equiv), TMSOTf (4.0 equiv), DIPEA (4.0 equiv), DCE, r.t., 1 h, 90%; e) DBU (4.0 equiv), toluene, 90°C, 30 min, 97%; f) $AgNTf_2$ (0.1 equiv), TMSOTf (4.0 equiv), DIPEA (4.0 equiv), DCE, 60°C, 2 h, 71%; g) PIFA (1.1 equiv), BF_3OEt_2 (1.5 equiv), CH_2Cl_2, –10°C, 1 h, 64%; h) $LiAlH_4$ (2.0 equiv), THF, reflux, 1 h, 85%. EDCI = *N*-Ethylcarbodiimide hydrochloride, DMAP = 4-Dimethylaminopyridine.

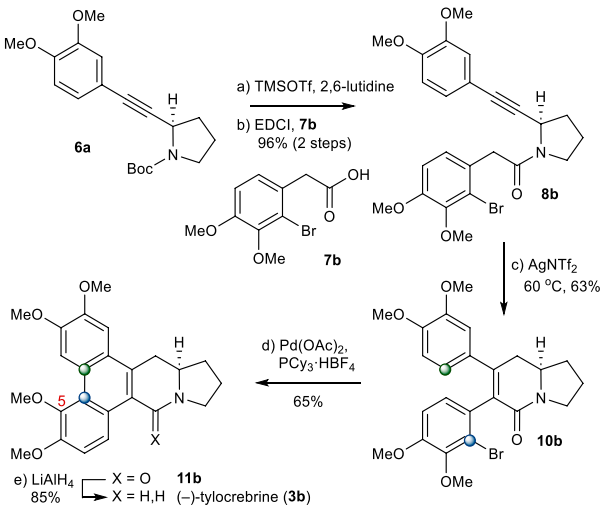

SCHEME 4
Synthesis of (–)-tylocrebrine (**3b**). Reagents and conditions: a) TMSOTf (2.0 equiv), 2,6-lutidine (3.0 equiv), CH_2Cl_2, 0°C, 10 min; b) **7b** (1.2 equiv), EDCI (1.1 equiv), DMAP (1.1 equiv), CH_2Cl_2, r.t., 20 h, 96% for 2 steps; c) $AgNTf_2$ (0.1 equiv), TMSOTf (4.0 equiv), DIPEA (4.0 equiv), DCE, 60°C, 2 h, 63%; d) $Pd(OAc)_2$ (0.2 equiv), $PCy_3{\cdot}HBF_4$ (0.4 equiv), K_2CO_3 (4.0 equiv), 1,4-dioxane, 110°C, 1 h, 65%; e) $LiAlH_4$ (2.0 equiv), THF, reflux, 1 h, 85%.

trials, we found that the treatment of **10b** with $Pd(OAc)_2$ and $PCy_3{\cdot}HBF_4$ as the palladium source and ligand in dioxane, respectively, led to the formation of **11b** as the only detectable regioisomer (Campeau et al., 2006; Yadav et al., 2010). After the reduction of the amide group in **11b**, (–)-tylocrebrine (**3b**) was obtained in 5 steps from **6a** (Scheme 4).

The same chemistry was used for the total synthesis of (–)-isotylocrebrine (**3c**). Total synthesis of **3c** started from alkyne **5**. The Sonogashira coupling of **5** with 2-bromo-1-iodo-3,4-dimethoxybenzene chemoselectively afforded **6c** in an excellent yield (Weijiang et al., 2013). After *N*-Boc group removal, 2-aryl acetic acid **7c** was introduced to give amide **8c** in a good yield. Under the aforementioned one-pot cyclization/isomerization conditions, **8c** would not yield 5,6-dihydropyridinone **10c**. Instead, **9c** was formed in a high yield. Isomerization to **10c** was achieved when **9c** was treated with DBU in toluene at 90°C. Palladium-catalyzed B-ring formation, followed by the reduction of the amide group, provided (–)-isotylocrebrine (**3c**), as shown in Scheme 5.

Using the same chemistry described for the synthesis of (–)-antofine (**3a**), we accomplished the total synthesis of the phenanthroquinolizidine alkaloid (–)-cryptopleurine (**4a**), as shown in Scheme 6. A notable difference is the use of 2-alkyne-

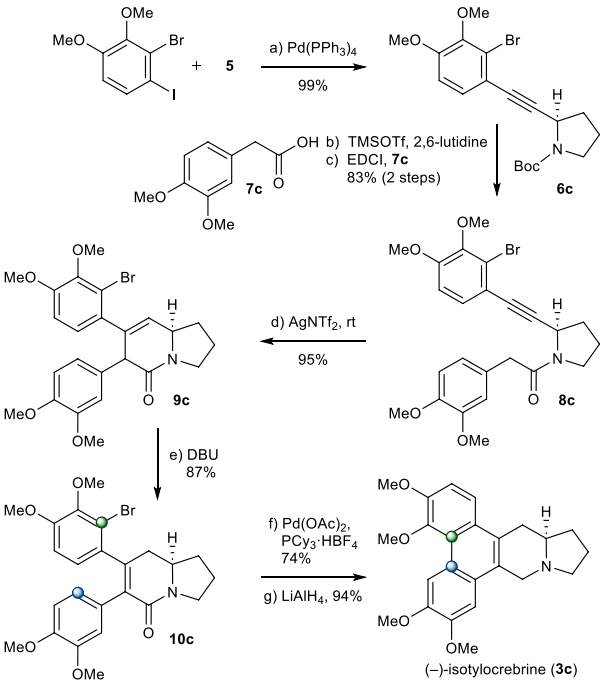

SCHEME 5
Synthesis of (–)-isotylocrebrine (**3c**). Reagents and conditions: a) $Pd(PPh_3)_4$ (0.05 equiv), CuI (0.1 equiv), iPr_2NH, r.t., 2 h, 99%; b) TMSOTf (2.0 equiv), 2,6-lutidine (3.0 equiv), CH_2Cl_2, 0°C, 10 min; c) **7c** (1.2 equiv), EDCI (1.1 equiv), DMAP (1.1 equiv), CH_2Cl_2, r.t., 12 h, 83% for 2 steps; d) $AgNTf_2$ (0.1 equiv), TMSOTf (4.0 equiv), DIPEA (4.0 equiv), DCE, r.t., 1 h, 95%; e) DBU (4.0 equiv), toluene, 90°C, 1.5 h, 87%; f) $Pd(OAc)_2$ (0.2 equiv), $PCy_3{\cdot}HBF_4$ (0.4 equiv), K_2CO_3 (4.0 equiv), 1,4-dioxane, 110°C, 12 h, 74%; g) $LiAlH_4$ (2.0 equiv), THF, reflux, 1 h, 94%.

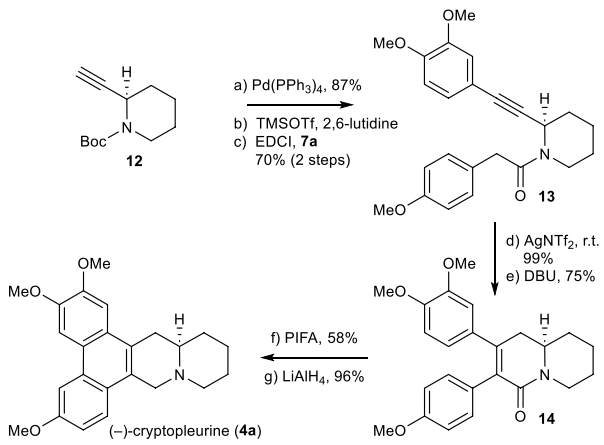

SCHEME 6
Synthesis of (–)-cryptopleurine (**4a**). Reagents and conditions: a) 3,4-dimethoxyiodobenzene, $Pd(PPh_3)_4$ (0.05 equiv), piperidine/MeCN (1:1), r.t., 14 h, 87%; b) TMSOTf (2.0 equiv), 2,6-lutidine (3.0 equiv), CH_2Cl_2, 0°C, 25 min; c) **7a** (1.2 equiv), EDCI (1.1 equiv), DMAP (1.1 equiv), CH_2Cl_2, r.t., 12 h, 70% for 2 steps; d) $AgNTf_2$ (0.1 equiv), TMSOTf (4.0 equiv), DIPEA (4.0 equiv), DCE, r.t., 2 h, 99%; e) DBU (4.0 equiv), toluene, 90°C, 6 h, 75%; f) PIFA (1.1 equiv), BF_3OEt_2 (3.0 equiv), CH_2Cl_2, −10°C, 30 min, 58%; g) $LiAlH_4$ (3.0 equiv), THF, reflux, 30 min, 96%.

piperidine **12** in place of **5**. The total synthesis of **4a** was accomplished from **12** in 7 steps, using the process shown in Scheme 3. The spectra data and optical rotations of obtained alkaloids **3a**, **3b**, **3c**, and **4a** were in good agreement with those reported in the literature (Abe et al., 1995; Suzuki et al., 1995; Stærk et al., 2002; Niphakis et al., 2011).

3 Conclusion

In conclusion, we successfully developed a new synthetic strategy for the construction of functionalized dihydropyridinone rings through the annulation of an amide *α*-carbon with a tethered alkyne moiety. An unexplored reaction between amide and alkyne was realized through an *O*-silyl *N*,*O*-ketene acetal. Our method was applied for the total synthesis of phenanthroindolizidine and phenanthroquinolizidine alkaloids. Varying the coupling partners allowed for the culminative total synthesis of (–)-antofine (**3a**), (–)-tylocrebrine (**3b**), (–)-isotylocrebrine (**3c**), and (–)-cryptopleurine (**4a**). Further applications of this reaction for the synthesis of various functional dihydropyridinones and investigation of its extension to the total synthesis of other types of heterocyclic compounds are underway in our laboratory.

Data availability statement

The original contributions presented in the study are included in the article/Supplementary Material, further inquiries can be directed to the corresponding author.

Author contributions

SL: Data curation, Formal Analysis, Writing-review and editing, Investigation, Validation. JS: Data curation, Formal Analysis, Writing-review and editing, Investigation, Validation. RY: Data curation, Formal Analysis, Writing-review and editing. HY: Data curation, Formal Analysis, Writing-review and editing. SK: Supervision, Writing-original draft, Writing-review and editing, Conceptualization, Funding acquisition, Investigation, Project administration, Validation.

Funding

The authors declare financial support was received for the research, authorship, and/or publication of this article. This work was supported by the National Research Foundation of Korea (NRF) grant funded by the Korean government (MSIT) (RS-2023-00209322).

Conflict of interest

The authors declare that the research was conducted in the absence of any commercial or financial relationships that could be construed as a potential conflict of interest.

Publisher's note

Supplementary material

The Supplementary Material for this article can be found online at: https://www.frontiersin.org/articles/10.3389/fchem.2023.1267422/full#supplementary-material

References

Abe, F., Iwase, Y., Yamauchi, T., Honda, K., and Hayshi, N. (1995). Phenanthroindolizidine alkaloids from *Tylophora tanakae*. *Phytochemistry* 39, 695–699. doi:10.1016/0031-9422(95)00034-5

Burtoloso, A. C. B., Bertonha, A. F., and Rosset, I. G. (2014). Synthesis of alkaloids: Recent advances in the synthesis of phenanthroindolizidine alkaloids. *Curr. Top. Med. Chem.* 14, 191–199. doi:10.2174/1568026613666131213154633

Campeau, L.-C., Parisien, M., Jean, A., and Fagnou, K. (2006). Catalytic direct arylation with aryl chlorides, bromides, and iodides: Intramolecular studies leading to new intermolecular reactions. *J. Am. Chem. Soc.* 128, 581–590. doi:10.1021/ja055819x

Chemler, S. R. (2009). Phenanthroindolizidines and phenanthroquinolizidines: Promising alkaloids for anti-cancer therapy. *Curr. Bioact. Compd.* 5, 2–19. doi:10.2174/157340709787580928

Chen, W., Cao, X., and Yang, X. (2023). Transition-metal-free methods for the remote C–H bond functionalization of cyclic amines. *Asian J. Org. Chem.* 12, e202200547. doi:10.1002/ajoc.202200547

De Fatima Pereira, M., Rochais, C., and Dallemagne, P. (2015). Recent advances in phenanthroindolizidine and phenanthroquinolizidine derivatives with anticancer activities. *Anti-Cancer Agents Med. Chem.* 15, 1080–1091. doi:10.2174/1871520615666150520143600

Dénes, F., Pérez-Luna, A., and Chemla, F. (2010). Addition of metal enolate derivatives to unactivated carbon-carbon multiple bonds. *Chem. Rev.* 110, 2366–2447. doi:10.1021/cr800420x

Downey, C. W., Ingersoll, J. A., Glist, H. M., Dombrowski, C. M., and Barnett, A. T. (2015). One-pot silyl ketene acetal-formation Mukaiyama–Mannich additions to imines mediated by trimethylsilyl trifluoromethanesulfonate. *Eur. J. Org. Chem.* 2015, 7287–7291. doi:10.1002/ejoc.201500958

Ghosh, T., Biswas, D., and Bhakta, S. (2022). Palladium-catalyzed synthesis of fused carbo-and heterocycles. *Chem. Asian J.* 17, e202200725. doi:10.1002/asia.202200725

Hack, D., Blümel, M., Chauhan, P., Philipps, A. R., and Enders, D. (2015). Catalytic Conia-ene and related reactions. *Chem. Soc. Rev.* 44, 6059–6093. doi:10.1039/C5CS00097A

He, Y., Zheng, Z., Yang, J., Zhang, X., and Fan, X. (2021). Recent advances in the functionalization of saturated cyclic amines. *Org. Chem. Front.* 8, 4582–4606. doi:10.1039/D1QO00171J

Iwao, M., Mahalanabis, K. K., Watanabe, M., De Silva, S. O., and Snieckus, V. (1983). Directed ortho metallation of tertiary aromatic amides: A new *N*-heteroring annelation method and synthesis of phenanthro-quinolizidine and -indolizidine alkaloids. *Tetrahedron* 39, 1955–1962. doi:10.1016/S0040-4020(01)91913-1

Jia, X. H., Zhao, H. X., Du, C. L., Tang, W. Z., and Wang, X. J. (2021). Possible pharmaceutical applications can be developed from naturally occurring phenanthroindolizidine and phenanthroquinolizidine alkaloids. *Phytochem. Rev.* 20, 845–868. doi:10.1007/s11101-020-09723-3

Kobayashi, S., Kiyohara, H., and Yamaguchi, M. (2011). Catalytic silicon-mediated carbon–carbon bond-forming reactions of unactivated amides. *J. Am. Chem. Soc.* 133, 708–711. doi:10.1021/ja108764d

Kwon, Y., Song, J., Lee, H., Kim, E.-Y., Lee, K., Lee, S. K., et al. (2015). Design, synthesis, and biological activity of sulfonamide analogues of antofine and cryptopleurine as potent and orally active antitumor agents. *J. Med. Chem.* 58, 7749–7762. doi:10.1021/acs.jmedchem.5b00764

Lappert, M., Poer, P., Protchenko, A., and Seeber, A. (2009). *Metal amide chemistry*. Weinheim: Wiley VCH.

Lee, S., Yoo, H., Park, S., Yoon, R., and Kim, S. (2023). Facile one-pot synthesis of polysubstituted pyridinium salts by annulation of enamines with alkynes. *Chem. Eur. J.* 29, e202300059. doi:10.1002/chem.202300059

Lin, E.-Z., Xu, Y., Ji, K., and Ye, L.-W. (2021). Recent advances towards catalytic asymmetric Conia-ene-type reactions. *Chin. Chem. Lett.* 32, 954–962. doi:10.1016/j.cclet.2020.08.012

Mercado-Marin, E., Garcia-Reynaga, P., Romminger, S., Pimenta, E. F., Romney, D. K., Lodewyk, M. W., et al. (2014). Total synthesis and isolation of citrinalin and cyclopiamine congeners. *Nature* 509, 318–324. doi:10.1038/nature13273

Minnihan, E. C., Colletti, S. L., Toste, F. D., and Shen, H. C. (2007). Gold(I)-catalyzed regioselective cyclizations of silyl ketene amides and carbamates with alkynes. *J. Org. Chem.* 72, 6287–6289. doi:10.1021/jo071014r

Nandakumar, A., Midya, S. P., Landge, V. G., and Balaraman, E. (2015). Transition-metal-catalyzed hydrogen-transfer annulations: Access to heterocyclic scaffolds. *Angew. Chem. Int. Ed.* 54, 11022–11034. doi:10.1002/anie.201503247

Niphakis, M. J., and Georg, G. I. (2011). Synthesis of tylocrebrine and related phenanthroindolizidines by VOF_3–mediated oxidative aryl–alkene coupling. *Org. Lett.* 13, 196–199. doi:10.1021/ol1023954

Paris, T. J., and Willand-Charnley, R. (2022). Modern synthesis and chemistry of stabilized ketene *N, O*-acetals. *Synthesis* 54, 1537–1550. doi:10.1055/a-1713-8481

Stærk, D., Lykkeberg, A. K., Christensen, J., Budnik, B. A., Abe, F., and Jaroszewski, J. W. (2002). *In vitro* cytotoxic activity of phenanthroindolizidine alkaloids from cynanchum vincetoxicum and *Tylophora tanakae* against drug-sensitive and multidrug-resistant cancer cells. *J. Nat. Prod.* 65, 1299–1302. doi:10.1021/np0106384

Suzuki, H., Aoyagi, S., and Kibayashi, C. (1995). Asymmetric total synthesis of (*R*)-(–)-cryptopleurine and (*R*)-(–)-julandine via highly enantioselective amidoalkylations with *N*-acylhydrazonium salts. *J. Org. Chem.* 60, 6114–6122. doi:10.1021/jo00124a025

Takeda, N., Futaki, E., Kobori, Y., Ueda, M., and Miyata, O. (2017). Nucleophilic arylation of *N,O*-ketene acetals with triaryl aluminum reagents: Access to alpha-aryl amides through an umpolung process. *Angew. Chem. Int. Ed.* 56, 16342–16346. doi:10.1002/anie.201708665

Thombal, R. S., Rubio, P. Y. M., Lee, D., Maiti, D., and Lee, Y. R. (2022). Modern palladium-catalyzed transformations involving C–H activation and subsequent annulation. *ACS Catal.* 12, 5217–5230. doi:10.1021/acscatal.2c00813

Vo, C.-V. T., and Bode, J. W. (2014). Synthesis of saturated *N*-heterocycles. *J. Org.Chem.* 79, 2809–2815. doi:10.1021/jo5001252

Weijiang, Y., and Herndon, James W. (2013). Total synthesis of (+)-antofine and (–)-cryptopleurine. *Eur. J. Org. Chem.* 2013, 3112–3122. doi:10.1002/ejoc.201300200

Yadav, A. K., Ila, H., and Junjappa, H. (2010). Synthesis of novel substituted phenanthrenes and polycyclic heteroarenes by Pd-catalyzed, direct, intramolecular arylation/heteroarylation. *Eur. J. Org. Chem.* 2010, 338–344. doi:10.1002/ejoc.200901036

Yamamoto, H., and Ishihara, K. (2008). *Acid catalysis in modern organic synthesis*. New York: Wiley.

Yamamoto, H. (2000). *Lewis acids in organic synthesis*. Weinheim: Wiley VCH.

frontiers | Frontiers in Chemistry

TYPE Original Research
PUBLISHED 29 September 2023
DOI 10.3389/fchem.2023.1272034

OPEN ACCESS

EDITED BY
Takashi Ohshima,
Kyushu University, Japan

REVIEWED BY
Tao Shi,
The Scripps Research Institute, United States
María De Gracia Retamosa,
University of Alicante, Spain

*CORRESPONDENCE
Kei Murakami,
kei.murakami@kwansei.ac.jp

RECEIVED 03 August 2023
ACCEPTED 18 September 2023
PUBLISHED 29 September 2023

CITATION
Hashimoto K, Higuchi D, Matsubara S and Murakami K (2023), Copper-catalyzed reaction of aziridine for the synthesis of substituted imidazolidine and imidazolidinone.
Front. Chem. 11:1272034.
doi: 10.3389/fchem.2023.1272034

Copper-catalyzed reaction of aziridine for the synthesis of substituted imidazolidine and imidazolidinone

Kota Hashimoto[1], Daiki Higuchi[1], Satoshi Matsubara[1] and Kei Murakami[1,2]*

[1]Department of Chemistry, School of Science, Kwansei Gakuin University, Sanda, Japan, [2]JST-PRESTO, Chiyoda, Japan

Herein we report a copper-catalyzed synthesis of imidazolidine by employing the reaction of aziridine with imine. The reaction smoothly provided a diverse range of 2-substituted imidazolidines with high compatibility with various functional groups. Moreover, during our investigation, we discovered that isocyanate also reacted with aziridine to yield substituted imidazolidinones efficiently. The versatility of these reactions was further demonstrated by their application in the synthesis of hybrid molecules derived from two pharmaceutical compounds. This approach opens new possibilities for the discovery of novel classes of bioactive molecules.

KEYWORDS

copper catalyst, aziridine, imine, isocyanate, imidazolidine, imidazolidinone, cyclization

1 Introduction

The construction of saturated nitrogen-containing heterocycles is of utmost importance as they are prevalent structures in a wide range of natural products and pharmaceuticals (Smith et al., 1999; Antonopoulos et al., 2008). Among such saturated azaheterocycles, the synthesis of substituted imidazolidines has received comparatively less attention than other mono-azaheterocycles, such as pyrrolidines. However, given that imidazolidine scaffolds have been identified in numerous bioactive molecules, the development of new synthetic methodologies for accessing these scaffolds is highly important (Figure 1A).

To access imidazolidine derivatives, aziridines have been widely employed as the starting materials (Figure 1B). Aziridines can be categorized into three types based on their reactivity: i) activated dipolar aziridines (Wu and Zhang, 2012; Shi et al., 2021), ii) activated vinyl aziridines (Lin et al., 2018; Spielmann et al., 2018), and iii) other substituted aziridines (Liu et al., 2017; Sengoden et al., 2017; Li et al., 2018; Tu et al., 2019; Pradhan et al., 2020). For type i), Shi et al. reported in 2021 the reaction of donor-accepter-type aziridines with 1,3,5-triazinanes through a [3 + 2] cycloaddition (Shi et al., 2021). This reaction demonstrated that aziridines can serve as efficient precursors for the synthesis of multi-substituted imidazolidines. Regarding type ii), Spielmann et al. reported the palladium-catalyzed [3 + 2] cycloaddition reaction of vinylaziridines with cyclic imines (Spielmann et al., 2018). The reaction proceeds through the formation of π-allylpalladium intermediate, which then reacts with the cyclic imine to yield the corresponding products. This approach allows for the

10.3389/fchem.2023.1272034

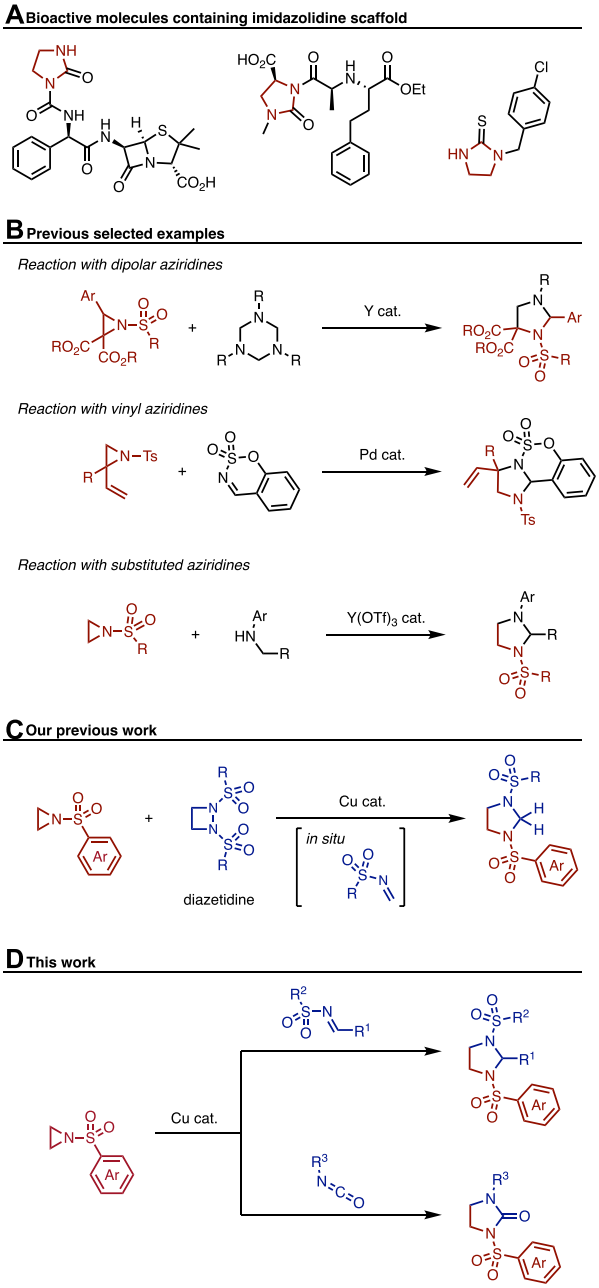

FIGURE 1
Background of this research.

diastereoselective synthesis of imidazolidine-fused tricyclic molecules. For type iii), Sengoden et al. reported copper-catalyzed reaction of aziridine with *N*-alkylanilines (Sengoden et al., 2017). This reaction involves the oxidation of aniline derivatives to generate an iminium intermediate *in situ*, which allows the efficient preparation of *N*-aryl-*N*-sulfonylimidazolidines. Despite the availability of various methods for accessing imidazolidines from aziridines, copper-catalyzed reactions of aziridines with imines or isocyanates have remained relatively underdeveloped (Zhu and Chiba, 2016; Bozorov et al., 2019; Pal et al., 2020; Pineschi, 2020; Zhang et al., 2022).

In this context, our previous study demonstrated the reaction of aziridine with diazetidine (Figure 1C), which led to the formation of imidazolidines (Higuchi et al., 2023). While the scope of this reaction was broad to construct various imidazolidines, the synthetic limitation associated with diazetidine hindered its widespread use for accessing imidazolidine derivatives. During our mechanistic investigation, we disclosed that an *in situ* formed imine reacted with aziridine to form the corresponding imidazolidine. This discovery motivated us to explore the reaction of aziridines with substituted imines to expand the scope of this transformation. Herein, we report the copper-catalyzed synthesis of imidazolidines through the reaction of aziridines with imines (Figure 1D). This transformation exhibits good functional group compatibility to afford the desired products efficiently. Additionally, we have successfully demonstrated that the use of isocyanates instead of imines allows accessing imidazolidinones. We have shown its application in the synthesis of hybrid molecules derived from Celecoxib and NLRP3 inflammasome inhibitor.

2 Results and discussions

We initiated our study by investigating the ligand effect for the reaction. The treatment of aziridine **1a** with imine **2a** in the presence of 10 mol% of CuBr and **L1** in toluene at 120 °C for 20 h afforded the corresponding imidazolidine **3a** in 72% isolated yield (Figure 2A). It is noteworthy that the ligand effect is critical where 6% of **3a** was obtained without the addition of **L1**. Furthermore, CuBr was found to be essential for the reaction, and no product was observed in the absence of both CuBr and **L1**. We then investigated the effect of ligands (Figure 2B). Although no clear correlation between ligand structure and catalytic activity was observed, 1,10-phenanthroline derivatives showed good results (^{1}H NMR yields using various ligands **L2**: 74% **L3**: 49%, **L4**: 43%). Similarly, 2,2-bipyridine derivatives also promoted the reaction (**L5**–**L8**: 14%–72% ^{1}H NMR yields.). After the screening, we decided to use **L1** as the optimal ligand because it provided the highest isolated yield.

The scope of the reaction was investigated (Figure 3). Initially, we examined the substituent effect on imines. The use of electron-withdrawing *p*-trifluoromethylphenyl group at the R^1 position allowed an efficient transformation to give **3b** in 80% yield. Other electron-withdrawing groups, such as *p*-bromo- or *p*-chlorophenyl groups, provided the corresponding products **3c** and **3d** in 88% and 84% yields, respectively. It is noteworthy that such halogen moieties can serve as footholds for further transformation. The reactions of electron-donating *p*-methyl- or

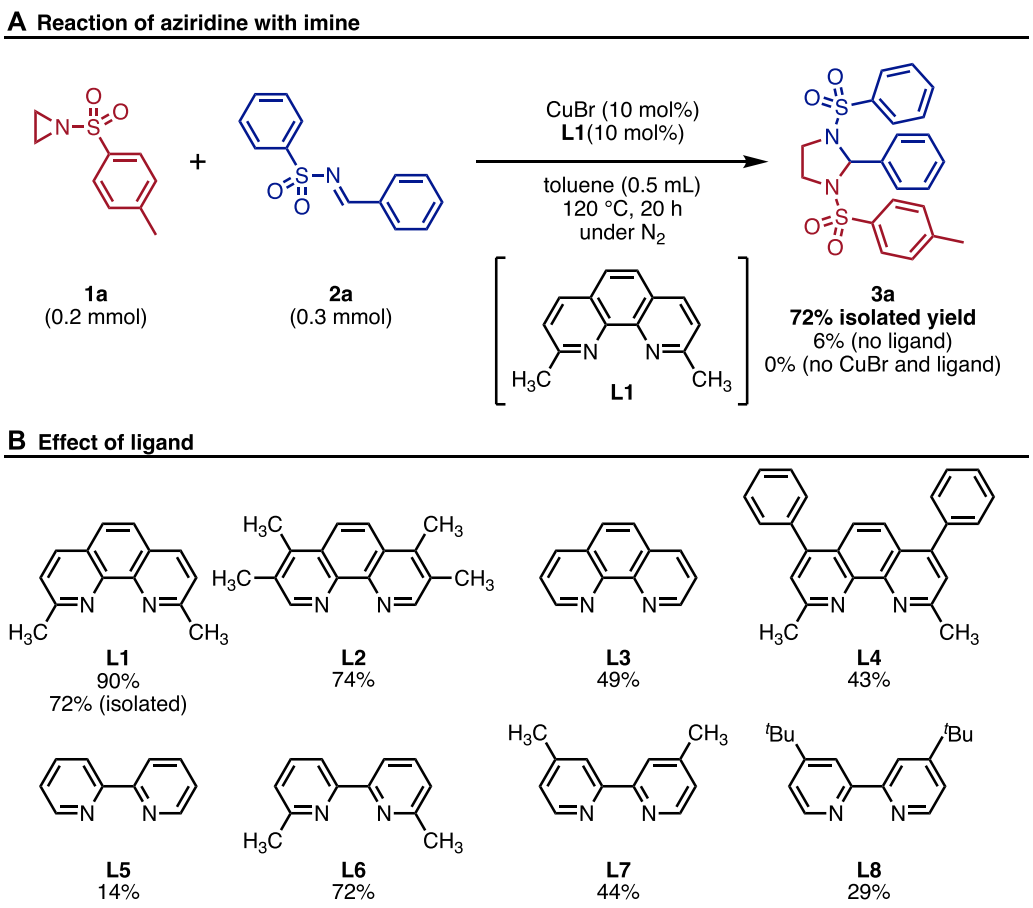

FIGURE 2
(A) Reaction of aziridine with imine. **(B)** Effect of ligand. ^{1}H NMR yields were shown using 1,1,2,2-tetrachloroethane.

p-methoxyphenyl-substituted imines were relatively sluggish, however, both starting materials were completely consumed. Not only *p*-substituted one but also *m*-substituted phenylsulfonylimine reacted smoothly converted to **3g** in 81% yield. Despite the bulky *o*-bromo-, or *o*-nitrophenyl groups, the corresponding products **3h** and **3i** were obtained in moderate to high yields. Although the yield was not high, imine **2j** derived from cinnamaldehyde, was applicable to the reaction to afford **3j** in 34% yield. A variety of sulfonyl groups were tolerated under the reaction conditions, where methylsulfonyl (Ms) or *o*-nitrophenylsulfonyl (Ns)-substituted imines provided **3k** and **3l** in 84% and 67% yields without the loss of these sulfonyl groups. When electron-donating group-substituted arylsulfonylaziridines were employed, the reactions were less effective and gave **3m** and **3n** in 25% and 49% yields, respectively. Furthermore, the reaction was applicable to cyclic imine to give **3o** in almost quantitative yield. Unsuccessful combinations of substrates are summarized at the bottom of Figure 3. The reactions of *N*-phenylimine or *N*-sulfoxyimine with **1a** failed to give the corresponding products. Although the reaction of unsubstituted aziridine **1a** with imine **2a** smoothly provided the products, the reaction of diphenylmethanimine or substituted aziridine failed. This can be attributed to steric hindrance, as the reaction of substituted aziridine proceeded smoothly with methanimine derivatives (Higuchi et al., 2023).

To expand the scope of the reaction, we employed isocyanate **4** as the coupling partner (Figure 4). The reaction of tosylaziridine **1a** with phenylisocyanate **4a** under the same optimized conditions afforded imidazolidinone **5a** in 74% yield. A variety of arylisocyanate was applicable to the reaction where electron-withdrawing *p*-acetyl-, *p*-chloro-, or electron-donating *p*-methoxyphenylisocyanate gave products **5b–5d** in 60%–83% yields. When tosylisocyanate was employed as the substrate, product **5e** was obtained in 64% yield. We then investigated the scope of substituted aziridines. Compared with the reaction with imine, the reaction with isocyanate showed a broader substrate scope of aziridines. The reaction of vinylaziridine afforded **5f** in 43% yield, and no isolable byproduct that reacted with the olefin was observed, leaving less than 20% of vinylaziridine remaining. Other substituents, such as methoxycarbonyl, benzyl, or

10.3389/fchem.2023.1272034

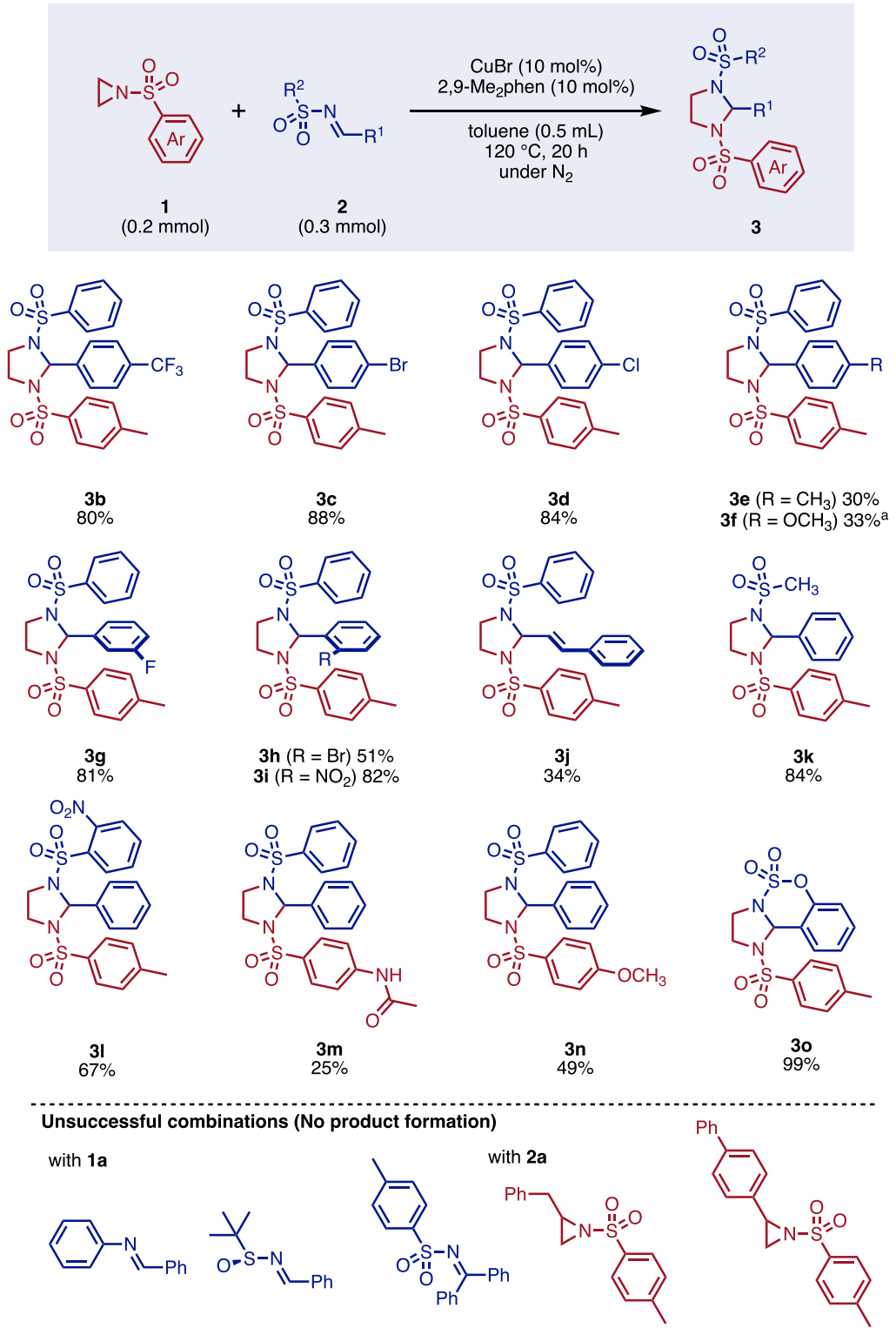

FIGURE 3
Scope of imidazolidine synthesis. [a] reaction time: 40 h.

biphenyl groups, were applicable to the reaction to give **5g**–**5i** in 36%–56% yields. Bicyclic aziridine **1h**, which can be prepared from cyclohexene, reacted to give **5j** in 22% yield. Although the yield was not high, the formal *cis*-diamination product can be obtained through this transformation (Minakata et al., 2021).

A proposed mechanism is shown in Figure 5. The reaction initiates with the coordination of aziridine **1** to copper catalyst **A**

10.3389/fchem.2023.1272034

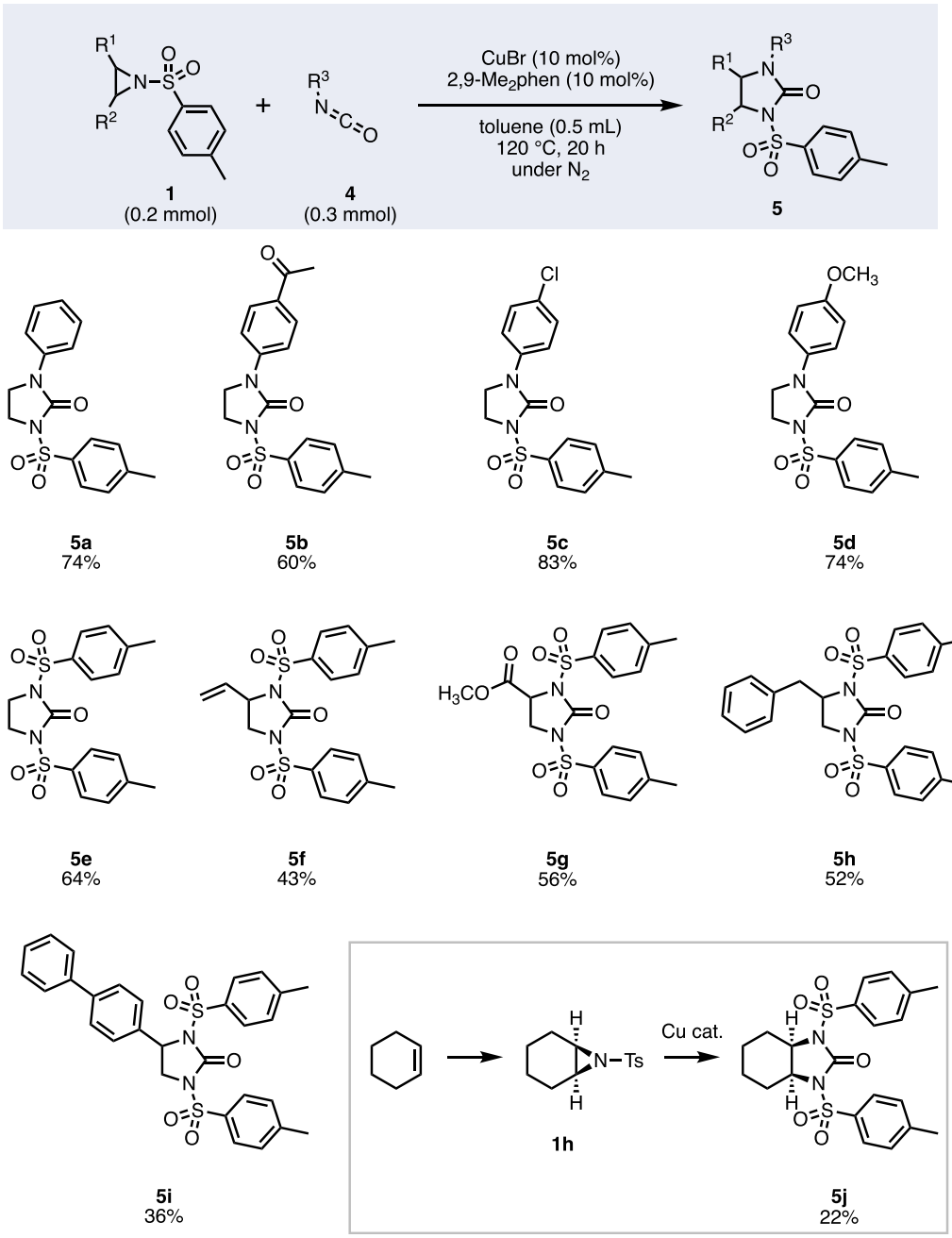

FIGURE 4
Scope of imidazolidinone synthesis.

to give the corresponding intermediate **B** (or **B′**). Subsequently, imine **2** attacks to open the aziridine ring to give intermediate **C** (or **C'**). Finally, a cyclization reaction takes place from **C** to give product **3**. From the result of the competitive experiment, the electron-donating group might reduce the reactivity of intermediate **C**, which hampers the cyclization and eventually the turnover of the catalyst. Note that another reaction mechanism can be depicted (see Supplementary Figure S1). At this stage, we considered that the reaction with isocyanate also proceeded through a similar reaction mechanism. Because it is difficult to elucidate the full reaction mechanism, further investigation is ongoing.

Finally, we applied the developed reaction to synthesize pharmaceutical hybrids (Figure 6). Firstly, we synthesized

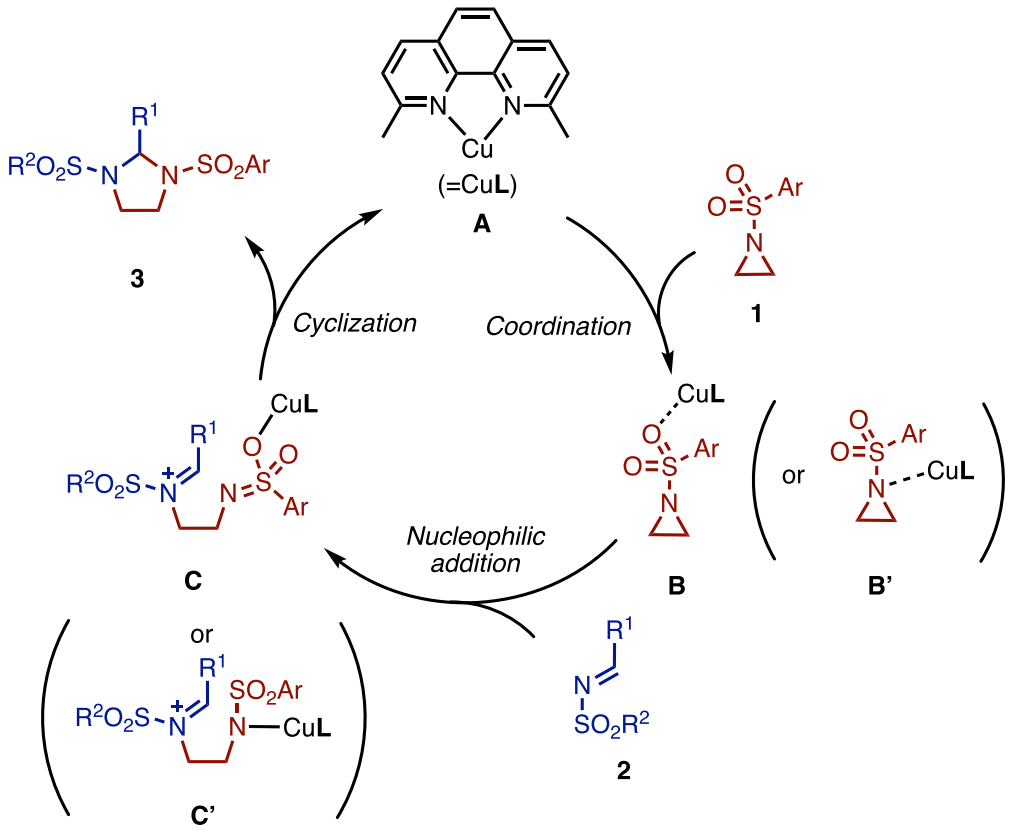

FIGURE 5
Proposed mechanism.

aziridine **1i** from Celecoxib (Ozaki et al., 2021). Aziridine **1i** was then reacted with imine **2m**, derived from an NLRP3 inflammasome inhibitor, to give **3p** in 51% yield. Furthermore, the reaction of aziridine **1i** with bis-isocyanate **4f** afforded product **5k** in 95% yield. These applications clearly demonstrate the excellent functional group compatibility that allows connecting various pharmaceuticals.

3 Conclusion

In conclusion, we have successfully reported the copper-catalyzed reaction of aziridine with imine and isocyanate, which afforded imidazolidine and imidazolidinone respectively. These developed reactions exhibited broad functional group compatibility to access a diverse array of potential bioactive 5-membered azaheterocycles. Furthermore, to demonstrate the practical applicability of these reactions, we prepared hybrids of pharmaceutical molecules using the developed reactions. These reactions surely facilitate the syntheses of complex azaheterocycles, which will accelerate the discovery of structurally new bioactive molecules in the future.

4 Materials and methods

For experimental procedures and compound characterization data, see the Supplementary Materials.

4.1 Experimental section

4.1.1 Experimental procedures and characterization data

4.1.1.1 General procedure for reaction of aziridine with imine

Aziridine (0.20 mmol, 1.0 equiv.), imine (0.30 mmol, 1.5 equiv.), copper bromide (3.0 mg, 0.020 mmol, 10 mol%), and 2,9-dimethyl-1,10-phenanthroline (4.2 mg, 0.020 mmol, 10 mol%) were added with a stirring bar to a dried Schlenk tube. The tube was filled with nitrogen. Toluene (0.5 mL) was added to the tube and the mixture was stirred at 120°C for 20 h. The crude mixture was passed through a short pad of silica gel and concentrated *in vacuo*. Purification by chromatography on silica gel provided the desired product.

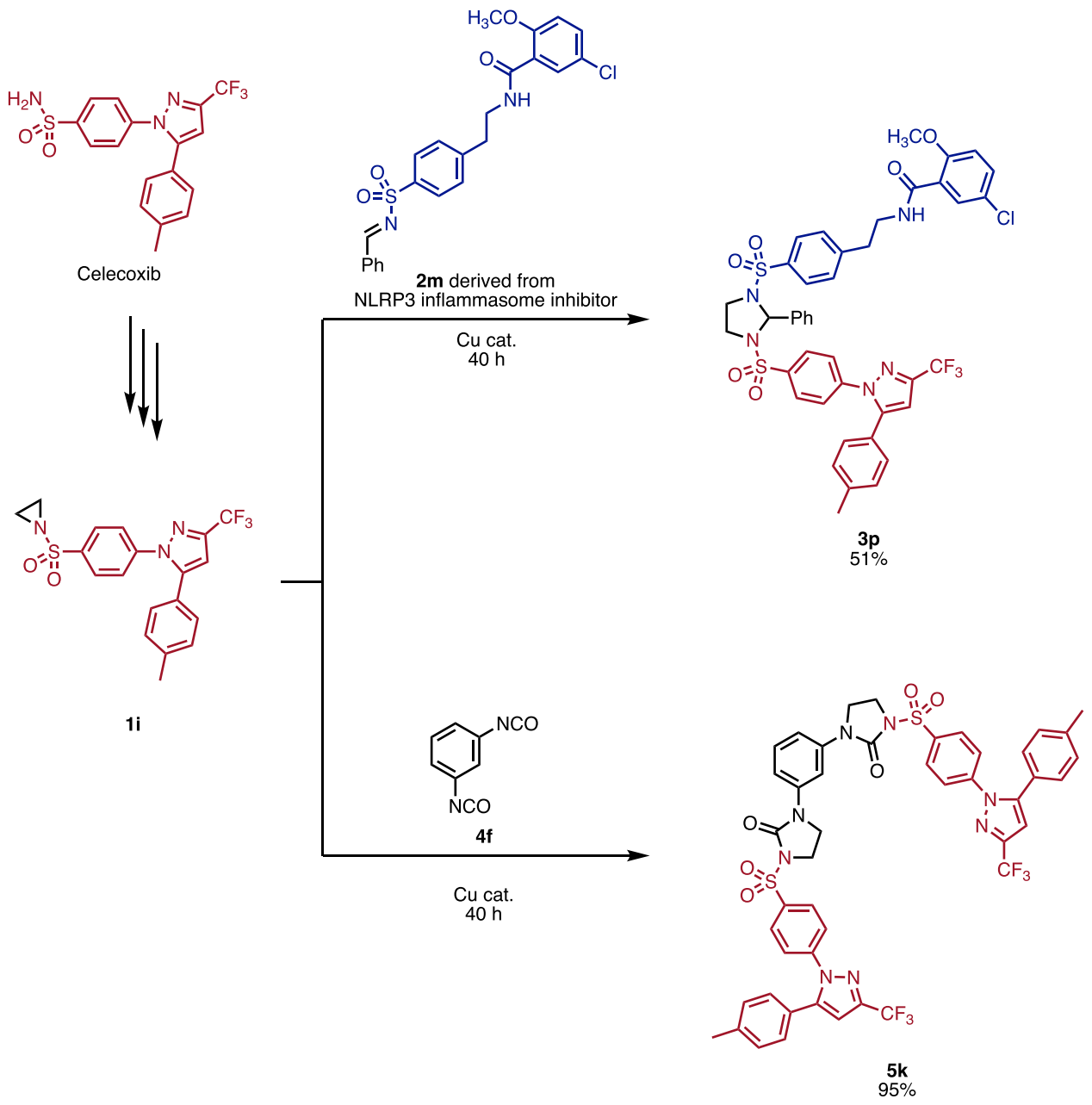

FIGURE 6
Application toward the syntheses of pharmaceutical hybrids.

4.1.1.2 General procedure for reaction of aziridine with isocyanate

Aziridine (0.20 mmol, 1.0 equiv.), isocyanate (0.30 mmol, 1.5 equiv.), copper bromide (3.0 mg, 0.020 mmol, 10 mol%), and 2,9-dimethyl-1,10-phenanthroline (4.2 mg, 0.020 mmol, 10 mol%) were added with a stirring bar to a dried Schlenk tube. The tube was filled with nitrogen. Toluene (0.5 mL) was added to the tube and the mixture was stirred at 120°C for 20 h. The crude mixture was passed through a short pad of silica gel and concentrated *in vacuo*. Purification by chromatography on silica gel provided the desired product.

Data availability statement

The original contributions presented in the study are included in the article/Supplementary Material, further inquiries can be directed to the corresponding author.

Author contributions

KH: Writing–review and editing. DH: Writing–review and editing. SM: Writing–review and editing. KM: Writing–original draft, Writing–review and editing.

Funding

The authors declare financial support was received for the research, authorship, and/or publication of this article. This work was supported by Japan Science and Technology Agency (JST) PRESTO Grant Number JPMJPR20D8 and the Kobayashi Foundation.

Conflict of interest

The authors declare that the research was conducted in the absence of any commercial or financial relationships that could be construed as a potential conflict of interest.

Publisher's note

Supplementary material

The Supplementary Material for this article can be found online at: https://www.frontiersin.org/articles/10.3389/fchem.2023.1272034/full#supplementary-material

References

Antonopoulos, S., Kokkoris, S., Gerakari, S., Mikros, S., Nitsotolis, T., Vikeli, D., et al. (2008). Comparison of monotherapy versus combination antihypertensive therapy in elderly patients with essential hypertension. *Angiology* 59, 230–235. doi:10.1177/0003319707304580

Bozorov, K., Zhao, J., and Aisa, H. A. (2019). 1,2,3-Triazole-containing hybrids as leads in medicinal chemistry: A recent overview. *Bioorg. Med. Chem.* 27, 3511–3531. doi:10.1016/j.bmc.2019.07.005

Higuchi, D., Matsubara, S., Kadowaki, H., Tanaka, D., and Murakami, K. (2023). Copper-catalyzed heterocyclic recombination of aziridine and diazetidine for the synthesis of imidazolidine. *Chem. Eur. J.* 29, e202301071. doi:10.1002/chem.202301071

Li, H., Huang, S., Wang, Y., and Huo, C. (2018). Oxidative dehydrogenative [2 + 3]-cyclization of Glycine esters with aziridines leading to imidazolidines. *Org. Lett.* 20, 92–95. doi:10.1021/acs.orglett.7b03448

Lin, T.-Y., Wu, H.-H., Feng, J.-J., and Zhang, J. (2018). Chirality transfer in rhodium(I)-Catalyzed [3 + 2]-cycloaddition of vinyl aziridines and oxime ethers: Atom-economical synthesis of chiral imidazolidines. *Org. Lett.* 20, 3587–3590. doi:10.1021/acs.orglett.8b01378

Liu, P., Xu, G., and Sun, J. (2017). Metal-free [2 + 1 + 2]-cycloaddition of tosylhydrazones with hexahydro-1,3,5-triazines to form imidazolidines. *Org. Lett.* 19, 1858–1861. doi:10.1021/acs.orglett.7b00600

Minakata, S., Miwa, H., Yamamoto, K., Hirayama, A., and Okumura, S. (2021). Diastereodivergent intermolecular 1,2-diamination of unactivated alkenes enabled by iodine catalysis. *J. Am. Chem. Soc.* 143, 4112–4118. doi:10.1021/jacs.1c00228

Ozaki, T., Yorimitsu, H., and Perry, G. J. P. (2021). Primary sulfonamide functionalization via sulfonyl pyrroles: Seeing the N-ts bond in a different light. *Chem. Eur. J.* 27, 15387–15391. doi:10.1002/chem.202102748

Pal, T., Lahiri, G. K., and Maiti, D. (2020). Copper in efficient synthesis of aromatic heterocycles with single heteroatom. *Eur. J. Org. Chem.* 2020, 6859–6869. doi:10.1002/ejoc.202000688

Pineschi, M. (2020). The binomial copper-catalysis and asymmetric ring opening of strained heterocycles: Past and future challenges. *Eur. J. Org. Chem.* 2020, 2643–2649. doi:10.1002/ejoc.201901853

Pradhan, S., Chauhan, N., Shahi, C. K., Bhattacharyya, A., and Ghorai, M. K. (2020). Stereoselective synthesis of hexahydroimidazo[1,2-*a*]quinolines via S_N2-type ring-opening hydroarylation–hydroamination cascade cyclization of activated aziridines with *N*-propargylanilines. *Org. Lett.* 22, 7903–7908. doi:10.1021/acs.orglett.0c02801

Sengoden, M., Bhowmick, A., and Punniyamurthy, T. (2017). Stereospecific copper-catalyzed domino ring opening and sp3 C–H functionalization of activated aziridines with N-alkylanilines. *Org. Lett.* 19, 158–161. doi:10.1021/acs.orglett.6b03458

Shi, Z., Fan, T., Zhang, X., Zhan, F., Wang, Z., Zhao, L., et al. (2021). Synthesis of diversely substituted imidazolidines *via* [3+2] cycloaddition of 1,3,5-triazinanes with donor-acceptor aziridines and their anti-tumor activity. *Adv. Synth. Catal.* 363, 2619–2624. doi:10.1002/adsc.202001569

Smith, A. L., Doershuk, C., Goldmann, D., Gore, E., Hilman, B., Marks, M., et al. (1999). Comparison of a β-lactam alone versus β-lactam and an aminoglycoside for pulmonary exacerbation in cystic fibrosis. *J. Pediatr.* 134, 413–421. doi:10.1016/s0022-3476(99)70197-6

Spielmann, K., van der Lee, A., de Figueriedo, R. M., and Campagne, J.-M. (2018). Diastereoselective palladium-catalyzed (3 + 2)-cycloadditions from cyclic imines and vinyl aziridines. *Org. Lett.* 20, 1444–1447. doi:10.1021/acs.orglett.8b00228

Tu, L., Li, Z., Feng, T., Yu, S., Huang, R., Li, J., et al. (2019). Access to imidazolidines via 1,3-dipolar cycloadditions of 1,3,5-triazinanes with aziridines. *J. Org. Chem.* 84, 11161–11169. doi:10.1021/acs.joc.9b01959

Wu, X., and Zhang, J. (2012). $Y(OTf)_3$-Catalyzed diastereoselective [3+2] cycloaddition of N-tosylaziridines and imines; efficient synthesis of multisubstituted imidazolidines. *Synthesis* 44, 2147–2154. doi:10.1055/s-0031-1290816

Zhang, Z., Chen, P., and Liu, G. (2022). Copper-catalyzed radical relay in $C(sp^3)$–H functionalization. *Chem. Soc. Rev.* 51, 1640–1658. doi:10.1039/d1cs00727k

Zhu, X., and Chiba, S. (2016). Copper-catalyzed oxidative carbon–heteroatom bond formation: A recent update. *Chem. Soc. Rev.* 45, 4504–4523. doi:10.1039/c5cs00882d

frontiers | Frontiers in Chemistry

TYPE Original Research
PUBLISHED 19 October 2023
DOI 10.3389/fchem.2023.1280633

OPEN ACCESS

EDITED BY
Hasan Küçükbay,
İnönü University, Türkiye

REVIEWED BY
Turan Ozturk,
Istanbul Technical University, Türkiye
Joel Teran,
Instituto de Ciencias, Mexico

*CORRESPONDENCE
Hyun-Joon Ha,
hjha@hufs.ac.kr

RECEIVED 21 August 2023
ACCEPTED 02 October 2023
PUBLISHED 19 October 2023

CITATION
Srivastava N and Ha H-J (2023), Regioselective ring opening of aziridine for synthesizing azaheterocycle. *Front. Chem.* 11:1280633. doi: 10.3389/fchem.2023.1280633

Regioselective ring opening of aziridine for synthesizing azaheterocycle

Nikhil Srivastava and Hyun-Joon Ha*

Department of Chemistry, Hankuk University of Foreign Studies, Yongin, Republic of Korea

Aziridine had different regioselective ring openings depending on the functional group of its alkyl substituent. In the case of the alkyl group bearing γ-ketone at the C2 substituent of aziridine, the ring opening by the hydroxy nucleophile from H_2O occurred by attacking the aziridine carbon at the C2 position. This reaction proceeded efficiently in the presence of CF_3CO_2H. Interestingly, the same starting aziridine ring bearing the alkyl substituent at the C2 position with the γ-silylated hydroxy group instead of γ-ketone led to the ring-opening reaction by the same oxygen nucleophile at the unsubstituted C3 position, with the breakage of the bond between aziridine N1 nitrogen and carbon at C3. These reaction products were cyclized to afford substituted pyrrolidine and piperidine rings with representative examples of congeners of pseudoconhydrine and monomorine.

KEYWORDS

aziridine, regioselectivity, ring opening, pyrrolidine, piperidine

Introduction

Aziridine, a nitrogen-containing three-membered ring, has been used for the synthesis of various azaheterocycles based on its chemical reactivity and unique regio- and stereoselectivity. In our lab, we have synthesized various azaheterocycles utilizing chiral aziridine in its optically pure forms (Ha et al., 2014; D'hooghe and Ha, 2016). Biologically active compounds including alkaloids with azaheterocycles have been prepared from enantiopure aziridines via aziridine ring formation from its acyclic compounds or its ring transformation (Srivastava et al., 2020). Transformation is mostly based on the formation of aziridinium ion with proper electrophiles and the subsequent ring-opening by nucleophiles either at C2 (pathway **b** in Scheme 1) or C3 (pathway **a** in Scheme 1) (Dolfen et al., 2016; Choi et al., 2017; Ranjith and Ha, 2021; Ranjith and Ha, 2022). The nucleophilic ring opening at C2 or C3 is controlled by substituents at the aziridine ring, electrophiles, and nucleophiles to provide acyclic amine **A** or **B**. The substituent cyclization gives rise to **Cyc-A** or **Cyc-B** (Scheme 1) (Eum et al., 2015; Yadav et al., 2016; Srivastava et al., 2020).

Herein, for the first time, we report the involvement of functionalization of 2-substituted aziridine-2-carboxylate to give piperidine alkaloids in an efficient regiochemical pathway of ring-opening reaction. More specifically, 2-(3 silylated-hydroxy and 3-keto alkyl) aziridine (**2** and **3**) prepared from the same chiral aziridine-2-carboxylate (**1**) reacted with nucleophiles for the ring-opening. These reactions proceeded in a regioselective manner through either pathway a or b to yield **4** or **5** which was then cyclized to give pyrrolidine (**6**) or piperidine (**7**) (Scheme 2).

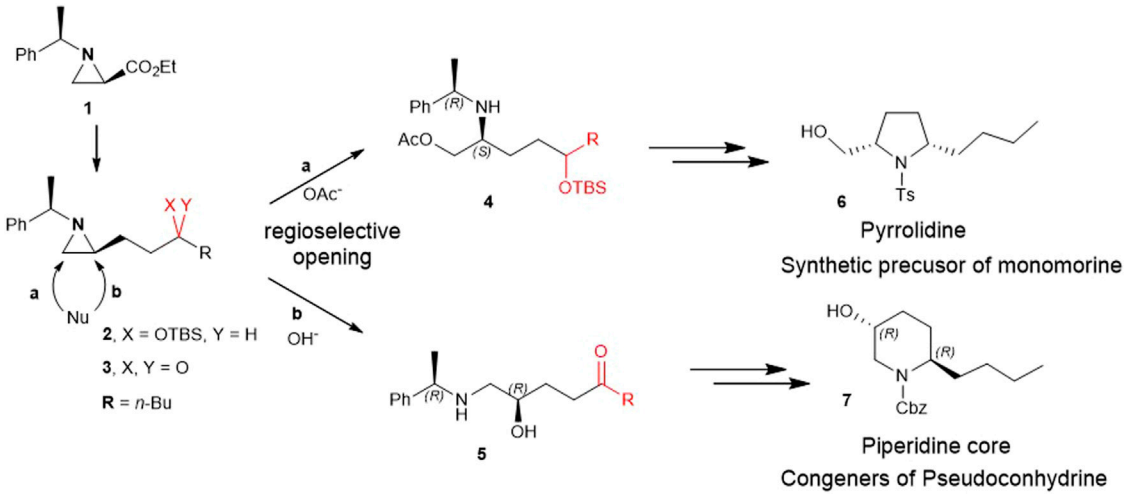

GRAPHICAL ABSTRACT
Regioselective ring opening of aziridine for synthesizing azaheterocycle.

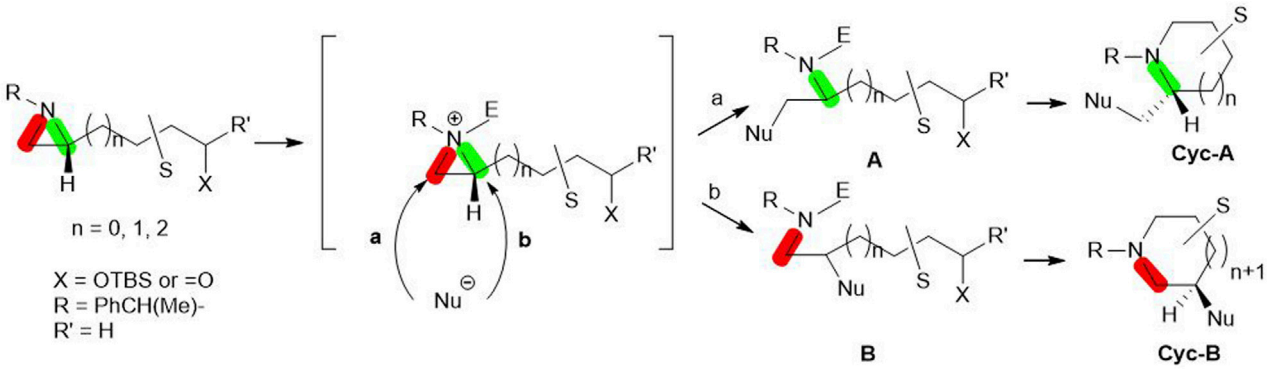

SCHEME 1
Aziridine ring-opening reactions by nucleophiles (either **a** or **b)** with breakage of bond C3-N (red) or C2-N (Green) to yield **A** or **B**. Subsequent cyclization of **A** or **B** decorated with the various functional groups(S) gives rise to either **Cyc-A** or **Cyc-B**.

Results and discussion

At first, the ring opening of aziridine was performed to give rise to either terminal amine or internal amines with the breakage of bonds N1-C2 or N1-C3, respectively. For the preparation of piperidine ring, screening of ring-opening reactions were carried out with the compound 1-((*S*)-1-((*R*)-1-phenylethyl)aziridin-2-yl) oct-7-en-3-one (**3a**) as a model substrate in Table 1, which was derived from (2*R*)-aziridine-2-carboxylates (**1**) (Its synthetic procedure is described in experimental section).

Starting with a typical protocol for the ring openings of aziridines with neat acetic acid for 4 h at room temperature over the compound ((*R*)-1-phenylethyl)aziridin-2-yl)oct-7-en-3-one **3a**, did not afford any ring-opening product (Table 1, entry 1). Up to date, almost all regiochemical pathway takes to yield internal amines regardless of substituents at the side chain functionality including simple halogen, amine, and hydroxyl groups (Stankovic et al., 2012; Ha et al., 2014). Therefore, we expected internal amine as a ring-opening product with breakage of the bond between N1 and C3 without any substituent. After varying solvents such as 1,4-dioxane and toluene and performing the reaction with acetic acid (1 equiv) at room temperature for 5 h, no ring-opened product was obtained (Table 1, entries 2 and 3) with all starting material stayed as they were. We then switched to another solvent, dichloromethane. A regioselective product with OAc group (*R*)-5-oxo-1-(((*R*)-1-phenylethyl)amino)dec-9-en-2-yl acetate **8** was obtained in less than 10% yield (Table 1, entry 4). To increase the yield, the experiment was further carried out with the same acetic acid (1 equiv) in 1,2-dichloroethane and THF for 6 h. However, reactions ended up with the recovery of starting material only (Table 1, entries 5 and 6). Then we switched over to trifluoracetic acid (TFA) as another protic acid. When the representative substrate ((*R*)-1-phenylmethyl)aziridine-2-yl)oct-7-en-3-one **3a** was treated with TFA (1 equiv) in CH_3CN:H_2O (9:1) for 5 h at the same room temperature, unexpectedly, only regioselective product (*R*)-2-hydroxy-1-(((*R*)-1-phenylmethyl)amino)dec-9-en-5-one **8** was obtained in 60% yield (Table 1, entry 7). Changing the mixed solvent ratio of CH_3CN:H_2O from 9:1 to 2:1, the yield for compound **8** was

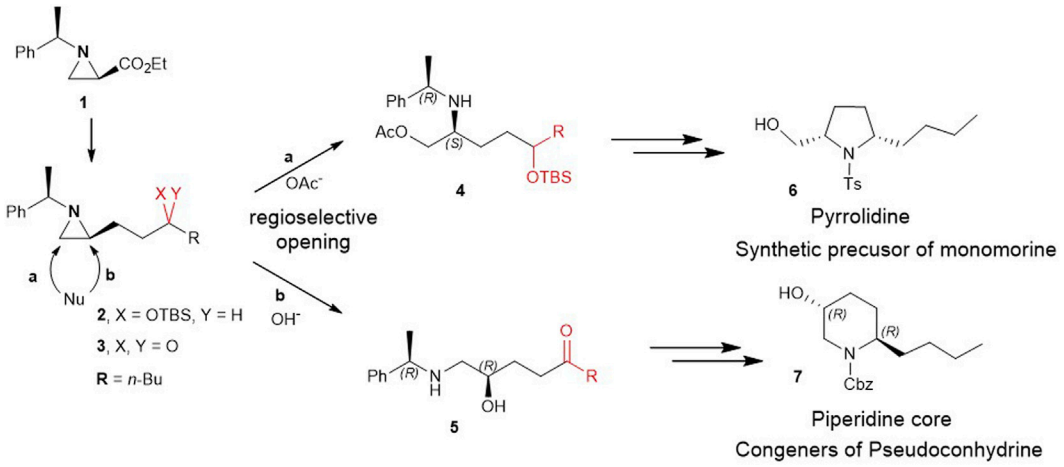

SCHEME 2
Ring-opening of 2-(3-hydroxy and 3-keto alkyl)aziridine (**2** and **3**) prepared from the same chiral aziridine-2-carboxylate (**1**) proceeds in a regioselective manner through either pathway **a** or **b** to yield **4** or **5** which is then cyclized to give pyrrolidine (**6**) or piperidine (**7**).

improved to 75% under the same condition with TFA (1 equiv) (Table 1, entry 8). Inspired by this outcome, the starting compound **3a** was treated with the TFA (1 equiv) at room temperature under acetone instead of CH_3CN. The yield was further improved to 80%. All these observations can be explained by the solubility and the way of the association between TFA and aziridine. This was further justified by changing the ratio of the acetone and H_2O solvent system with the ratio from 9:1 to 2:1 to give its ring-opened product (*R*)-2-hydroxy-1-(((*R*)-1-phenylmethyl)amino)dec-9-en-5-one (**8**) as a single isomer in a 90% yield (Table 1, entry 10). In continuation, switching to strong bronsted acid i,e. sulfuric acid (H_2SO_4) (1N) (1 equiv) also gave efficient regioselective ring opened product **8** in 82% yield under same acetone and H_2O (2:1) solvent system (Table 1, entry 11).

TABLE 1 Screening of regioselective opening of ((*R*)-1-phenylethyl)aziridin-2-yl)oct-7-en-3-one (3a).

Entry	Protic acid[b]	Solvent	t [h][c]	Yield of 8 (%)[d]
1	AcOH	Neat	4	No rxn
2	AcOH	1,4-Dioxane	5	No rxn
3	AcOH	Toluene	5	No rxn
4	AcOH	1,2-Dichloromethane	5	<8[e]
5	AcOH	1,2-Dichloroethane	6	No rxn
6	AcOH	THF	6	No rxn
7	TFA	CH_3CN/H_2O (9:1)	5	60
8	TFA	CH_3CN/H_2O (2:1)	5	75
9	TFA	Acetone/H_2O(9:1)	4	80
10	**TFA**	**Acetone/H_2O (2:1)**	**4**	**90**
11	H_2SO_4	Acetone/H_2O (2:1)	4	82

[a]Reaction performed at 0.6 mmol of compound A.
[b]Protic acid (1.0 equiv.).
[c]Time in hours.
[d]Isolated yield.
[e]Acylated product 8.

On the basis of the above experiments described in Table 1, a plausible mechanism is proposed as shown in Figure 1. Possibly the reaction is mediated by the protonation of aziridine-nitrogen to form *in situ* aziridinium ion via a transition state (**Ta**). In this transition state, nitrogen attached proton, simultaneously interacted with oxygen attached to carbonyl carbon-oxygen *via* hydrogen bonding. Due to this transition state (**Ta**), the hydroxy nucleophile from H_2O selectively approaches to attack at C2 carbon of the aziridinium ring exclusively in a regioselective manner (Figure 1) (Lopez and Salazar, 2013; Dalabehera et al., 2020). Under the same reaction conditions, other aziridinyl ketones such as 2-β- or 2-δ-ketoalkyl substituted aziridine yielded the mixture of the regioisomers of the ring-opened products which means that the conformation with fluorine is a driving force to determine the position of the nucleophilic attacks.

In order to support the plausible mechanistic pathway proposed above, we investigated ^{1}H-NMR spectral change studies for the regioselective ring opening reaction over compound **3a** with TFA under deuterated acetone (d_6)/D_2O (2:1) solvent system (See in Supplementary Material S2; Figure 1). It was interesting to observe firstly an increase in δ ppm values in both N- benzylic (quartet at 4.00 ppm) and methyl protons (doublet at 1.85 ppm) after 20 min. It happened due to the formation of *in situ* N-aziridinium ion via transition state (**Ta**). Then after 1 h, the formation of a new quartet (at 4.63 ppm) of N-benzylic and a doublet of newly methyl protons at 1.81 ppm were observed, which confirmed the regioselective ring opening reaction process happened in a concerted manner. Finally, after 4 h formation of product **8** in a protonated form, via the regioselective ring opened process was fully confirmed during ^{1}H-NMR change studies (See in Supplementary Material S2, Figure 1).

After establishing standard reaction conditions for regioselective aziridine ring opening, we then utilized this method for the synthesis of piperidine core **7** bearing substituents at C2. Those structures are cores of congeners analog to pseudoconhydrine (Scheme 3). Accordingly, we started our synthesis from chiral (2*R*)-aziridine-2-carboxylates (**1a**) as a

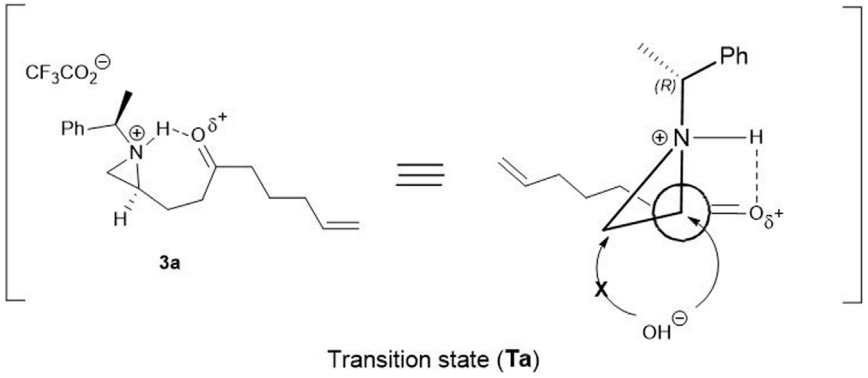

FIGURE 1
A schematic representation of plausible transition state (**Ta**) with keto compound **3a** for the regioselective opening of aziridine moiety.

starting material. The preparation of compound (*E*)-methyl 3-((*S*)-1-((*R*)-1-phenylethyl)aziridin-2-yl)acrylate (**1c**) was easily achieved from Swern oxidation of ((*R*)-1-((*R*)-1-phenylethyl)aziridin-2-yl)methanol (**1b**), followed by a Wittig reaction for the two carbon extension, resulting compound **1c** in a yield of 82% of isomers with the *cis: trans* ratio 88:12 using protocols for previously known sequential reactions (Scheme 3) (Lee and Ha, 2003; Yoon et al., 2010). After treatment with 2-nitrobenzenesulfonylhydrazide (NBSH), this olefinic product **1c** was then saturated to afford compound **1d** in 95% yield (Lee et al., 2009). The saturated methyl ester **1d** was then converted to Weinreb amide **1e**, followed by a reaction with *n*-C_4H_9MgCl, which afforded γ-aziridinyl ketone **2** in 80% yield (Macha and Ha, 2019). Based on the outcomes shown in Table 1, we then treated compound **2** following our established protocol for the regioselective aziridine ring-opening reaction with TFA under the mixed solvent system, acetone and H_2O (2:1), at room temperature for 4 h. This yielded a hydroxy opened product **5** in 90% yield. Compound (*R*)-2-hydroxy-1-(((*R*)-1-phenylethyl)amino)nonan-5-one (**5**) was then treated with atmospheric H_2 at room temperature under the catalytic amount of $Pd(OH)_2$, yielding cyclic compound, followed by the reaction with CbzCl. These sequential reactions afforded *N*-Cbz-protected (2*S*,5*R*)-benzyl 2-butyl-5-hydroxypiperidine-1-carboxylate (**7**) (*dr* > 98:2) in 80% yield

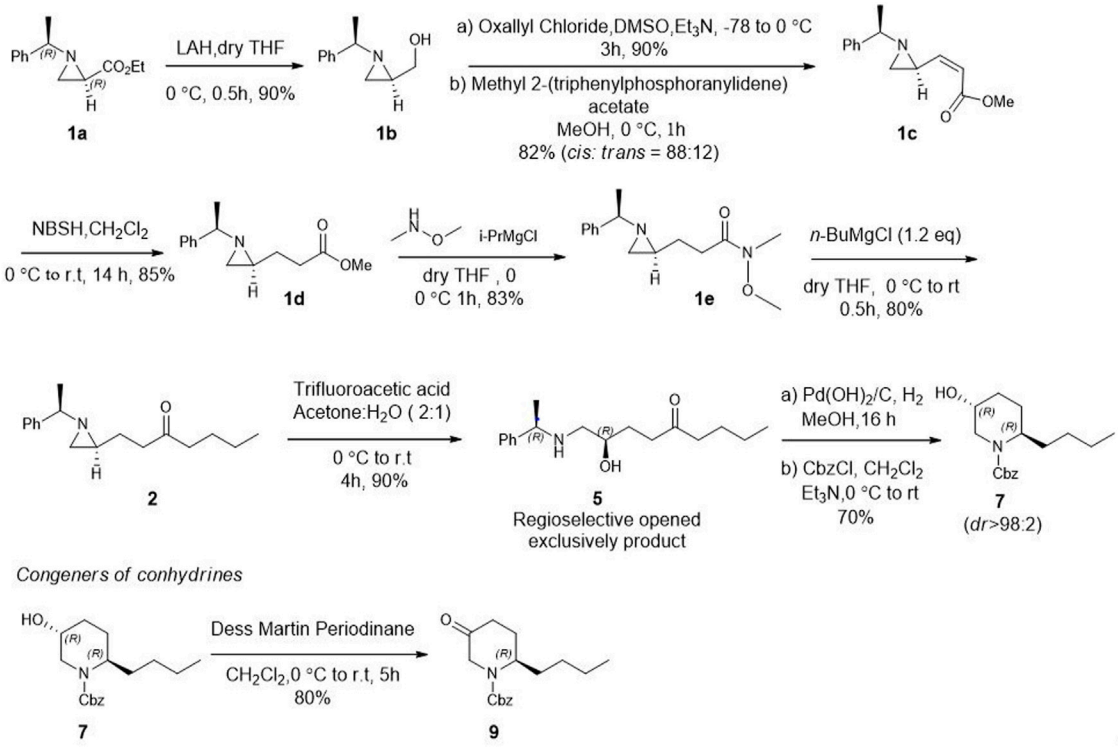

SCHEME 3
Asymmetric synthesis of congeners of pseudoconhydrine from (2*R*)-aziridine-2-carboxylate (**1**) via regioselective aziridine ring opening reaction as a key step.

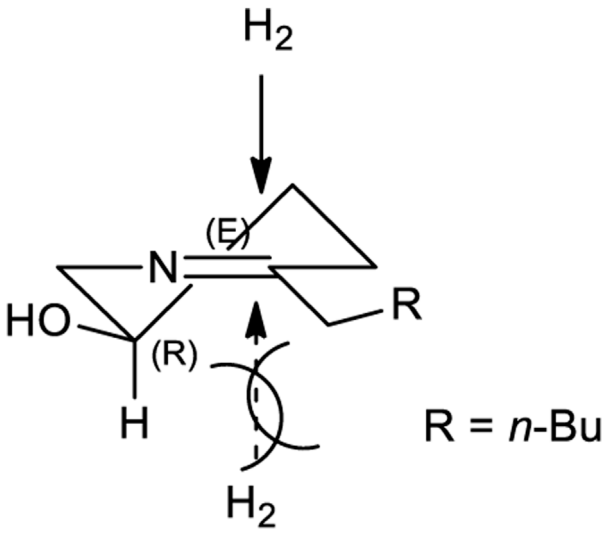

FIGURE 2
A Stereochemical aspect for one-pot hydrogenation of reductive amination for the synthesis of 2,5-*trans* piperidine core (**7**).

of two steps. The formation of compound **7** as a piperidine core skeleton (Macha et al., 2019) was obtained as a congener of pseudoconhydrine piperidine alkaloid (Bates et al., 2011). The formation of piperidine core **7** was executed with one-pot sequential debenzylation under hydrogenolysis followed by *in situ* cyclized via intramolecular reductive amination. Diastereoselectivity and assigned stereochemistry at the newly created center were then accessed. It was found that hydrogenation of a more stable intermediate imine could derive from a less hindered *β*-face of the molecule, resulting in a 2,5-*trans*-piperidine (Lee et al., 2003; Rao and Kumar, 2006) (Figure 2).

In addition, when compound **7** was further treated for oxidation under Dess-Martin periodinane, it produced 2-butyl-5-oxopiperidine (**9**) in 80% yield. Synthesizing this structural type of piperidone **9** (Ying et al., 2018; Lin et al., 2022) is an important intermediate to preparing various other biologically important 3-substituted piperidines (Vataku et al., 2014). The synthesis of 2-alkyl 5-hydroxy piperidine (**7**) and 2-alkyl 5-piperidone (**9**) with diverse substituents at C2 can be achieved efficiently using our regioselective opening protocol for γ-aziridinyl ketone which is prepared from commercially available (2*R*) aziridine −2 carboxylate at ease.

Encouraged by the synthesis of piperidine core, we decided to synthesize pyrrolidine core moiety **11** in which two alkyl groups at C2 and C5 of pyrrolidine are in a *cis*-stereo relationship (Scheme 4). Accordingly, a regioselective aziridine ring opening driven by the breakage of the bond between N1 and C3 of 2-alkyl aziridine is needed. This could be again prepared from the same starting substrate **1d**, which was achieved from chiral aziridine-2-carboxylate (**1a**) at ease. Ester **1d** was reduced to aldehyde by DIBAL and then alkylated with *n*-butyl magnesium chloride in dry THF to give alcohol (**10**) in

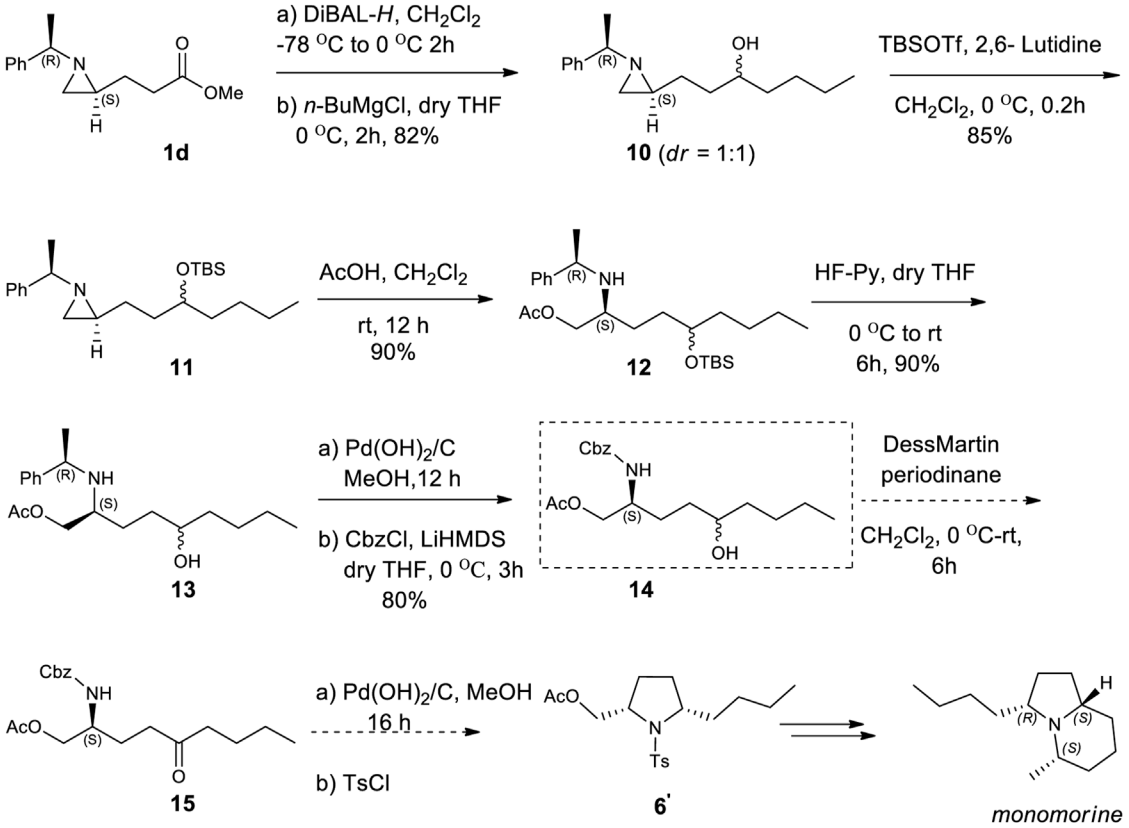

SCHEME 4
Asymmetric synthesis of monomorine from (2*R*)-aziridine-2-carboxylate (**1**) via regioselective aziridine ring opening reaction as a key step.

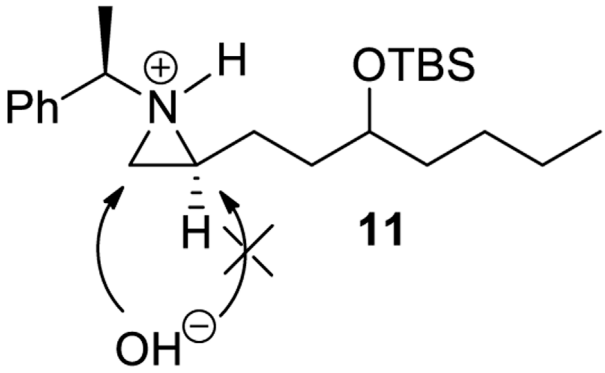

FIGURE 3
A plausible transition state for a regioselective opening of **11**.

82% yield for both diastereomers. The stereoselectivity of this alcohol was almost 1:1, which was not important because it would be oxidized for the formation of a pyrrolidine ring (Scheme 4). Both diastereomeric products **10** were treated with TBSOTf under 2,6-lutidine to afford silyl-protected **11** with a yield of 85%. Compound **11** was then subject to a regioselective aziridine ring-opening reaction under acetic acid conditions to give acetate-opened product **12** in a 90% yield (Singh et al., 2011). The drastic difference in the regioselectivity of **11** from the case of γ-ketoalkyl substituent (**2**) could be explained by the difference in the transition state (Figures 1, 3). A plausible transition state for the regioselective opening of **11** is only protonation of aziridine ring to form aziridinium ion in transition state **11**, followed by opening of aziridinium ion by oxygen nucleophiles from less-hindered C3 site (Figure 3).

As expected from the previous studies, we observed a ring-opened product with breakage of N1 and C3 bearing substituent which was different from a ring-opened product of γ-keto aziridine. To determine the regiochemical difference by acid, we treated compound **11** with CF_3CO_2H as shown in entry 10 of Table 1. It failed to give a ring-opened product with a decent yield. After achieving acetate compound **12**, it was treated under HF·Pyridine condition in dry THF to give hydroxy compound **13** in a yield of 80%. Surprisingly, the triers to oxidize **13** under various oxidation conditions were unable to yield an oxidized product in a decent yield. Changing the 2-phenylethyl to N-Cbz as protecting group from sequential reactions consisting of debenzylation followed by CbzCl in LiHMDS base at 0 °C afforded compound **14** in 80% yield. With the known established protocol of oxidation (Srivastava and Ha, 2022) followed by deprotection of Cbz and cyclization under hydrogen in catalytic $Pd(OH)_2$ gave 2,5-*cis* pyrrolidine (**6′**), the essential core skeleton of many pyrrolidines and indolizidine alkaloids including monomorine (Wang et al., 2009; Michael, 2016).

Conclusion

In conclusion, we have successfully developed a regioselective ring opening reaction of aziridine moiety. The key feature includes the involvement of the functional group (γ-ketone or γ-silylated hydroxy group) present at the alkyl substituent of aziridine, which played a crucial role in the regioselective ring opening reaction of aziridine. In the case of γ-ketone group, the ring opening of aziridine occurred at carbon C2 position by hydroxy nucleophile from H_2O under TFA condition in an efficient manner. Interestingly, in the case of γ-silylated hydroxy group present at the alkyl substituent of aziridine, the regioselective ring-opening reaction occurred at unsubstituted carbon C3 position of aziridine by the acetate oxygen nucleophile under acetic acid condition. These reaction products were cyclized to afford substituted pyrrolidine and piperidine rings with representative examples of congeners of pseudoconhydrine and monomorine.

Experimental section

Materials and methods

General Remarks. Chiral aziridine-2-carboxylates were obtained as their methyl ester from Sigma-Aldrich as reagents and from Imagene Co., Ltd. (http://www.imagene.co.kr/) in bulk quantities. Their corresponding ethyl esters were also obtained either from the transesterification of methyl ester or from Imagene (http://www.imagene.co.kr/) in bulk quantities. All commercially available compounds were used as received unless stated otherwise. All reactions were carried out under an atmosphere of nitrogen in oven-dried glassware with a magnetic stirrer. Reactions were monitored by thin layer chromatography (TLC) with 0.25 mm·E. Merck pre-coated silica gel plates (60 F254). Visualization was accomplished with either UV light or by immersion in a solution of ninhydrin, p-anisaldehyde, or phosphomolybdic acid (PMA) followed by heating on a hot plate for about 10 s. Purification of the reaction product was carried out by flash chromatography using Kieselgel 60 Art 9385 (230–400 mesh). 1H NMR and 13C NMR spectra were obtained using Varian unity INOVA 400WB (400 MHz) or Bruker AVANCE III HD (400 MHz) spectrometer. Chemical shifts are reported relative to chloroform (δ = 7.26) for 1H NMR and chloroform (δ = 77.0) for 13C {1H} proton-decoupled carbon NMR. Data are reported as (br = broad, s = singlet, d = doublet, t = triplet, q = quartet, p = quintet, m = multiplet). Coupling constants are given in Hz. Ambiguous assignments were resolved based on standard one-dimensional proton decoupling experiments. Optical rotations were obtained using a Rudolph Autopol III digital polarimeter and a JASCO P-2000. Optical rotation data are reported as follows [α]20 (concentration c = g/100 mL, solvent). High-resolution mass spectra were recorded on a 4.7 T Ion Spec ESI-TOFMS, JEOL (JMS-700). An AB Sciex 4800 Plus MALDI TOFTM (2,5-dihydroxybenzoic acid (DHB) matrix was used to prepare samples for MS. Data were obtained in the reflector positive mode with internal standards for calibration.

Typical procedure and characteristic data

1-((S)-1-((R)-1-phenylethyl)aziridin-2-yl) oct-7-en-3-one compound: (3a)

To a stirred solution of chiral N-methoxy-N-methyl-3-((*S*)-1-((*R*)-1-phenylethyl)aziridin-2-yl)propanamide (1e) (500 mg,

1.9 mmol, 1.0 equiv.) in dry THF (25 mL) at 0°C, 4-pentenylmagnesium bromide solution C_5H_9MgBr (4.0 mL, 0.5 M in THF, 3.81 mmol) was added. The reaction mixture was slowly warmed to room temperature and stirred for 0.5 h. After completion as per TLC indication, the reaction was quenched with saturated NH_4Cl (3 mL). The crude mixture was extracted with EtOAc (3 × 15 mL), dried over anhydrous Na_2SO_4, and concentrated under vacuum to afford crude product 3a, which was then purified by column chromatography to give compound 1-((*S*)-1-((*R*)-1-phenylethyl)aziridin-2-yl)oct-7-en-3-one (**3a**) as a viscous liquid (415 mg, 80% yield), TLC R_f (30% EtOAc/hexane = 0.30).

$[\alpha]^{20}_D$ = + 25.8 (*c* = 0.7, MeOH); **^{1}H NMR** (400 MHz, $CDCl_3$): δ 7.40–7.25 (m, 5 H), 5.87–5.73 (m, 1 H), 5.08–4.97 (m, 2 H), 2.68–2.57 (m, 2 H), 2.48 (t, *J* = 7.4 Hz, 2 H), 2.41 (q, *J* = 6.2 Hz, 1 H), 2.13–2.04 (m, 1 H), 2.02–1.89 (m, 1 H), 1.80–1.66 (m, 2 H), 1.60–1.53 (m, 2 H), 1.51–1.48 (m, 1 H), 1.43 (d, *J* = 6.6 Hz, 3 H), 1.32–1.27 (m, 1 H); **^{13}C NMR** (101 MHz, $CDCl_3$): 210.43, 144.44, 137.95, 128.24, 126.90, 126.73, 115.20, 69.60, 41.83, 40.48, 39.32, 33.47, 33.06, 27.05, 23.31, 22.70; **HRMS-ESI** (*m/z*) $[M+H]^+$ calcd. for $C_{18}H_{26}NO^+$ 272.2014; found 272.2006.

(R)-2-hydroxy-1-(((R)-1-phenylethyl)amino) dec-9-en-5-one: (8)

To a stirred solution of 1-((*S*)-1-((*R*)-1-phenylethyl)aziridin-2-yl) oct-7-en-3-one (3a) (165 mg, 0.60 mmol) in acetone (2.0 mL) and water (1.0 mL) solvent system, trifluoro acetic acid (TFA) (0.05 mL, 0.87 mmol, 1.0 equiv.) was added at 0°C. The mixture was then stirred at room temperature for 4 h. After completion of the reaction per TLC indication, the reaction was quenched with a saturated solution of $NaHCO_3$ (1 mL) and extracted with CH_2Cl_2 (4 × 10 mL). After concentrating under vacuum, the crude product was purified by flash column chromatography on silica gel to afford a pure product **8** (157 mg, 90%) TLC R_f (90% EtOAc/hexane = 0.1).

$[\alpha]^{20}_D$ = + 18.2 (*c* = 0.14, MeOH); **^{1}H NMR** (400 MHz, $CDCl_3$): δ 7.40–7.20 (m, 5 H), 5.86–5.68 (m, 1 H), 5.06–4.91 (m, 2 H), 3.81–3.70 (m, 1 H), 3.53–3.37 (m, 1 H), 2.63–2.45 (m, 2 H), 2.45–2.36 (m, 2 H), 2.11–1.96 (m, 2 H), 1.74–1.51 (m, 3 H), 1.42–1.33 (m, 3 H); **^{13}C NMR** (101 MHz, $CDCl_3$): δ 211.26, 144.82, 137.94, 128.55, 127.15, 126.45, 115.18, 69.36, 58.61, 53.38, 41.97, 38.91, 33.04, 28.55, 23.83, 22.77; **HRMS-ESI** (m/z) $[M+H]^+$calcd. for $C_{18}H_{28}NO_2^+$ 290.2120; found 290.2115.

(Z)-methyl 3-((S)-1-((R)-1-phenylethyl) aziridin-2-yl)acrylate: (1c)

To a stirred solution of oxalyl chloride (3.62 mL, 42.31 mmol, 1.5 equiv) in CH_2Cl_2 (80 mL) at −78°C, dimethyl sulfoxide (6.01 mL, 84.63 mmol, 3.0 equiv.) was added over 15 min. The resulting mixture was stirred for another 40 min. Then a solution of ((*R*)-1-((*R*)-1-phenylethyl)aziridin-2-yl)methanol **1b** (5.0 g, 28.21 mmol) in CH_2Cl_2 (30 mL) was added dropwise at the same temperature. The reaction mixture was stirred for 1.5 h at the same temperature. Triethylamine (11.81 mL, 42.31 mmol, 3.0 equiv.) was then added at −78°C and allowed to stir at the same temperature for 30 min. It was then warmed to 0°C and stirred for 30 min. After completion of the reaction per TLC indication, the reaction mixture was quenched with water (80 mL) and extracted with CH_2Cl_2 (2 × 100 mL). Combined organic layers were dried over anhydrous Na_2SO_4 and concentrated under reduced pressure to obtain a crude aldehyde which was used for the Wittig reaction without further purification.

To a solution of [(1*R*)-phenylethylaziridine]-(2*R*)-carboxaldehyde (3.0 g, 17.12 mmol, 1.0 equiv) in MeOH (34 mL), methyl triphenylphosphoranylideneacetate (6.86 g, 20.54 mmol, 1.2 equiv.) was added at 0°C. The resulting mixture was allowed to stir for 1 h at 0°C. After completion of the reaction, methanol was removed under vacuum and H_2O (2 × 50 mL) was added to the reaction mixture. The organic layer was then extracted with CH_2Cl_2 (3 × 100 mL), dried over anhydrous Na_2SO_4, and concentrated under a vacuum. The crude product was purified by flash column chromatography on silica gel to afford a pure product (Z)-methyl 3-((S)-1-((R)-1-phenylethyl) aziridin-2-yl)acrylate **1c** (3.2 g, 82%) TLC R_f (30% EtOAc/hexane = 0.4).

$[\alpha]_D$ = +58.3 (*c* = 16.20, in $CHCl_3$); **^{1}H NMR** (400 MHz, $CDCl_3$): δ 7.43–7.22 (m, 6 H), 6.78 (dt, *J* = 13.1, 6.6 Hz, 1 H), 6.20–6.09 (m, 1 H), 5.98–5.82 (m, 2 H), 3.78 (s, 3 H), 2.66–2.59 (m, 1 H), 2.21–2.10 (m, 1 H), 1.86–1.72 (m, 2 H), 1.70–1.63 (m, 1 H), 1.47 (t, *J* = 6.8 Hz, 1 H), 1.43 (dd, *J* = 6.5, 1.6 Hz, 1 H); **^{13}C NMR** (101 MHz, $CDCl_3$): δ 166.57, 150.51, 148.54, 143.78, 128.25, 127.01, 126.64, 126.61, 121.22, 120.17, 69.62, 51.09, 39.45, 37.32, 22.89; **HRMS-ESI** (*m/z*) $[M+1]^+$calcd. for $C_{14}H_{18}NO_2^+$ 231.1337; found $C_{14}H_{18}NO_2^+$- H+ 231.1331.

Methyl 3-((S)-1-((R)-1-phenylethyl)aziridin-2-yl)propanoate (1d)

To a stirred solution of olefin, **1c** (2.0 g, 8.64 mmol) in CH_2Cl_2 (24 mL) at 0°C, 2-nitrobenzenesulfonylhydrazide (NBSH) (7.5 g, 34.58 mmol, 4.0 equiv) was added. Then triethylamine (10.0 mL, 69.17 mmol, 8.0 equiv) was added in a dropwise manner at the same 0°C. The reaction mixture was then allowed to stir at room temperature for an additional 12 h. After completion of starting material as confirmed by TLC, the reaction mixture was quenched with saturated $NaHCO_3$ solution, extracted with CH_2Cl_2 (3 × 50 mL), and concentrated under vacuum to give a crude product 1d, which was then purified by column chromatography to give compound methyl 3-((*S*)-1-((*R*)-1-phenylethyl)aziridin-2-yl) propanoate (**1d**) as a viscous liquid (1.72 g, 85% yield), TLC R_f (40% EtOAc/hexane = 0.30).

$[\alpha]^{20}_D$ = + 35.4 (*c* = 0.32, MeOH); **^{1}H NMR** (400 MHz, $CDCl_3$): δ 7.40–7.23 (m, 5 H), 3.72 (s, 3 H), 2.58–2.51 (m, 2 H), 2.42 (q, *J* = 6.5 Hz, 1 H), 2.02–1.93 (m, 1 H), 1.65–1.58 (m, 2 H), 1.52 (d, *J* = 3.2 Hz, 1H), 1.44 (d, *J* = 6.6 Hz, 3 H), 1.36–1.27 (m, 1 H); **^{13}C NMR** (101 MHz, $CDCl_3$) δ 173.71, 144.49, 128.22, 126.87, 126.71, 69.60, 51.52, 39.10, 33.41, 31.91, 28.26, 23.27; **HRMS-ESI** (*m/z*) $[M+H]^+$calcd. for $C_{14}H_{20}NO_2^+$ 234.1494; found 234.1486.

N-methoxy-N-methyl-3-((S)-1-((R)-1-phenylethyl)aziridin-2-yl)propanamide (1e)

To a stirred solution of saturated ester **1d** (1.5 g, 6.42 mmol, 1.0 equiv.) and N,O-dimethylhydroxylamine hydrochloride (1.15 g, 9.64 mmol, 1.5 equiv.) in dry THF (22 mL) at 0°C, *i*-PrMgCl

(9.6 mL, 2.0 M in THF, 19.28 mmol, 3.0 equiv.) was slowly added. The reaction mixture was stirred for 1 h at the same 0°C. After completion of the reaction as per TLC, the reaction mixture was quenched with saturated NH_4Cl solution (2 mL) and extracted with EtOAc (4 × 50 mL). Combined organic layers were dried over anhydrous Na_2SO_4. Under vacuum, solvents were removed to obtain a crude amide product, which was purified by column chromatography to give a pure Weinreb amide product (**1e**) (1.40 g, 83% yield), TLC R_f (90% EtOAc/hexane = 0.1).

$[\alpha]^{20}_D$ = + 28.3 (*c* = 0.70, MeOH); **^{1}H NMR** (400 MHz, CDCl3): δ 7.37–7.15 (m, 5 H), 3.63 (d, *J* = 14.7 Hz, 3 H), 3.17–3.09 (m, 3 H), 2.60 (dd, *J* = 14.3, 8.6 Hz, 2 H), 2.37 (q, *J* = 6.5 Hz, 1 H), 1.98–1.86 (m, 1 H), 1.65–1.51 (m, 2 H), 1.46 (d, *J* = 3.3 Hz, 1 H), 1.39 (d, *J* = 6.6 Hz, 3 H), 1.25 (d, *J* = 6.3 Hz, 1 H);**^{13}C NMR** (101 MHz, $CDCl_3$): δ 173.76, 144.20, 127.90, 126.54, 126.43, 69.23, 60.81, 39.24, 33.25, 31.83, 29.36, 27.46, 23.01; **HRMS-ESI** (*m/z*) [M+H]$^+$calcd. for $C_{15}H_{23}N_2O_2^+$ 263.1759; found 263.1751.

1-((S)-1-((R)-1-phenylethyl)aziridin-2-yl) heptan-3-one: (2)

To a stirred solution of Weinreb amide **1e** (1.0 g, 3.8 mmol, 1.0 equiv.) in dry THF (50 mL) at 0°C, *n*-Butylmagnesium chloride solution C_4H_9MgCl (1.9 mL, 2.0 M in Ether, 1.90 mmol) was added. The reaction mixture was slowly warmed to room temperature and stirred for 0.5 h. After completion of the reaction as per TLC, the reaction mixture was quenched with NH_4Cl solution and extracted with EtOAc (3 × 80 mL). Combined organic layers were dried over Na_2SO_4 and concentrated *in vacuo*, which was then purified by silica gel column chromatography to afford ketone product **2** (830 mg, 80% yield) TLC R_f (60% EtOAc/hexane = 0.5).

$[\alpha]^{20}_D$ = + 51.0 (*c* = 0.06, MeOH); **^{1}H NMR** (400 MHz, $CDCl_3$): δ 7.42–7.32 (m, 3 H), 7.31–7.21 (m, 2 H), 2.70–2.58 (m, 1 H), 2.47 (dd, *J* = 9.3, 5.6 Hz, 2 H), 2.41 (q, *J* = 6.5 Hz, 1 H), 2.01–1.89 (m, 3 H), 1.66–1.53 (m, 1 H), 1.52–1.48 (m, 1 H), 1.43 (d, *J* = 6.6 Hz, 3 H), 1.40–1.26 (m, 1 H), 0.98–0.90 (m, 3 H); **^{13}C NMR** (101 MHz, $CDCl_3$): δ 210.77, 144.51, 128.26, 126.91, 126.75, 69.64, 42.52, 40.40, 39.36, 33.49, 27.10, 25.94, 23.32, 22.35, 13.85; **HRMS-ESI** (*m/z*) [M+H]$^+$calcd. for $C_{17}H_{26}NO^+$ 260.2014; found 260.2003.

(R)-2-hydroxy-1-(((R)-1-phenylethyl)amino) nonan-5-one: (5)

The procedure was analogous to that used for preparing compound **8** using 1-((*S*)-1-((*R*)-1-phenylethyl)aziridin-2-yl) heptan-3-one (**2**) (800 mg, 3.084 mmol, 1.0 equiv.) in an acetone (10.0 mL) and water (5.0 mL) solvent system with trifluoro acetic acid (TFA) (0.23 mL, 3.08 mmol, 1.0 equiv) to afford compound (*R*)-2-hydroxy-1-(((*R*)-1-phenylethyl)amino)nonan-5-one (**5**) (760 mg, 90% yield), TLC R_f (90% EtOAc/hexane = 0.1).

$[\alpha]^{20}_D$ = + 87.2 (*c* = 0.14, MeOH); **^{1}H NMR** (400 MHz, $CDCl_3$): 7.49–7.11 (m, 5H), 3.87–3.66 (m, 1H), 3.54–3.32 (m, 1H), 2.63–2.43 (m, 3H), 2.40–2.31 (m, 3H), 1.77–1.63 (m, 1H), 1.61–1.46 (m, 3H), 1.44–1.36 (m, 3H), 1.32–1.20 (m, 2H), 0.96–0.82 (m, 3H); **^{13}C NMR** (101 MHz, $CDCl_3$): δ 211.63, 144.80, 128.57, 127.19, 126.48, 69.35, 58.61, 53.37, 42.64, 38.82, 28.56, 25.96, 23.79, 22.32, 13.83; **HRMS**-ESI (*m/z*) [M+H]$^+$calcd. for $C_{17}H_{28}NO_2^+$ 278.2120; found 278.2114.

(2R,5R)-benzyl 2-butyl-5-hydroxypiperidine-1-carboxylate: (7)

Compound **5** (600 mg, 2.16 mmol) was taken in MeOH (10 mL) and degassed with N_2 for 2 h. Then 20% $Pd(OH)_2/C$ (242 mg, 1.7 mmol, 0.8 equiv) was added and the mixture was hydrogenated under an atmospheric pressure of hydrogen for 16 h. After completion of the reaction as per TLC, the reaction mixture was diluted with MeOH (20 mL) and filtered on a pad of Celite using MeOH as solvent. The filtrate was concentrated under vacuum and crude product was used for N-Cbz protection reaction without purification.

To a solution of crude product (325 mg) in dry CH_2Cl_2 (5 mL), triethyl amine (0.5 mL, 3.25 mmol, 1.6 equiv.) and benzyl chloroformate (CbzCl) (0.43 mL, 3.05 mmol, 1.5 equiv.) were added at 0°C. Then resulting mixture was allowed to stir at room temperature for 3 h. After completion of the reaction, the reaction was quenched with H_2O (2 mL). The organic layer was then extracted with CH_2Cl_2 (2 × 20 mL), dried over anhydrous Na_2SO_4, and concentrated under vacuum to give an *N*-Cbz protected piperidine crude product, which was then purified by flash column chromatography on silica gel to afford a pure product (2*R*,5*R*)-benzyl 2-butyl-5-hydroxypiperidine-1-carboxylate (**7**) (412 mg, 70% yield for 2 steps) TLC R_f (40% EtOAc/hexane = 0.3).

$[\alpha]^{20}_D$ = −9.3 (*c* = 0.30, MeOH); **^{1}H NMR** (400 MHz, $CDCl_3$): δ 7.44–7.29 (m, 5H), 5.16 (q, *J* = 12.3 Hz, 2H), 4.33 (s, 1H), 4.12 (s, 1H), 3.90 (d, *J* = 38.5 Hz, 1H), 3.05 (d, *J* = 14.0 Hz, 1H), 2.21–1.93 (m, 2H), 1.84–1.58 (m, 3H), 1.46–1.11 (m, 6H), 0.88 (t, *J* = 6.4 Hz, 3H); **^{13}C NMR** (101 MHz, $CDCl_3$): δ 156.52, 136.76, 128.42, 127.89, 127.77, 67.08, 64.47, 50.59, 44.76, 28.73, 28.46, 25.40, 22.54, 14.05; **HRMS**-ESI (*m/z*) [M+H]$^+$calcd. for $C_{17}H_{26}NO_3^+$ 292.1912; found 292.1905.

(R)-*benzyl 2-butyl-5-oxopiperidine-1-carboxylate:* (9)

To a stirred solution of **7** (200 mg, 0.68 mmol, 1.0 equiv) in CH_2Cl_2 (15 mL), Dess-Martin periodinane (DMP) (581 mg, 1.37 mmol, 2.0 equiv) was added at 0°C. After 10 min, the reaction mixture was allowed to stir for an additional 8 h at room temperature. After completion of the reaction as per TLC, the reaction mixture was filtered on a pad of Celite using CH_2Cl_2 (2 × 5 mL) as solvent. The saturated $NaHCO_3$ (5 mL) was used to treat the filtrate. Combined organic extracts were washed with CH_2Cl_2 (2 × 15 mL), dried over anhydrous Na_2SO_4, and concentrated *in vacuo*. The residue was purified by flash chromatography on silica gel to provide keto compound **9** (158 mg, 80%) as a liquid, TLC R_f (30% EtOAc/hexane = 0.5).

$[\alpha]^{20}_D$ = +48.0 (*c* = 0.55, MeOH); **^{1}H NMR** (400 MHz, $CDCl_3$): δ 7.50–7.32 (m, 5H), 5.28–5.08 (m, 2H), 4.68–4.44 (m, 1H), 4.40–4.18 (m, 1H), 3.62 (d, *J* = 17.7 Hz, 1H), 2.44 (t, *J* = 6.7 Hz, 2H), 2.24 (m, 1H), 1.68 (m, 2H), 1.54 (m, 1H), 1.32 (m, 4H), 0.98–0.84 (m, 3H); **^{13}C NMR** (101 MHz, $CDCl_3$): δ 207.37, 166.95, 136.29, 128.52, 128.16, 127.99, 67.50, 50.81, 50.40, 35.69, 27.90, 22.51, 13.97; **HRMS-ESI** (*m/z*) [M+H]$^+$calcd. for $C_{17}H_{24}NO_3^+$ 290.1756; found 290.1748.

1-((S)-1-((R)-1-phenylethyl)aziridin-2-yl) heptan-3-ol: (10)

To a stirred solution of methyl 3-((*S*)-1-((*R*)-1-phenylethyl) aziridine-2-yl)propanoate **(1d)** (2 g, 8.57 mmol, 1.0 equiv) in dry CH_2Cl_2 (40 mL), a solution of diisobutylaluminum hydride solution (DIBAL-*H*) (9.4 mL, 1.0 M in Toluene, 9.43 mmol) was added dropwise at—78°C. The reaction mixture was allowed to stir for 2 h at the same temperature. After completion of the reaction as per TLC indication, the reaction was quenched with a saturated solution of Na-k tartarate (10 mL) at 0°C. The reaction mixture was then stirred for an additional 1 h. The crude mixture was extracted with CH_2Cl_2 (3 × 20 mL), dried over anhydrous Na_2SO_4, and concentrated under vacuum to afford crude aldehyde, which was used for the next step without further purification.

To a stirred solution of crude aldehyde in dry THF (40 mL) at 0°C, *n*-butylmagnesium chloride solution C_4H_9MgCl (4.1 mL, 2.0 M in ether, 4.0 mmol) was added. The reaction mixture was allowed to stir for 2 h at the same temperature. After completion of the reaction per TLC indication, the reaction mixture was quenched with saturated NH_4Cl solution and extracted with EtOAc (2 × 100 mL). Combined organic layers were dried over Na_2SO_4 and concentrated *in vacuo* to afford a crude product which was then purified by silica gel column chromatography to afford diastereomeric (1:1) hydroxy compound **10** (1.82 g, 80% yield for two steps) at the same R_f, TLC R_f (40% EtOAc/hexane = 0.5).

$[\alpha]^{20}_D$ = + 55.2 (*c* = 0.11, MeOH);**^{1}H NMR** (400 MHz, $CDCl_3$): δ 7.43–7.24 (m, 10H), 3.67–3.52 (m, 1H), 2.56–2.50 (m, 1H), 2.49–2.43 (m, 1H), 2.06–1.88 (m, 1H), 1.79–1.69 (m, 2H), 1.69–1.64 (m, 2H), 1.60 (qd, *J* = 4.0, 1.9 Hz, 3H), 1.54–1.42 (m, 11H), 1.41–1.31 (m, 4H), 1.30–1.26 (m, 1H), 1.04–0.85 (m, 6H); **^{13}C NMR** (101 MHz, $CDCl_3$): δ 144.22, 144.04, 128.31, 127.00, 126.75, 71.56, 69.81, 39.96, 39.68, 37.34, 33.88, 33.21, 28.82, 28.67, 27.97, 23.37, 22.84, 14.08; **HRMS-ESI** (*m/z*) $[M+H]^+$calcd. for $C_{17}H_{27}NO^+$ 262.2171; found 262.2160.

(2S)-2-(3-((tert-butyldimethylsilyl)oxy) heptyl)-1-((R)-1-phenylethyl)aziridine: (11)

Tert-butyldimethylsilyltrifluoromethane sulfonate (TBSOTf) (1.5 mL, 6.73 mmol, 1.1 equiv) was slowly added to a cooled solution (0°C) of alcohol **10** (1.6 g, 6.12 mmol, 1.0 equiv) and 2,6-lutidine (1.4 mL, 12.24 mmol, 2.0 equiv) in dry CH_2Cl_2 (30 mL). After 20 min, the reaction mixture was diluted with CH_2Cl_2 (20 mL), quenched with water, and extracted with CH_2Cl_2 (2 × 15 mL). Combined organic layers were dried over anhydrous Na_2SO_4 and concentrated *in vacuo* to obtain a crude product which was purified by flash column chromatography to afford TBS protected compound **11** (1.92 g, 85% yield) TLC R_f (20% EtOAc/hexane = 0.6).

$[\alpha]^{20}_D$ = + 26.2 (*c* = 0.5, MeOH); **^{1}H NMR** (400 MHz, $CDCl_3$): δ 7.46–7.26 (m, 10H), 3.90–3.53 (m, 2H), 2.46–2.34 (m, 2H), 1.85–1.51 (m, 3H), 1.51–1.43 (m, 10H), 1.39–1.23 (m, 6H), 0.96–0.86 (m, 18H), 0.12–0.06 (m, 6H), 0.04 (s, 6H); **^{13}C NMR** (101 MHz, $CDCl_3$): δ 144.65, 128.24, 126.84, 72.27, 72.21, 71.92, 71.84, 69.89, 40.76, 37.12, 36.57, 35.14, 34.98, 33.36, 29.42, 28.64, 27.50, 25.95, 25.91, 25.70, 25.66, 23.29, 22.87, 18.14, 18.11, 14.11, −2.96, −4.37; **HRMS-ESI** (*m/z*) $[M+H]^+$calcd. for $C_{23}H_{42}NOSi^+$ 376.3035; found 376.3023.

(2S)-5-((tert-butyldimethylsilyl)oxy)-2-(((R)-1-phenylethyl)amino)nonyl acetate (12)

To (2*S*)-2-(3-((*tert*-butyldimethylsilyl)oxy)heptyl)-1-((*R*)-1-phenylethyl)aziridine (**11**) (800 mg, 2.12 mmol) in CH_2Cl_2 (10 mL), acetic acid (0.3 mL, 4.25 mmol, 2.5 equiv) was added at 0°C. The reaction mixture was allowed to stir at room temperature for 12 h. After completion of the reaction per TLC indication, the reaction mixture was quenched with a saturated solution of $NaHCO_3$ (5 mL), extracted with CH_2Cl_2 (3 × 15 mL), and concentrated under *vacuum* to obtain a crude product which was then purified by flash column chromatography on silica gel to afford a pure product **12** (820 mg, 89%) TLC R_f (20% EtOAc/hexane = 0.5).

$[\alpha]^{20}_D$ = + 38.2 (*c* = 0.70, MeOH);**^{1}H NMR** (400 MHz, $CDCl_3$): δ 7.40–7.16 (m, 10H), 4.05–3.94 (m, 1H), 3.92–3.81 (m, 3H), 3.71–3.53 (m, 1H), 2.72–2.45 (m, 1H), 2.07–2.01 (m, 6H), 1.62–1.53 (m, 3H), 1.50–1.38 (m, 3H), 1.36–1.31 (m, 4H), 1.30–1.21 (m, 3H), 0.92–0.85 (m, 18H), 0.05–0.00 (m, 12H); **^{13}C NMR** (101 MHz, $CDCl_3$): δ 171.01, 145.76, 145.72, 128.40, 126.93, 126.52, 72.06, 72.02, 66.86, 66.83, 55.23, 55.17, 53.61, 36.62, 32.59, 27.49, 26.50, 25.91, 24.79, 22.86, 20.92, 18.10, 14.11, −4.47; **HRMS-ESI** (*m/z*) $[M+H]^+$calcd. for $C_{25}H_{46}NO_3Si^+$ 436.3247; found 436.3234.

(2S)-5-hydroxy-2-(((R)-1-phenylethyl) amino)nonyl acetate (13)

To a stirred solution of **12** (500 mg, 1.14 mmol) in dry THF (12 mL) in a polypropylene vial HF-Py complex (70%, 0.4 mL) at 0°C was added. The reaction mixture was slowly raised to room temperature and stirred for 12 h. After completion of the reaction per TLC indication, the reaction mixture was cautiously quenched with saturated aqueous $NaHCO_3$ and stirred for 20 min. Then both layers were separated. The aqueous layer was further extracted with EtOAc (2 × 20 mL). Combined organic layers were washed with saturated aqueous $CuSO_4$ (5 mL), water (5 mL), and brine (5 mL), dried over Na_2SO_4, and concentrated *in vacuo* to obtain a crude product, which was then purified by flash column chromatography on silica gel to afford a pure product **13** (295 mg, 80%) TLC R_f (70% EtOAc/hexane = 0.2).

$[\alpha]^{20}_D$ =—51.2 (*c* = 0.22, MeOH); **^{1}H NMR** (400 MHz, $CDCl_3$): δ 7.51–7.12 (m, 10H), 4.17–4.02 (m, 2H), 4.02–3.94 (m, 2H), 3.93–3.81 (m, 2H), 3.63–3.43 (m, 1H), 3.06–2.81 (m, 1H), 2.81–2.60 (m, 1H), 2.13–1.94 (m, 6H), 1.84–1.45 (m, 4H), 1.46–1.16 (m, 9H), 1.03–0.71 (m, 6H); **^{13}C NMR** (101 MHz, $CDCl_3$): δ 170.77, 170.67, 144.95, 144.65, 128.51, 128.47, 127.18, 127.12, 126.38, 126.26, 71.66, 71.25, 66.17, 65.82, 55.22, 54.92, 54.20, 52.68, 37.22, 37.15, 34.45, 32.82, 29.59, 27.95, 27.92, 27.59, 23.78, 23.00, 22.71, 22.69, 20.71, 13.99; **HRMS-ESI** (*m/z*) $[M+H]^+$calcd. for $C_{19}H_{32}NO_3^+$ 322.2382; found 322.2372.

(2S)-2-(((benzyloxy)carbonyl)amino)-5-hydroxynonyl acetate: (14)

Compound **13** (250 mg, 0.77 mmol) was taken in MeOH (10 mL) and degassed with N_2 for 1 h. Then 20% $Pd(OH)_2/C$ (218 mg, 1.55 mmol, 2.0 equiv) was added and the mixture was

hydrogenated under an atmospheric pressure of hydrogen for 16 h. The reaction mixture was diluted with MeOH (15 mL) and filtered on a pad of Celite using MeOH as a solvent. The filtrate was concentrated under a *vacuum* to obtain a crude product which was used for the *N*-Cbz protection reaction without purification.

To a solution of crude product in dry THF (8 mL), LiHMDS (0.4 mL, 0.44 mmol, 1.2 equiv), benzyl chloroformate (CbzCl) (0.2 mL, 0.58 mmol, 1.6 equiv) were added at 0°C. The resulting mixture was allowed to stir at the same temperature for 3 h. After completion of the reaction, the mixture was quenched with H_2O (3 mL). The organic layer was extracted with EtOAc (2 × 15 mL), dried over anhydrous Na_2SO_4, and concentrated under *vacuum* to obtain an *N*-Cbz protected crude product, which was purified by flash column chromatography on silica gel to afford a pure product **14** (120 mg, 80% yield for 2 steps) TLC R_f (80% EtOAc/hexane = 0.2).

$[\alpha]^{20}_D$ = + 28.5 (*c* = 0.07, MeOH); **^{1}H NMR** (400 MHz, $CDCl_3$): δ 7.51–7.31 (m, 10H), 5.24–5.08 (m, 4H), 4.28–4.08 (m, 5H), 3.67–3.52 (m, 2H), 3.38–3.15 (m, 2H), 1.99–1.90 (m, 6H), 1.77–1.49 (m, 3H), 1.47–1.19 (m, 10H), 1.18–1.08 (m, 3H), 1.01–0.73 (m, 6H); **^{13}C NMR** (101 MHz, $CDCl_3$) δ 170.18, 170.15, 155.08, 155.07, 134.91, 128.66, 128.61, 128.44, 71.40, 69.93, 69.89, 69.45, 69.18, 48.36, 48.32, 37.30, 34.43, 33.11, 33.04, 27.81, 27.75, 27.46, 23.20, 22.64, 14.76, 14.00; **HRMS-ESI** (*m/z*) $[M+H]^+$calcd. for $C_{19}H_{30}NO_5^+$ 352.2124; found 352.2114.

Data availability statement

The original contributions presented in the study are included in the article/Supplementary Material, further inquiries can be directed to the corresponding author.

Author contributions

NS: Conceptualization, Data curation, Formal Analysis, Funding acquisition, Investigation, Methodology, Project administration, Resources, Supervision, Validation, Visualization, Writing–original draft, Writing–review and editing. H-JH: Conceptualization, Data curation, Formal Analysis, Investigation, Methodology, Validation, Visualization, Writing–original draft, Writing–review and editing.

Funding

The authors declare financial support was received for the research, authorship, and/or publication of this article. This work was supported by a grant (NRF-2012M3A7B4049645 with Centre for New Directions in Organic Synthesis) of the National Research Foundation of Korea and HUFS fund 2023.

Conflict of interest

The authors declare that the research was conducted in the absence of any commercial or financial relationships that could be construed as a potential conflict of interest.

Publisher's note

All claims expressed in this article are solely those of the authors and do not necessarily represent those of their affiliated organizations, or those of the publisher, the editors and the reviewers. Any product that may be evaluated in this article, or claim that may be made by its manufacturer, is not guaranteed or endorsed by the publisher.

Supplementary material

The Supplementary Material for this article can be found online at: https://www.frontiersin.org/articles/10.3389/fchem.2023.1280633/full#supplementary-material

References

Bates, R. W., Sivarajan, K., and Straub, B. F. (2011). A Synthesis of pseudoconhydrine and its epimer via hydroformylation and dihydroxylation. *J. Org. Chem.* 76 (16), 6844–6848. doi:10.1021/jo2008912

Choi, J., Yadav, N. N., and Ha, H.-J. (2017). Preparation of a stable bicyclic aziridinium ion and its ring expansion toward piperidines and azepanes. *Asian J. Org. Chem.* 6, 1292–1307. doi:10.1002/ajoc.201700080

Dalabehera, N. R., Meher, S., Palai, B. B., and Sharma, N. K. (2020). Instability of amide bond with trifluoroacetic acid (20%): synthesis, conformational analysis, and mechanistic insights into cleavable amide bond comprising β-troponylhydrazino acid. *ACS Omega* 5, 26141–26152. doi:10.1021/acsomega.0c03729

D'hooghe, M., and Ha, H.-J. (2016). *Synthesis of 4- to 7-Membered heterocycles by ring expansion: aza-, oxo-and thiaheterocyclic Small-Ring Systems. Heidelberg*. Springer, 1–367.

Dolfen, J., Yadav, N. N., De Kimpe, N., D'hooghe, M., and Ha, H.-J. (2016). Front cover picture: bicyclic aziridinium ions in azaheterocyclic chemistry – preparation and synthetic application of 1-Azoniabicyclo[n.1.0]alkanes (adv. Synth. Catal. 22/2016). *Adv. Synth. Catal.* 358, 3483–3511. doi:10.1002/adsc.201601081

Eum, H., Choi, J., Cho, C.-G., and Ha, H.-J. (2015). Cover picture: regiochemistry-directed syntheses of polyhydroxylated alkaloids from chiral aziridines (asian J. Org. Chem. 12/2015). *Asian J. Org. Chem.* 4, 1325–1340. doi:10.1002/ajoc.201500380

Ha, H.-J., Jung, J.-H., and Lee, W. K. (2014). Application of regio- and stereoselective functional group transformations of chiral aziridine-2-carboxylates. *Asian J. Org. Chem.* 3, 1020–1035. doi:10.1002/ajoc.201402098

Lee, B. K., Lee, W. K., Yoon, D.-H., and Ha, H.-J. (2009). Selective reduction of C-C double bonds of 2-vinylaziridnes: preparation of enationmerically pure 2-alkylaziridines. *Bull. Kor. Chem. Soc.* 30, 3123–3126. doi:10.5012/bkcs.2009.30.12.3123

Lee, W.-K., and Ha, H.-J. (2003). High light of the chemistry of enantiomerically pure aziridine-2-carboxylates. *Aldrichimica Acta* 36 (2), 57–63. doi:10.1002/chin.200428252

Lee, Y.-S., Shin, Y.-H., Kim, Y.-H., Lee, K.-Y., Oh, C.-Y., Pyun, S.-J., et al. (2003). Stereoselective synthesis of (+)-spectaline. *Tetrahedron Asymm* 14, 87–93. doi:10.1016/S0957-4166(02)00794-2

Lin, S., Liu, C., Zhao, X., Han, X., Li, X., Ye, Y., et al. (2022). Recent advances of pyridinone in medicinal chemistry. *Front. Chem.* 23, 869860. doi:10.3389/fchem.2022.869860

Lopez, S. E., and Salazar, J. (2013). Trifluoroacetic acid: uses and recent applications in organic synthesis. *J. Fluor. Chem.* 156, 73–100. doi:10.1016/j.jfluchem.2013.09.004

Macha, L., D'hooghe, M., and Ha, H.-J. (2019). Deployment of aziridines for the synthesis of alkaloids and their derivatives. *Synthesis* 51, 1491–1515. doi:10.1055/s-0037-1611715

Macha, L., and Ha, H.-J. (2019). Total synthesis and absolute stereochemical assignment of microgrewiapine A and its stereoisomers. *J. Org. Chem.* 84, 94–103. doi:10.1021/acs.joc.8b02342

Michael, J. P. (2016). Simple indolizidine and quinolizidine alkaloids. *Alkaloids Chem. Biol.* 75, 1–498. doi:10.1016/bs.alkal.2014.12.001

Ranjith, J., and Ha, H.-J. (2022). *Strained aziridinium ion, more synthetic approaches to nonaromatic nitrogen heterocycles*, 1. John Wiley and Sons, Ltd., 499–528. doi:10.1002/9781119757153.ch15

Ranjith, J., and Ha, H.-J. (2021). Synthetic Applications of aziridinium ions. *Molecules* 26 (6), 1774. doi:10.3390/molecules26061774

Rao, V. K. S., and Kumar, P. (2006). An asymmetric aminohydroxylation route to cis-2,6-disubstituted piperidine-3-ol: application to the synthesis of (−)-deoxocassine. *Tetrahedron* 62, 9942–9948. doi:10.1016/j.tet.2006.08.014

Singh, A., Kim, B., Lee, W. K., and Ha, H.-J. (2011). Asymmetric synthesis of 1-deoxyazasugars from chiral aziridines. *Org. Biomol. Chem.* 9, 1372–1380. doi:10.1039/C0OB00730G

Srivastava, N., and Ha, H.-J. (2022). Highly efficient and stereoselective Mukaiyama aldol reaction with chiral aziridine-2-carboxaldehyde and its synthetic applications. *Asian J. Org. Chem.* 11 (1), 72–81. doi:10.1002/ajoc.202100567

Srivastava, N., Macha, L., and Ha, H.-J. (2020). Stereoselective synthesis of 2,6-disubstituted piperidine alkaloids. *Org. Biomol. Chem.* 18, 5493–5512. doi:10.1039/D0OB00918K

Stankovic, S., D'hooghe, M., Catak, S., Eum, H., Waroquier, M., Van Speybroeck, V., et al. (2012). Regioselectivity in the ring opening of non-activated aziridines. *Chem. Soc. Rev.* 41, 643–665. doi:10.1039/C1CS15140A

Vataku, E., Smith, D. T., and Njardarson, J. T. (2014). Analysis of the structural diversity, substitution patterns, and frequency of nitrogen heterocycles among U.S. FDA approved pharmaceuticals. *J. Med. Chem.* 57, 10257–10274. doi:10.1021/jm501100b

Wang, Y.-G., Kumano, T., Kano, T., and Maruoka, K. (2009). Organocatalytic approach to enantioselective one-pot synthesis of pyrrolidine, hexahydropyrrolizine, and octahydroindolizine Core Structures. *Org. Lett.* 11 (9), 2027–2029. doi:10.1021/ol900477x

Yadav, N. N., Choi, J., and Ha, H.-J. (2016). One-pot multiple reactions: asymmetric synthesis of 2,6-cis-disubstituted piperidine alkaloids from chiral aziridine. *Org. Biomol. Chem.* 14, 6426–6434. doi:10.1039/C6OB00806B

Ying, X., Zhang, J., Wang, C., Huang, M., Ji, Y., Cheng, F., et al. (2018). Characterization of a carbonyl reductase from rhodococcus erythropolis WZ010 and its variant Y54F for the asymmetric synthesis of (*S*)-N- Boc-3-hydroxypiperidine. *Molecules* 23 (12), 3117. doi:10.3390/molecules23123117

Yoon, D.-H., Ha, H.-J., Kim, B. C., and Lee, W. K. (2010). Conjugate addition of amines to chiral 3-aziridin-2-yl-acrylates. *Tetrahedron Lett.* 51, 2181–2183. doi:10.1016/j.tetlet.2010.02.087

frontiers | Frontiers in Chemistry

TYPE Perspective
PUBLISHED 30 October 2023
DOI 10.3389/fchem.2023.1279418

OPEN ACCESS

EDITED BY
Florenci Vicent González,
University of Jaume I, Spain

REVIEWED BY
Praveen Reddy Adiyala,
Indian Institute of Chemical Technology (CSIR), India

*CORRESPONDENCE
Hyun-Joon Ha,
hjha@hufs.ac.kr

RECEIVED 18 August 2023
ACCEPTED 13 October 2023
PUBLISHED 30 October 2023

CITATION
Ha H-J (2023), Recent advances in synthesizing and utilizing nitrogen-containing heterocycles.
Front. Chem. 11:1279418.
doi: 10.3389/fchem.2023.1279418

Recent advances in synthesizing and utilizing nitrogen-containing heterocycles

Hyun-Joon Ha*

Department of Chemistry, Hankuk University of Foreign Studies, Yongin, Republic of Korea

The use of organocatalysts and a pot economy has strengthened recent organic syntheses. Synthetic methodologies may be applicable in laboratory preparation or in the industrial production of valuable organic compounds. In most cases, synthetic challenges are overcome by highly efficient and environmentally benign organocatalysts in a pot-economical manner. This is exemplified by the recent synthesis of tetrahydropyridine-containing (–)-quinine.

KEYWORDS

organocatalyst, pot-economy, tetrahydropyridine, (–)-quinine, environmentally benign

In the last several decades, great progress has been made in organic synthesis. However, we are still quite far away from the ideal goal. In particular, synthetic reactions should be environmentally benign and should remove costly purification procedures derived from the step-by-step procedures used in a myriad of protecting and deprotecting protocols. In recent years, great success was achieved in overcoming these drawbacks by using several techniques, including fluorous catalysis (De Wolf et al., 1999; Mika and Horvath, 2018), solid-supported catalysis (Nafiu et al., 2023), biocatalysis (Pyser et al., 2021), and organocatalysis with green chemistry metrics (Martínez J. et al., 2022). Various trials with solvent-free and aqueous reactions (Ruiz-Lopez et al., 2020) or ionic liquids (Earle and Seddon, 2000) also succeeded in organic synthesis, with certain limitations. In addition, multicomponent reactions (Boukis et al., 2018; Cimarelli, 2019) were also applied based on pot-economical synthesis (Grondal C. et al., 2010). In recent years, great success has been achieved using a combination of organocatalysis and pot-economical synthesis. The one-pot synthesis of a target molecule in the same reaction vessel is widely considered to be an efficient approach in synthetic organic chemistry.

Although catalytic reactions have been known for a long time (List, 2010; Vogel et al., 2016), including various metallic compounds and a few organic molecules, no systematic investigation has been performed (Hajos and Parrish, 1974; Bernhard and Wolfgang, 1978). The concept and the term "organocatalyst" were established in earnest by the novel laurates B. List (List, 2007) and D. MacMillan (MacMillan, 2008) in 2007. They carried out various reactions, such as the addition of electron-deficient olefins like aldol and even Diels-Alder reactions (Chen et al., 2022). The advantages of organocatalysts include their lack of sensitivity to moisture and oxygen, making them easy to handle. In addition, most of them are readily available at low cost, with relatively low toxicity compared with metal catalysts (Albrecht et al., 2022). Diverse organocatalysts were developed as chiral catalysts to warrant the streamlined synthesis of optically active and/or pure products needed in many areas, including pharmaceutical industries (Hughes, 2018; Han, et al., 2021).

In terms of the great synthetic challenges of any organic compounds requiring many steps, all the necessary reactions should proceed in a highly efficient manner, including a pot-economy. A minimum reaction vessel required for the reaction to complete is an economical

approach, such as in a pot economy. (Grondal C. et al., 2010). Reactions utilizing step-by-step protocols under different conditions require costly work-up and purification procedures. For example, the following flowchart shows three different reactions needed to get **D** as a product from three different reactions **I**, **II**, and **III**, yielding **B** and **C** as synthetic intermediate molecules. However, when we want to get **D** from the starting material **A** through several reactions, without isolating **B** and **C**, we are able to save laborious costly work-up and purification.

$$A \xrightarrow{\text{ReactionI}} B \xrightarrow{\text{ReactionII}} C \xrightarrow{\text{ReactionIII}} D$$

The best way to perform the different reactions in an efficient and easy way is to carry out all necessary reactions **I** to **III** in one pot under the same condition with the same reagents in the same solvent. For example, the synthesis of substituted 2,6-disubstituted piperidine from 3-alkynyl-2-(N-α-methylbenzylaziridine) was successfully achieved in the same way as shown in Scheme 1 by using a one-pot reaction under catalytic hydrogenation, without isolating any synthetic intermediate (Yadav et al., 2016). Under this condition, four different reactions, entailing the hydrogenation of alkyne, aziridine ring opening, reductive cyclization, and deprotection of the α-methylbenzyl group at the nitrogen ring occurred, without changing anything else throughout the whole reaction sequences.

This is quite an exceptional case. In most cases, a preparative amount of product is accessible from reactions with different reagents under very specific conditions. Obtaining a decent amount of the final product in an efficient and handy protocol is possible with a one-pot synthesis. One-pot synthesis involves successive chemical reactions in just one reactor, from which sufficient purity is secured further in the sequence, without any purification. To carry out this synthesis properly, a decent reaction yield should be provided, with different reagents for the reaction to proceed to the specific position and functional group, even under different solvents. The reagents used for the previous reactions should not harm the subsequent reactions. For example, reactions **II** and **III** should be carried out by selecting proper reagents after killing the reactivity from the previous reactions to avoid harming the next reaction, i.e., reaction **II** from **I** and reaction **III** from both **I** and **II**. For this purpose, the synthetic intermediates in most cases are not stable for the next reaction, or they are in equilibrium for the next reaction. Selecting solvents is also a crucial factor for the specific reaction. In most cases, changing the solvents should be simple after one reaction, owing to the relatively low boiling points for them to be removed via simple evaporation.

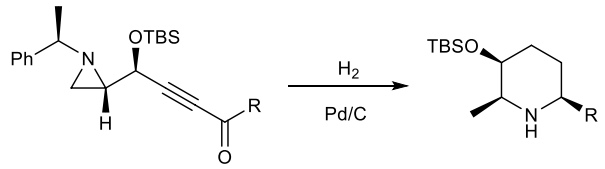

SCHEME 1
Synthesis of piperidine from multi-reactions of the starting material 3-alkynyl-2-(N-α-methylbenzyl)aziridine.

For an efficient and environmentally benign synthesis, a pot-economical method is better for use in conjunction with organocatalysts. For example, the Michael reactions of nitroalkenes shown in Scheme 2 were investigated intensively, taking advantage of their superior reactivity toward the nucleophile and its practicability. Proper selection of organocatalysts derived from proline makes this transformation asymmetric, with high yields, and these are used in many cases. Though various organocatalysts were developed and utilized to make these reactions possible, diarylprolinol silyl ethers (**Cat**) are the most widely used as simple and very efficient catalysts. They carry out the reactions, including Michael reactions of nitroalkanes between **2** and **3**, in a highly efficient manner to yield products **4** with high optically purities (Y. Hayashi et al., 2005; Jensen et al., 2012; Reyes-Rodríguez et al., 2019) (Scheme 2). Once the key bond has been made, the others are followed by stereoselective reactions, with carbocyclic or heterocyclic ring transformations. The newly constructed bonds formed from organocatalysts are green, with specific examples indicated by the green-colored bonds in Scheme 2. In this manner, there are many reports showing that the organocatalytic reactions were very efficient ways of making the bonds needed in biologically important molecules, including pharmaceuticals and natural products such as acyclic and cyclic molecules. Some representative examples of organocatalyst proline derivatives, including diarylprolinol silyl ethers (**Cat**) are gabapentin (Gotoh et al., 2007), sacubitril (Hughes, 2018), prostaglandin PGF2α (Coulthard et al., 2012; Scheffler and Mahrwald, 2013), oseltamivir (Ishikawa et al., 2009; Ishikawa et al., 2010; Hayashi and Ogasawara, 2016), (+)-(α)-lycorane (Meng et al., 2014), (+)-microminutinin (Huang et al., 2017), and pyrrolysine (Han et al., 2013).

Recently, one outstanding publication that is worth looking into in detail deals with the two important aspects, pot-economical and organocatalytic synthesis, and was carried out by Professor Y. Hayashi's lab. They performed a very impressive synthesis of a (−)-quinine (**1**) natural product consisting of core azaheterocycle tetrahydropyridine (Terunuma and Hayashi, 2022). The synthesis, with a piperidine ring needed for the preparation of unnatural enantiomer, was previously published with an organocatalyst via (3 + 3) cyclization and Strecker-type cyanation (Shiomi, et al., 2019). However, a strategically different method was used to obtain azaheterocycle tetrahydropyridine as a core ring of the natural enantiomer (−)-quinine. The addition of aldehyde **5** to 2-phenylnitroalkene (**6**) for an aza-Henry reaction was initiated in the presence of 20 mol% of diphenyl prolinol trimethylsilyl ether as a catalyst (Scheme 3). Moreover, their synthesis was in conjunction with the pot-economical manner, leading to several reactions in the same vessel without any extra procedures or work-up (Hayashi, 2016). The imine needed to make a tetrahydropiperidine ring from the initial adduct between **5** and **6** would enhance the synthesis of **9** in the same vessel for a reaction completed in one pot.

The initial acyclic adduct **7**, as a Niro-Michael product, was reacted with imine generated from the corresponding sulfonyl precursor DBU (1,8-diazabicyclo [5.4.0]undec-7-ene, 3.0 equiv) in a single pot manner. This synthetic intermediate was converted, with the elimination of HNO_2 in the presence of DBU as a base, to yield the cyclic product **9** in high yield (66%) and high e. e. (98%), with 1:1 at C2 d.e. The hydroxy substituent at C2 is eventually eliminated. All the reactions starting from **5**, **6**, and the iminocarboxylate to **9** proceed sequentially in the one-pot

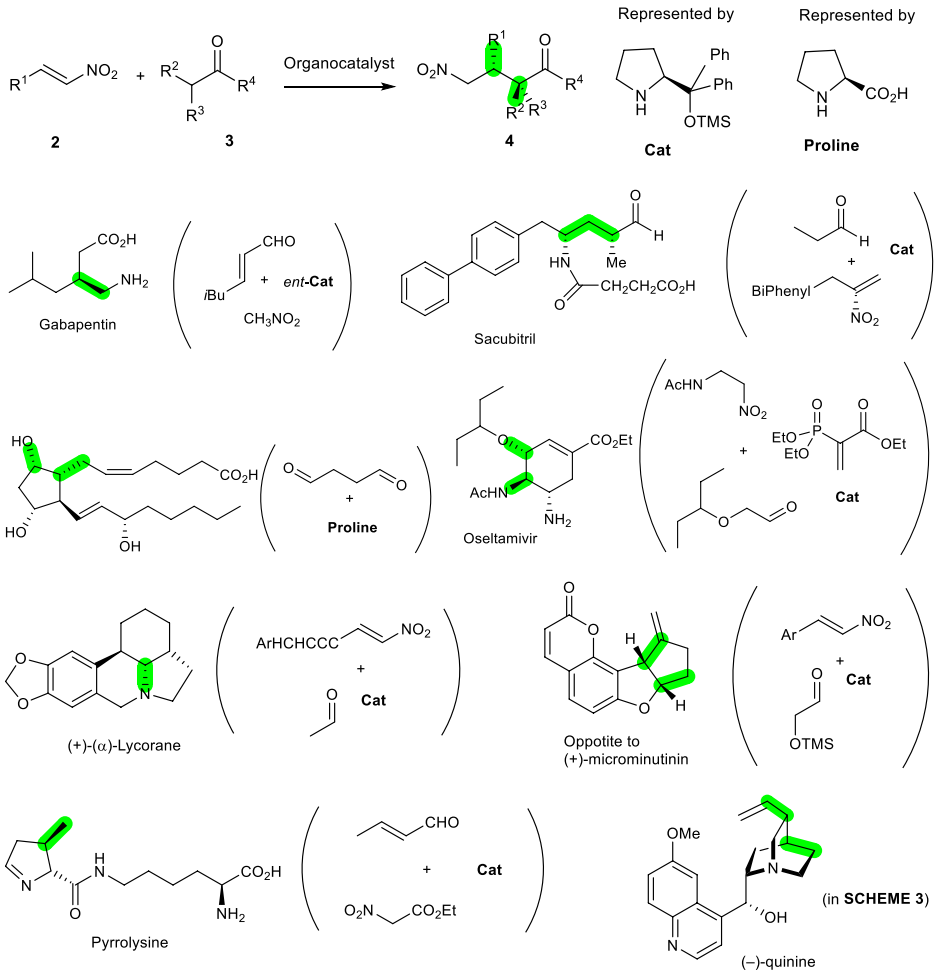

SCHEME 2
General synthetic scheme of bond formation and stereochemistry shown in green in adduct **4** based on organocatalytic nitro-Michael reactions from **2** and **3**. The catalyst used was proline or its diarylprolinol silyl ethers (**Cat**) derivatives. The specific cases of initial organocatalytic reactions with starting materials and catalysts are shown in parenthesis on the right side of the examples, with the construction of green-colored bonds.

protocol. To succeed in this reaction sequence, all synthetic intermediates were kinetically and thermodynamically favorable to afford the next product without any hindrance from the previous reagents, as shown in Scheme 3. The best way to perform this synthetic strategy is for all necessary reactions to succeed in a single operation without changing the reagents and solvents. However, this is very rare, with the assumption that the same reagents under the same solvent can carry out different reactions in a certain direction. Except for rare cases, almost all the reactions require different reagents under different solvents. Therefore, the reaction should be well designed to perform the steps in a pot-economical manner. As a diastereomeric mixture, the initial crude cyclic compound **9** from Pot 1 proceeded further for dehydroxylative reduction by CF_3CO_2H and Et_3SiH. Then, the reduction of enamine to amine was followed by the reducing agent $NaBH(OAc)_3$. All the excessive reductive reagents were destroyed by the reaction with additional acetaldehyde. This second one-pot reaction (Pot 2) afforded the azaheterocycle **10** as an almost single stereoisomer, with the correct stereochemistry. In Pot 3, it is relatively straightforward to obtain olefin **11** with the release of aryl thiol according to the Matsuo protocol (Matsuo et al., 2006) with 2,4,6-trimethylphenylsulfonylamide. The substituent carboxy ester was then reduced by DIBAL under low temperatures to give rise to aldehyde **11**. Then, 2-bromo-6-methoxyquinoline was added to this aldehyde, generating a diastereomeric mixture of hydroxy carbon without much stereoselectivity between *re-* or *si* face addition. However, this problem was overcome by oxidation of the alcohol adduct to ketone by DMP (Dess-Martin Periodinane), followed by the stereoselective reduction by LDBBA (lithium diisobutyl-*tert*-butoxyaluminum hydride), leading to the right isomer **12** needed for target **1** with more than 80% yield (Pot 4). The next steps in Pot 5 are the removal of bromine in the aryl ring and deprotecting the TBDPS and Boc groups from the free hydroxy group by treatment with Zn and AcCl. This primary hydroxy group was mesylated for the final cyclization with nitrogen to give quinuclidine under mild conditions using NaI and K_2CO_3. These four reactions are performed in a one-pot sequence with 77% yield. All these reactions are highly stereospecific, as seen in the synthesis of the expected (−)-quinine (**1**) in a pot economical manner. This report brings up two important and challenging synthetic methodologies in organic chemistry, i.e., the use of environmentally benign organocatalysts and pot economy.

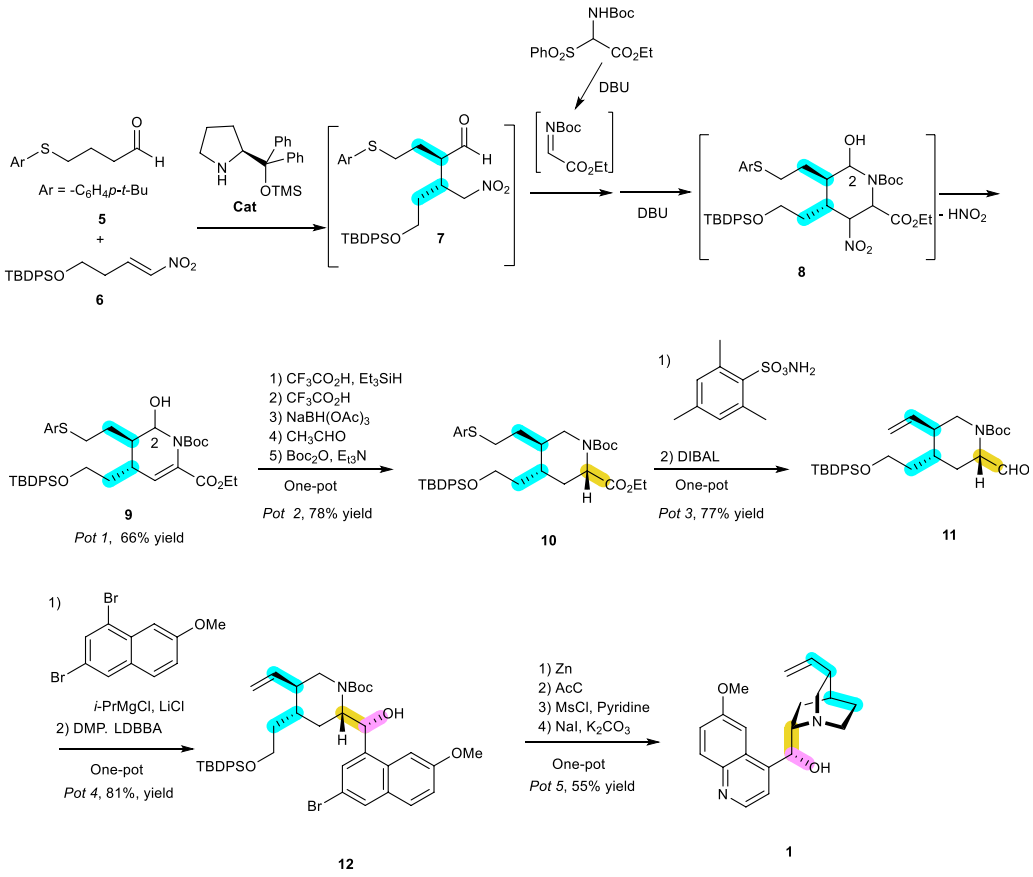

SCHEME 3
(–)-Quinine (**1**) synthesis reported by Professor Y. Hayashi's lab (Terunuma and Hayashi, 2022) using an organocatalyst in a pot-economical manner as a key step in constructing the initial important bonds, highlighted in blue, followed by stereoselective reduction and aryl Grignard addition, as shown by the yellow and red bonds.

This perspective focuses on the use of organocatalysts in a pot-economical manner for the recent synthesis of tetrahydropyridine-containing (–)-quinine. These synthetic methodologies may be applicable in laboratory preparation or in the industrial production of valuable organic compounds (Bernardi, et al., 2021). Most synthetic challenges are highly efficient and environmentally benign with organocatalysts in a pot-economical manner.

Data availability statement

The datasets presented in this article are not readily available because there are not any restrictions for readers to request. Requests to access the datasets should be directed to hjha@hufs.ac.kr.

Author contributions

H-JH: Conceptualization, Funding acquisition, Investigation, Project administration, Resources, Supervision, Validation, Visualization, Writing–original draft, Writing–review and editing.

Funding

The author(s) declare financial support was received for the research, authorship, and/or publication of this article. This work was supported by the National Research Foundation of Korea (SRC NRF 2021R1A5A6002803, Centre for New Directions in Organic Synthesis) and the HUFS fund 2024.

Conflict of interest

The author declares that the research was conducted in the absence of any commercial or financial relationships that could be construed as a potential conflict of interest.

Publisher's note

References

Albrecht, L., Albrecht, A., and Dell'Amico, L. (2022). *Asymmetric organocatalysis: new Strategies, catalysts, and opportunities*. Wiley VCH. ISBN-13, 978-3527349074.

Bernardi, L., Carlone, A., and Fini, F. (2021). Industrial relevance of asymmetric organocatalysis in the preparation of chiral amine derivatives. in *The book "Methodologies in amine synthesis: challenges and Applications* (A. Ricci and L. Bernardi) Wiley VCH, Weinheim.

Bernhard, N., and Wolfgang, S. (1978). Simple method for the esterification of carboxylic acids. *Angew. Chem. Int. Ed.* 17, 522–524. doi:10.1002/anie.197805221

Boukis, A. C., Reiter, K., Frölich, M., Hofheinz, D., and Meier, M. A. (2018). Multicomponent reactions provide key molecules for secret communication. *Nat. Commun.* 9, 1–10. doi:10.1038/s41467-018-03784-x

Chen, Z., Yang, Q.-Q., Du, W., and Chen, Y. C. (2022). Asymmetric organocatalysis involving double activation. *Tetrahedron Chem.* 2, 100017. doi:10.1016/j.tchem.2022.100017

Cimarelli, C. (2019). Multicomponent reactions. *Molecules* 24, 2372. doi:10.3390/molecules24132372

Coulthard, G., Erb, W., and Aggarwal, V. K. (2012). Stereocontrolled organocatalytic synthesis of prostaglandin PGF2a in seven steps. *Nature* 489, 278. doi:10.1038/nature11411

De Wolf, E., van Koten, G., and Deelman, B.-J. (1999). Fluorous phase separation techniques in catalysis. *Chem. Soc. Rev.*, 37–41. doi:10.1039/A805644G

Earle, M. J., and Seddon, K. R. (2000). Ionic liquids. Green solvents for the future. *Pure Appl. Chem.* 72, 1391–1398. doi:10.1351/pac200072071391

Gotoh, H., Ishikawa, H., and Hayashi, Y. (2007). Diphenylprolinol silyl ether as catalyst of an asymmetric, catalytic, and direct Michael reaction of nitroalkanes with α,β-unsaturated Aldehydes. *Org. Lett.* 9, 5307. doi:10.1021/ol702545z

Grondal, C., Jeanty, M., and Enders, D. (2010). Organocatalytic cascade reactions as a new tool in total synthesis. *Nat. Chem.* 2, 167–178. doi:10.1038/nchem.539

Hajos, Z. G., and Parrish, D. R. (1974). Asymmetric synthesis of bicyclic intermediates of natural product chemistry. *J. Org. Chem.* 39, 1615–1621. doi:10.1021/jo00925a003

Han, B., He, X.-H., Liu, Y.-Q., He, G., Peng, C., and Li, J.-L. (2021). Asymmetric organocatalysis: an enabling technology for medicinal chemistry. *Chem. Soc. Rev.* 50, 1522–1586. doi:10.1039/D0CS00196A

Han, M.-Y., Wang, H.-Z., An, W.-K., Jia, J.-Y., Ma, B.-C., Zhang, Y., et al. (2013). A Concise synthesis of L-pyrrolysine. *Chem. Eur. J.* 19, 8078. doi:10.1002/chem.201300403

Hayashi, Y. (2016). Pot-economy and one-pot synthesis. *Chem. Sci.* 7, 866–880. doi:10.1039/C5SC02913A

Hayashi, Y., Gotoh, H., Hayashi, T., and Shoji, M. (2005). Diphenylprolinol silyl ethers as efficient organocatalysts for the asymmetric Michael reaction of aldehydes and nitroalkenes. *Angew. Chem. Int. Ed.* 49, 4212–4315. PMID 20175175. doi:10.1002/anie.200906900

Hayashi, Y., and Ogasawara, S. (2016). Time economical total synthesis of (−)-oseltamivir. *Org. Lett.* 18, 3426–3429. doi:10.1021/acs.orglett.6b01595

Huang, W.-L., Raja, A., Hong, B. C., and Lee, G. H. (2017). Organocatalytic enantioselective Michael–acetalization reduction Nef reaction for a one-pot entry to the functionalized aflatoxin system. total synthesis of (-)-dihydroaflatoxin D2 and (-) and (+)-microminutinin. *Org. Lett.* 19, 3494. doi:10.1021/acs.orglett.7b01473

Hughes, D. L. (2018). Asymmetric organocatalysis in drug development—highlights of recent patent lterature. *Org. Process. Res. Dep.* 22, 574–584. doi:10.1039/D0CS00196A

Ishikawa, H., Suzuki, T., and Hayashi, Y. (2009). High-yielding synthesis of the anti-influenza neuramidase inhibitor (−)-oseltamivir by three "one-pot" operations. *Angew. Chem. Int. Ed.* 48, 1304–1307. doi:10.1002/anie.200804883

Ishikawa, H., Suzuki, T., Orita, H., Uchimaru, T., and Hayashi, Y. (2010). High-yielding synthesis of the anti-influenza neuraminidase inhibitor (−)-oseltamivir by two "one-pot" sequences. *Chem. Eur. J.* 16, 12616–12626. doi:10.1002/chem.201001108

Jensen, K. L., Dickmeiss, G., Jiang, H., Albrecht, L., and Jørgensen, K. A. (2012). The diarylprolinol silyl ether system: a general organocatalyst. *Acc. Chem. Res.* 45, 248–264. doi:10.1021/ar200149w

List, B. (2007). Introduction: organocatalysis. *Chem. Rev.* 107 (12), 5413–5415. doi:10.1021/cr078412e

List, B. (2010). Emil Knoevenagel and the roots of aminocatalysis. *Angew. Chem. Int. Ed.* 49, 1730–1734. doi:10.1002/anie.200906900

MacMillan, D. W. C. (2008). The advent and development of organocatalysis. *Nature* 455, 304–308. doi:10.1038/nature07367

Martínez, J., Cortés, J. F., and Miranda, R. (2022). Green chemistry, metrics, A Review. *Processes* 10, 1274. doi:10.3390/pr10071274

Matsuo, J., Kozai, T., and Ishibashi, H. (2006). Mild preparation of alkenes from phenyl sulfides: one-pot elimination of phenylthio group via sulfilimine at ambient temperature. *Org. Lett.* 8, 6095–6098. doi:10.1021/ol062620w

Meng, X.-L., Liu, T., Sun, Z.-W., Wang, J.-C., Peng, F.-Z., and Shao, Z.-H. (2014). Asymmetric catalytic conjugate addition of acetaldehyde to nitrodienynes/nitroenynes: applications to the syntheses of (+)-α-lycorane and chiral β-alkynyl acid. *Org. Lett.* 16, 3044–3047. doi:10.1021/ol501158b

Mika, L. T., and Horváth, I. T. (2018). *Fluorous Catalysis in the book green techniques for organic synthesis and medicinal chemistry*, (W. Zhang and B. W. Cue) John Wiley and Sons. Hoboken, USA.

Nafiu, S. A., Ajeebi, A. M., Alghamdi, H. S., Aziz, M. A., and Shaikh, M. N. (2023). Solid-supported catalysts for organic functional group transformations. *Asian J. Org. Chem.* 12, e202300051. doi:10.1002/ajoc.202300051

Pyser, J. B., Chakrabarty, S., Romero, E. O., and Narayan, A. R. H. (2021). State-of-the-art biocatalysis. *ACS Cent. Sci.* 7, 1105–1116. doi:10.1021/acscentsci.1c00273

Reyes-Rodríguez, G. J., Rezayee, N. M., Vidal-Albalat, A., and Jørgensen, K. A. (2019). Prevalence of diarylprolinol silyl ethers as catalysts in total synthesis and patents. *Chem. Rev.* 119, 4221–4260. doi:10.1021/acs.chemrev.8b00583

Ruiz-Lopez, M. F., Francisco, J. S., Martins-Costa, M. T. C., and Anglada, J. M. (2020). Molecular reactions at aqueous interfaces. *Nat. Rev. Chem.* 4, 459–475. doi:10.1038/s41570-020-0203-2

Scheffler, U., and Mahrwald, R. (2013). Recent advances in organocatalytic methods for asymmetric C-C bond formation. *Chem. Eur. J.* 19, 14346–14396. doi:10.1002/chem.201301996

Shiomi, S., Misaka, R., Kaneko, M., and Ishikawa, H. (2019). Enantioselective total synthesis of the unnatural enantiomer of quinine. *Chem. Sci.* 10, 9433. doi:10.1039/c9sc03879e

Terunuma, T., and Hayashi, Y. (2022). Organocatalyst-mediated five-pot synthesis of (−)-quinine. *Nat. Commun.* 13, 7503. doi:10.1038/s41467-022-34916-z

Vogel, P., Lam, Y.-H., Simon, A., and Houk, K. N. (2016). Organocatalysis: fundamentals and comparisons to metal and enzyme catalysis. *Catalysts* 6, 128. doi:10.3390/catal6090128

Yadav, N. N., Choi, J., and Ha, H.-J. (2016). Asymmetric synthesis of 2,6-cis-disubstituted piperidine alkaloids from chiral aziridine. *Org. Biomol. Chem.* 14, 6426–6434. doi:10.1039/C6OB00806B

frontiers | Frontiers in Chemistry

TYPE Original Research
PUBLISHED 03 November 2023
DOI 10.3389/fchem.2023.1271896

OPEN ACCESS

EDITED BY
Hsyueh-Liang Wu,
National Taiwan Normal University, Taiwan

REVIEWED BY
Rajendra Rohokale,
University of Florida, United States
Gary W. Breton,
Berry College, United States

*CORRESPONDENCE
Hidetoshi Noda,
hnoda@bikaken.or.jp
Masakatsu Shibasaki,
mshibasa@bikaken.or.jp

RECEIVED 03 August 2023
ACCEPTED 23 October 2023
PUBLISHED 03 November 2023

CITATION
Noda H, Asada Y and Shibasaki M (2023), Examining the effects of additives and precursors on the reactivity of rhodium alkyl nitrenes generated from substituted hydroxylamines. *Front. Chem.* 11:1271896. doi: 10.3389/fchem.2023.1271896

Examining the effects of additives and precursors on the reactivity of rhodium alkyl nitrenes generated from substituted hydroxylamines

Hidetoshi Noda*, Yasuko Asada and Masakatsu Shibasaki*

Institute of Microbial Chemistry (BIKAKEN), Tokyo, Japan

In this study, the reactivity of the alkyl nitrenes, generated from the substituted hydroxylamine precursors, was determined using the same rhodium catalyst. The results revealed that in competitive C–H insertion experiments, the regioselectivity between benzylic and tertiary C–H bonds could be modulated by adding Brønsted acids or changing the substituents on oxygen. This study enhances our understanding of the metallonitrene structures and provides valuable insights for further development of selective N-heterocycle syntheses.

KEYWORDS

nitrene, N-heterocycle, rhodium, C-H insertion, kinetic isotope effect

1 Introduction

Nitrogen-containing compounds prevail over biologically active compounds (Lovering et al., 2009; Vitaku et al., 2014). Therefore, the synthetic chemists have made considerable efforts to introduce nitrogen atoms at desired positions in the molecular skeleton (Park et al., 2017; Trowbridge et al., 2020). Among various approaches, utilizing nitrenes is preferred, as they can functionalize the otherwise inert C–H bonds (Müller and Fruit, 2003; Díaz-Requejo and Pérez, 2008; Darses et al., 2017). Given the high reactivity of free nitrenes, metallonitrenes are primarily used for nitrogen insertion as their reactivity can be regulated by the structure of the metal complexes (Ju and Schomaker, 2021). Metalated nitrenes are typically generated from oxidized precursors, either prepared *in situ* or from those containing a labile bond (Breslow and Gellman, 1982; Nägeli et al., 1997; Lebel et al., 2005).

The substituents on the nitrogen can be used to classify nitrene structures such as carbamoyl (Cui and He, 2004), sulfamoyl (Espino et al., 2001), aryl (Stokes et al., 2007), acyl (Hong et al., 2018), and alkyl (Hennessy and Betley, 2013) nitrenes. The class of nitrenes determines the structure of the resulting product. For instance, intramolecular C–H insertion of sulfamoyl nitrenes provides a 1,3-aminoalcohol unit, whereas that of alkyl nitrenes delivers a saturated N-heterocycle. Therefore, the advancement in nitrene chemistry is directed toward expanding the product structures and its evolution has resulted in the development of efficient catalysts and new precursors (Roizen et al., 2012; Alderson et al., 2017; Hong et al., 2021). The chemoselective amination reactions have garnered considerable interest in this area that has triggered the identification of various catalyst-controlled aminations (Noda et al., 2021). However, there are limited studies in the literature investigating the reactivity difference between various nitrene classes using identical catalysts. The comparison of the same nitrene class obtained from different precursors is

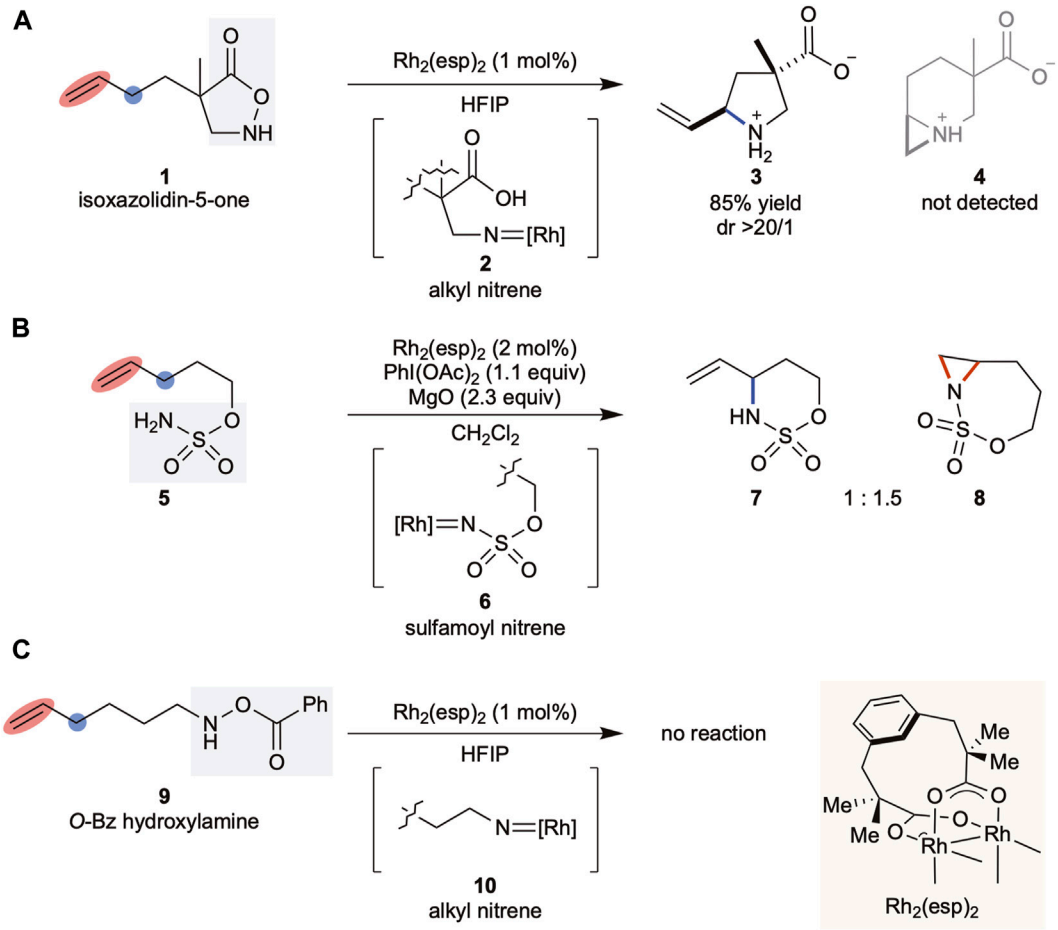

SCHEME 1
(A–C) Background of this work. esp: α, α, α′, α′-tetramethyl-1,3-benzenedipropionic acid, HFIP: 1,1,1,3,3,3-hexafluoroisopropanol.

also lacking. This could be attributed to the lack of a suitable system for studying the reactivities.

We previously reported that substituted isoxazolidin-5-ones (Annibaletto et al., 2017; Noda, 2021) acted as alkyl nitrene precursors in the presence of rhodium (Yu et al., 2019) or copper catalysts (Tak et al., 2021a). The generated metallonitrene reacted intramolecularly with an aromatic ring (Tak et al., 2021b) or C(sp^3)–H bond (Espinosa et al., 2019) to afford the corresponding unprotected cyclic β-amino acids. In our study to synthesize remotely decorated trisubstituted pyrrolidines via C(sp^3)–H insertion (Tang et al., 2022) using $Rh_2(esp)_2$, a Du Bois catalyst (Espino et al., 2004), it was observed that the alkyl nitrene derived from the heterocycle selectively aminated the C(sp^3)–H bond at the allylic position without touching the double bond (Scheme 1A), which was in contrast to the sulfamoyl nitrene favoring aziridination over C(sp^3)–H insertion, using the same rhodium catalyst (Scheme 1B) (Fiori et al., 2009). These results highlighted the unique nature of the nitrene reactivities associated with their structural classes.

Driven by the significance of saturated N-heterocycles in drug discovery programs, we further investigated alkyl nitrenes and identified *O*-benzoyl hydroxylamines as efficient alkyl nitrene precursors for the transformation of a linear primary amine into the corresponding five-membered cyclic amine (Noda et al., 2020). When we subjected substrate **9** to the catalytic conditions to explore the scope of the method, no reaction was observed, resulting in full recovery of the substrate (Scheme 1C). As both substrates **1** and **9** were expected to generate similar alkyl rhodium nitrene species **2** and **10**, respectively, as shown in Scheme 2, this difference in the outcomes could be attributed to the precursor structure. However, the lack of insight into the structure-reactivity relationship between nitrene precursors and the reaction conditions required a further detailed examination of these factors. Herein, we report our study on the reactivity of alkyl nitrenes derived from substituted hydroxylamines.

2 Results

From the outset, we focused on the reactivities of alkyl nitrenes, as the products obtained from the intramolecular amination are medicinally important saturated N-heterocycles. In addition to isoxazolidin-5-ones and *O*-Bz hydroxylamines, alkyl azides (Thacker et al., 2016; Bagh et al., 2017; Shing et al., 2018; Qin et al., 2019), and *O*-Ts hydroxylamines (Munnuri et al., 2017) act as nitrene precursors. Owing to their stability and facile structural modification, *O*-Bz hydroxylamines were used as model substrates in this study, and $Rh_2(esp)_2$ was used as the catalyst. Examination of the presumed nitrene structures **2** and **10**

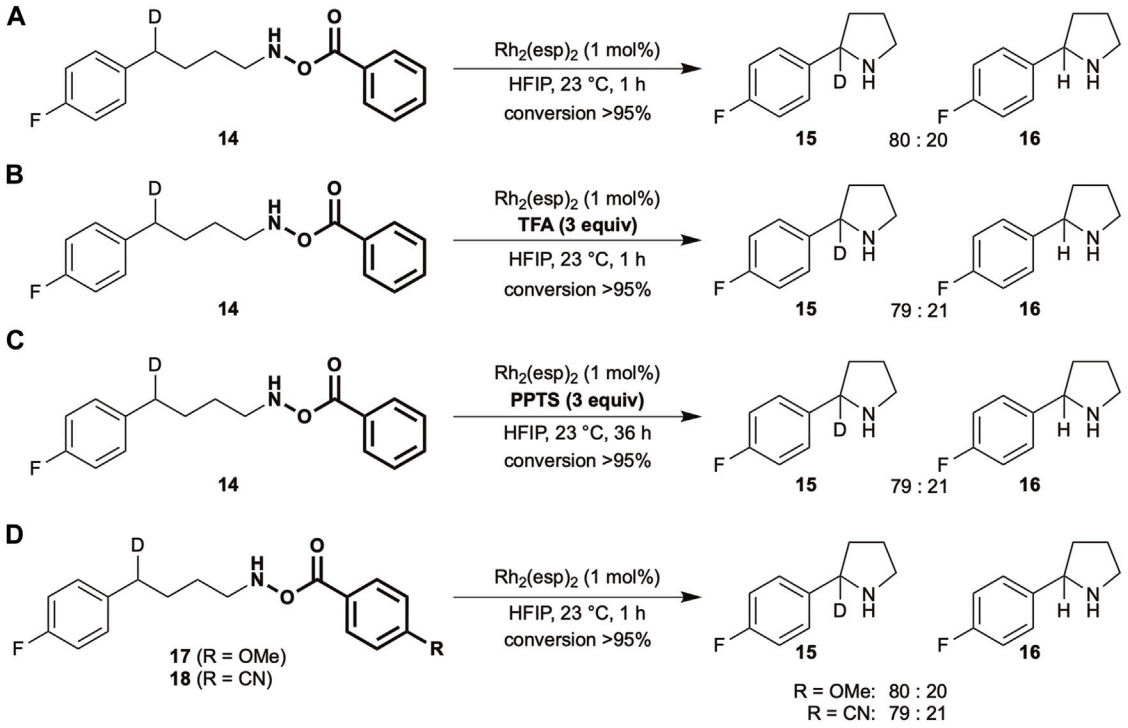

SCHEME 2
KIE experiments using $Rh_2(esp)_2$ as a catalyst under various conditions.

TABLE 1 Evaluation of additives on the regioselectivity of Rh-alkyl nitrene.

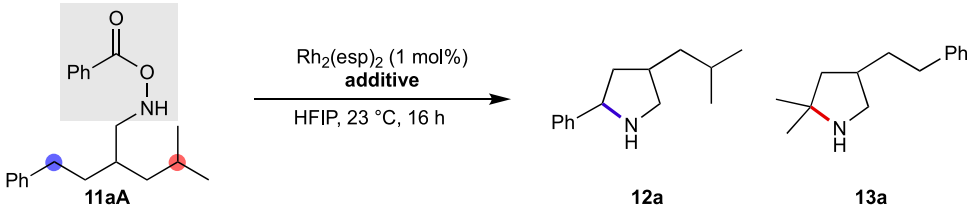

Entry	Additive (x equiv)	Conversion (%)[a]	12a:13a[b]
1	—	>95	21:79
2	TFA (3)	>95	29:71
3	TFA (10)	>95	31:69
4[c]	TfOH (3)	12 (21)	4:>96 (4: > 96)
5	PPTS (3)	27	4:>96
6	2,6-Lutidine (3)	>95	24:76
7	Et_3N (3)	>95	26:74
8	Cs_2CO_3 (3)	>95	19:81
9	Barton's base (3)	Complex mixture	

[a]Conversion was determined using 1H NMR, analysis of unpurified reaction mixture.
[b]The regioselectivity was determined using 1H NMR, and reverse-phase HPLC, analysis of unpurified reaction mixture.
[c]The values in parentheses were obtained after 48 h. TFA, trifluoroacetic acid; TfOH, trifluoromethanesulfonic acid; PPTS, pyridinium *p*-toluenesulfonate.

implied that a suitably located acidic proton in **2** played an important role in determining the reactivity, which was the driving force to investigate the additive effect using Brønsted acids and bases.

Table 1 summarizes the influence of additives on the regioselectivity of reactions, where the selectivity between benzylic and tertiary C–H bonds was used as a reactivity probe.

10.3389/fchem.2023.1271896

TABLE 2 Comparison between *O*-Bz and *O*-Ts hydroxylamines using rhodium catalyst.[a]

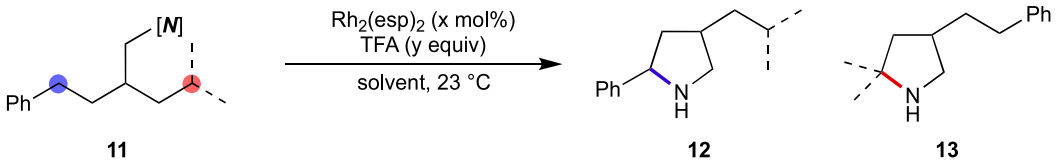

Entry	11	Conditions	Yield (%)	12:13	*anti*/*syn* (12)
1	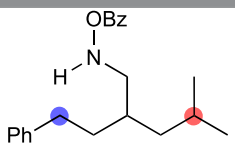 **11aA**	A	73	31:69	83/17
2	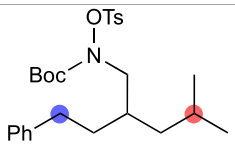 **11aB**	B	77	43:57	84/16
3	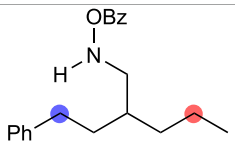 **11bA**	A	83	>96:4	81/19
4	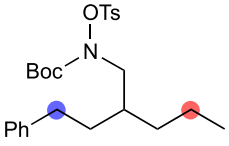 **11bB**	B	84	>96:4	88/12
5	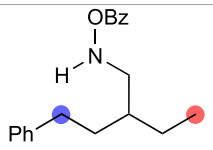 **11cA**	A	82	>96:4	83/17
6	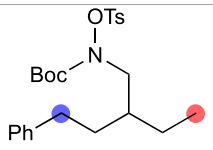 **11cB**	B	83	>96:4	89/11

Conditions A: $Rh_2(esp)_2$ (1 mol%), TFA (10 equiv), HFIP., Conditions B: $Rh_2(esp)_2$ (2 mol%), TFA (2 equiv), TFE.
[a]Products were isolated after conversion into the corresponding *N*-Ts adducts. TFE; 2,2,2-trifluoroethanol, Ts; *p*-toluenesulfonyl.

In the absence of additives, the site selectivity of **11aA** is close to 1:4, favoring the tertiary C–H bond (entry 1). The ratio marginally decreases in the presence of trifluoroacetic acid (TFA) (entry 2), suggesting that an acidic proton source plays a vital role in the selectivity-determining transition state. Higher acid loadings do not decrease the selectivity further (entry 3). It was observed that all the acids do not lower the selectivity, and the addition of a stronger acid, trifluoromethanesulfonic acid (TfOH), creates a strong bias in the reaction site for the tertiary C–H bond, although with a considerably slower kinetics (entry 4). Similar trend is observed for pyridinium *p*-toluenesulfonate (PPTS), which is a milder Brønsted acid compared to the TFA (entry 5). In contrast to acidic additives, the addition of a Brønsted base does not lead to a noticeable shift in the regioselectivity (entries 6–8).

10.3389/fchem.2023.1271896

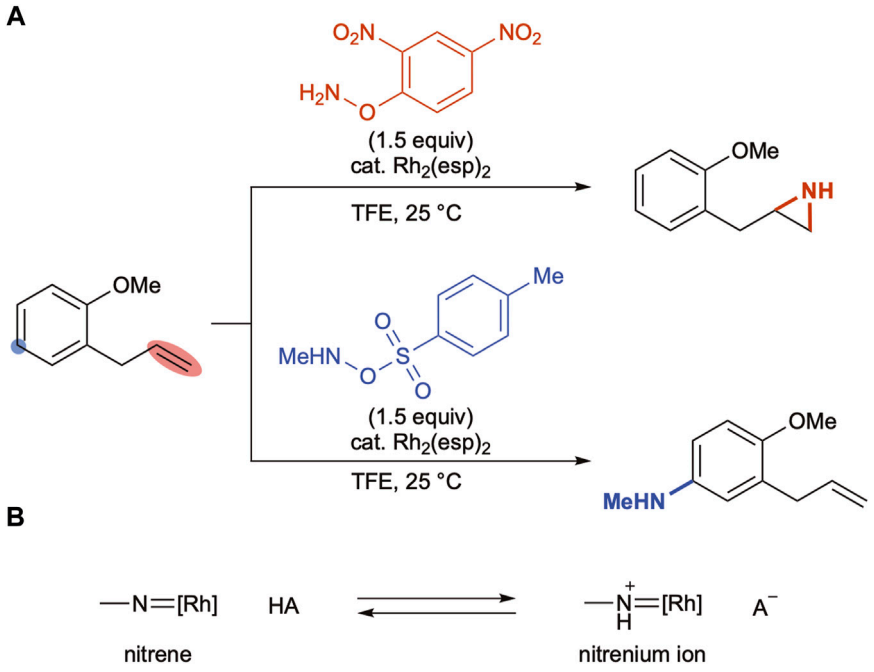

SCHEME 3
(A) Reagent-controlled chemoselectivity switch under rhodium-catalyzed conditions. **(B)** Possible interconversion between nitrenes and nitrenium ions.

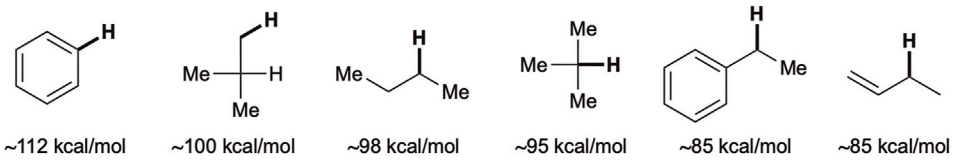

FIGURE 1
BDEs for various representative C–H bonds.

A change in the selectivity is often accompanied by a change in the reaction mechanism. Therefore, to understand the nature of reactive intermediates under Brønsted acidic conditions, kinetic isotope effect (KIE) experiments were conducted (Scheme 2). Fluorine-substituted compounds were used for this purpose as the high sensitivity of ^{19}F nuclei in nuclear magnetic resonance (NMR) is beneficial for determining the selectivity. Under standard conditions, using 1 mol % $Rh_2(esp)_2$ as a catalyst in 1,1,1,3,3,3-hexafluoroisopropanol (HFIP) at ambient temperature, a KIE value of 4.0 is obtained (Scheme 2A). The value remains the same in the presence of TFA (Scheme 2B), suggesting similar properties of the reactive intermediate in both cases. Despite the distinct selectivity trend observed in Table 1, the addition of PPTS does not change the KIE value (Scheme 2C). The KIE value of a similar *N*-Boc-*O*-Ts substrate was reported to be 5.3 (Munnuri et al., 2017), therefore, electronically tuned benzoate substrates were subjected to identical conditions. The obtained values are approximately same to those of the unmodified substrate (Scheme 2D).

We questioned whether the difference in the KIE values between *O*-Bz and *O*-Ts hydroxylamines would be translated into a difference in regioselectivities. Although the reactivity trend of *O*-Ts hydroxylamines has been previously studied using a different rhodium catalyst, a comparison with three classes of substrates was carried out for ranking the reactivities of various C–H bonds (benzylic, tertiary, secondary, and primary). In addition to regioselectivity, diastereoselectivity was utilized as the other reactivity probe.

The instability of the *N*-H form of *O*-Ts hydroxylamines requires *in situ* removal of a protective group from the nitrogen. Following the previous reports, the *N*-Boc group was used to mask the nitrogen atom and TFA was used as the proton source in TFE. Thus, TFA was included in the reactions with *O*-Bz substrates for a fair comparison (Table 2). All the products were isolated after conversion to their *N*-Ts forms. Examining the regioselectivity between benzylic and tertiary C–H bonds, a marginally lower selectivity is obtained using the *O*-Ts substrate compared to that of *O*-Bz substrate, although the diastereoselectivity is similar for both (entries 1 and 2). Owing to their diminished reactivity toward metallonitrene, cyclization products are not obtained at the secondary or primary C–H bonds for either of the substrates. However, better diastereoselectivities are recorded with *O*-Ts substrates compared to those with *O*-Bz substrates (entries 3 vs. 4 and 5 vs. 6).

3 Discussion

Falck and coworkers reported aziridination of olefins with *O*-(2,4-dinitrophenyl)hydroxylamine under the influence of a $Rh_2(esp)_2$ catalyst (Jat et al., 2014). The group revealed in a subsequent report that the combination of the same rhodium catalyst with *O*-Ts hydroxylamine aminated an aromatic C–H bond keeping the olefin moiety intact (Scheme 3A) (Paudyal et al., 2016). The authors proposed that the rhodium nitrene generated upon N–O bond cleavage was in equilibrium with the protonated nitrenium ion and the two species exhibited distinct reactivity, which justified the remarkable chemoselectivity switch (Scheme 3B). Moreover, acidity of the liberated Brønsted acids determined the equilibrium positions; the nitrophenol was not strong enough to protonate metallonitrenes, whereas a stronger sulfonic acid propelled the equilibrium forward to yield nitrenium ions.

Given that the acidity of the reaction medium is responsible for the equilibrium position, it was hypothesized that the addition of external Brønsted acids should play an identical role. The results in Table 1 reveal that the inclusion of sulfonic acids drastically changes the regioselectivity trend (entries 4,5, Table 1), which can be explained by a possible shift in the equilibrium. The observed lower reactivity could be ascribed to either the lower C–H insertion activity of the nitrenium ion intermediate or the slower N–O bond cleavage to form a reactive intermediate. However, the addition of external Brønsted acids does not alter the KIE values (Scheme 2A–C), suggesting that a similar reactive intermediate is involved in the C–H amination step in the absence or presence of acids.

Over the years, KIE experiments have been used to assess and elucidate the nature of reactive intermediates in various C–H functionalization reactions. It is well-known in nitrene chemistry that KIE values lower than three indicate the presence of a concerted mechanism involving a singlet nitrene. For instance, the KIE values of sulfamoyl nitrenes using a similar rhodium catalyst were in the range of 1.9–2.9 (Fiori et al., 2009; Varela-Álvarez et al., 2016). In contrast, a stepwise mechanism displays higher KIE values (Badiei et al., 2008; Harvey et al., 2011). The difference in KIE values between *O*-Bz (4.0) and *O*-Ts (5.3) hydroxylamines using the same catalyst inferred that precursor structures play a significant role in determining the nature of reactive intermediate but the acidity of the reaction medium. As a slight modification of the benzoic acid derivatives (pKa in H_2O: *p*-CN-C_6H_4 3.55, C_6H_5 4.21, *p*-MeO-C_6H_4 4.47) did not affect the KIE values (Scheme 2D), a considerably drastic change in the acidity of the leaving groups might be required to induce a change.

The precursor structure-dependent KIE value implies that the reactive intermediate generated from *O*-Ts substrates possesses a triplet, radical-like nature. Radical-like intermediates typically follow the bond dissociation energy (BDE) order, which is the enthalpy change associated with the homolytic scission of the bond (Figure 1). The results summarized in Table 2 agree with this trend. Therefore, the *O*-Ts substrate undergoes the benzylic amination preferably compared to that for *O*-Bz (entry 1 vs. 2, Table 2). Comparable results are obtained in HFIP using **11aB** (76% yield, **12a**:**13a** 41:59, *anti*/*syn* 83/17), excluding the possibility that the choice of solvent governs the selectivity. The observed diastereoselectivities support the different natures of the reactive intermediates generated from *O*-Bz and *O*-Ts hydroxylamines.

4 Conclusion

We have investigated the reactivity of rhodium alkyl nitrenes generated from substituted hydroxylamines. The addition of Brønsted acids modulated the regioselectivity of the intramolecular C–H insertion between the benzylic and tertiary positions. Despite the distinct regioselectivities, approximately identical KIE values were observed for various Brønsted acids. In contrast to external acids, the KIE values fluctuated as a function of the precursor structures. The conditions that produced the more radical-like reactive intermediate followed the expected reaction tendency. Although further efforts are required to completely understand the nature of reactive intermediates, particularly with the external addition of Brønsted acids, our results comprehensively confirmed that the reactivities of seemingly similar reactive intermediates could be regulated by incorporating additives or changing the precursor structures. This work significantly enhances our understanding of the rhodium nitrene structures, which are typically devoid of precursor residues, and opens up new avenues for a substrate-controlled approach to fine-tune the reactivity, as with other hydroxylamine-involving reactions (Noda et al., 2014; Niu and Buchwald, 2015).

Data availability statement

The original contributions presented in the study are included in the article/Supplementary Material, further inquiries can be directed to the corresponding authors.

Author contributions

HN: Writing–original draft, Writing–review and editing. YA: Writing–original draft. MS: Writing–review and editing.

Funding

The author(s) declare financial support was received for the research, authorship, and/or publication of this article. This work was supported by the JSPS KAKENHI grant numbers JP20K06957 and JP22H05383 (Digi-TOS). HN is grateful to the Naito Foundation and the Takahashi Industrial and Economic Research Foundation for their financial support.

Acknowledgments

We are grateful to Dr. Ryuichi Sawa, Yumiko Kubota, Dr. Kiyoko Iijima, and Dr. Shinya Adachi at the Institute of Microbial Chemistry for their technical assistance with the NMR and MS analyses.

Conflict of interest

The authors declare that the research was conducted in the absence of any commercial or financial relationships that could be construed as a potential conflict of interest.

Publisher's note

All claims expressed in this article are solely those of the authors and do not necessarily represent those of their affiliated organizations, or those of the publisher, the editors and the reviewers. Any product that may be evaluated in this article, or claim that may be made by its manufacturer, is not guaranteed or endorsed by the publisher.

Supplementary material

The Supplementary Material for this article can be found online at: https://www.frontiersin.org/articles/10.3389/fchem.2023.1271896/full#supplementary-material

References

Alderson, J. M., Corbin, J. R., and Schomaker, J. M. (2017). Tunable, chemo- and site-selective nitrene transfer reactions through the rational design of silver(I) catalysts. *Acc. Chem. Res.* 50, 2147–2158. doi:10.1021/acs.accounts.7b00178

Annibaletto, J., Oudeyer, S., Levacher, V., and Brière, J.-F. (2017). Catalytic enantioselective syntheses of isoxazolidin-5-ones. *Synthesis* 49, 2117–2128. doi:10.1055/s-0036-1588765

Badiei, Y. M., Dinescu, A., Dai, X., Palomino, R. M., Heinemann, F. W., Cundari, T. R., et al. (2008). Copper–nitrene complexes in catalytic C–H amination. *Angew. Chem. Int. Ed.* 47, 9961–9964. doi:10.1002/anie.200804304

Bagh, B., Broere, D. L. J., Sinha, V., Kuijpers, P. F., van Leest, N. P., de Bruin, B., et al. (2017). Catalytic synthesis of N-Heterocycles via direct C(sp^3)–H amination using an Air-stable Iron(III) species with a redox-active ligand. *J. Am. Chem. Soc.* 139, 5117–5124. doi:10.1021/jacs.7b00270

Breslow, R., and Gellman, S. H. (1982). Tosylamidation of cyclohexane by a cytochrome P-450 model. *J. Chem. Soc. Chem. Commun.* 1982, 1400–1401. doi:10.1039/c39820001400

Cui, Y., and He, C. (2004). A silver-catalyzed intramolecular amidation of saturated C–H bonds. *Angew. Chem. Int. Ed.* 43, 4210–4212. doi:10.1002/anie.200454243

Darses, B., Rodrigues, R., Neuville, L., Mazurais, M., and Dauban, P. (2017). Transition metal-catalyzed iodine(iii)-mediated nitrene transfer reactions: efficient tools for challenging syntheses. *Chem. Commun.* 53, 493–508. doi:10.1039/c6cc07925c

Díaz-Requejo, M. M., and Pérez, P. J. (2008). Coinage metal catalyzed C-H bond functionalization of hydrocarbons. *Chem. Rev.* 108, 3379–3394. doi:10.1021/cr078364y

Espino, C. G., Fiori, K. W., Kim, M., and Du Bois, J. (2004). Expanding the scope of C–H amination through catalyst design. *J. Am. Chem. Soc.* 126, 15378–15379. doi:10.1021/ja0446294

Espino, C. G., Wehn, P. M., Chow, J., and Du Bois, J. (2001). Synthesis of 1,3-difunctionalized amine derivatives through Selective C–H bond oxidation. *J. Am. Chem. Soc.* 123, 6935–6936. doi:10.1021/ja011033x

Espinosa, M., Noda, H., and Shibasaki, M. (2019). Synthesis of unprotected spirocyclic β-Prolines and β-Homoprolines by Rh-catalyzed C-H insertion. *Org. Lett.* 21, 9296–9299. doi:10.1021/acs.orglett.9b03198

Fiori, K. W., Espino, C. G., Brodsky, B. H., and Du Bois, J. (2009). A mechanistic analysis of the Rh-catalyzed intramolecular C–H amination reaction. *Tetrahedron* 65, 3042–3051. doi:10.1016/j.tet.2008.11.073

Harvey, M. E., Musaev, D. G., and Du Bois, J. (2011). A diruthenium catalyst for selective, intramolecular allylic C–H amination: reaction development and mechanistic insight gained through experiment and theory. *J. Am. Chem. Soc.* 133, 17207–17216. doi:10.1021/ja203576p

Hennessy, E. T., and Betley, T. A. (2013). Complex N-heterocycle synthesis via iron-catalyzed, direct C-H bond amination. *Science* 340, 591–595. doi:10.1126/science.1233701

Hong, S. Y., Hwang, Y., Lee, M., and Chang, S. (2021). Mechanism-guided development of transition-metal-catalyzed C-N bond-forming reactions using dioxazolones as the versatile amidating source. *Acc. Chem. Res.* 54, 2683–2700. doi:10.1021/acs.accounts.1c00198

Hong, S. Y., Park, Y., Hwang, Y., Kim, Y. B., Baik, M.-H., and Chang, S. (2018). Selective formation of γ-lactams via C–H amidation enabled by tailored iridium catalysts. *Science* 359, 1016–1021. doi:10.1126/science.aap7503

Jat, J. L., Paudyal, M. P., Gao, H., Xu, Q. L., Yousufuddin, M., Devarajan, D., et al. (2014). Direct stereospecific synthesis of unprotected N-H and N-Me aziridines from olefins. *Science* 343, 61–65. doi:10.1126/science.1245727

Ju, M., and Schomaker, J. M. (2021). Nitrene transfer catalysts for enantioselective C–N bond formation. *Nat. Rev. Chem.* 5, 580–594. doi:10.1038/s41570-021-00291-4

Lebel, H., Huard, K., and Lectard, S. (2005). *N*-Tosyloxycarbamates as a source of metal nitrenes: rhodium-catalyzed C-H insertion and aziridination reactions. *J. Am. Chem. Soc.* 127, 14198–14199. doi:10.1021/ja0552850

Lovering, F., Bikker, J., and Humblet, C. (2009). Escape from flatland: increasing saturation as an approach to improving clinical success. *J. Med. Chem.* 52, 6752–6756. doi:10.1021/jm901241e

Müller, P., and Fruit, C. (2003). Enantioselective catalytic aziridinations and asymmetric nitrene insertions into CH bonds. *Chem. Rev.* 103, 2905–2920. doi:10.1021/cr020043t

Munnuri, S., Adebesin, A. M., Paudyal, M. P., Yousufuddin, M., Dalipe, A., and Falck, J. R. (2017). Catalyst-controlled diastereoselective synthesis of cyclic amines via C-H functionalization. *J. Am. Chem. Soc.* 139, 18288–18294. doi:10.1021/jacs.7b09901

Nägeli, I., Baud, C., Bernardinelli, G., Jacquier, Y., Moraon, M., and Müllet, P. (1997). Rhodium(II)-catalyzed CH insertions with [(4-Nitrophenyl)sulfonyl]iminophenyl-λ^3-iodane. *Helv. Chim. Acta* 80, 1087–1105. doi:10.1002/hlca.19970800407

Niu, D., and Buchwald, S. L. (2015). Design of modified amine transfer reagents allows the synthesis of α-chiral secondary amines via CuH-catalyzed hydroamination. *J. Am. Chem. Soc.* 137, 9716–9721. doi:10.1021/jacs.5b05446

Noda, H. (2021). Imbuing an old heterocycle with the power of modern catalysis: an isoxazolidin-5-one Story. *Chem. Pharm. Bull.* 69, 1160–1169. doi:10.1248/cpb.c21-00750

Noda, H., Asada, Y., and Shibasaki, M. (2020). *O*-Benzoylhydroxylamines as alkyl nitrene precursors: synthesis of saturated N-heterocycles from primary amines. *Org. Lett.* 22, 8769–8773. doi:10.1021/acs.orglett.0c02842

Noda, H., Erős, G., and Bode, J. W. (2014). Rapid ligations with equimolar reactants in water with the potassium acyltrifluoroborate (KAT) amide formation. *J. Am. Chem. Soc.* 136, 5611–5614. doi:10.1021/ja5018442

Noda, H., Tang, X., and Shibasaki, M. (2021). Catalyst-controlled chemoselective nitrene transfers. *Helv. Chim. Acta* 104, e2100140. doi:10.1002/hlca.202100140

Park, Y., Kim, Y., and Chang, S. (2017). Transition metal-catalyzed C–H amination: scope, mechanism, and applications. *Chem. Rev.* 117, 9247–9301. doi:10.1021/acs.chemrev.6b00644

Paudyal, M. P., Adebesin, A. M., Burt, S. R., Ess, D. H., Ma, Z., Kürti, L., et al. (2016). Dirhodium-catalyzed C-H arene amination using hydroxylamines. *Science* 353, 1144–1147. doi:10.1126/science.aaf8713

Qin, J., Zhou, Z., Cui, T., Hemming, M., and Meggers, E. (2019). Enantioselective intramolecular C–H amination of aliphatic azides by dual ruthenium and phosphine catalysis. *Chem. Sci.* 10, 3202–3207. doi:10.1039/c9sc00054b

Roizen, J. L., Harvey, M. E., and Du Bois, J. (2012). Metal-catalyzed nitrogen-atom transfer methods for the oxidation of aliphatic C-H bonds. *Acc. Chem. Res.* 45, 911–922. doi:10.1021/ar200318q

Shing, K.-P., Liu, Y., Cao, B., Chang, X.-Y., You, T., and Che, C.-M. (2018). N-heterocyclic carbene Iron(III) porphyrin-catalyzed intramolecular C(sp^3)-H amination of alkyl azides. *Angew. Chem. Int. Ed.* 57, 12123–12127. doi:10.1002/ange.201806059

Stokes, B. J., Dong, H., Leslie, B. E., Pumphrey, A. L., and Driver, T. G. (2007). Intramolecular C–H amination reactions: exploitation of the Rh_2(II)-catalyzed decomposition of azidoacrylates. *J. Am. Chem. Soc.* 129, 7500–7501. doi:10.1021/ja072219k

Tak, R. K., Amemiya, F., Noda, H., and Shibasaki, M. (2021a). Generation and application of Cu-bound alkyl nitrenes for the catalyst-controlled synthesis of cyclic β-amino acids. *Chem. Sci.* 12, 7809–7817. doi:10.1039/d1sc01419f

Tak, R. K., Noda, H., and Shibasaki, M. (2021b). Ligand-Enabled, copper-catalyzed electrophilic amination for the asymmetric synthesis of β-amino acids. *Org. Lett.* 23, 8617–8621. doi:10.1021/acs.orglett.1c03328

Tang, X., Tak, R. K., Noda, H., and Shibasaki, M. (2022). A missing link in multisubstituted pyrrolidines: remote stereocontrol forged by Rhodium-alkyl nitrene. *Angew. Chem. Int. Ed.* 61, e202212421. doi:10.1002/anie.202212421

Thacker, N. C., Lin, Z., Zhang, T., Gilhula, J. C., Abney, C. W., and Lin, W. (2016). Robust and porous β-diketiminate-functionalized metal–organic frameworks for earth-abundant-metal-catalyzed C–H amination and hydrogenation. *J. Am. Chem. Soc.* 138, 3501–3509. doi:10.1021/jacs.5b13394

Trowbridge, A., Walton, S. M., and Gaunt, M. J. (2020). New strategies for the transition-metal catalyzed synthesis of aliphatic amines. *Chem. Rev.* 120, 2613–2692. doi:10.1021/acs.chemrev.9b00462

Varela-Álvarez, A., Yang, T., Jennings, H., Kornecki, K. P., MacMillan, S. N., Lancaster, K. M., et al. (2016). Rh_2(II,III) catalysts with chelating carboxylate and carboxamidate supports: electronic structure and nitrene transfer reactivity. *J. Am. Chem. Soc.* 138, 2327–2341. doi:10.1021/jacs.5b12790

Vitaku, E., Smith, D. T., and Njardarson, J. T. (2014). Analysis of the structural diversity, substitution patterns, and frequency of nitrogen heterocycles among U.S. FDA approved pharmaceuticals. *J. Med. Chem.* 57, 10257–10274. doi:10.1021/jm501100b

Yu, J.-S., Espinosa, M., Noda, H., and Shibasaki, M. (2019). Traceless electrophilic amination for the synthesis of unprotected cyclic β-amino acids. *J. Am. Chem. Soc.* 141, 10530–10537. doi:10.1021/jacs.9b05476

frontiers | Frontiers in Chemistry

TYPE Original Research
PUBLISHED 22 January 2024
DOI 10.3389/fchem.2024.1355636

OPEN ACCESS

EDITED BY
Hyun-Joon Ha,
Hankuk University of Foreign Studies, Republic of Korea

REVIEWED BY
Prakash Sekar,
Syganture Discovery Ltd., United Kingdom
Jung Min Joo,
Kyung Hee University, Republic of Korea
Cheon-Gyu Cho,
Hanyang University, Republic of Korea
Sanghee Kim,
Seoul National University, Republic of Korea

*CORRESPONDENCE
Sunkyu Han,
sunkyu.han@kaist.ac.kr

RECEIVED 14 December 2023
ACCEPTED 08 January 2024
PUBLISHED 22 January 2024

CITATION
Kim S, Lee H-S and Han S (2024), Transformation of (allo)securinine to (allo)norsecurinine via a molecular editing strategy. *Front. Chem.* 12:1355636. doi: 10.3389/fchem.2024.1355636

Transformation of (allo)securinine to (allo)norsecurinine via a molecular editing strategy

Seoyoung Kim, Hee-Seung Lee and Sunkyu Han*

Department of Chemistry, Korea Advanced Institute of Science & Technology (KAIST), Daejeon, Republic of Korea

Securinega alkaloids have intrigued chemists since the isolation of securinine in 1956. This family of natural products comprises a securinane subfamily with a piperidine substructure and norsecurinane alkaloids featuring a pyrrolidine core. From a biosynthetic perspective, the piperidine moiety in securinane alkaloids derives from lysine, whereas the pyrrolidine moiety in norsecurinane natural products originates from ornithine, marking an early biogenetic divergence. Herein, we introduce a single-atom deletion strategy that enables the late-stage conversion of securinane to norsecurinane alkaloids. Notably, for the first time, this method enabled the transformation of piperidine-based (allo) securinine into pyrrolidine-based (allo)norsecurinine. Straightforward access to norsecurinine from securinine, which can be readily extracted from the plant *Flueggea suffruticosa*, abundant across the Korean peninsula, holds promise for synthetic studies of norsecurinine-based oligomeric securinega alkaloids.

KEYWORDS

securinega alkaloids, ring contraction, molecular editing, natural products, atom deletion strategy, heterocycle

Introduction

Securinega alkaloids, composed of over 100 members, have fascinated the synthetic community owing to their structural diversity (Wehlauch and Gademann, 2017; Kang et al., 2023) and potent bioactivities (Hou et al., 2023) since the isolation of securinine (**2**) in 1956 (Muraveva and Bankovskii, 1956). Securinane alkaloids, exemplified by allosecurinine (**1**) and securinine (**2**), are characterized by an azabicyclo[3.2.1]octane core (B/C rings), fused with a piperidine (A) and butenolide (D) rings (Scheme 1A). Norsecurinane alkaloids such as allonorsecurinine (**3**) (Alibés et al., 2004; Antien et al., 2019; Hetzler et al., 2022) and norsecurinine (**4**) share a structural resemblance with securinanes. However, they feature a pyrrolidine moiety in place of the piperidine-based A ring. It is established that the piperidine (A) ring of the securinane alkaloids is derived from 1-piperideine (**5**), the biosynthetic downstream derivative of lysine (**6**) (Marek Golebiewski et al., 1976). On the other hand, the pyrrolidine (A) ring of the norsecurinane alkaloids is envisioned to have originated from 1-pyrroline (**7**), the biosynthetic derivative of ornithine (**8**). Hence, the size of the A ring is determined at the early stage of the biogenesis.

Notably, various dimeric and oligomeric high-order securinega alkaloids such as flueggenines A (**9**), C (**10**), and fluevirosines A (**11**), G (**12**) have been isolated (Scheme 1B) (Jeon et al., 2017; Kang et al., 2023). In 2017, we reported the total synthesis of flueggenine C (**10**) via an accelerated Rauhut–Currier (RC) reaction (Jeon and Han, 2017). Subsequently, we also succeeded in the total synthesis of flueggenines D and I via a Stille cross-coupling and stereoselective conjugate reduction dimerization strategy (Jeon et al., 2020). Notably, the primary constituent among

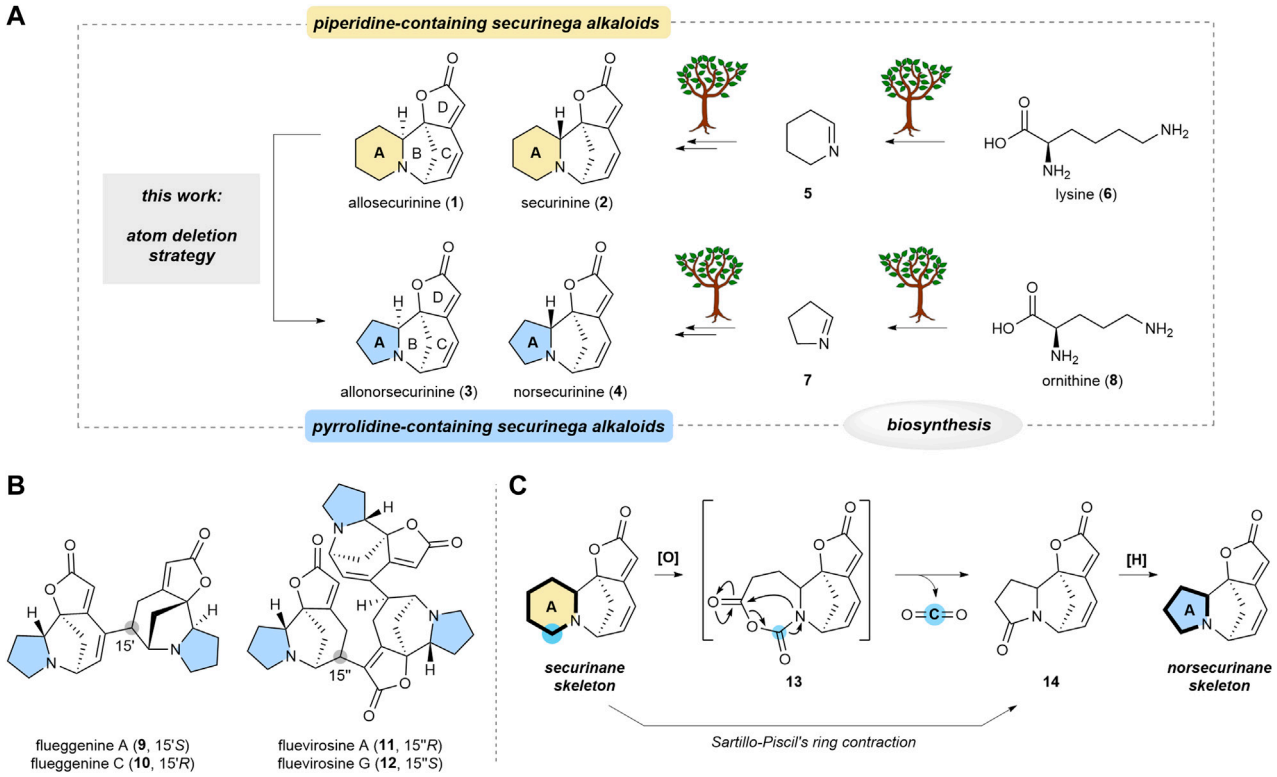

SCHEME 1
Transformation of securinane framework to norsecurinane framework via molecular editing strategy. **(A)** Parallel biosynthesis of (allo)securinine and (allo)norsecurinine and the direct transformation of the former natural products to the latter natural product (this work). **(B)** Representative high-order securinega alkaloids with the pyrrolidine core. **(C)** Overview of our atom deletion strategy that is based on Sartillo-Piscil's ring contraction method.

the monomeric units forming high-order securinega alkaloids is norsecurinine (**4**). In pursuit of a synthetic program centered on direct RC-based conjugations among norsecurinines (**4**) (Han, 2023; Park et al., 2023), we sought a solution for obtaining a substantial quantity of norsecurinine (**4**). In consideration of this goal, we conceived a semisynthetic method to derive (allo)norsecurinine (**3** and **4**) from (allo)securinine (**1** and **2**), natural substances abundantly found in *Flueggea suffruticosa*, a widely distributed plant in the Korean peninsula.

Single-atom skeletal editing has emerged as a powerful approach to efficiently diversify the molecular framework (Jurczyk et al., 2022). This molecular editing strategy has also been applied in natural product synthesis (Hui et al., 2022). We envisioned that the securinane skeleton could be transformed into the norsecurinane skeleton via a single-atom deletion logic (Ha, 2023). Herein, we describe a synthetic protocol that enables a single carbon deletion of the piperidine (A) (Srivastava and Ha, 2023) ring of securinanes to yield pyrrolidine-based norsecurinanes via the intermediacy of *N*-carboxyanhydride intermediate **13** and lactam **14** (Scheme 1C) based on Sartillo-Piscil's ring contraction method (Romero-Ibañez et al., 2019).

Results and discussion

Our synthesis commenced with regioselective double oxidation of C5 and C6 carbons of allosecurinine (**1**) to produce lactam **20** in 60% yield as a 4:1 diastereomeric mixture (Scheme 2). In 2016, Sartillo-Piscil and coworkers reported a double sp^3 C–H oxidation of cyclic amines to α-alkoxyamine lactams (Osorio-Nieto et al., 2016; Romero-Ibañez et al., 2023). In the instance of allosecurinine (**1**), the oxoammonium cation of TEMPO (**15**) selectively abstracted the C6 hydridic α-hydrogen from the amine moiety due to its greater steric accessibility consistent with Sartillo-Piscil's reports (Osorio-Nieto et al., 2016; Romero-Ibañez et al., 2023). This led to the formation of the iminium ion intermediate **16**, which subsequently underwent tautomerization, resulting in the formation of enamine **17**. Subsequently, enamine **17** reacted with the oxoammonium cation of TEMPO (**15**) to produce iminium ion **18**, which is consequently trapped by the chlorine dioxide anion to afford intermediate **19** (Osorio-Nieto et al., 2016). The extrusion of hypochlorous acid from intermediate **19** resulted in lactam **20**. The structure of the major diastereomer of **20** was unambiguously confirmed by a single crystal X-ray diffraction (SCXD) analysis. To our delight, when the TEMPO adduct **20** was allowed to react with 3 equiv of *m*-CPBA, the ring contraction product **14** was obtained in 54% yield (Romero-Ibañez et al., 2019). The structure of lactam **14** was confirmed by a single crystal X-ray diffraction (SCXD) analysis. Chemoselective reduction of the lactam moiety of **14** in the presence of the lactone group was achieved by a synthetic sequence involving the conversion of the lactam moiety to the thiolactam group (96% yield), the methylation of the resulting thiolactam moiety, and the sodium cyanoborohydride-mediated

10.3389/fchem.2024.1355636

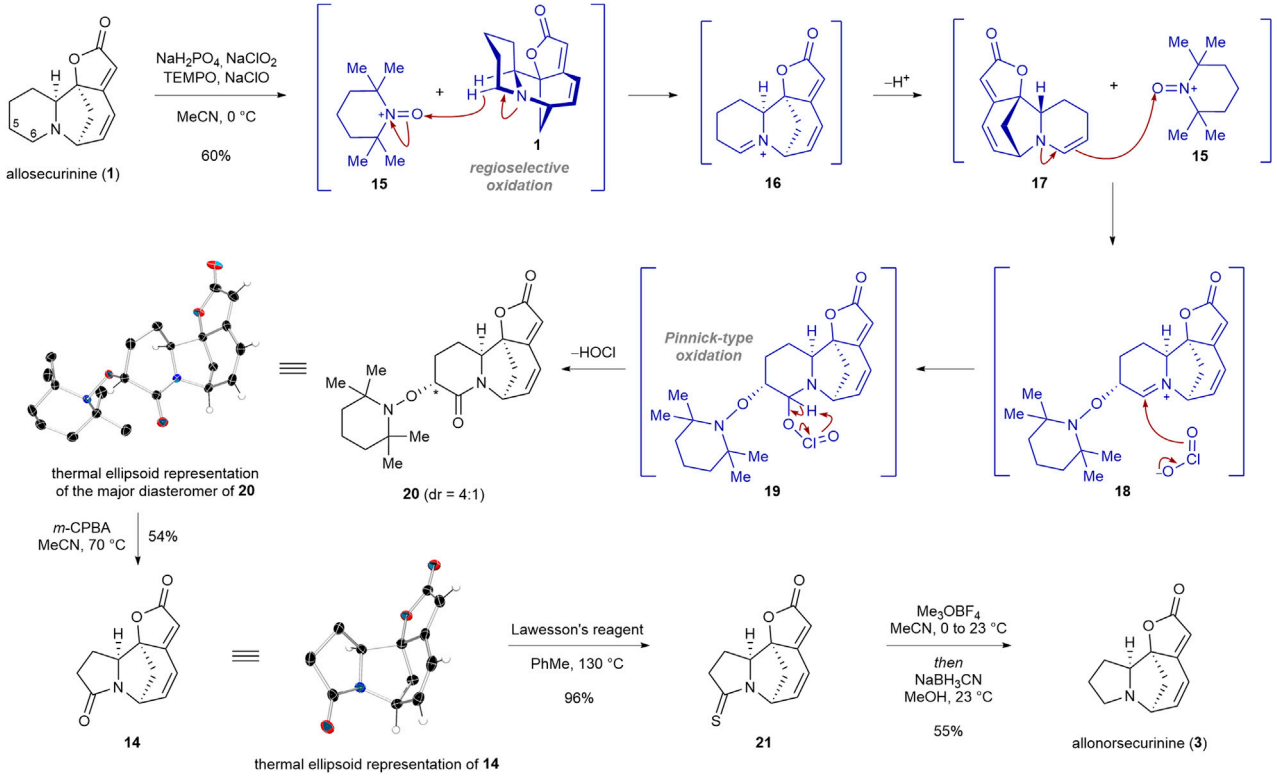

SCHEME 2
Transformation of allosecurinine (**1**) to allonorsecurinine (**3**) via an atom deletion strategy.

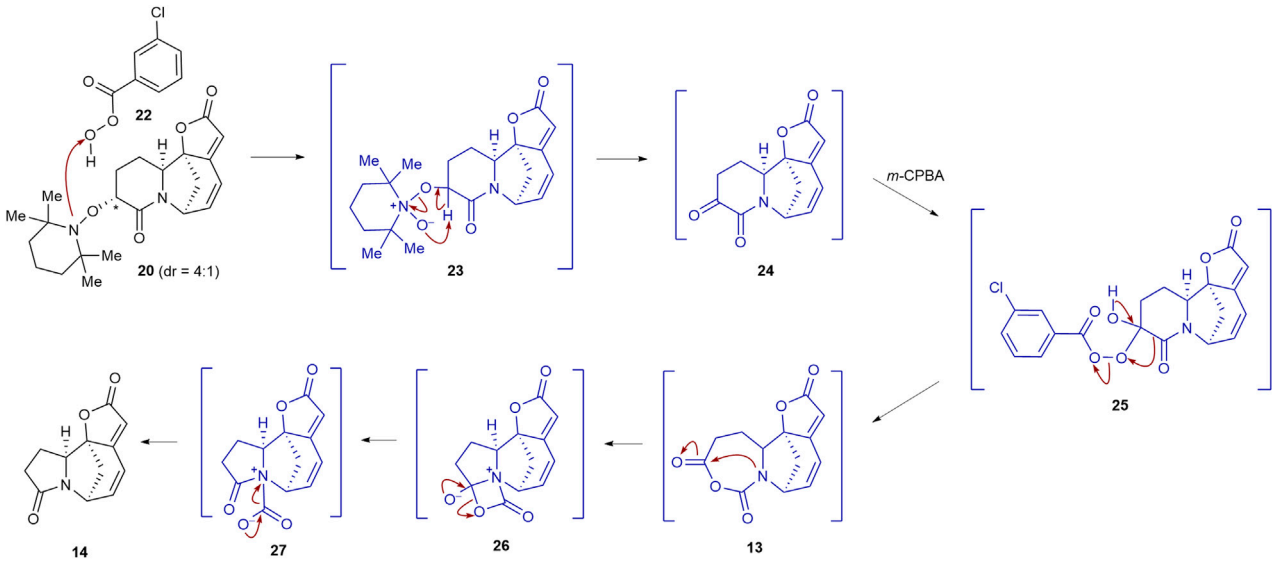

SCHEME 3
Plausible reaction mechanism for the formation of **14** from **20** in the presence of *m*-CPBA.

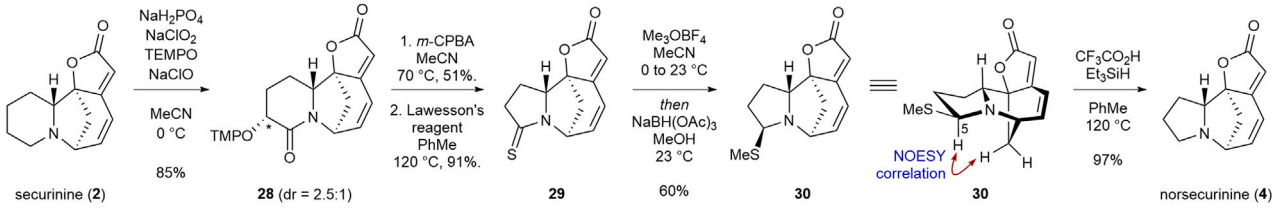

SCHEME 4
Transformation of securinine (**2**) to norsecurinine (**4**).

reduction of the consequent thioimidate ester salt (55% yield for the conversion of **21** to **3**).

The plausible reaction mechanism for converting TEMPO adduct **20** to lactam **14** is depicted in Scheme 3 (Romero-Ibañez et al., 2019). The *m*-CPBA-mediated oxidation of TEMPO adduct **20** would result in the formation of *N*-oxide intermediate **23**. Extrusion of TEMPOH from **23** would afford α-ketolactam intermediate **24**. Ketone **24** would then undergo a regioselective Baeyer–Villiger oxidation via intermediate **25** to produce *N*-carboxyanhydride intermediate **13**. Transannular 1,2-addition of the nitrogen nucleophile in **13** would yield pentacyclic intermediate **26**, which subsequently undergoes a carbon dioxide extrusion via intermediate **27** to forge lactam **14**.

After establishing a synthetic protocol for the "methylene deletion" of allosecurinine (**1**), we set out to transform securinine (**2**) to norsecurinine (**4**) in an analogous manner. In the event, treatment of securinine (**2**) with monosodium phosphate, sodium chlorite, TEMPO, sodium hypochlorite in acetonitrile resulted in TEMPO adduct **28** in 85% yield as a 2.5:1 mixture of diastereomers (Scheme 4). Subsequent *m*-CPBA-mediated ring contraction (51% yield) and the thionylation of the resulting lactam with Lawesson's reagent (91%) afforded thiolactam **29**. Interestingly, when thiolactam **29** was allowed to react with Meerwein's salt and subsequently with sodium triacetoxyborohydride, thioaminal product **30** was obtained in 60% yield. This was in stark contrast to the aforementioned reduction of thioamide **21** to the amine product under analogous reduction conditions. 2D-NMR analysis of compound **30** revealed that the proton at C5 is axially positioned. Hence, we reasoned that the stereoelectronic misalignment of the N1-lone pair p-orbital and the C5–S σ* orbital hindered the formation of the iminium ion intermediate. To our pleasure, we discovered that exposure of thioaminal product **30** to more forcing conditions (TFA and triethylsilane in refluxing toluene) afforded norsecurinine (**4**) in 97% yield.

Conclusion

In summary, a molecular editing protocol for the transformation of (allo)securinine to (allo)norsecurinine was established. The key to our success was the employment of the oxidative ring contraction method pioneered by the Sartillo-Piscil group (Romero-Ibañez et al., 2019). Chemoselective reduction of the lactam moiety over the lactone moiety was possible via selective conversion of the amide group to the thioamide group and its subsequent chemoselective reduction. Our findings enabled a straightforward transformation of securinine into norsecurinine, leveraging the abundant supply of securinine derived from the *F. suffruticosa* plant commonly found across the Korean peninsula. Norsecurinine, a pyrrolidine-based compound, serves as the monomeric unit within the high-order securinega alkaloids. Hence, our discovery stands poised to enable the synthesis of more complex securinega alkaloids. Those studies are currently ongoing and will be the subject of forthcoming reports.

Materials and methods

General information

All reactions were performed in oven-dried or flame-dried round-bottomed flasks and vials. Unless otherwise noted, the flasks were fitted with rubber septa and reactions were conducted under a positive pressure of argon, and vials were tightly sealed with plastic septa, Teflon tape, and parafilm. Stainless steel syringes were used to transfer air- and moisture-sensitive liquids. Flash column chromatography was performed as described by Still et al. using silica gel (60-Å pore size, 40–63 μm, 4%–6% H_2O content, Merck) (Still et al., 1978). Analytical thin–layer chromatography (TLC) was performed using glass plates pre-coated with 0.25 mm silica gel impregnated with a fluorescent indicator (254 nm). Thin layer chromatography plates were visualized by exposure to ultraviolet light, and/or a basic aqueous potassium permanganate ($KMnO_4$).

Unless otherwise stated, all commercial reagents and solvents were used without additional purification.

^1H and ^{13}C nuclear magnetic resonance spectra were recorded with Bruker Avance III HD (400 MHz), Bruker Avance NEO (500 MHz), Agilent DD-2 (600 MHz) and calibrated by using the residual undeuterated chloroform (δ_H = 7.24 ppm) and $CDCl_3$ (δ_C = 77.23 ppm) as internal references. Data are reported in the following manners: chemical shift in ppm [multiplicity (s = singlet, d = doublet, t = triplet, q = quartet, p = quintet, m = multiplet, app = apparent, br = broad), coupling constant(s) in Hertz, integration]. The NMR solvent $CDCl_3$ was taken from a stock containing anhydrous K_2CO_3 to remove residual DCl. High resolution mass spectra were obtained from KAIST Analysis Center for Research (Daejeon) by using ESI method. Specific rotation $[\alpha]_D^T$ was obtained by JASCO P-2000 polarimeter.

Data availability statement

The original contributions presented in the study are included in the article/Supplementary Material, further

inquiries can be directed to the corresponding author. Single crystal X-ray diffraction analysis data of compounds **14** (deposition number: 2314385) and **20** (deposition number: 2314384) were deposited in the Cambridge Crystallographic Data Center (CCDC).

Author contributions

SK: Conceptualization, Investigation, Writing–original draft, Writing–review and editing. H-SL: Funding acquisition, Supervision, Writing–review and editing. SH: Conceptualization, Funding acquisition, Investigation, Supervision, Writing–original draft, Writing–review and editing.

Funding

The author(s) declare financial support was received for the research, authorship, and/or publication of this article. This work was supported by the National Research Foundation of Korea (NRF-2021R1A2C2011203). Furthermore, we acknowledge support by the National Research Foundation of Korea (NRF-2018R1A5A1025208). This research was also supported by the KAIST UP project. We finally thank the support by the KAIST Grand Challenge 30 project.

Acknowledgments

We thank Dongwook Kim for the assistance with the single crystal X-ray diffraction analyses of compounds **14** and **20**.

Conflict of interest

The authors declare that the research was conducted in the absence of any commercial or financial relationships that could be construed as a potential conflict of interest.

Publisher's note

Supplementary material

The Supplementary Material for this article can be found online at: https://www.frontiersin.org/articles/10.3389/fchem.2024.1355636/full#supplementary-material

References

Alibés, R., Ballbé, M., Busqué, F., de March, P., Elias, L., Figueredo, M., et al. (2004). A new general access to either type of securinega alkaloids: synthesis of securinine and (−)-Allonorsecurinine. *Org. Lett.* 6, 1813–1816. doi:10.1021/ol049455+

Antien, K., Lacambra, A., Cossío, F. P., Massip, S., Deffieux, D., Pouységu, L., et al. (2019). Bio-inspired total synthesis of twelve securinega alkaloids: structural reassignments of (+)-Virosine B and (−)-Episecurinol A. *Chem. Eur. J.* 25, 11574–11580. doi:10.1002/chem.201903122

Ha, H.-J. (2023). Recent advances in synthesizing and utilizing nitrogen-containing heterocycles. *Front. Chem.* 11, 1279418. doi:10.3389/fchem.2023.1279418

Han, S. (2023). "K-synthesis": recent advancements in natural product synthesis enabled by unique methods and strategies development in Korea. *Bull. Korean Chem. Soc.* 44, 172–201. doi:10.1002/bkcs.12654

Hetzler, B. E., Trauner, D., and Lawrence, A. L. (2022). Natural product anticipation through synthesis. *Nat. Rev. Chem.* 6, 170–181. doi:10.1038/s41570-021-00345-7

Hou, W., Huang, H., Wu, X.-Q., and Lan, J.-X. (2023). Bioactivities and mechanism of action of securinega alkaloids derivatives reported prior to 2022. *Biomed. Pharmacother.* 158, 114190. doi:10.1016/j.biopha.2022.114190

Hui, C., Wang, Z., Wang, S., and Xu, C. (2022). Molecular editing in natural product synthesis. *Org. Chem. Front.* 9, 1451–1457. doi:10.1039/D2QO00043A

Jeon, S., and Han, S. (2017). An accelerated intermolecular rauhut–currier reaction enables the total synthesis of (−)-flueggenine C. *J. Am. Chem. Soc.* 139, 6302–6305. doi:10.1021/jacs.7b02751

Jeon, S., Lee, J., Park, S., and Han, S. (2020). Total synthesis of dimeric Securinega alkaloids (−)-flueggenines D and I. *Chem. Sci.* 11, 10934–10938. doi:10.1039/d0sc03057k

Jeon, S., Park, J., and Han, S. (2017). Syntheses of dimeric securinega alkaloids. *Synlett* 28, 2353–2359. doi:10.1055/s-0036-1590864

Jurczyk, J., Woo, J., Kim, S. F., Dherange, B. D., Sarpong, R., and Levin, M. D. (2022). Single-atom logic for heterocycle editing. *Nat. Synth.* 1, 352–364. doi:10.1038/s44160-022-00052-1

Kang, G., Park, S., and Han, S. (2023). Synthesis of high-order and high-oxidation state securinega alkaloids. *Acc. Chem. Res.* 56, 140–156. doi:10.1021/acs.accounts.2c00719

Marek Golebiewski, W., Horsewood, P., and Spenser, I. D. (1976). Biosynthesis of securinine: the mode of incorporation of lysine. *J. Chem. Soc. Chem. Comm.* 24, 217–218. doi:10.1039/C39760000217

Muraveva, V. I., and Bankovskii, A. I. (1956). Chemical study of alkaloids of Securinega suffruticosa. *Dokl. Akad. Nauk. SSSR.* 110, 998–1000.

Osorio-Nieto, U., Chamorro-Arenas, D., Quintero, L., Höpfl, H., and Sartillo-Piscil, F. (2016). Transition metal-free selective double sp^3 C-H oxidation of cyclic amines to 3-alkoxyamine lactams. *J. Org. Chem.* 81, 8625–8632. doi:10.1021/acs.joc.6b01566

Park, S., Kim, D., Yang, W., and Han, S. (2023). Total synthesis of 4α-hydroxyallosecurinine and securingine F, securinega alkaloids with a C4-hydroxy handle for biofunctional derivatizations. *Synlett* 34. doi:10.1055/a-2047-9680

Romero-Ibañez, J., Cruz-Gregorio, S., Sandoval-Lira, J., Hernández-Pérez, J. M., Quintero, L., and Sartillo-Piscil, F. (2019). Transition-metal-free deconstructive lactamization of piperidines. *Angew. Chem. Int. Ed.* 58, 8867–8871. doi:10.1002/anie.201903880

Romero-Ibañez, J., Sandoval-Lira, J., Cruz-Gregorio, S., Hernández-Pérez, J. M., Quintero, L., and Sartillo-Piscil, F. (2023). On the reaction mechanism of the selective C(sp^3)–H functionalization of N-benzylpiperidines mediated by TEMPO oxoammonium cation. *Synthesis* 55, 3662–3669. doi:10.1055/a-2053-9558

Srivastava, N., and Ha, H.-J. (2023). Regioselective ring opening of aziridine for synthesizing azaheterocycle. *Front. Chem.* 11, 1280633. doi:10.3389/fchem.2023.1280633

Still, W. C., Kahn, M., and Mitra, A. (1978). Rapid chromatographic technique for preparative separations with moderate resolution. *J. Org. Chem.* 43, 2923–2925. doi:10.1021/jo00408a041

Wehlauch, R., and Gademann, K. (2017). Securinega alkaloids: complex structures, potent bioactivities, and efficient total syntheses. *Asian J. Org. Chem.* 6, 1146–1159. doi:10.1002/ajoc.201700142

frontiers | Frontiers in Chemistry

TYPE Original Research
PUBLISHED 01 March 2024
DOI 10.3389/fchem.2024.1361266

OPEN ACCESS

EDITED BY
Takashi Ohshima,
Kyushu University, Japan

REVIEWED BY
Vinay S. Sharma,
Gujarat University, India
Raman Khurana,
O2M Technologies, LLC, United States

*CORRESPONDENCE
Farzaneh Mohamadpour,
f_mohamadpour@sums.ac.ir,
mohamadpour.f.7@gmail.com
Ali Mohammad Amani,
amani_a@sums.ac.ir,
aliamani@sums.ac.ir

RECEIVED 25 December 2023
ACCEPTED 15 February 2024
PUBLISHED 01 March 2024

CITATION
Mohamadpour F and Amani AM (2024), Halogenated dicyanobenzene-based photosensitizer (3DPAFIPN) as a thermally activated delayed fluorescence (TADF) used in gram-scale photosynthesis 3,4-dihydropyrimidin-2-(1*H*)-one/thione derivatives via a consecutive visible-light-induced electron-transfer pathway. *Front. Chem.* 12:1361266. doi: 10.3389/fchem.2024.1361266

Halogenated dicyanobenzene-based photosensitizer (3DPAFIPN) as a thermally activated delayed fluorescence (TADF) used in gram-scale photosynthesis 3,4-dihydropyrimidin-2-(1*H*)-one/thione derivatives via a consecutive visible-light-induced electron-transfer pathway

Farzaneh Mohamadpour* and Ali Mohammad Amani*

Department of Medical Nanotechnology, School of Advanced Medical Sciences and Technologies, Shiraz University of Medical Sciences, Shiraz, Iran

Background: Organic dyes often have shorter lifetimes in the excited state, which is a major obstacle to the development of effective photoredox methods. The scientific community has shown a great deal of interest in a certain class of organic chromophores because of their unique characteristics and effectiveness. One characteristic of the molecules under research is thermally activated delayed fluorescence (TADF), which is only observed in molecules with a tiny energy gap (often less than 0.2 eV) between their lowest two excited states, i.e., singlet excited state (S_1) and triplet excited state (T_1). The extended singlet excited states arising from TADF and the simplicity with which their redox potentials may be altered make the isophthalonitrile family of chromophores an attractive option for organic photocatalyst applications.

Methods: The Biginelli reaction between *β*-ketoesters, arylaldehydes, and urea/thiourea has been used to build a sustainable technique for the production of 3,4-dihydropyrimidin-2-(1*H*)-one/thione derivatives. In the present study, the development of a green radical synthesis approach for this class of compounds is addressed in depth. As a photocatalyst, a new halogenated dicyanobenzene-based photosensitizer was employed in this study. As a renewable energy source activated by a blue LED, it was dissolved in ethanol, at room temperature in air atmosphere. The primary objective of this research is to employ a novel donor-acceptor (D-A) based on halogenated cyanoarene that is affordable, easily available, and innovative.

Findings: The 3DPAFIPN [2,4,6-tris(diphenylamino)-5-fluoroisophthalonitrile] photocatalyst, a thermally activated delayed fluorescence (TADF), induces single-electron transfer (SET) in response to visible light, offering a

straightforward, eco-friendly, and highly efficient process. Additionally, we determined the 3,4-dihydropyrimidin-2-(1*H*)-one/thione derivatives turnover frequency (TOF) and turnover number (TON). It has also been demonstrated that gram-scale cyclization is a workable method for industrial purposes.

KEYWORDS

dicyanobenzene-based photosensitizer (3DPAFIPN), renewable energy source, visible-light-induced electron-transfer, photosynthesis, 3, 4-dihydropyrimidin-2-(1H)-one/thione derivatives

Introduction

In recent literature, photoredox catalysis has served as a foundation for novel approaches in organic chemistry (Mohamadpour, 2021a; Mohamadpour, 2023a). The field of photoredox catalysis, which combines metal-promoted reactions with photoredox cycles, is gaining significant attention from both academia and industry (Pinosa et al., 2022). The main focus of research is the use of inexpensive, readily manufactured, and efficient organic dyes to help create novel, powerful, and selective metal-promoted reactions (Gualandi et al., 2021). In this sector, organic dyes must take the place of the commonly employed inorganic complexes that are dependent on Ir(III) and Ru(II). When compared to organic molecules, these compounds are known for their long excited state lifetimes, which may tend toward dynamic quenching. Organic dyes often have shorter lifetimes in the excited state, which is a major obstacle to the development of effective photoredox methods. The scientific community has shown a great deal of interest in a specific class of organic chromophores because of their unique characteristics and effectiveness (Bryden and Zysman-Colman, 2021). One characteristic of the molecules under study is thermally activated delayed fluorescence (TADF), which is only observed in molecules with a tiny energy gap (often less than 0.2 eV) between their lowest two excited states, i.e., S_1 and T_1. Under ambient conditions, the molecules under study undergo reverse intersystem crossing (RISC), aided by a thermally activated pathway from the triplet excited state (T_1) to the singlet excited state (S_1). This results in a delayed fluorescence phenomenon that is commonly observed in systems similar to this one. The present goal is to combine reduced instruction set computing's (RISC) exceptional efficiency with fluorescence's great quantum yield. 2012 saw a significant advancement in the field of organic light-emitting diodes (OLEDs) with the release of a basic work by Adachi (Uoyama et al., 2012). This approach covers the efficient usage of dicyanobenzene molecules with suitable photophysical properties as well as their demonstrated application in OLEDs. Similar TADF chromophores have been used in other domains, such as photocatalysis, since these initial discoveries (Yang et al., 2017; Bryden and Zysman-Colman, 2021). The extended singlet excited states arising from TADF and the simplicity with which their redox potentials may be altered make the isophthalonitrile family of chromophores a viable option for organic photocatalyst applications (Speckmeier et al., 2018). 2,4,6-tris(diphenylamino)-5-fluoroisophthalonitrile (3DPAFIPN) is a chemical that is widely used in a number of visible light-triggered synthetic procedures. Intramolecular cyclizations (Flynn et al., 2020; Wu et al., 2020) and the formation of C–C (Cardinale et al., 2020; Donabauer et al., 2020), N–C (Zhou et al., 2020), and P–C (Rothfelder et al., 2021) bonds (Pinosa et al., 2022) are a few examples of these processes.

Because visible light irradiation has a large energy reserve, is inexpensive, and can be used to access sustainable energy sources, it is considered a reliable method for creating organic compounds (Mohamadpour, 2021b; Mohamadpour, 2021c; Mohamadpour, 2022a).

It is expected that dihydropyrimidine structures have potent biological and pharmacological effects (Figure 1). Calcium channel blockers, antihypertensive effects (Sujatha et al., 2006), anticancer (Wisen et al., 2008), anti HIV agent (Heys et al., 2000), antibacterial and antifungal (Ashok et al., 2007), antiviral (Hurst and Hull, 1961), antioxidative (Magerramow et al., 2006), and anti-inflammatory (Bahekar and Shinde, 2004).

To produce 3,4-dihydropyrimidin-2-(1*H*)-one/thione derivatives, a number of catalysts are employed, including Na_2 eosin Y (Mohamadpour, 2022b), copper (II)sulfamate (Liu et al., 2012), bakers, yeast (Kumar and Maurya, 2007), hydrotalcite (Lal et al., 2012), hexaaquaaluminium (III) tetrafluoroborate (Litvic et al., 2010), TBAB (Ahmed et al., 2009), copper (II) tetrafluoroborate (Kamal et al., 2007), [Btto][*p*-TSA] (Zhang et al., 2015), triethylammonium acetate (Attri et al., 2017), saccharin (Mohamadpour et al., 2016), caffeine (Mohamadpour and Lashkari, 2018), zirconium (IV)-salophen perfluorooctanesulfonate (Li et al., 2020), $H_3[PW_{12}O_{40}]$ (Chopda and Dave, 2020), Dioxane-HCl (Choudhare et al., 2021), WSi/A15 (Bosica et al., 2021), $H_4[W_{12}SiO_{40}]$ (V Chopda and Dave, 2020), $Zr(H_2PO_4)_2$ (KÜÇÜKİSLAMOĞLU et al., 2010), and GO-chitosan (Maleki and Paydar, 2016). Complex procedures, lengthy reaction times, the use of costly chemicals, and lower yields are just a few of the variables that significantly impact the management and disposal of waste. Moreover, it might be challenging to extract homogeneous catalysts from reaction mixtures. Due to our interest in the development of photocatalytic reactions (Mohamadpour, 2022c; Mohamadpour, 2022d; Mohamadpour, 2023b; Mohamadpour, 2023c; Mohamadpour, 2023d), the current work discusses the use of photocatalysts in the synthesis of heterocyclic compounds, emphasizing the use of environmentally acceptable practices. The investigation indicates that using

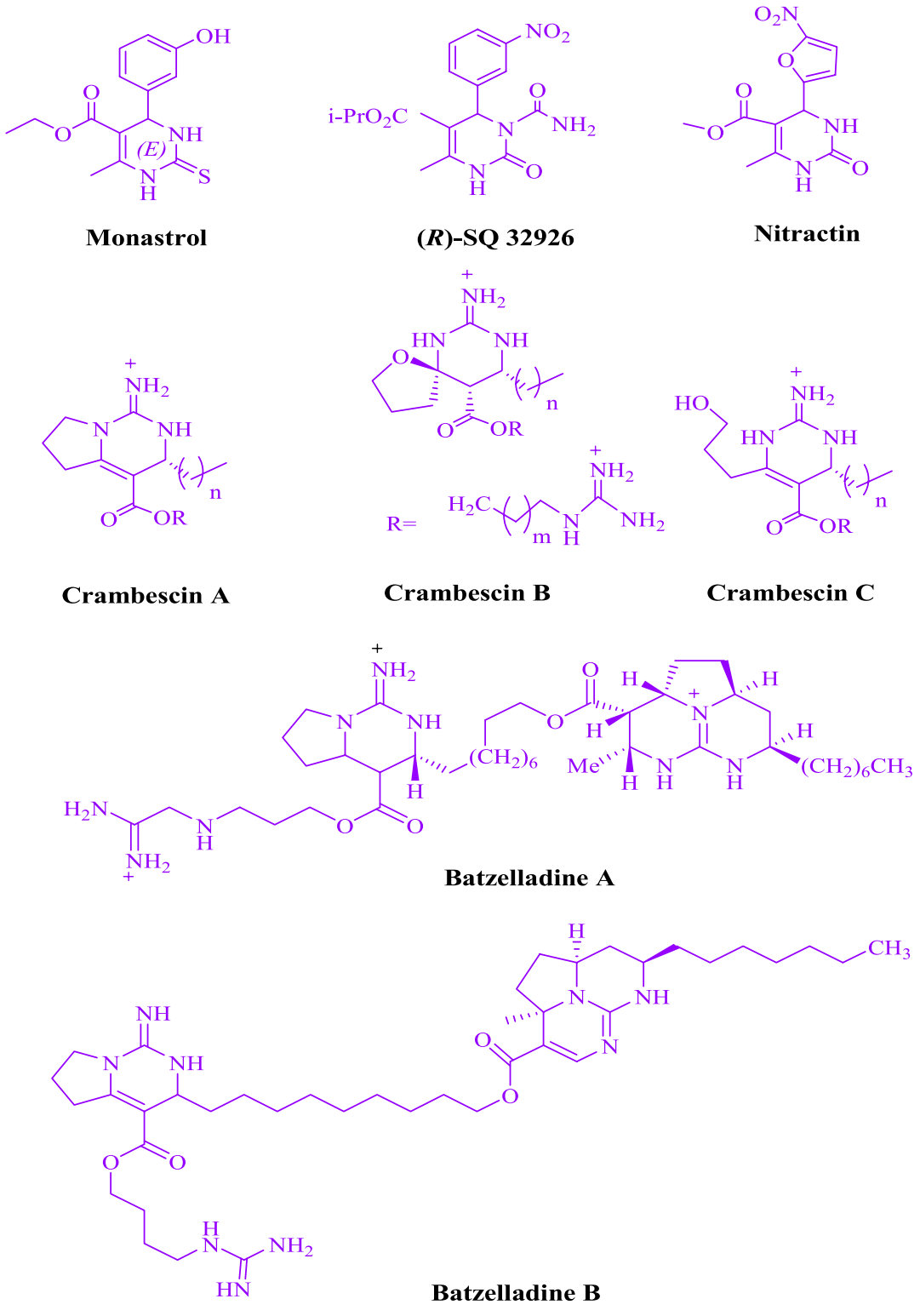

FIGURE 1
The dihydropyrimidine motifs exhibit pharmacological activity.

photo-redox catalysts for halogenated organic dyes is also financially feasible. A potent donor-acceptor (D-A) cyanoarene is employed as an efficient organo-photocatalyst by employing the previously outlined technique.

The primary focus of the investigation was 2,4,6-tris(diphenylamino)-5-fluoroisophthalonitrile (3DPAFIPN) because of its exceptional photophysical and photochemical properties. Organic chemists now have access to a wider range

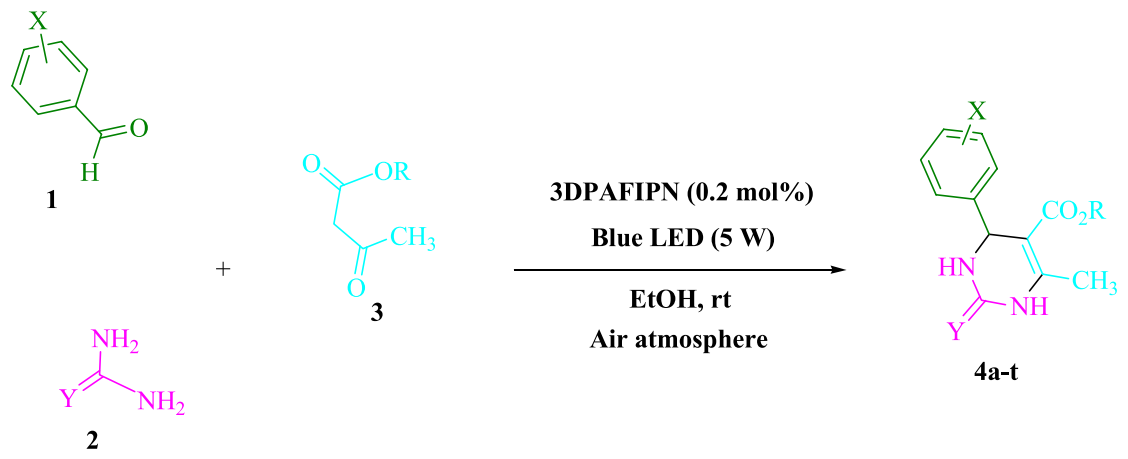

SCHEME 1
Light-mediated synthesis of 3,4-dihydropyrimidin-2-(1*H*)-one/thione derivatives.

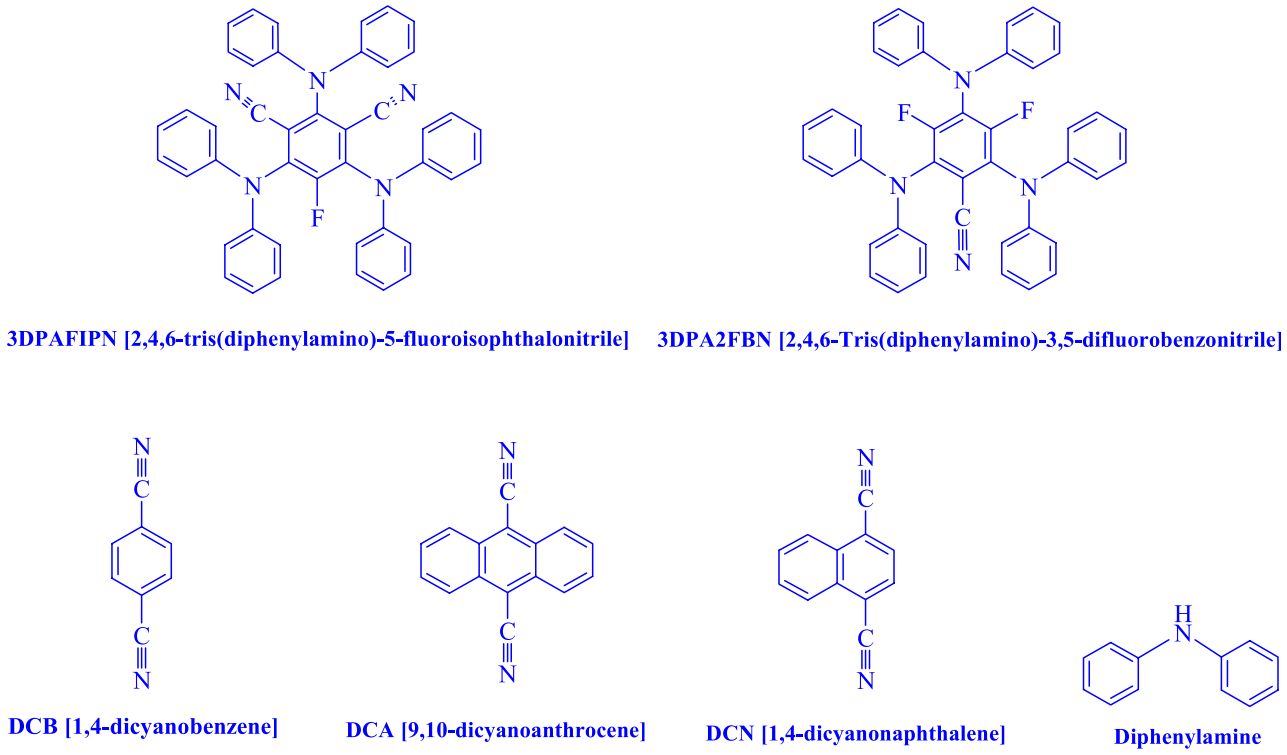

FIGURE 2
The suitability of the catalyst was evaluated in this study.

of photocatalysts thanks to the development of dicyanobenzene-based photosensitizers, which demonstrate exceptional photoelectric activity and thermally activated delayed fluorescence (TADF).

The current study has investigated 3DPAFIPN, a new halogenated cyanoarene-based donor-acceptor (D-A) photocatalyst that works by a sequence of visible-light-induced electron transfers. The three-condensation domino Biginelli

TABLE 1 This table optimizes the photocatalyst for the synthesis of 4j[a].

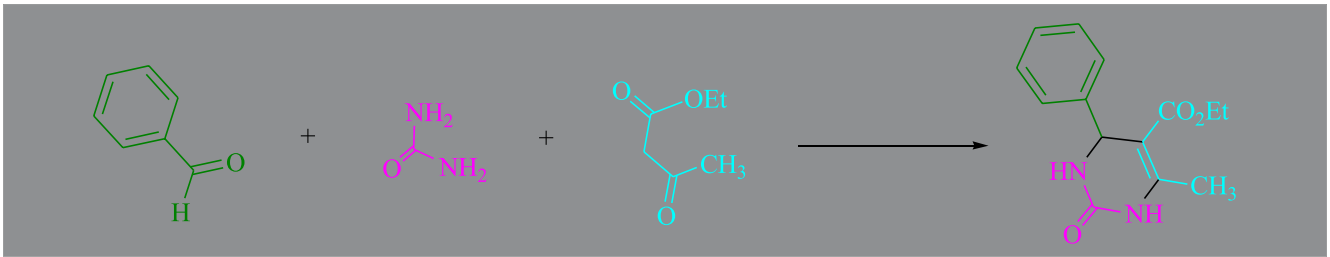

Entry	Photocatalyst	Solvent (3 mL)	Time (min)	Isolated Yields (%)
1	3DPAFIPN (0.1 mol%)	EtOH	5	84
2	3DPAFIPN (0.2 mol%)	EtOH	5	97
3	3DPA2FBN (0.2 mol%)	EtOH	5	82
4	DCB (0.2 mol%)	EtOH	5	19
5	DCA (0.2 mol%)	EtOH	5	27
6	DCN (0.2 mol%)	EtOH	5	22
7	Diphenylamine (0.2 mol%)	EtOH	5	31
8	3DPAFIPN (0.3 mol%)	EtOH	5	97
9	—	EtOH	20	trace

[a]Reaction conditions: several photocatalysts were combined with benzaldehyde (1.0 mmol), ethyl acetoacetate (1.0 mmol), and urea (1.5 mmol) at room temperature.

reaction arylaldehydes with urea/thiourea and β-ketoesters are used in this procedure. In addition, this process employs blue LED, a sustainable and environmentally friendly energy source, in a room-temperature, ethanol medium as a green solvent. Regardless of the timely and effective completion of all obligations and adherence to the agreed-upon budget.

Experimental

General

To find each compound's melting point, an electrothermal instrument, a 9,100, was employed. ^{1}HNMR spectra were collected using Bruker DRX-300 Avance equipment with DMSO-d_6. Materials and reagents were acquired from Acros, Merck, and Fluka and utilized right away.

The sustainable method for 3,4-dihydropyrimidin-2-(1H)-one/thione derivatives (4a-t)

At room temperature in EtOH (3 mL), urea/thiourea (**2**, 1.5 mmol), ethyl/methyl acetoacetate (**3**, 1.0 mmol), and arylaldehyde derivatives (**1**, 1.0 mmol) were stirred with 3DPAFIPN (0.2 mol%) and blue light (5 W) (Scheme 1). We used thin-layer chromatography (TLC) to track the reaction's development. Without requiring any additional purification procedures, the pure substance was obtained by screening, washing with water and ethanol, and crystallizing the crude solid from ethanol following the reaction. The Supplementary Material file contains a report on spectroscopic data.

Results and discussion

The reaction was optimized in the current study using a 3 mL ethanol medium containing 1.0 mmol of benzaldehyde, 1.5 mmol of urea, and 1.0 mmol of ethyl acetoacetate. Without the aid of a photocatalyst, a trace quantity of **4j** was produced for 20 min at room temperature in the presence of 3 mL of EtOH. The pace of reaction was enhanced by the inclusion of photocatalysts. The compounds include 3DPAFIPN, 3DPA2FBN, DCB, DCA, DCN, and diphenylamine, as indicated by the data in Figure 2

The present technique can create **4j** with varying yields. The aforementioned data showed that 3DPAFIPN's operational efficacy has increased. A reaction with 0.2 mol% 3DPAFIPN yielded a 97% yield, based on the data in Table 1, entry 2. Results for solvent-free conditions, EtOAc, DMSO, toluene, H_2O, EtOH, MeOH, $CHCl_3$, CH_3CN, THF, and are displayed in Table 2. In the presence of EtOH, the reaction was demonstrated to have a notably enhanced rate and subsequent yield. Based on the data in Table 2, especially entry 5, a 97% yield was achieved. Table 2 lists the light sources that have been used in studies to assess the impact of blue light on production. In the assessment that was conducted

TABLE 2 The table for optimizing solvent and visible light in the synthesis of 4j[a].

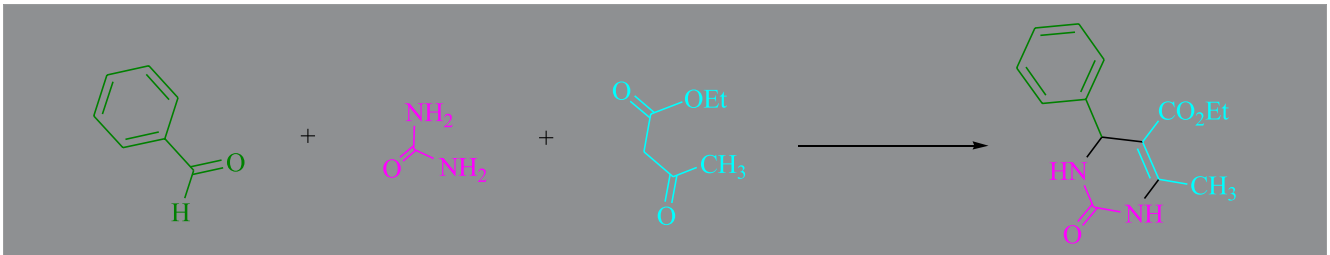

Entry	Light source	Solvent (3 mL)	Time (min)	Isolated yields (%)
1	Blue light (5 W)	EtOAc	5	68
2	Blue light (5 W)	DMSO	25	29
3	Blue light (5 W)	toluene	25	26
4	Blue light (5 W)	H2O	6	71
5	Blue light (5 W)	EtOH	5	97
6	Blue light (5 W)	MeOH	8	59
7	Blue light (5 W)	—	8	46
8	Blue light (5 W)	CHCl3	30	17
9	Blue light (5 W)	CH3CN	5	75
10	Blue light (5 W)	THF	25	15
11	White light (5 W)	EtOH	5	82
12	Green light (5 W)	EtOH	5	90
13	Blue light (3 W)	EtOH	5	89
14	Blue light (7 W)	EtOH	5	97
15	—	EtOH	20	trace

[a]Reaction conditions: a mixture of urea (1.5 mmol), benzaldehyde (1.0 mmol), and ethyl acetoacetate (1.0 mmol) was added to 0.2 mol% 3DPAFIPN.

without the use of an illumination tool, the **4j** was discovered in extremely little amounts. The results of this investigation demonstrate that 3DPAFIPN and visible light are essential for the effective synthesis of product **4j**. The top designs were determined using blue light-emitting diode (LED) intensities of 3 W, 5 W, and 7 W. The results of the investigation showed that the greatest results were obtained when blue light-emitting diodes (LEDs) with a 5 W power output were used. The outcomes of studies conducted on a range of substrates under optimal conditions are displayed in Table 3; Scheme 1 (and also Supplementary Table S1). The benzaldehyde substituent has no effect on the reaction's result (Table 3). Both polar and halide substitutions were permitted in this reaction. In the current state of the reaction, reactions involving both electron-donating and electron-withdrawing functional groups are acceptable. Aromatic aldehydes that are *ortho*, *meta*, and *para*-substituted have a very high yield potential. The reactions of methyl and ethyl acetoacetate are comparable. Urea and thiourea have comparable reactivities.

Table 4 presents the turnover number (TON) and turnover frequency (TOF) as objective value measures. Yield/Amount of Catalyst (mol) and Yield/Time/Amount of Catalyst (mol) are two distinct forms of yield that are commonly expressed as TON and TOF, respectively, in academic literature. The catalyst performance may be enhanced by higher turnover number (TON) and turnover frequency (TOF) values as they need less catalyst to provide the required yields. A TOF of 97 and a TON of 485 are considered high values for **4j**. In relation to **4s**, a TON of 480 is likewise regarded as high, although a TOF of 96 is deemed excessive. The aim of the inquiry was to reduce reaction times, increase production, and utilize the fewest amount of catalysts.

Gram-scale synthesis

The main emphasis of current research is whether the aforementioned chemicals can be produced on a gram-scale for use in pharmaceutical (R&D) procedures. In one experiment, 50 mmol of 4-methoxybenzaldehyde, 75 mmol of thiourea, and 50 mmol of ethyl acetoacetate were utilized. To retrieve the final product, a standard filtering process was applied after the 6-min reaction period. The ^{1}HNMR spectroscopy results show that the

TABLE 3 Using 3DPAFIPN, a halogenated dicyanobenzene-based photosensitizer, 3,4-dihydropyrimidin-2-(1*H*)-one/thione derivatives be produced.

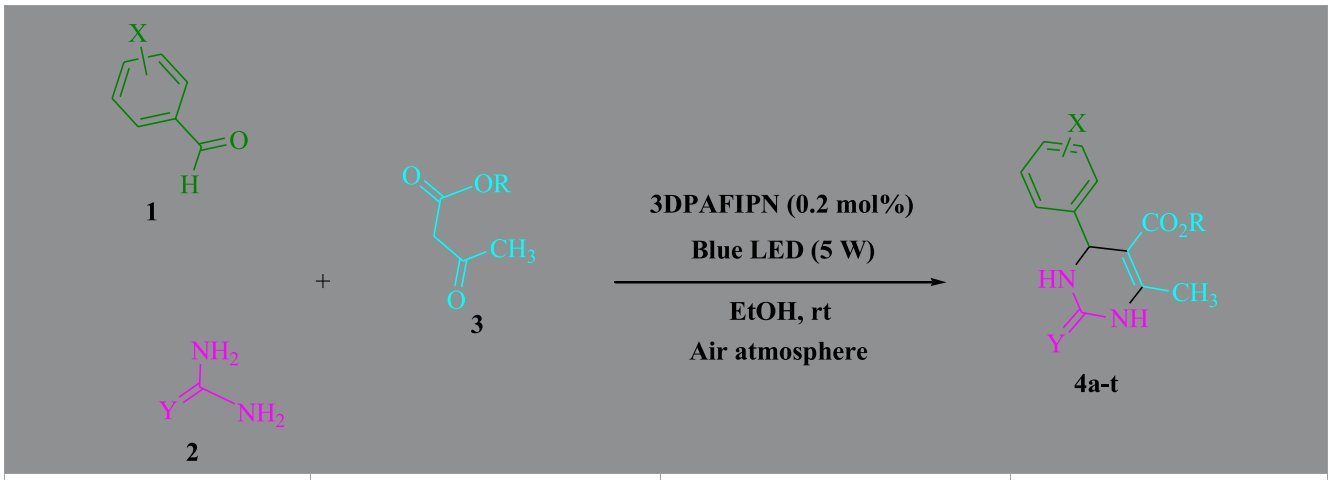

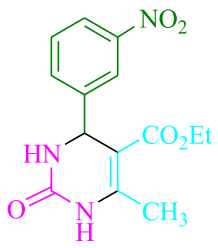 **4a** (5 min, 96%)	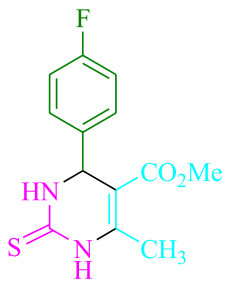 **4b** (5 min, 93%)	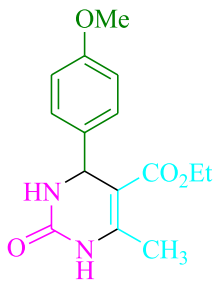 **4c** (6 min, 95%)	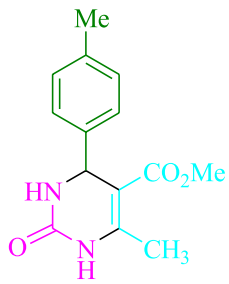 **4d** (4 min, 96%)
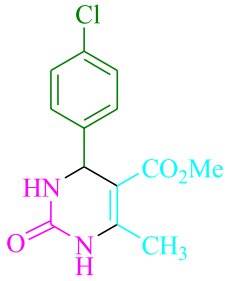 **4e** (7 min, 89%)	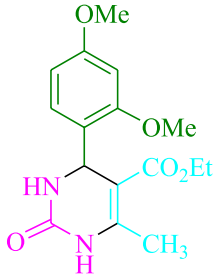 **4f** (6 min, 91%)	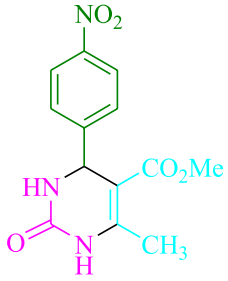 **4g** (4 min, 97%)	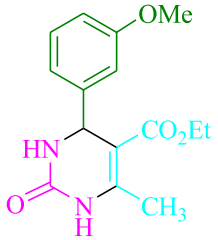 **4h** (6 min, 93%)
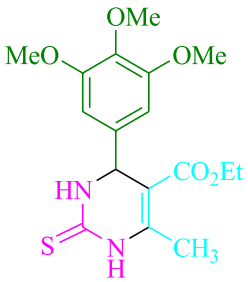 **4i** (7 min, 90%)	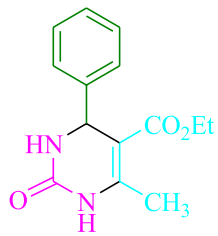 **4j** (5 min, 97%)	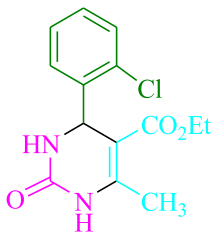 **4k** (6 min, 92%)	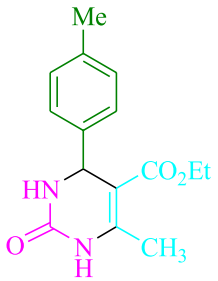 **4l** (4 min, 97%)

(Continued on following page)

TABLE 3 (*Continued*) Using 3DPAFIPN, a halogenated dicyanobenzene-based photosensitizer, 3,4-dihydropyrimidin-2-(1*H*)-one/thione derivatives be produced.

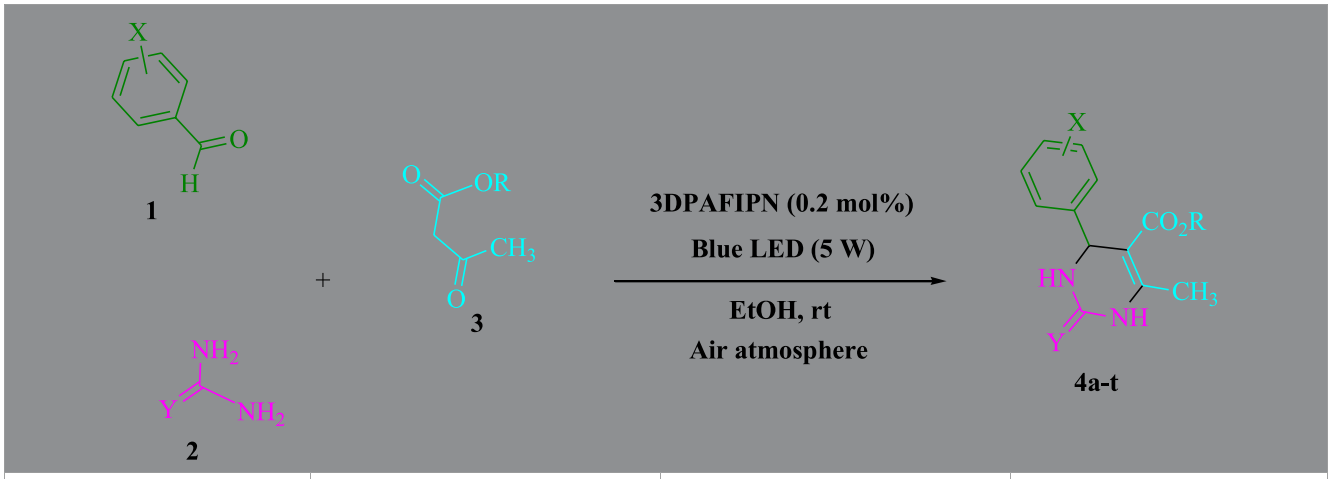

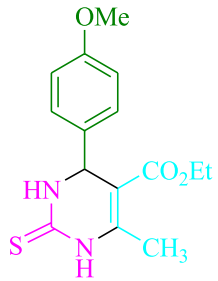 **4m** (6 min, 92%)	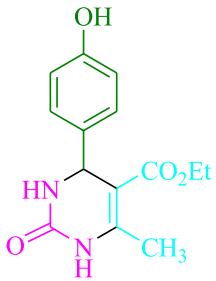 **4n** (7 min, 88%)	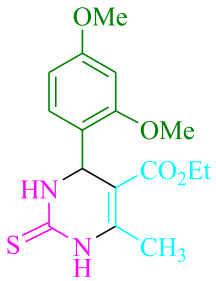 **4o** (6 min, 89%)	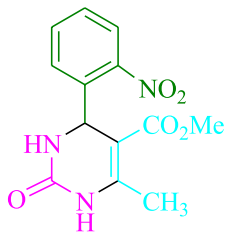 **4p** (4 min, 92%)
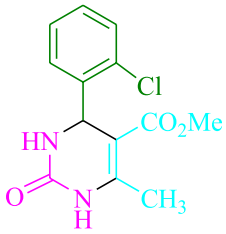 **4q** (6 min, 91%)	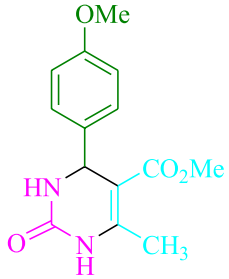 **4r** (6 min, 94%)	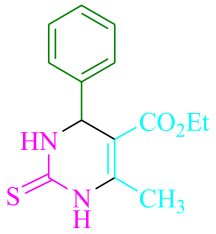 **4s** (5 min, 96%)	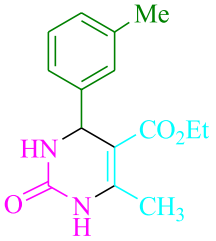 **4t** (4 min, 95%)

chemical compound in question exhibits a high degree of spectroscopic purity.

Control experiments

Scheme 2 displays the outcomes of the control experiments used to elucidate the process utilizing the visible-light-induced. The synthesis of benzylideneurea (**I**) in the first stage and its condensation with ethyl acetoacetate (**3**) in the second are considered to be the two steps of the Biginelli reaction. Under standard circumstances (3DPAFIPN in EtOH under blue LED), benzaldehyde (**1**) and urea (**2**) were condensed by reducing H_2O to produce benzylideneurea (**I**). As a consequence, in 97% of reactions between the iminium intermediate (**I**) and cation radical (**II**), under normal conditions, the expected product **4j** was generated. Even though the reaction was carried out in total darkness, there was still a trace of product **4j** created. The results of this experiment indicate that Scheme 3 presents a convincing and rational chemical process.

The suggested mechanism

Scheme 3 provides a thorough description of the suggested methodology. Using single-electron transfer (SET) processes, the cyanoarene organic dye 3DPAFIPN has been utilized to develop photocatalytic reactions that use visible light energy as a

TABLE 4 The following calculated were used to determine the turnover frequency (TOF) and turnover number (TON).

Entry	Product	TON	TOF	Entry	Product	TON	TOF
1	4a	480	96	11	4k	460	76.6
2	4b	465	93	12	4l	485	121.2
3	4c	475	79.1	13	4m	460	76.6
4	4d	480	120	14	4n	440	62.8
5	4e	445	63.5	15	4o	445	74.1
6	4f	455	75.8	16	4p	460	115
7	4g	485	121.2	17	4q	455	75.8
8	4h	465	77.5	18	4r	470	78.3
9	4i	450	64.2	19	4s	480	96
10	4j	485	97	20	4t	475	118.7

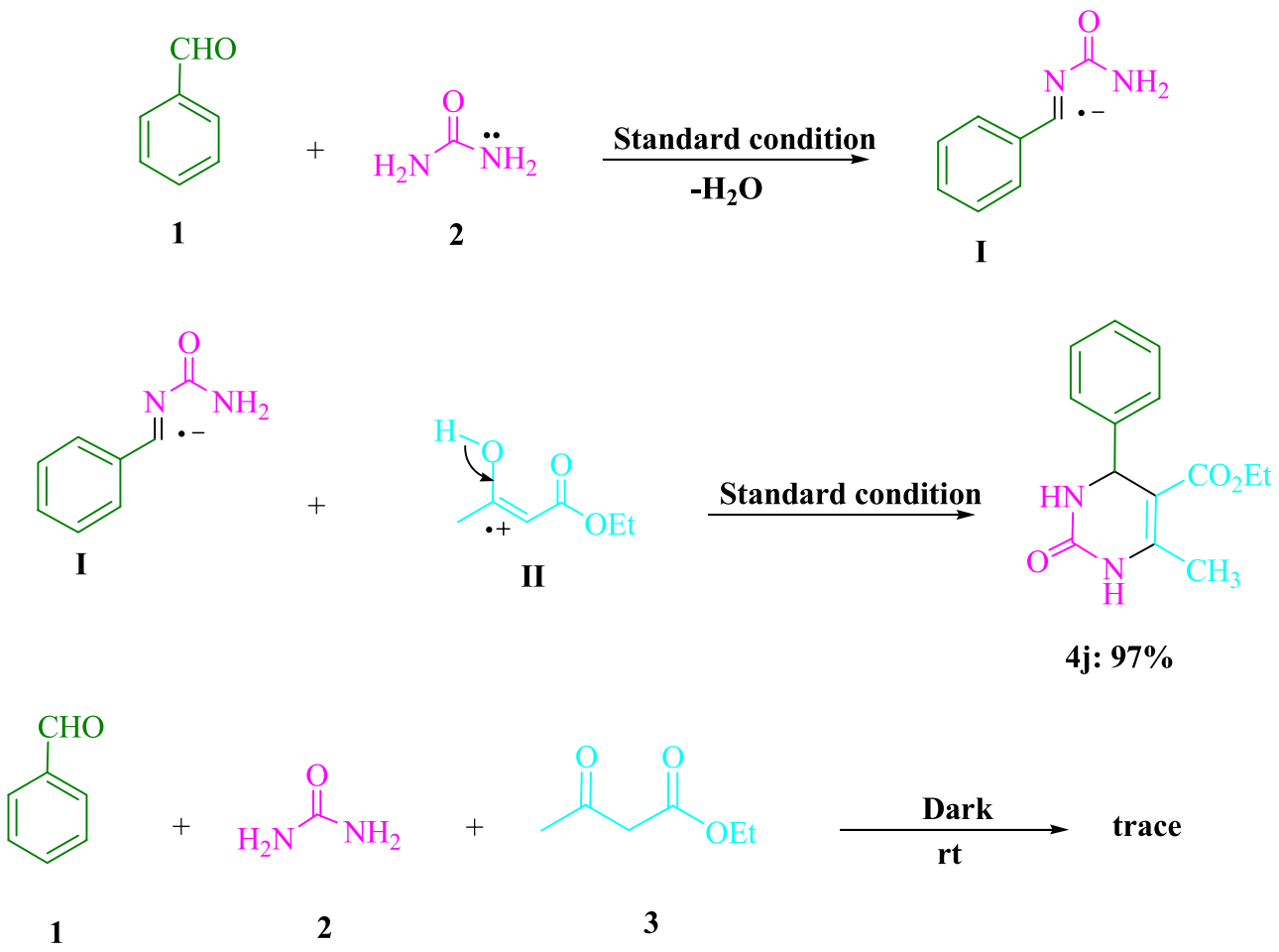

SCHEME 2
To comprehend the condensations of urea (**2**, 1.5 mmol), ethyl acetoacetate (**3**, 1.0 mmol), and benzaldehyde (**1**, 1.0 mmol), significant control tests are conducted.

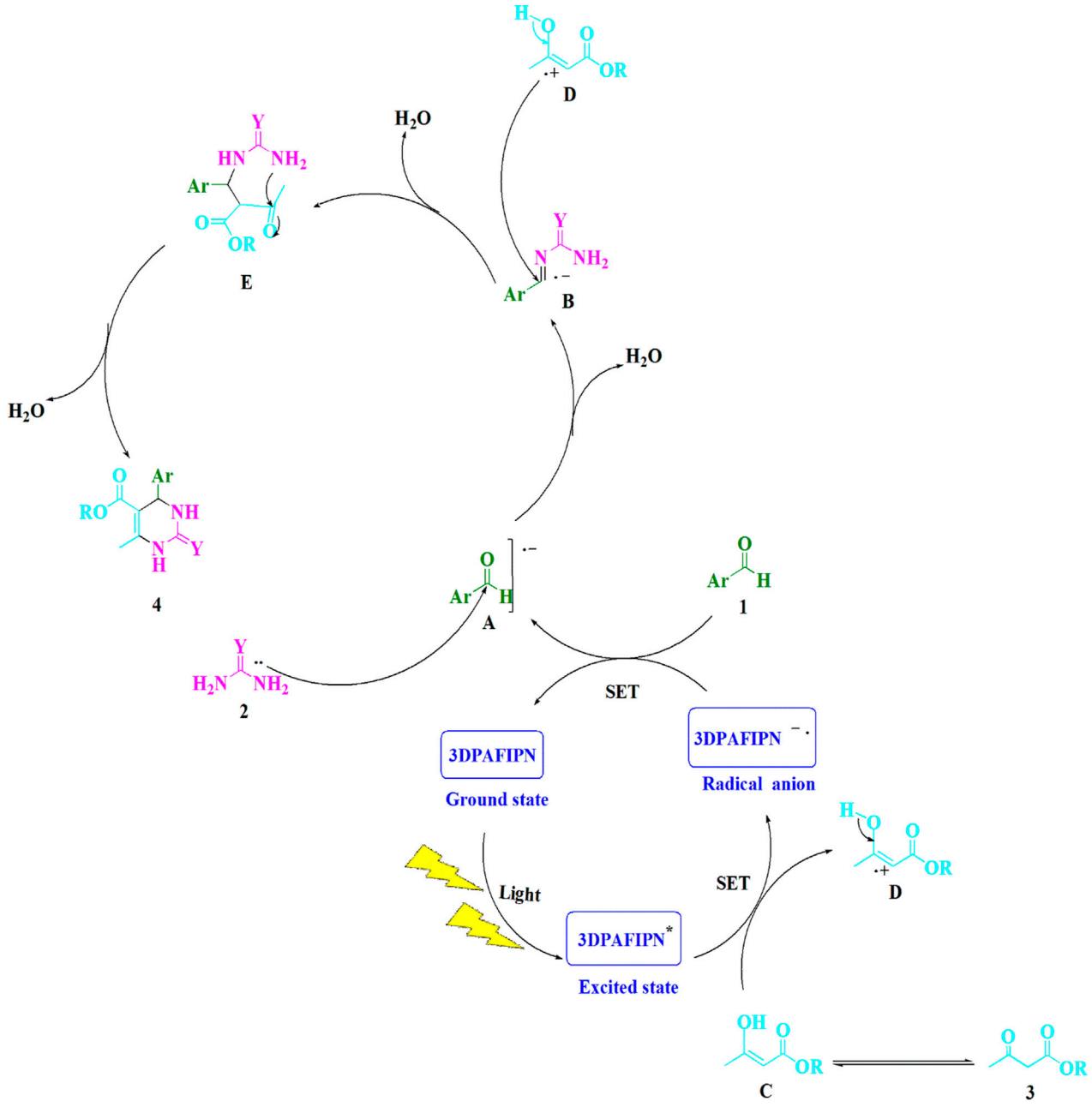

SCHEME 3
This is a detailed illustration of the synthetic procedure that yields 3,4-dihydropyrimidin-2-(1*H*)-one/thione derivatives.

sustainable resource. Utilizing visible light expedites the procedure. The ground-state 3DPAFIPN and the intermediate (**A**) regenerate as a result of the electron transfer (ET) activity between the arylaldehydes (**1**) and the 3DPAFIPN radical anion. A reactive iminium intermediate (**B**) is formed when this radical anion (**A**) is added nucleophilically to urea/thiourea (**2**). The single-electron transfer (SET) technique is utilized to enhance 3DPAFIPN*, which is produced by visible light, and produce the cation radical (**D**). The iminium intermediate (**B**) is attacked by the cation radical (**D**), leading to the formation of the cyclized dehydrated (**4**).

Comparison of the catalytic activity of different catalysts with 3DPAFIPN

Table 5 compares how well various catalysts work to encourage the synthesis of 3,4-dihydropyrimidin-2-(1*H*)-one/thione derivatives. The process in question precipitates rapid chemical changes without generating any waste by using tiny quantities of photocatalyst. When there are quantifiable light wavelengths present, this approach can be used. At multigram scales, atom-economical processes are very efficient and have a big impact on the industrial domain.

TABLE 5 The results of assessing the various catalysts' catalytic efficacy for the synthesis of 4j[a].

Entry	Catalyst	Conditions	Time/Yield (%)	References
1	Bakers' yeast	Room temperature	1,440 min/84	Kumar and Maurya (2007)
2	Hydrotalcite	Solvent-free, 80°C	35 min/84	Lal et al. (2012)
3	$[Al(H_2O)_6](BF_4)_3$	MeCN, Reflux	1,200 min/81	Litvic et al. (2010)
4	$Cu(BF_4)_2.xH_2O$	Room temperature	30 min/90	Kamal et al. (2007)
5	[Btto][*p*-TSA]	Solvent-free, 90°C	30 min/96	Zhang et al. (2015)
6	triethylammonium acetate	Solvent-free, 70°C	45 min/90	Attri et al. (2017)
7	saccharin	Solvent-free, 80°C	15 min/88	Mohamadpour et al. (2016)
8	caffeine	Solvent-free, 80°C	25 min/91	Mohamadpour and Lashkari (2018)
9	3DPAFIPN	Blue LED, EtOH, rt	5 min/97	This work

[a]The synthesis requires three ingredients: urea, ethyl acetoacetate, and benzaldehyde.

Conclusion

We have green photosynthesized 3,4-dihydropyrimidin-2-(1*H*)-one/thione derivatives from arylaldehydes, *β*-ketoesters, and urea/thiourea by means of the radical-induced Biginelli reaction. In the current work, a new halogenated dicyanobenzene-based photosensitizer; 3DPAFIPN was employed as a donor-acceptor (D-A) photocatalyst. It works by causing a sequence of electron transfers that are triggered by visible light. Blue light-emitting diode (LED) technology has been demonstrated to generate a sustained energy-generating mechanism at room temperature and in an air environment when used in an ethanol medium. The suggested method has significant advantages for the field of chemical synthesis. Fast reaction times, the removal of hazardous solvents, higher product yields, streamlined reaction mechanisms, and the utilization of a sustainable energy source are some of these benefits. The separation method does not need chromatography. By preserving the result, it is possible to accelerate a multigram-scale reaction of model substrates. As a result, the method may be used in an environment that promotes long-term ecological and financial sustainability.

Data availability statement

The original contributions presented in the study are included in the article/Supplementary Material, further inquiries can be directed to the corresponding authors.

Author contributions

FM: Investigation, Methodology, Project administration, Supervision, Validation, Visualization, Writing–original draft, Writing–review and editing. AMA: Investigation, Methodology, Project administration, Supervision, Validation, Visualization, Writing–original draft, Writing–review and editing.

Funding

The author(s) declare that no financial support was received for the research, authorship, and/or publication of this article.

Acknowledgments

This work is financially supported by Iran National Science Foundation (INSF) (no. 4015618), financially supported by Iran's National Elites Foundation (no. 4015618), and also, Shiraz University of Medical Sciences.

Conflict of interest

The authors declare that the research was conducted in the absence of any commercial or financial relationships that could be construed as a potential conflict of interest.

Publisher's note

Supplementary material

The Supplementary Material for this article can be found online at: https://www.frontiersin.org/articles/10.3389/fchem.2024.1361266/full#supplementary-material

References

Ahmed, B., Khan, R. A., Habibullah, A., and Keshai, M. (2009). An improved synthesis of Biginelli-type compounds via phase-transfer catalysis. *Tetrahydron Lett.* 50, 2889–2892. doi:10.1016/j.tetlet.2009.03.177

Ashok, M., Holla, B. S., and Kumara, N. S. (2007). Convenient one pot synthesis of some novel derivatives of thiazolo [2,3-b] dihydropyrimidinone possessing 4-methylthiophenyl moiety and evaluation of their antibacterial and antifungal activities. *Eur. J. Med. Chem.* 42, 380–385. doi:10.1016/j.ejmech.2006.09.003

Attri, P., Bhatia, R., Gaur, J., Arora, B., Gupta, A., Kumar, N., et al. (2017). Triethylammonium acetate ionic liquid assisted one-pot synthesis of dihydropyrimidinones and evaluation of their antioxidant and antibacterial activities. *Arabian J. Chem.* 10, 206–214. doi:10.1016/j.arabjc.2014.05.007

Bahekar, S. S., and Shinde, D. B. (2004). Synthesis and anti-inflammatory activity of some 4,6-(4-substituted aryl)-2-thioxo-1. *Bioorg. Med. Chem. Lett. 14* 23. doi:10.1016/j.bmcl.2004.01.039

Bosica, G., Cachia, F., De Nittis, R., and Mariotti, N. (2021). Efficient one-pot synthesis of 3,4-dihydropyrimidin-2(1H)-ones via a three-component Biginelli reaction. *Molecules* 26, 3753. doi:10.3390/molecules26123753

Bryden, M. A., and Zysman-Colman, E. (2021). Organic thermally activated delayed fluorescence (TADF) compounds used in photocatalysis. *Chem. Soc. Rev.* 50, 7587–7680. doi:10.1039/D1CS00198A

Cardinale, L., Konev, M. O., and Jacobi von Wangelin, A. (2020). Photoredox-catalyzed addition of carbamoyl radicals to olefins: a 1,4-dihydropyridine approach. *Chemistry–A Eur. J.* 26, 8239–8243. doi:10.1002/chem.202002410

Chopda, L. V., and Dave, P. N. (2020). Heteropoly-12-tungstophosphoric acid $H_3[PW_{12}O_{40}]$ over natural bentonite as a heterogeneous catalyst for the synthesis of 3,4-dihydropyrimidin-2-(1H)-ones. *Arabian J. Chem.* 13, 5911–5921. doi:10.1016/j.arabjc.2020.04.034

Choudhare, T. S., Wagare, D. S., Kadam, V. T., Kharpe, A. A., and Netankar, P. D. (2021). Rapid one-pot multicomponent dioxane-HCl complex catalyzed solvent-free synthesis of 3,4-dihydropyrimidine-2-one derivatives. *Polycycl. Aromat. Compd.* 42, 3865–3873. doi:10.1080/10406638.2021.1873808

Donabauer, K., Murugesan, K., Rozman, U., Crespi, S., and Konig, B. (2020). Photocatalytic reductive radical-polar crossover for a base-free corey-seebach reaction. *Chemistry–A Eur. J.* 26, 12945–12950. doi:10.1002/chem.202003000

Flynn, A. R., McDaniel, K. A., Hughes, M. E., Vogt, D. B., and Jui, N. T. (2020). Hydroarylation of arenes via reductive radical-polar crossover. *J. Am. Chem. Soc.* 142, 9163–9168. doi:10.1021/jacs.0c03926

Gualandi, A., Anselmi, M., Calogero, F., Potenti, S., Bassan, E., Ceroni, P., et al. (2021). Metallaphotoredox catalysis with organic dyes. *Org. Biomol. Chem.* 19, 3527–3550. doi:10.1039/D1OB00196E

Heys, L., Moore, C. G., and Murphy, P. (2000). The guanidine metabolites of Ptilocaulis spiculifer and related compounds; isolation and synthesis. *Chem. Soc. Rev.* 29, 57–67. doi:10.1039/A903712H

Hurst, E. W., and Hull, R. (1961). Two new synthetic substances active against viruses of the psittacosis-lymphogranuloma-trachoma group. *J. Med. Chem.* 3, 215–229. doi:10.1021/jm50015a002

Kamal, A., Krishnaji, T., and Azhar, M. A. (2007). Copper(II)tetrafluoroborate as a mild and efficient catalyst for the one-pot synthesis of 3,4-dihydropyrimidin-2(1H)-ones under solvent-free conditions. *Catal. Commun.* 8, 1929–1933. doi:10.1016/j.catcom.2007.03.009

KÜÇÜKİSLAMOĞLU, M., BEŞOLUK, Ş., Zengin, M., Arslan, M., and Nebioğlu, M. (2010). An efficient one-pot synthesis of dihydropyrimidinones catalyzed by zirconium hydrogen phosphate under solvent-free conditions. *Turkish J. Chem.* 34, 411–416. doi:10.3906/kim-0912-357

Kumar, A., and Maurya, R. A. (2007). An efficient bakers' yeast catalyzed synthesis of 3,4-dihydropyrimidin-2-(1H)-ones. *Tetrahedron Lett.* 48, 4569–4571. doi:10.1016/j.tetlet.2007.04.130

Lal, J., Sharma, M., Gupta, S., Parashar, P., Sahu, P., and Agarwal, D. D. (2012). Hydrotalcite: a novel and reusable solid catalyst for one-pot synthesis of 3,4-dihydropyrimidinones and mechanistic study under solvent free conditions. *J. Mol. Catal. A Chem.* 352, 31–37. doi:10.1016/j.molcata.2011.09.009

Li, N., Wang, Y., Liu, F., Zhao, X., Xu, X., An, Q., et al. (2020). Air-stable zirconium (IV)-salophen perfluorooctanesulfonate as a highly efficient and reusable catalyst for the synthesis of 3,4-dihydropyrimidin-2-(1H)-ones/thiones under solvent-free conditions. *Appl. Organomet. Chem.* 34, e5454. doi:10.1002/aoc.5454

Litvic, M., Vecani, I., Ladisic, Z. M., Lovric, M., Voncovic, V., and Filipan-Litvic, M. (2010). First application of hexaaquaaluminium(III)tetrafluoroborate as a mild, recyclable, non-hygroscopic acid catalyst in organic synthesis: a simple and efficient protocol for the multigram scale synthesis of 3,4-dihydropyrimidinones by Biginelli reaction. *Tetrahedron* 66, 3463–3471. doi:10.1016/j.tet.2010.03.024

Liu, J. N., Li, J., Zhang, L., Song, L. P., Zhang, M., Cao, W. J., et al. (2012). Facile one-pot three-component reaction to synthesize trifluoromethylated cyclopenta[b]pyran derivatives and their further transformation. *Tetrahedron Lett.* 53, 2469–2472. doi:10.1016/j.tetlet.2012.03.023

Magerramow, A. M., Kurbanova, M. M., Abdinbekova, R. T., Rzaeva, I. A., Farzaliev, V. M., and Allokhverdiev, M. A. (2006). Synthesis and antioxidative properties of some 3,4-dihydropyrimidin-2(1H)ones (-thiones),Russian. *J. Appl. Chem.* 79, 787–790.

Maleki, A., and Paydar, R. (2016). Bionanostructure-catalyzed one-pot three-component synthesis of 3, 4-dihydropyrimidin-2 (1H)-one derivatives under solvent-free conditions. *React. Funct. Polym.* 109, 120–124. doi:10.1016/j.reactfunctpolym.2016.10.013

Mohamadpour, F. (2021a). New role for photoexcited organic dye, Na_2 eosin Y via the direct hydrogen atom transfer (HAT) process in photochemical visible-light-induced synthesis of spiroacenaphthylenes and 1*H*-pyrazolo[1,2-*b*]phthalazine-5,10-diones under air atmosphere. *Dyes Pigments* 194, 109628. doi:10.1016/j.dyepig.2021.109628

Mohamadpour, F. (2021b). Catalyst-free, visible light irradiation promoted synthesis of spiroacenaphthylenes and 1*H*-pyrazolo[1,2-*b*]phthalazine-5,10-diones in aqueous ethyl lactate. *J. Photochem. Photobiol. A Chem.* 407, 113041. doi:10.1016/j.jphotochem.2020.113041

Mohamadpour, F. (2021c). Catalyst-free and solvent-free visible light irradiation-assisted Knoevenagel–Michael cyclocondensation of aryl aldehydes, malononitrile, and resorcinol at room temperature. *Monatsh. für Chemie-Chemical Mon.* 152, 507–512. doi:10.1007/s00706-021-02763-1

Mohamadpour, F. (2022a). Catalyst-free and solvent-free visible light assisted synthesis of tetrahydrobenzo[*b*]Pyran scaffolds at room temperature. *Polycycl. Aromat. Compd.* 42, 7607–7615. doi:10.1080/10406638.2021.2006244

Mohamadpour, F. (2022b). Visible-light-induced radical condensation cyclization to synthesize 3,4-dihydropyrimidin-2-(1*H*)-ones/thiones using photoexcited Na_2 eosin Y as a direct hydrogen atom transfer (HAT) catalyst. *ACS Omega* 7, 8429–8436. doi:10.1021/acsomega.1c05808

Mohamadpour, F. (2022c). The development of imin-based tandem Michael–Mannich cyclocondensation through a single-electron transfer (SET)/energy transfer (EnT) pathway in the use of methylene blue (MB^+) as a photoredox catalyst. *RSC Adv.* 12, 10701–10710. doi:10.1039/D2RA01190E

Mohamadpour, F. (2022d). Visible-light-driven radical Friedländer heteroannulation of 2-aminoaryl ketone and α-methylene carbonyl compound via organic dye fluorescein through a single-electron transfer (SET) pathway. *BMC Chem.* 16, 116. doi:10.1186/s13065-022-00910-1

Mohamadpour, F. (2023a). Acridine yellow G-catalyzed visible-light-promoted synthesis of 2-amino-4*H*-chromene scaffolds via a photo-induced electron transfer process in an aqueous media. *Catal. Surv. Asia* 27, 306–317. doi:10.1007/s10563-023-09397-9

Mohamadpour, F. (2023b). 3DPAFIPN as a halogenated dicyanobenzene-based photosensitizer catalyzed gram-scale photosynthesis of pyrano[2,3-*d*]pyrimidine scaffolds. *Sci. Rep.* 13, 13142. doi:10.1038/s41598-023-40360-w

Mohamadpour, F. (2023c). Acridine yellow G as a photo-induced electron transfer catalyzed radical metal-free synthesis of tetrahydrobenzo[b]pyran scaffolds in an aqueous media. *Curr. Res. Green Sustain. Chem.* 6, 100356. doi:10.1016/j.crgsc.2023.100356

Mohamadpour, F. (2023d). Carbazole-based photocatalyst (4CzIPN) as a novel donor-acceptor fluorophore-catalyzed visible-light-induced photosynthesis of dihydropyrano[2,3-*c*]pyrazole scaffolds via a proton-coupled electron transfer process. *J. Chem. Sci.* 135, 74. doi:10.1007/s12039-023-02204-y

Mohamadpour, F., and Lashkari, M. (2018). Three-component reaction of β-keto esters, aromatic aldehydes and urea/thiourea promoted by caffeine, a green and natural, biodegradable catalyst for eco-safe Biginelli synthesis of 3,4-dihydropyrimidin-2(1*H*)-ones/thiones derivatives under solvent-free conditions. *J. Serbian Chem. Soc.* 83, 673–684. doi:10.2298/JSC170712041M

Mohamadpour, F., Maghsoodlou, M. T., Heydari, R., and Lashkari, M. (2016). Saccharin: a green, economical and efficient catalyst for the one-pot, multi-component synthesis of 3,4-dihydropyrimidin-2-(1*H*)-one derivatives and 1*H*-pyrazolo[1,2-*b*]phthalazine-5,10-dione derivatives and substituted dihydro-2-oxypyrrole. *J. Iran. Chem. Soc.* 13, 1549–1560. doi:10.1007/s13738-016-0871-5

Pinosa, E., Bassan, E., Cetin, S., Villa, M., Potenti, S., Calogero, F., et al. (2022). Light-induced access to carbazole-1, 3-dicarbonitrile: a thermally activated delayed fluorescent (TADF) photocatalyst for cobalt-mediated allylations. *J. Org. Chem.* 88, 6390–6400. doi:10.1021/acs.joc.2c01825

Rothfelder, V., Streitferdt, U., Lennert, J., Cammarata, D., Scott, J., Zeitler, K., et al. (2021). Photocatalytic arylation of P4 and PH3: reaction development through mechanistic insight. *Angew. Chem.* 60, 24855–24863. doi:10.1002/ange.202110619

Speckmeier, E., Fischer, T. G., and Zeitler, K., A toolbox approach to construct broadly applicable metal-free catalysts for photoredox chemistry: deliberate tuning of redox potentials and importance of halogens in donor-acceptor cyanoarenes, *J. Am. Chem. Soc.* 140 (2018) 15353 –15365. doi:10.1021/jacs.8b08933

Sujatha, K., Shanmugam, P., Perumal, P. T., Muralidharan, D., and Rajendran, M. (2006). Synthesis and cardiac effects of 3,4-dihydropyrimidin-2(1H)-one-5carboxylates. *Bioorg. Med. Chem. Lett.* 16, 4893–4897. doi:10.1016/j.bmcl.2006.06.059

Uoyama, H., Goushi, K., Shizu, K., Nomura, H., and Adachi, C. (2012). Highly efficient organic light-emitting diodes from delayed fluorescence. *Nature* 492, 234–238. doi:10.1038/nature11687

V Chopda, L., and Dave, P. N. (2020). 12-Tungstosilicic acid $H_4[W_{12}SiO_{40}]$ over natural bentonite as a heterogeneous catalyst for the synthesis of 3,4-dihydropyrimidin-2(1H)-Ones. *ChemistrySelect* 5, 2395–2400. doi:10.1002/slct.201904962

Wisen, S., Androsavich, J., Evans, C. G., Chang, L., and Gestwi cki, J. E. (2008). Chemical modulators of heat shock protein 70 (Hsp70) by sequential, microwave-accelerated reactions on solid phase. *Bioorg. Med. Chem. Lett.* 18, 60–65. doi:10.1016/j.bmcl.2007.11.027

Wu, Q. A., Chen, F., Ren, C. C., Liu, X. F., Chen, H., Xu, L. X., et al. (2020). Donor-acceptor fluorophores as efficient energy transfer photocatalysts for [2 + 2] photodimerization. *Org. Biomol. Chem.* 18, 3707–3716. doi:10.1039/C9OB02735A

Yang, Z., Mao, Z., Xie, Z., Zhang, Y., Liu, S., Zhao, J., et al. (2017). Recent advances in organic thermally activated delayed fluorescence materials. *Chem. Soc. Rev.* 46, 915–1016. doi:10.1039/C6CS00368K

Zhang, Y., Wang, B., Zhang, X., Huang, J., and Liu, C. (2015). An efficient synthesis of 3,4-dihydropyrimidin-2(1H)-Ones and thiones catalyzed by a novel brønsted acidic ionic liquid under solvent-free conditions. *Molecules* 20, 3811–3820. doi:10.3390/molecules20033811

Zhou, C., Lei, T., Wei, X. Z., Ye, C., Liu, Z., Chen, B., et al. (2020). Metal-free, redox-neutral, site-selective access to heteroarylamine via direct radical-radical cross-coupling powered by visible light photocatalysis. *J. Am. Chem. Soc.* 142, 16805–16813. doi:10.1021/jacs.0c07600

frontiers | Frontiers in Chemistry

TYPE Original Research
PUBLISHED 22 May 2024
DOI 10.3389/fchem.2024.1378746

OPEN ACCESS

EDITED BY
Naohiko Yoshikai,
Tohoku University, Japan

REVIEWED BY
Raman Khurana,
O2M Technologies, LLC, United States
Satyajit Roy,
The University of Texas at Dallas, United States

*CORRESPONDENCE
Takashi Ohshima,
ohshima@phar.kyushu-u.ac.jp
Hiroyuki Morimoto,
morimoto@che.kyutech.ac.jp

RECEIVED 30 January 2024
ACCEPTED 01 March 2024
PUBLISHED 22 May 2024

CITATION
Choi J, Nawachi A, Saito N, Kondo Y, Morimoto H and Ohshima T (2024), Evaluation of functional group compatibility and development of reaction-accelerating additives in ammonium salt-accelerated hydrazinolysis of amides.
Front. Chem. 12:1378746.
doi: 10.3389/fchem.2024.1378746

Evaluation of functional group compatibility and development of reaction-accelerating additives in ammonium salt-accelerated hydrazinolysis of amides

Jeesoo Choi[1], Anna Nawachi[1], Natsuki Saito[1], Yuta Kondo[1], Hiroyuki Morimoto[2]* and Takashi Ohshima[1]*

[1]Graduate School of Pharmaceutical Sciences, Kyushu University, Fukuoka, Japan, [2]Department of Applied Chemistry, Graduate School of Engineering, Kyushu Institute of Technology, Fukuoka, Japan

Functional group compatibility in an amide bond cleavage reaction with hydrazine was evaluated for 26 functional groups in the functional group evaluation (FGE) kit. Accurate and rapid evaluation of the compatibility of functional groups, such as nitrogen-containing heterocycles important in drug discovery research, will enhance the application of this reaction in drug discovery research. These data will be used for predictive studies of organic synthesis methods based on machine learning. In addition, these studies led to discoveries such as the unexpected positive additive effects of carboxylic acids, indicating that the FGE kit can propel serendipitous discoveries.

KEYWORDS

amide bond cleavage, functional group compatibility, functional group evaluation kit, carboxylic acid, zinc trifluoromethanesulfonate

1 Introduction

Amide bonds are among the most abundant chemical bonds in nature and are widely found in various organic molecules, such as peptides, natural products, and pharmaceuticals (Pattabiraman and Bode, 2011; Kaspar and Reichert, 2013; Brown and Bostrom, 2016). The chemical stability of amide bonds is extremely high due to their tendency to form resonance structures (Kemnitz and Loewen, 2007; Wang and Cao, 2011; Mahesh et al., 2018), and this stability affords beneficial properties to amide compounds. Due to their stability, except for biochemical cleavage by enzymes such as peptidases (Dai et al., 1995; Wu et al., 2020), chemical cleavage of amide bonds is quite difficult and often requires harsh reaction conditions (Thorner et al., 2000; Rashed et al., 2019; Lv et al., 2023). If amide bonds can be cleaved under mild conditions, the corresponding carboxylic acid equivalents and amines can be synthesized from various amides. Therefore, the development of amide bond cleavage reactions under mild conditions has attracted increased attention in recent years. Although several excellent reactions have been reported (Chaudhari and Gnanaprakasam, 2019; Li and Szostak, 2020), cleavage of common unactivated amides still requires the use of highly reactive metal catalysts, strict anhydrous conditions, and higher reaction temperatures.

To overcome these problems, we took advantage of the high nucleophilicity of hydrazine and found that simple inorganic ammonium salts, such as ammonium

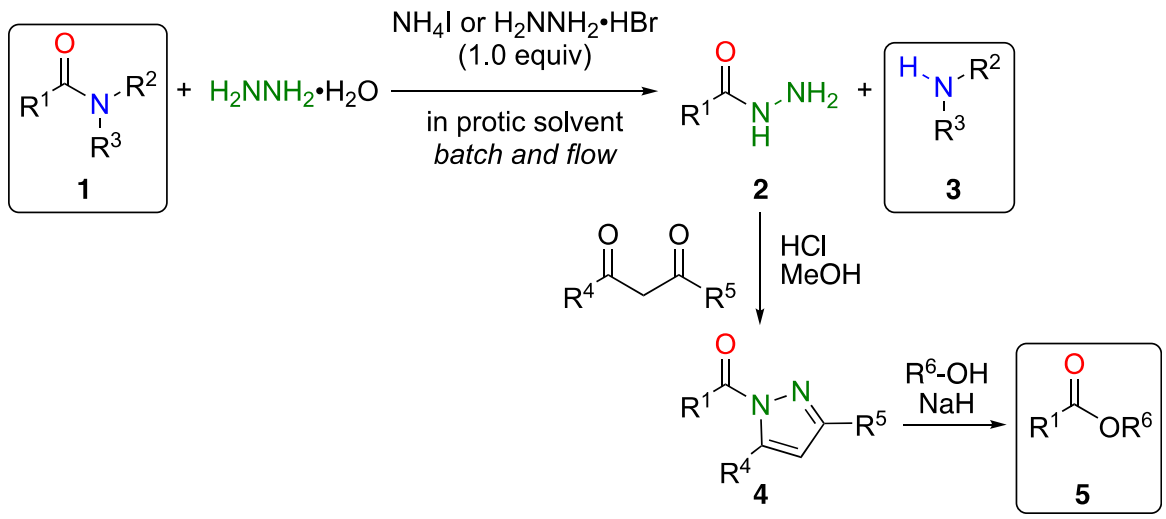

SCHEME 1
Ammonium salts promoted cleavage of amide bond with hydrazine and further transformation to esters.

iodide, efficiently accelerated bond cleavage of unactivated amides **1** under mild conditions to afford the corresponding acyl hydrazides **2** and amines **3** in high yields (Scheme 1) (Shimizu et al., 2014). Furthermore, by employing a continuous microwave flow reactor, the reaction was easily scaled up (100 mmol scale, 23 mmol h^{-1}) (Noshita et al., 2019). The obtained acyl hydrazides were easily converted into the corresponding ester **5** by reacting with β-diketone, such as acetylacetone, to the active amide acylpyrazole **4** (Kashima et al., 1994). By combining these reactions, both the carboxylic acid and amine portions of the amide **1** can be effectively utilized for further transformations.

If this reaction could be applied to amides with various functional groups, its usefulness would be greatly enhanced. The functional groups (FGs) are involved in the properties and reactivity of molecules and form the basis for organic chemistry and pharmaceutical chemistry (Dreos et al., 2011; Ertl, 2017). Although several functionalized amide substrates were investigated, comprehensive information on the functional group compatibility in this reaction has not yet been collected due to difficulties in synthesizing such functionalized amide substrates. Therefore, we used a functional group evaluation (FGE) kit (Saito et al., 2023), which allows for accurate and rapid assessment of information on the functional group compatibility using 26 FGE compounds, including the nitrogen-containing heterocycles imidazole and indole, important in drug discovery research (Collins and Glorius, 2013). In this system, the functional group compatibility of a given reaction is assessed by adding 26 external additives with various functional groups. Using this method, comprehensive data on functional group compatibility can be collected and entered into our "Digitization-driven Transformative Organic Synthesis (Digi-TOS)" database (https://en.digi-tos.jp). Artificial intelligence (AI) and digitization show great potential in next-generation organic synthesis, and data-driven prediction research of synthesis is essential to do so. In this regard, reliable information about functional group compatibility and chemoselectivity is important to understand the applicability of the reaction. This Digi-TOS database will be used for the development of a machine learning-based organic synthesis prediction method, such as a retrosynthetic analysis method (Mikulak-Klucznik et al., 2020; Zhang et al., 2023). For this purpose, it is essential to ensure the reliability of data, and therefore, statistical methods are used for handling the data. Another purpose of the FGE kit is to discover unexpected chemoselectivity and unexpected "positive" additive effects. Such unexpected discoveries, which are commonly referred to as "serendipitous," frequently result in the development of reactions (Maegawa et al., 2011). In fact, in the present study, we found the unexpected positive additive effect of carboxylic acids, and further investigation allowed us to develop a new Lewis acid-catalyzed reaction system. Our results demonstrate that FGE kit effectively promotes serendipitous discovery.

2 Results and discussion

2.1 Evaluation of functional group compatibility using FGE kit

2.1.1 Optimization of reaction conditions

Previously, we successfully developed ammonium salt-accelerated hydrazinolysis of unactivated amides using ammonium iodide and hydrazine monohydrate under mild conditions (Shimizu et al., 2014). To evaluate this reaction using the FGE kit, we selected *N*-(4-(trifluoromethoxy)phenyl)-4-(trifluoromethyl)benzamide (**1**) as the substrate because yields of the corresponding products 4-(trifluoromethyl)benzohydrazide (**2**) and 4-(trifluoromethoxy)aniline (**3**) can be determined by ^{19}F NMR analysis of the crude mixture without affecting ^{1}H-based contaminants such as additives in the FGE kit.

We first optimized reaction conditions for the hydrazinolysis of amide **1aa** using General Procedure A (Table 1) (See Supplementary Material for detailed information). Under the standard conditions of our previous studies using 10 equiv of hydrazine hydrate and 1.0 equiv of ammonium iodide at 70 °C for 48 h, the reaction gave only 20% of benzohydrazide **2a** (Entry 1). The reaction in

10.3389/fchem.2024.1378746

TABLE 1 Optimization of reaction condition using amide 1aa.

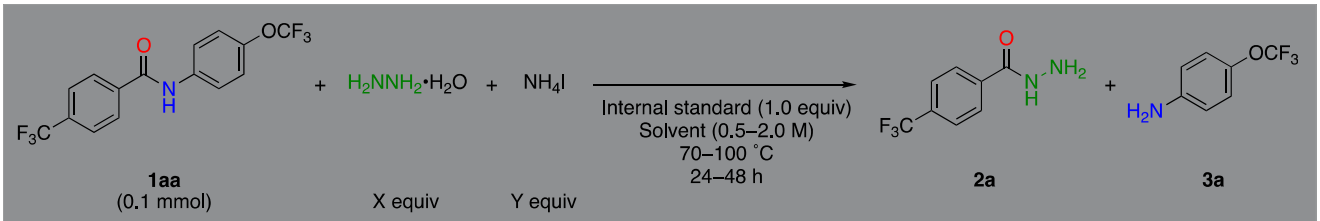

Entry	X equiv	Y equiv	Solvent	(M)	Temp. (°C)	Time (h)	Yield (%)[a]		
							2a	3a	1aa
1	10	1.0	ethanol	1.0	70	48	20	17	82
2	10	1.0	–	–	70	24	N.D[b]	N.D[b]	≥99
3	10	1.0	ethanol	1.0	100	24	85	81	17
4	10	1.0	hexafluoroisopropanol	1.0	100	24	82	82	18
5	10	1.0	trifluoroethanol	1.0	100	24	93	93	7
6	10	–	trifluoroethanol	1.0	100	24	52	53	48
7	10	2.0	trifluoroethanol	1.0	100	24	69	67	32
8	10	1.0[c]	trifluoroethanol	1.0	100	24	57	60	42
9	–	1.0	trifluoroethanol	1.0	100	24	N.D[b]	N.D[b]	≥99
10	20	1.0	trifluoroethanol	1.0	100	24	≥99	≥99	N.D[b]
11	2.0	1.0	trifluoroethanol	1.0	100	24	15	14	85
12	10	1.0	trifluoroethanol	0.5	100	24	66	67	33
13	10	1.0	trifluoroethanol	1.4	100	24	78	78	22
14	10	1.0	trifluoroethanol	2.0	100	24	76	76	24

[a]Determined by ^{19}F NMR analysis of the crude mixture using 4-(trifluoromethoxy)anisole (0.1 mmol) as an internal standard.
[b]Not detected.
[c]NH_4OAc was used instead of NH_4I.

the absence of solvent did not proceed (Entry 2). Increasing the reaction temperature to 100 °C increased the yield of **2a** to 85% in 24 h (Entry 3). Aiming to accelerate the reaction, we performed the reaction using acidic solvent hexafluoroisopropanol (Zhang et al., 2018; Kabi et al., 2020; Bhattacharya et al., 2021) and trifluoroethanol (Entries 4 and 5) (Smithrud et al., 1990; Bautista et al., 1999; Bai et al., 2019); the use of trifluoroethanol led to desired product **2a** in 93% yield. Using trifluoroethanol as the solvent in the absence of ammonium iodide decreased the reaction rate, however, clearly indicating that ammonium salt is important for achieving high reactivity (Entry 6) (Shimizu et al., 2012). On the other hand, the addition of 2 equiv of ammonium iodide decreased the yield of the product (Entry 7). NH_4OAc (Kumar et al., 2022) instead of NH_4I resulted in the lower yield of **2a** (Entry 8). When hydrazine monohydrate was not added, the reaction did not proceed and amide **1aa** was recovered quantitatively (Entry 9). Although increasing the amount of hydrazine from 10 to 20 equiv. improved the yield (Entry 10), the change was not significant (Entry 5). On the other hand, two equivalents of hydrazine gave **2a** in 14% yield (Entry 11); therefore, 10 equiv was considered optimal. The concentration of the solvent also affected the reaction (Entries 12–14), and a 1 M solvent concentration was optimal (Entry 5). As shown in this table, the yields of benzohydrazide **2a** and aniline **3a** were nearly identical, so only the yields of **2a** are listed in the following tables (See Table 1).

2.1.2 Additive compounds A0–A26 for FGE kit

After determining the optimized reaction conditions (Table 1, Entry 5), we applied the FGE kit to the reaction. Additive compounds **A0–A26** for our FGE kit contain the 4-chlorophenyl moiety as the parent backbone to facilitate ^{1}H NMR monitoring of the remaining additives (See Table 2). Because of its UV absorption, the 4-chlorophenyl moiety also enables HPLC analysis of the remaining additives. Furthermore, the isotopic distribution of the chlorine atoms facilitates the detection of chlorine-containing additive molecules as well as side products associated with the additives using mass spectroscopic analysis. We selected 26 functional groups found in many organic molecules, including amino acid residues such as the nitrogen-containing heterocycles imidazole **A7** and indole **A22**.

10.3389/fchem.2024.1378746

TABLE 2 Experimental results for hydrazinolysis of amides using FGE kit.

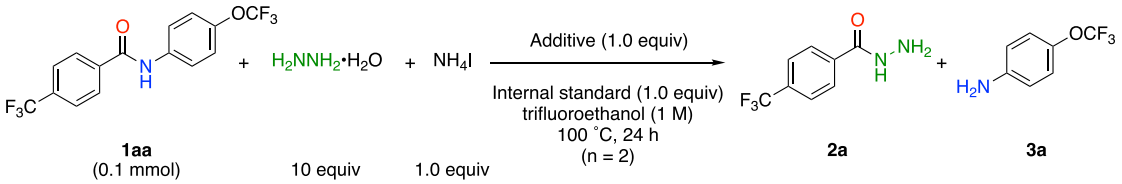

1aa (0.1 mmol) | 10 equiv | 1.0 equiv | **2a** | **3a**

Additive	Structure	Yield of **2a** (%)[a] (± SE)[b]		Additive remaining (%)[c]	
A0[d]	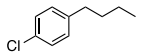	73 (±0.4)		97	
A1	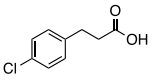	96 (±0.2)	+	14	X
A2[e]	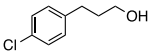	71 (±1.7)	±	99	±
A3	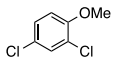	80 (±0.5)	+	99	±
A4	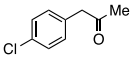	63 (±0.3)	−	0	X
A5	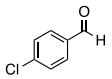	78 (±2.5)	±	0	X
A6[e]	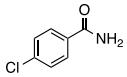	72 (±1.7)	±	0	X
A7[e]	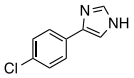	79 (±2.5)	±	95	±
A8	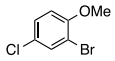	68 (±1.6)	±	>99	±
A9	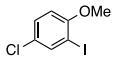	73 (±2.7)	±	95	±
A10	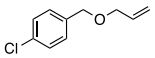	60 (±1.8)	±	44	X
A11	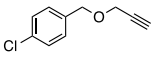	61 (±1.4)	±	27	X
A12	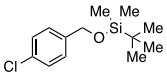	54 (±3,3)	±	84	±
A13		65 (±0.4)	−	64	±

Additive	Structure	Yield of **2a** (%)[a] (± SE)[b]		Additive remaining (%)[c]	
A14	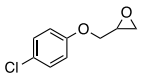	86 (±0.6)	+	95	±
A15	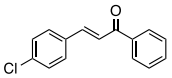	34 (±8.9)	±	0	X
A16	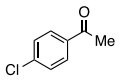	56 (±0.3)	−	0	X
A17	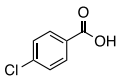	98 (±0.3)	+	28	X
A18	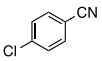	71 (±5.0)	±	9	X
A19	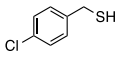	63 (±1.2)	±	>99	±
A20	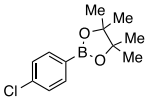	61 (±0.1)	−	81	±
A21	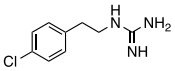	52 (±2.8)	±	0	X
A22	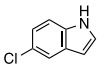	75 (±1.0)	±	96	±
A23	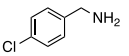	81 (±3.8)	±	98	±
A24	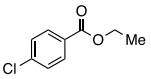	82 (±1.1)	±	0	X
A25	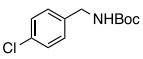	60 (±0.7)	−	94	±
A26	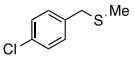	66 (±6.6)	±	92	±

[a]Determined by ^{19}F NMR analysis of the crude mixture using 4-(trifluoromethoxy)anisole (0.1 mmol) as an internal standard.
[b]Standard error.
[c]Determined by ^{1}H NMR analysis of the mixture using 4-(trifluoromethoxy)anisole (0.1 mmol) as an internal standard.
[d]n = 5.
[e]n = 4.

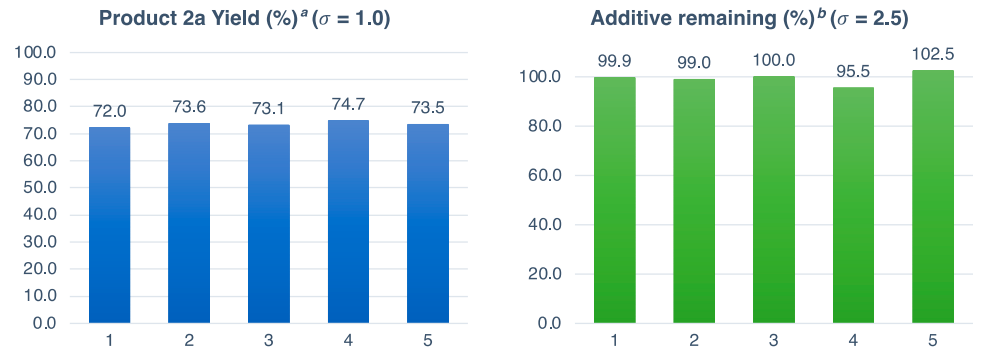

FIGURE 1
Reaction with additive **A0**. [a]Determined by ^{19}F NMR analysis of the crude mixture using 4-(trifluoromethoxy)anisole (0.1 mmol) as an internal standard. [b]The amount of additives were calculated by ^{1}H NMR analysis of the crude mixture using 4-(trifluoromethoxy)anisole (0.1 mmol) as an internal standard.

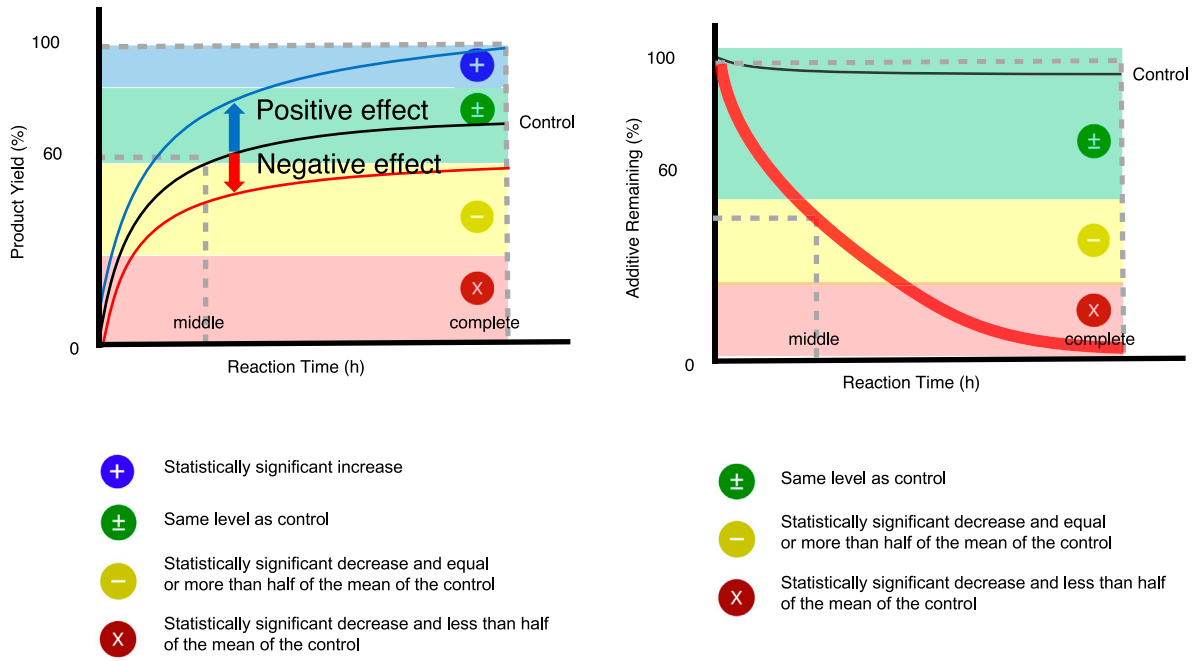

FIGURE 2
The symbols in FGE kit.

2.1.3 Control experiment with additive A0

Before starting the evaluation with the FGE kit, it was necessary to check whether the 4-chlorophenyl structure in the additive affects the reaction. Therefore, a control experiment was carried out by adding 1.0 equiv of additive **A0** (1-butyl-4-chlorobenzene), which does not contain an additional functional group, to the amide bond cleavage reaction. Another objective of the control experiment with additive **A0** was to check for reproducibility using the criterion of the standard deviation (σ) of the product yield (%) within 5 ($\sigma \leq 5$) in five experiments (n = 5). Detailed experimental methods for using the FGE kit are reported in our previous work (Saito et al., 2023) (See Supplementary Material for detailed information).

Under optimized reaction conditions, the reaction was carried out five times with 1.0 equiv of additive **A0** (Figure 1). The average yield decreased to 73% due to the decrease in the concentration caused by the addition of **A0**. Therefore, evaluation of the additive effect using **A1**–**A26** is based on this yield. The standard deviation of the yield (%) was 0.97, suggesting that sufficient reproducibility could be obtained even under the conditions with additives. No decreases in the remaining additive (%) were observed (97%), and high reproducibility was obtained with a standard deviation of 2.52, indicating that the 4-chlorophenyl structure is tolerant to the reaction conditions (Supplementary Table S1).

10.3389/fchem.2024.1378746

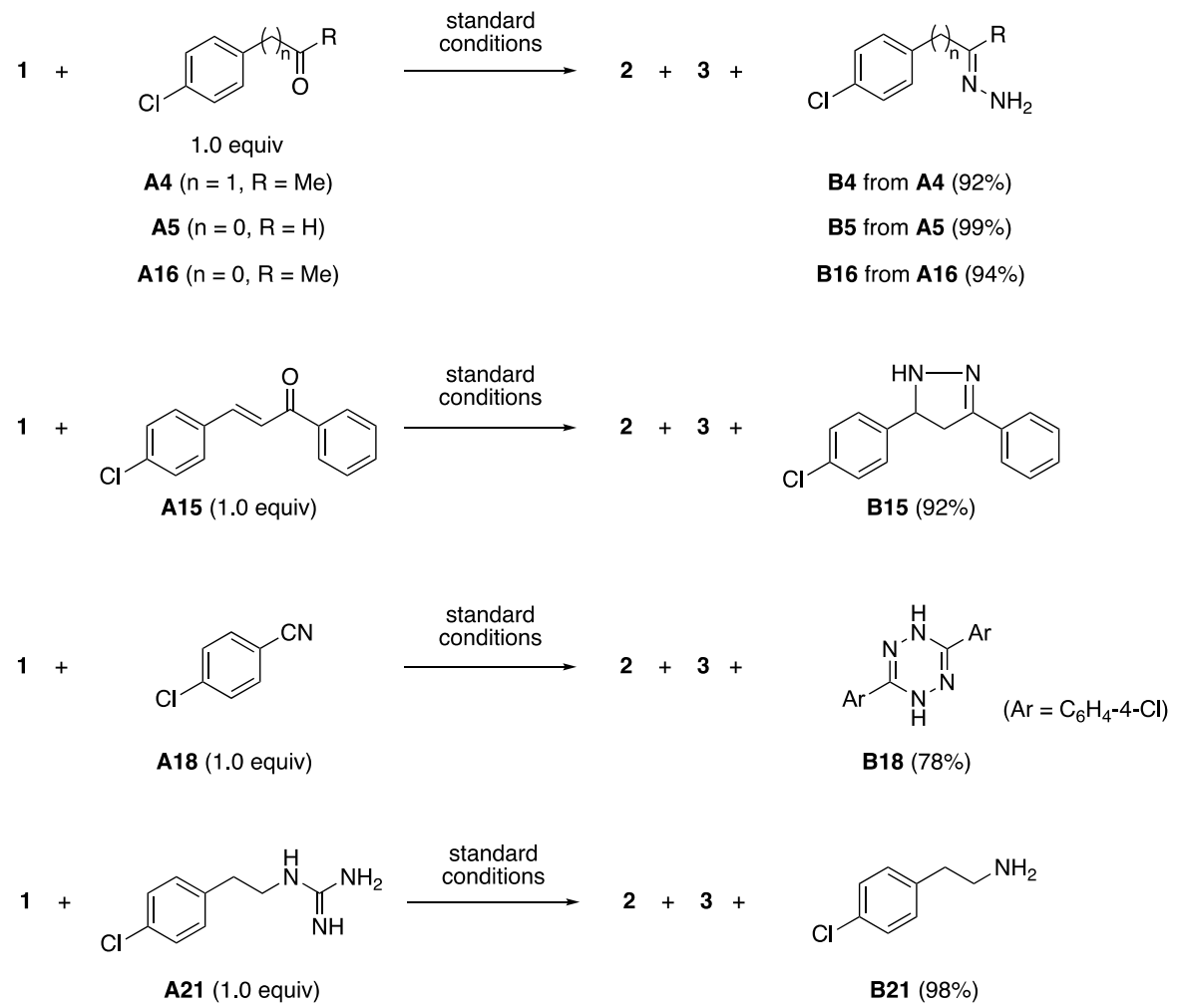

SCHEME 2
Formation of byproducts derived from additives **A4**, **A5**, **A15**, **A16**, **A18** and **A21**.

2.1.4 Evaluation functional group compatibility with additive A1–A26

After fulfilling the reproducibility criteria of additive **A0**, we examined the additive effects of the other additives, **A1**–**A26**, in the FGE kit. Each additive was subjected to an F-test through duplicate experiments (n = 2). Only when the F-test indicated that the variance differed and the variability was too high, two additional experiments with the same additives were performed. The following symbols are used in the experimental results (Figure 2; Table 2). The blue plus sign (+) indicates a statistically significant increase effect. The green plus/minus sign (±) indicates no statistically significant effect, but a result that was comparable to that of the control experiment. The yellow dash sign (−) indicates a statistically significantly decrease effect. When there was a significant decrease of more than half compared with the control experiment, a red "X" was used. Significant differences were determined by a t-test.

The effects of 26 additives **A1**–**A26** in the FGE kit were examined using General Procedure B (Table 2) (See Supplementary Material). Additives **A2**, **A7**–**A9**, **A12**, **A19**, **A22**, **A23**, and **A26** with alcohol, imidazole, aryl bromide, iodide, silyl ether, thiol, indole, primary amine, thioester moieties had no effect on product yield nor remaining additives. It is particularly important that highly reactive thiol **A19** and thioether **A26**, as well as *N*-unprotected imidazole **A7** and indole **A22**, were tolerated. Additives **A5**, **A6**, **A10**, **A11**, **A15**, **A18**, **A21** and **A24** with aldehyde, primary amine, terminal alkene, alkyne, enone, nitrile, guanidine and ester moieties did not affect the product yields, but the remaining additives were decreased, suggesting that the functional groups of these additives reacted under the reaction conditions (*vide infra*). In the case of additives **A3** and **A14** with aryl chloride and epoxide moieties, the yield of the product slightly increased and the remaining additive was unchanged. On the other hand, additives **A1** and **A17** with carboxylic acid moieties provided significantly higher product yields than the control reaction with additive **A0** although the remaining additives were decreased due to the formation of byproducts (*vide infra*). For additives **A4**, **A13** and **A16** with alkyl ketone, naphthol and aryl ketone moieties, both the yield of the product and the remaining additive were decreased. The addition of **A20** and **A25** with Bpin and Boc-protected amine moieties decreased the product yields but did not change the remaining additives.

10.3389/fchem.2024.1378746

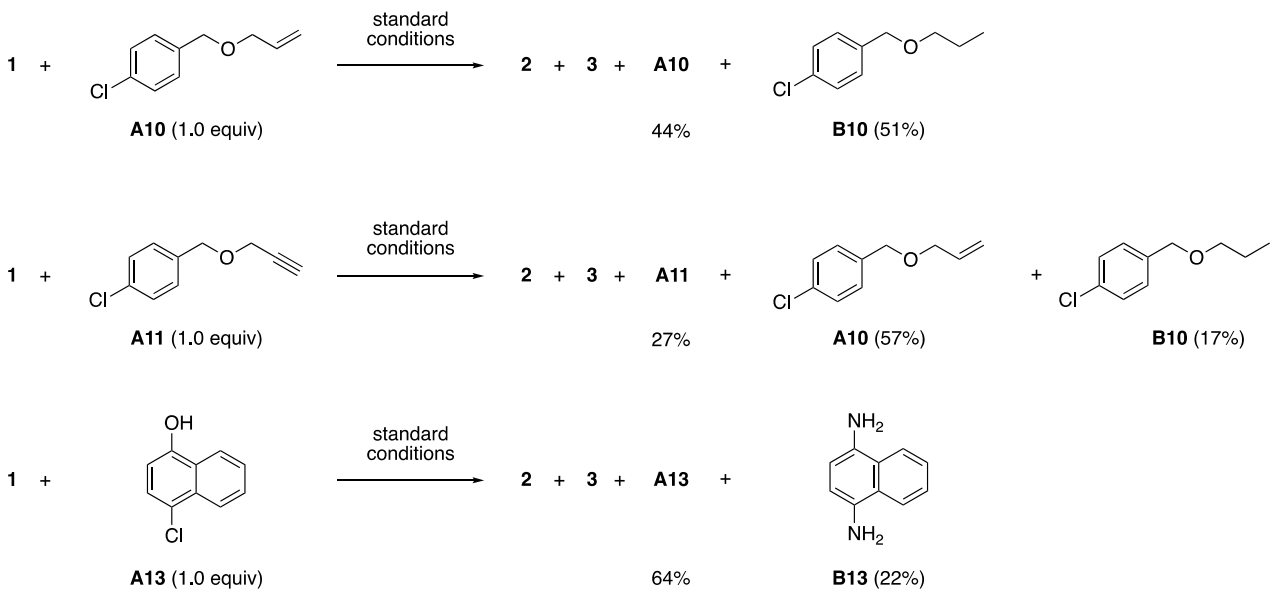

SCHEME 3
Formation of byproducts derived from additives **A10**, **A11**, and **A13**.

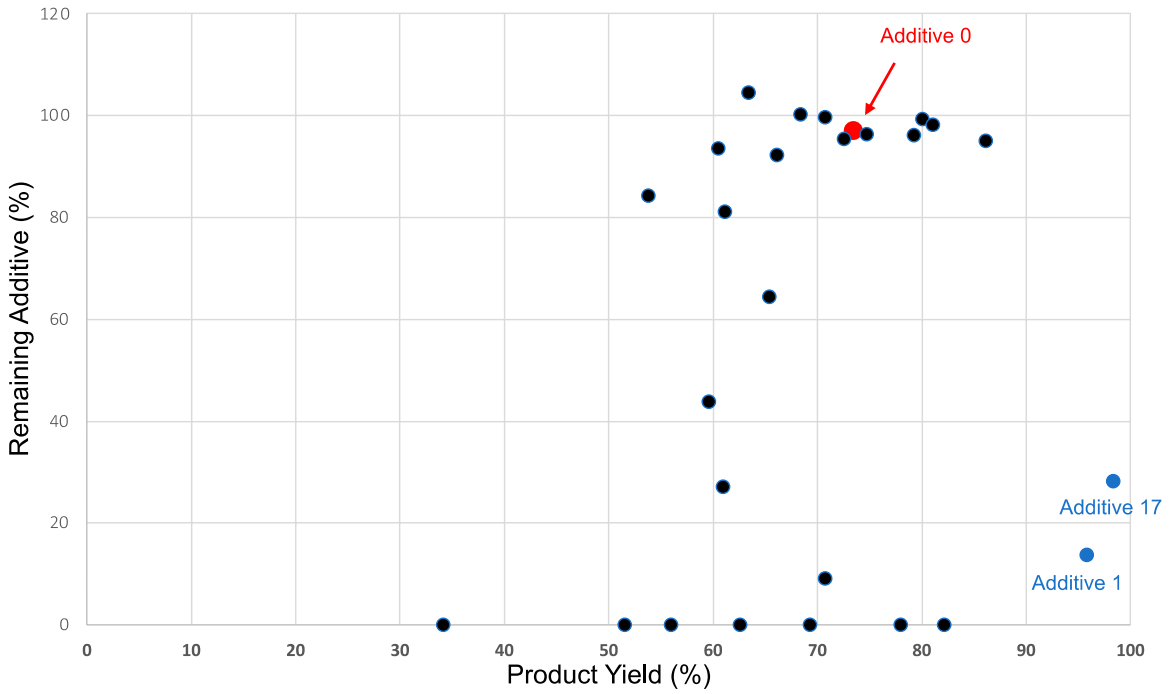

FIGURE 3
Two-dimensional representations of the product yield (%) and remaining additives (%).

The decrease in the remaining additives was mainly due to the formation of the corresponding byproducts by a competitive reaction between the additives and hydrazine. The byproducts that formed from the additives were either isolated from the crude mixture or, if difficult to isolate, synthesized by methods reported in the literature, and their structures were confirmed using NMR and mass spectrometry analysis (See Supplementary Material).

As expected, carboxyl groups in additives **A1** and **A17**, the amide group in additive **A6**, and the ester group in additive **A24** reacted with hydrazine to afford the corresponding acyl hydrazides such as **B1**.

The carbonyl groups in additive **A4**, **A5**, and **A16** also reacted with hydrazine to form the corresponding hydrazones such as **B4**, **B5**, and **B16** (Scheme 2). Additive **A15** with an enone moiety and additive **A18** with a nitrile moiety also reacted with hydrazine to give

10.3389/fchem.2024.1378746

TABLE 3 Screening of Brønsted acid additives.

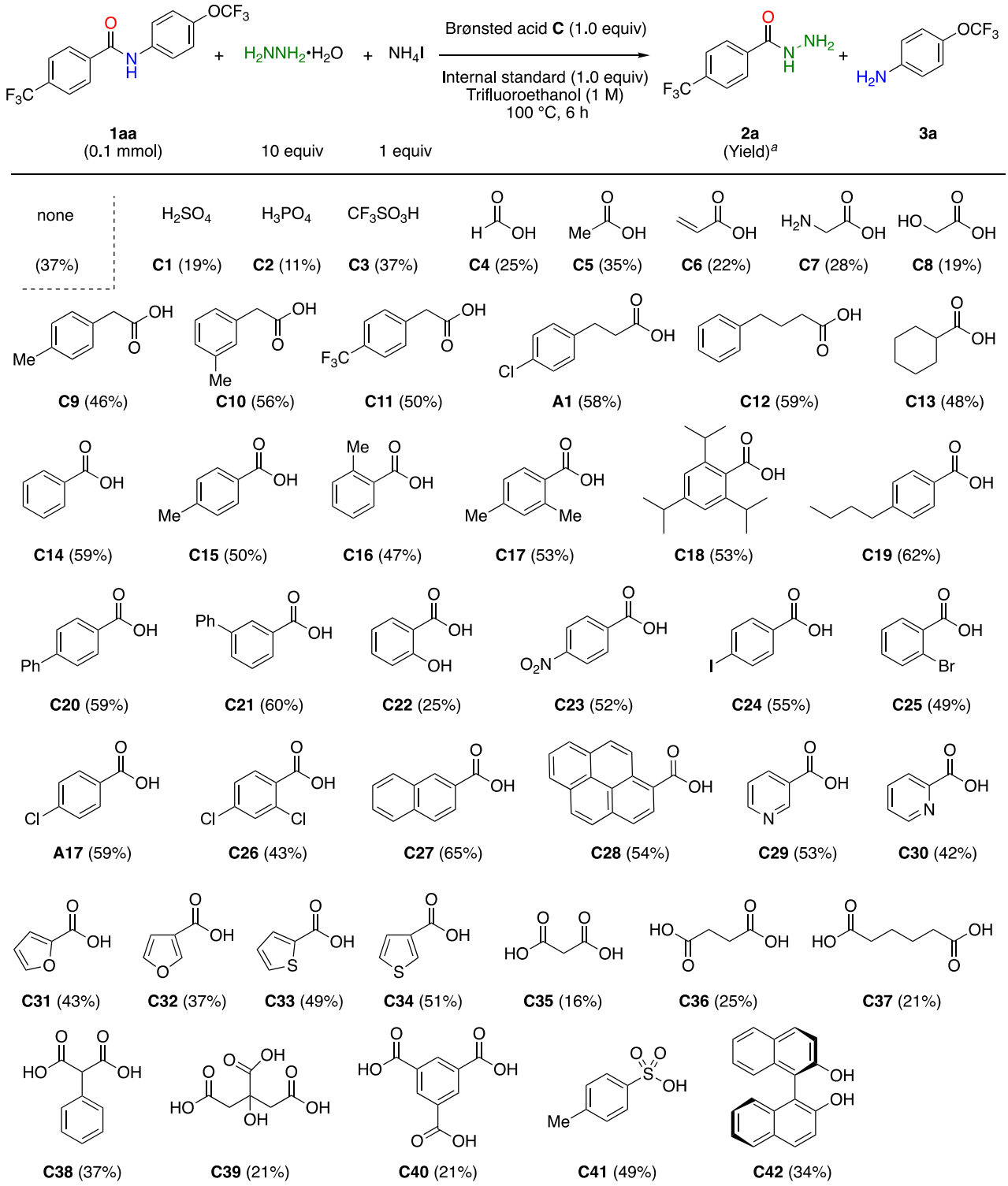

[a]Determined by ^{19}F NMR analysis of the mixture using 4-(trifluoromethoxy)anisole (0.1 mmol) as an internal standard.

nitrogen-containing heterocycles pyrazoline **B15** and tetrazine **B18** in good yields. On the other hand, some unexpected reactions were also observed. Additive **A21** with a guanidine moiety reacted with hydrazine to give amine **B21**.

In the reactions using additives **A10** and **A11** containing terminal alkene and alkyne, a partial reduction proceeded to produce alkane **B10** and alkene **A10** (Scheme 3). This type of reduction of olefins by hydrazine was reported by Imada et al., where hydrazine was in situ-oxidized to diimide and the reduction was promoted by Brønsted acids (Arakawa et al., 2017). Surprisingly, the phenolic hydroxyl group and Ar-Cl moiety in additive **A13** were converted to amino groups to give naphthalene-

10.3389/fchem.2024.1378746

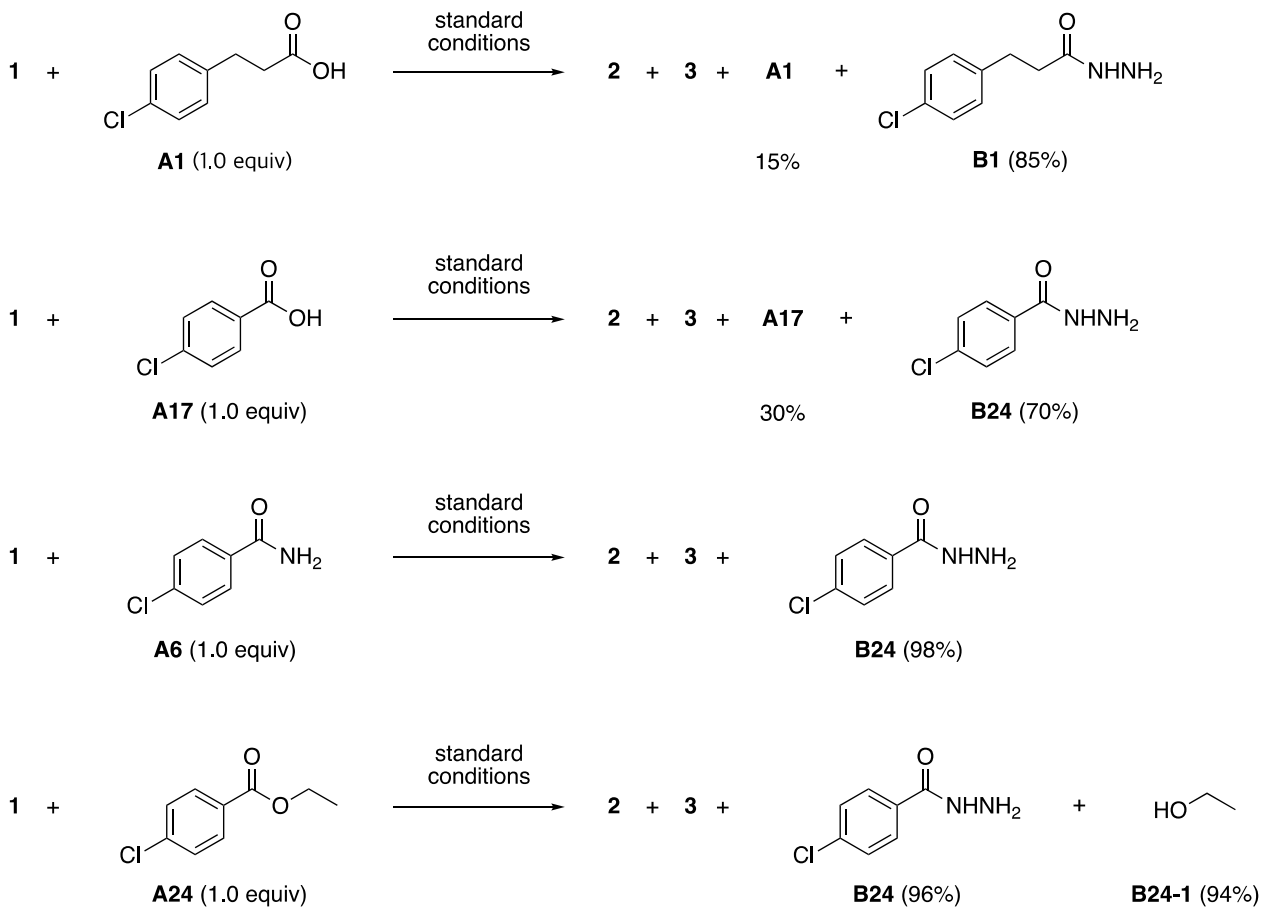

SCHEME 4
Formation of byproducts derived from additives **A1**, **A17**, **A6** and **A24**.

1,4-diamine (**B13**). The discovery of these unexpected reactions is an advantage of using the FGE kit.

Functional group compatibility of a reaction is evaluated from two aspects: the effect of the functionalized additive on the product yield and the remaining additive. The two-dimensional plot in Figure 3 shows the degree of the functional group compatibility for each reaction at a glance. In this plot, dots positioned near additive **A0** (red dot in the plot) indicate that the functional groups in the corresponding additive are tolerant in this reaction. On the other hand, dots father away from additive **A0** suggest that the reaction is significantly (often negatively) affected by the presence of the functional groups in the additives. This plot clearly shows that under the conditions of this amide bond cleavage reaction, although some functional groups reacted (reducing the recovery of the additive), many functional groups did not inhibit the reaction itself (reducing the yield). In addition, there are many additives with positive effects, and additives **A1** and **A17** with a carboxyl group significantly increased the product yield.

2.2 Acidic additives for accelerating the amide bond cleavage reaction

Because the above results suggested that carboxyl groups accelerate the ammonium salt-promoted amide bond cleavage reaction, we next examined various acidic additives.

2.2.1 Screening of Brønsted acid additives

Carboxylic acids are easy to handle and often inexpensive (Gooßen et al., 2008; Pichette Drapeau and Gooßen, 2016). Therefore, even if the amide bond cleavage reaction requires an equivalent amount of additive, the carboxylic acid addition conditions can be a useful reaction system.

First, we screened various inorganic and organic Brønsted acids as additives using General Procedure B (See Supplementary Material). To evaluate the additive effects on the reaction rate, product yields were examined for 6 h during the course of the reaction. The use of inorganic acids **C1**–**C3** significantly decelerated the reactions (Table 3). Next, we examined a wide variety of mono-carboxylic acids **C4**–**C34** including **A1** and **A17** as additives to evaluate changes in the product yield. Overall, aliphatic or aromatic carboxylic acids were not very important, and the correlation between the electrical effects and reactivity was low. On the other hand, it is important to have a certain molecular size, and carboxylic acids, especially those with aromatic rings such as benzene rings, exhibited a good tendency. *Ortho*-substituted Benzoic acids **C16**–**C18** and **C26** were expected to have excellent effects because their carboxylic acid moieties did not react with hydrazine due to steric hindrance. They, however, did not significantly impact the product yields, suggesting that carboxylic acids without steric hindrance should be considered as additives to accelerate the reaction. The acceleration effect of heterocyclic rings is low (**C29**–**C34**). The presence of hydroxyl (**C8** and **C22**) and amino (**C7**) groups in the vicinity of carboxylic acids

10.3389/fchem.2024.1378746

TABLE 4 Comparison of carboxylic acids and hydrazides.

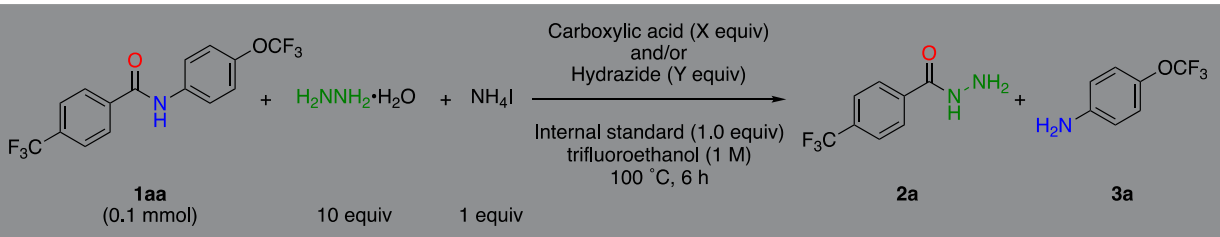

Entry	Additive	X equiv/Y equiv	Yield of 2a (%)[a]
1	none	–	37
2	benzoic acid	1.0	59
3	benzoic acid/benzohydrazide	0.5/0.5	48
4	benzohydrazide	1.0	38
5	4-chlorobenzoic acid	1.0	59
6	4-chlorobenzoic acid/4-chlorobenzohydrazide	0.5/0.5	44
7	4-chlorobenzohydrazide	1.0	43

[a]Determined by ^{19}F NMR analysis of the crude mixture using 4-(trifluoromethoxy)anisole (0.1 mmol) as an internal standard.

TABLE 5 Screening of Lewis acid catalysts.

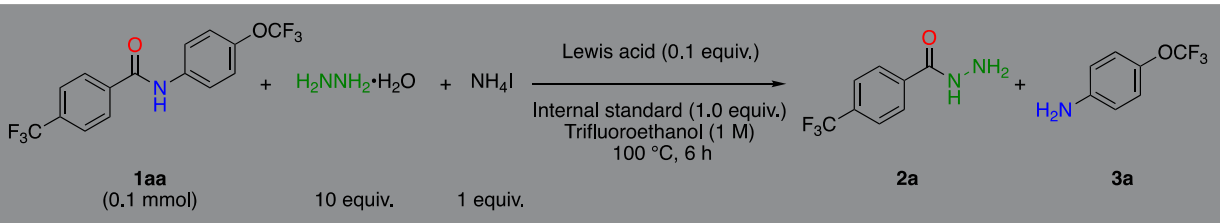

Entry	Lewis acid	Yield of 2a (%)[a]	Entry	Lewis acid	Yield of 2a (%)[a]
1	none	37	11	AgOTf	27
2	CuBr	20	12	$Cu(OTf)_2$	28
3	$CuBr_2$	27	13	$Ni(OTf)_2$	51
4	$CuCl_2$	28	14	$Co(OTf)_2$	48
5	$PdCl_2$	34	15	$Fe(OTf)_3$	63
6	$Zn(OAc)_2$	52	16	$Fe(OTf)_3$[b]	38
7	$Cu(OAc)_2$	28	17	$Sc(OTf)_3$	36
8	$Pd(OAc)_2$	32	18	$Y(OTf)_3$	42
9	$Zn(OTf)_2$	66	19	$Yb(OTf)_3$	41
10	$Zn(OTf)_2$[b]	89	20	$La(OTf)_3$	32
			21	$Bi(OTf)_3$	34

[a]Determined by ^{19}F NMR analysis of the crude mixture using 4-(trifluoromethoxy)anisole (0.1 mmol) as an internal standard. [b]Without addition of NH_4I.

was not desirable, and dicarboxylic and tricarboxylic acids (**C34**–**C42**) rather inhibited the reaction. Other types of acidic compounds, 4-toluenesulfonic acid (**C41**) and BINOL (**C42**), were also ineffective. Based on this screening study, we concluded that 4-butyl benzoic acid (**C19**) and 2-naphthoic acid (**C27**) were the most effective additives for the amide bond cleavage reaction.

2.2.2 Control experiments between carboxylic acid and hydrazide

As mentioned above, although several carboxylic acids had positive additive effects, the carboxyl groups reacted with hydrazine to form the corresponding hydrazide (Scheme 4). Therefore, control experiments between carboxylic acids and hydrazides were performed to determine whether the positive

10.3389/fchem.2024.1378746

TABLE 6 Substrate scope of amides with acidic additive/catalyst.

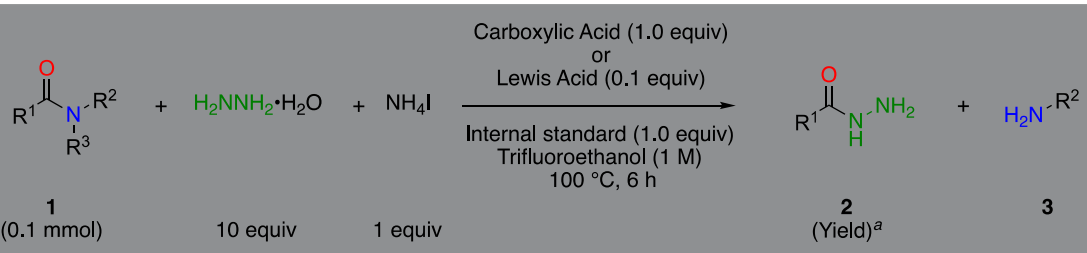

1 (0.1 mmol) | 10 equiv | 1 equiv | **2** (Yield)[a] | **3**

Amide	none	C19	C27	$Fe(OTf)_3$	$Zn(OTf)_2$	$Zn(OTf)_2$ without NH_4I
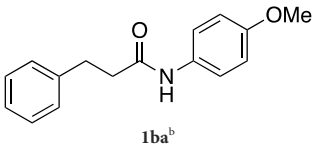 **1ba**[b]	69%	73%	70%	63%	67%	45%
	83% (12 h)	91% (12 h)	88% (12 h)		84% (12 h)	
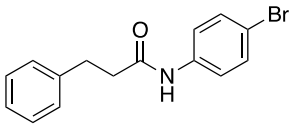 **1bb**	40%	71%	76%	40%	51%	76%
	67% (12 h)	>99% (12 h)	93% (12 h)			90% (12 h)
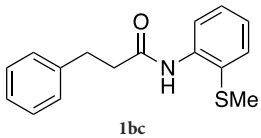 **1bc**	39%	53%	55%	44%	45%	77%
	67% (12 h)	76% (12 h)	76% (12 h)			87% (12 h)
		>99% (24 h)	>99% (24 h)			>99% (24 h)
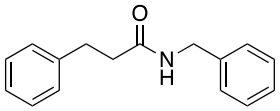 **1bd**	42%	51%	56%	62%	50%	38%
	67% (12 h)	>99% (24 h)	>99% (24 h)	79% (24 h)	82% (24 h)	
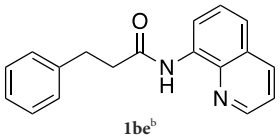 **1be**[b]	30%	57%	54%	53%	76%	>99%
	54% (12 h)	80% (12 h)	82% (12 h)			
			>99% (24 h)			

[a]Determined by ^1H NMR analysis of the mixture using an internal standard.
[b]At 90 °C.

effect was due to the carboxylic acid or the in situ-formed hydrazide.

We selected benzoic acid (**C14**) and 4-chlorobenzoic acid (**A17**) as representative carboxylic acids, and the corresponding hydrazides were synthesized to study their effects. As shown in Table 4, the addition of hydrazides had lower effects (Entries 4 and 7) than carboxylic acids (Entries 2 and 5). Furthermore, the addition of equal amounts of carboxylic acid and hydrazide gave intermediate-level results (Entries 3 and 6). These results clearly suggest that carboxylic acids accelerated the amide bond cleavage reaction, not hydrazides.

2.2.3 Lewis acid additives for accelerating the amide bond cleavage reaction

Because carboxylic acids are gradually converted to less effective hydrazides under the reaction conditions, we next examined Lewis acids as additives. Some Lewis acids are reported to accelerate C–H/C–C/C–O/C–N bond cleavage reactions and improve reaction efficiencies (Kita et al., 2013; Baglia et al., 2016; Gao et al., 2021).

In fact, the addition of 1.0 equiv of $Zn(OTf)_2$ greatly accelerated the reaction, increasing the yield of **2a** from 37% to 91% under the conditions shown in Supplementary Table S9. Furthermore, when the amount of Lewis acid was reduced to 0.1 equiv, the additive effect was maintained, although the yield was reduced to 66% (Table 5, Entry 9). In this case, no products other than the substrate **1aa** and the target products **2a** and **3a** were observed.

We then screened various Lewis acid catalysts for the amide bond cleavage reaction using General Procedure B (Table 5) (See Supplementary Material). Although many Lewis acids showed no positive effects, a catalytic amount of $Fe(OTf)_3$ along with $Zn(OTf)_2$ efficiently accelerated the amide bond cleavage reactions and increased the yield of product **2a** (Entry 15). Furthermore, in the case of $Zn(OTf)_2$, the reaction was accelerated more efficiently in the absence of ammonium iodide (Entry 10). On the other hand, in the case of Fe, no acceleration effect was observed under conditions without NH_4I (Entry 16).

2.2.4 Scope of amide substrates with acidic additive/catalyst

Finally, with the optimized activation systems using carboxylic acids **C19** and **C27** (1.0 equiv) and Lewis acid catalysts $Fe(OTf)_3$ and $Zn(OTf)_2$ (0.1 equiv) in hand, the substrate generality of amide was examined using General Procedure B (Table 6) (See Supplementary Material).

We found that the additives also had a reaction-accelerating effect on other amide substrates. Again, to clarity the differences in the effects of these four systems, the results are shown for a reaction time of 6 h before the reaction is complete. Although the degree of effectiveness of each system varied depending on the substrates, in all cases the addition of 1.0 equiv of carboxylic acid was effective. In the case of 8-aminoquinoline amide **1be**, a highly effective and frequently used directing group amide, the system using a zinc catalyst without the addition of NH_4I showed drastic acceleration effects, increasing the yield from 30% to 99% at 6 h. With acidic additives/catalysts, the reactions using amides **1bb**–**1bf** were almost completed by prolonging the reaction time. The addition of carboxylic or Lewis acids to the amide bond cleavage reaction is expected to be useful for cleavage of less reactive amide bonds.

3 Conclusion

In conclusion, we evaluated functional group compatibility in amide bond cleavage reactions using the FGE kit, which allows for accurate and rapid assessment of functional group compatibility using 26 FGE compounds with different functional groups. Except for some functional groups that react with hydrazine, we found many functional groups that are compatible. These evaluation experiments revealed that an unprecedented substitution reaction of additive **A13** with phenolic hydroxyl group proceeded. Moreover, carboxylic acids were discovered to accelerate the reaction, leading to the development of a new catalytic amide bond cleavage reaction with $Zn(OTf)_2$. These results revealed the clear advantage of the FGE kit for both collecting data that can be applied for machine learning and discovering seeds for the development of new reactions.

Data availability statement

The raw data supporting the conclusion of this article will be made available by the authors, without undue reservation.

Author contributions

JC: Data curation, Formal Analysis, Investigation, Methodology, Resources, Validation, Visualization, Writing–original draft, Writing–review and editing. AN: Data curation, Formal Analysis, Investigation, Methodology, Resources, Validation, Writing–review and editing. NS: Data curation, Formal Analysis, Investigation, Methodology, Resources, Validation, Writing–review and editing. YK: Formal Analysis, Investigation, Methodology, Writing–review and editing. HM: Investigation, Methodology, Supervision, Writing–review and editing. TO: Conceptualization, Data curation, Funding acquisition, Investigation, Methodology, Project administration, Supervision, Visualization, Writing–original draft, Writing–review and editing.

Funding

The author(s) declare that financial support was received for the research, authorship, and/or publication of this article. This work was supported by a Grant-in-Aid for Transformative Research Areas (A) Digitalization-driven Transformative Organic Synthesis (Digi-TOS) (MEXT KAKENHI Grant JP21A204, JP21H05207, and JP21H05208) from MEXT, and Grants-in-Aid for Scientific Research (B) (JSPS KAKENHI Grant JP17H03972 and JP21H02607 to TO) and (C) (JSPS KAKENHI Grant JP21K06477 to HM) from JSPS, Basis for Supporting Innovative Drug Discovery and Life Science Research (BINDS) (AMED Grant Numbers JP21am0101091 and JP22ama121031) from AMED. JC thanks the Japan Science and Technology Agency (JST) SPRING (JPMJSP2136).

Acknowledgments

The authors acknowledge Taro Tsuji, Shunsuke Kataoka, Asuka Kudo, and Yunosuke Koga for synthesizing additive compounds and Prof. Nobuyuki Mase and his students at Shizuoka University for synthesizing the compounds **A10**, **A11** and **A25** in the FGE kit by flow reaction system. We also thank Yumiko Hirakawa for her management and operation of the FGE kit.

Conflict of interest

The authors declare that the research was conducted in the absence of any commercial or financial relationships that could be construed as a potential conflict of interest.

Publisher's note

Supplementary material

The Supplementary Material for this article can be found online at: https://www.frontiersin.org/articles/10.3389/fchem.2024.1378746/full#supplementary-material

References

Arakawa, Y., Kohda, T., Minagawa, K., and Imada, Y. (2017). Brønsted acid catalysed aerobic reduction of olefins by diimide generated *in situ* from hydrazine. *SynOpen* 1 (01), 11–14. doi:10.1055/s-0036-1588790

Baglia, R. A., Krest, C. M., Yang, T., Leeladee, P., and Goldberg, D. P. (2016). High-valent manganese–oxo valence tautomers and the influence of lewis/bronsted acids on C–H bond cleavage. *Inorg. Chem.* 55 (20), 10800–10809. doi:10.1021/acs.inorgchem.6b02109

Bai, Z., Zheng, S., Bai, Z., Song, F., Wang, H., Peng, Q., et al. (2019). Palladium-catalyzed amide-directed enantioselective carboboration of unactivated alkenes using a chiral monodentate oxazoline ligand. *ACS Catal.* 9 (7), 6502–6509. doi:10.1021/acscatal.9b01350

Bautista, J. A., Connors, R. E., Raju, B. B., Hiller, R. G., Sharples, F. P., Gosztola, D., et al. (1999). Excited state properties of peridinin: observation of a solvent dependence of the lowest excited singlet state lifetime and spectral behavior unique among carotenoids. *J. Phys. Chem. B* 103 (41), 8751–8758. doi:10.1021/jp9916135

Bhattacharya, T., Ghosh, A., and Maiti, D. (2021). Hexafluoroisopropanol: the magical solvent for Pd-catalyzed C–H activation. *Chem. Sci.* 12 (11), 3857–3870. doi:10.1039/D0SC06937J

Brown, D. G., and Bostrom, J. (2016). Analysis of past and present synthetic methodologies on medicinal chemistry: where have all the new reactions gone? Miniperspective. *J. Med. Chem.* 59 (10), 4443–4458. doi:10.1021/acs.jmedchem.5b01409

Chaudhari, M. B., and Gnanaprakasam, B. (2019). Recent advances in the metal-catalyzed activation of amide bonds. *Chemistry–An Asian J.* 14 (1), 76–93. doi:10.1002/asia.201801317

Collins, K. D., and Glorius, F. (2013). A robustness screen for the rapid assessment of chemical reactions. *Nat. Chem.* 5 (7), 597–601. doi:10.1038/NCHEM.1669

Dai, X., De Mesmaeker, A., and Joyce, G. F. (1995). Cleavage of an amide bond by a ribozyme. *Science* 267 (5195), 237–240. doi:10.1126/science.7809628

Dreos, R., Geremia, S., Randaccio, L., and Siega, P. (2011). *The chemistry of amidines and imidates (Patai's Chemistry of Functional Groups)*. Chichester, UK: John Wiley & Sons, Ltd.

Ertl, P. (2017). An algorithm to identify functional groups in organic molecules. *J. cheminformatics* 9 (1), 36–37. doi:10.1186/s13321-017-0225-z

Gao, H., Hu, L., Hu, Y., Lv, X., Wu, Y. B., and Lu, G. (2021). Origins of Lewis acid acceleration in nickel-catalysed C–H, C–C and C–O bond cleavage. *Catal. Sci. Technol.* 11 (13), 4417–4428. doi:10.1039/D1CY00660F

Gooßen, L. J., Rodríguez, N., and Gooßen, K. (2008). Carboxylic acids as substrates in homogeneous catalysis. *Angew. Chem. Int. Ed.* 47 (17), 3100–3120. doi:10.1002/anie.200704782

Kabi, A. K., Gujjarappa, R., Vodnala, N., Kaldhi, D., Tyagi, U., Mukherjee, K., and etal (2020). HFIP-mediated strategy towards β-oxo amides and subsequent Friedel-Craft type cyclization to 2-quinolinones using recyclable catalyst. *Tetrahedron Lett.* 61 (46), 152535. doi:10.1016/j.tetlet.2020.152535

Kashima, C., Harada, H., Kita, I., Fukuchi, I., and Hosomi, A. (1994). The preparation of N-acylpyrazoles and their behavior toward alcohols. *Synthesis* 1994 (01), 61–65. doi:10.1055/s-1994-25406

Kaspar, A. A., and Reichert, J. M. (2013). Future directions for peptide therapeutics development. *Drug Discov. today* 18 (17-18), 807–817. doi:10.1016/j.drudis.2013.05.011

Kemnitz, C. R., and Loewen, M. J. (2007). "Amide resonance" correlates with a breadth of C– N rotation barriers. *J. Am. Chem. Soc.* 129 (9), 2521–2528. doi:10.1021/ja0663024

Kita, Y., Nishii, Y., Onoue, A., and Mashima, K. (2013). Combined catalytic system of scandium triflate and boronic ester for amide bond cleavage. *Adv. Synthesis Catal.* 355 (17), 3391–3395. doi:10.1002/adsc.201300819

Kumar, D., Sharma, H., Saha, N., and Chakraborti, A. K. (2022). Domino synthesis of functionalized pyridine carboxylates under gallium catalysis: unravelling the reaction pathway and the role of the nitrogen source counter anion. *Chem. – Asian J.* 17 (15), e202200304. doi:10.1002/asia.202200304

Li, G., and Szostak, M. (2020). Transition-metal-free activation of amides by N– C bond cleavage. *Chem. Rec.* 20 (7), 649–659. doi:10.1002/tcr.201900072

Lv, C., Zhao, R., Wang, X., Liu, D., Muschin, T., Sun, Z., et al. (2023). Copper-catalyzed transamidation of unactivated secondary amides via C–H and C–N bond simultaneous activations. *J. Org. Chem.* 88 (4), 2140–2157. doi:10.1021/acs.joc.2c02551

Maegawa, Y., Ohshima, T., Hayashi, Y., Agura, K., Iwasaki, T., and Mashima, K. (2011). Additive effect of N-heteroaromatics on transesterification catalyzed by tetranuclear zinc cluster. *ACS Catal.* 1 (10), 1178–1182. doi:10.1021/cs200224b

Mahesh, S., Tang, K. C., and Raj, M. (2018). Amide bond activation of biological molecules. *Molecules* 23 (10), 2615. doi:10.3390/molecules23102615

Mikulak-Klucznik, B., Gołębiowska, P., Bayly, A. A., Popik, O., Klucznik, T., Szymkuć, S., et al. (2020). Computational planning of the synthesis of complex natural products. *Nature* 588 (7836), 83–88. doi:10.1038/s41586-020-2855-y

Noshita, M., Shimizu, Y., Morimoto, H., Akai, S., Hamashima, Y., Ohneda, N., et al. (2019). Ammonium salt-accelerated hydrazinolysis of unactivated amides: mechanistic investigation and application to a microwave flow process. *Org. Process Res. Dev.* 23 (4), 588–594. doi:10.1021/acs.oprd.8b00424

Pattabiraman, V. R., and Bode, J. W. (2011). Rethinking amide bond synthesis. *Nature* 480 (7378), 471–479. doi:10.1038/nature10702

Pichette Drapeau, M., and Gooßen, L. J. (2016). Carboxylic acids as directing groups for C– H bond functionalization. *Chemistry–A Eur. J.* 22 (52), 18654–18677. doi:10.1002/chem.201603263

Rashed, M. N., Siddiki, S. H., Touchy, A. S., Jamil, M. A., Poly, S. S., Toyao, T., et al. (2019). Direct phenolysis reactions of unactivated amides into phenolic esters promoted by a heterogeneous CeO_2 catalyst. *Chemistry–A Eur. J.* 25 (45), 10594–10605. doi:10.1002/chem.201901446

Saito, N., Nawachi, A., Kondo, Y., Choi, J., Morimoto, H., and Ohshima, T. (2023). Functional group evaluation kit for digitalization of information on the functional group compatibility and chemoselectivity of organic reactions. *Bull. Chem. Soc. Jpn.* 96 (5), 465–474. doi:10.1246/bcsj.20230047

Shimizu, Y., Morimoto, H., Zhang, M., and Ohshima, T. (2012). Microwave-assisted deacylation of unactivated amides using ammonium-salt-accelerated transamidation. *Angew. Chem. Int. Ed.* 51 (34), 8564–8567. doi:10.1002/anie.201202354

Shimizu, Y., Noshita, M., Mukai, Y., Morimoto, H., and Ohshima, T. (2014). Cleavage of unactivated amide bonds by ammonium salt-accelerated hydrazinolysis. *Chem. Commun.* 50 (84), 12623–12625. doi:10.1039/C4CC02014F

Smithrud, D. B., Sanford, E. M., Chao, I., Ferguson, S. B., Carcanague, D. R., Evanseck, J. D., et al. (1990). Solvent effects in molecular recognition. *Pure Appl. Chem.* 62 (12), 2227–2236. doi:10.1351/pac199062122227

J. Thorner, S. D. Emr, and J. N. Abelson (2000). *Applications of chimeric genes and hybrid proteins, Part A: gene expression and protein purification* (San Diego, USA: Academic Press).

Wang, B., and Cao, Z. (2011). Acid-catalyzed reactions of twisted amides in water solution: competition between hydration and hydrolysis. *Chemistry–A Eur. J.* 17 (42), 11919–11929. doi:10.1002/chem.201101274

Wu, Z., Liu, C., Zhang, Z., Zheng, R., and Zheng, Y. (2020). Amidase as a versatile tool in amide-bond cleavage: from molecular features to biotechnological applications. *Biotechnol. Adv.* 43, 107574. doi:10.1016/j.biotechadv.2020.107574

Zhang, S. Q., Xu, L. C., Li, S. W., Oliveira, J. C., Li, X., Ackermann, L., et al. (2023). Bridging chemical knowledge and machine learning for performance prediction of organic synthesis. *Chemistry–A Eur. J.* 29 (6), e202202834. doi:10.1002/chem.202202834

Zhang, Z., Zheng, D., Wan, Y., Zhang, G., Bi, J., Liu, Q., et al. (2018). Selective cleavage of inert aryl C–N bonds in *N*-aryl amides. *J. Org. Chem.* 83 (3), 1369–1376. doi:10.1021/acs.joc.7b02880

Frontiers in Chemistry

Explores all fields of chemical science across the periodic table

Advances our understanding of how atoms, ions, and molecules come together and come apart. It explores the role of chemistry in our everyday lives - from electronic devices to health and wellbeing.

Discover the latest Research Topics

See more →

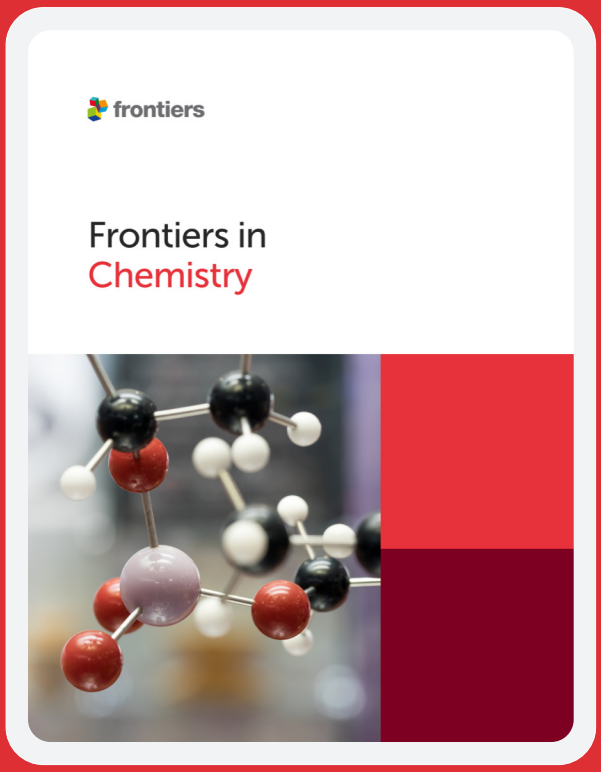

Frontiers

Avenue du Tribunal-Fédéral 34
1005 Lausanne, Switzerland
frontiersin.org

Contact us

+41 (0)21 510 17 00
frontiersin.org/about/contact